Clinical Projects on Biophotonics

CePOF paper collection

CEPOF
CENTRO DE PESQUISAS EM ÓPTICA E FOTÔNICA

2015

Photomedicine and Laser Surgery
Volume 30, Number 2, 2012

Pp. 96–101
DOI: 10.1089/pho.2011.3053

Overall-Mouth Disinfection by Photodynamic Therapy Using Curcumin

Natália Costa Araújo, M.D.,[1] Carla Raquel Fontana, Ph.D.,[2,3]
Marleny Elizabeth Martinez Gerbi, Ph.D.[1] and Vanderlei Salvador Bagnato, Ph.D.[3]

Abstract

Background data: Photodynamic therapy is a technique that involves the activation of photosensitizers by light in the presence of tissue oxygen, resulting in the production of reactive radicals capable of inducing cell death. ***Objective:*** The present study assessed the overall susceptibility of pathogens of salivary flora to photodynamic therapy after sensitization with curcumin and exposure to blue light at 450 nm. ***Methods:*** A randomized trial was executed with 13 adult volunteers. Three different groups were analyzed: L-D- (no light, no drug; control group), L-D+ (treated only with the drug; curcumin group) and L+D+ (treated with drug and light; photodynamic therapy group). Non-stimulated saliva samples were collected for bacterial counts at baseline and after the experimental phase, and adverse events experienced were recorded. Serial dilutions were performed, and the resulting samples were cultured on blood agar plates in microaerophilic conditions. The number of colony-forming units was then determined. ***Results:*** There was a considerable difference between the two experimental groups with regard to effectiveness of bacterial reduction. In the L-D+ group, the bacterial decline was considerably smaller (9%) than in the L+D+ group, with a 68% decrease in bacteria. A statistically significant reduction in the bacterial population was observed only in the photodynamic therapy group ($p < 0.05$). ***Conclusions:*** Photodynamic therapy was found to be effective in the reduction of salivary microorganisms. No significant reduction was found for the group in which only curcumin was used, proving the absence of dark toxicity of the drug. This work shows that overall disinfection of the mouth can be done with a simple procedure involving photodynamic action.

Introduction

The diversity of biological surfaces in the oral cavity provides many ecological sites for colonization by a variety of oral bacterial species. The mouth is a favorable habitat for >700 bacterial species because of the presence of nutrients, epithelial debris, and secretions.[1] Therefore, the risk of infection is increased in intra-oral surgical procedures, because it is practically impossible to attain aseptic conditions, as a result of the large number of bacteria in the normal mouth. Local postoperative infections are one of the main causes of morbidity in oral surgery.[2] In some cases, the mouth cavity can even be the main cause of contamination for many types of surgery. Some surgeons advocate the routine use of prophylactic systemic antibiotics to decrease the risk of postoperative infection. However, antibiotics may be associated with unfavorable side effects, ranging from gastrointestinal disturbances to anaphylactic shock and development of resistance.[3]

Another option for decreasing the risk of postoperative infection by temporary reduction of intra-oral bacterial counts is the use of oral antiseptics. Disinfecting solutions, ideally, should be safe to use and effective against pathogens, and should not cause adverse tissue reaction. The most frequently used are chlorhexidine solutions.[4]

Chlorhexidine causes an immediate reduction in the number of salivary bacteria because of its broad activity spectrum.[5] Its mechanism of action involves interactions with external cell components and the cytoplasmic membrane, causing a high rate of leakage of intracellular components and interactions with cytoplasmic constituents.[6] Alteration in taste; burning sensation; increase of calculus formation; staining of the teeth and restorative materials; and, more rarely, oral mucosa desquamation and parotid swelling are effects related to its use.[7]

Recently, alternatives that might offer the possibility of efficient intra-oral bacterial count reduction with minimum

[1]Dental School of Pernambuco, University of Pernambuco, Camaragibe, PE, Brazil.
[2]Department of Clinical Analysis, School of Pharmaceutical Sciences, University of São Paulo State (UNESP), Araraquara, SP, Brazil.
[3]Institute of Physics of São Carlos, University of São Paulo (USP), São Carlos, SP, Brazil.

damage to systemic health have been sought. In these circumstances, photodynamic therapy (PDT) may offer the possibility of a new approach to oral disinfection.

PDT has been used as a treatment for cancer as well as other nonmalignant diseases.[8,9] PDT involves the use of a photosensitizer (PS) that is activated by exposure to light of a specific wavelength in the presence of oxygen. The excited PS binds to the target cell and induces the formation of oxygen species, causing localized photodamage and cell death.[9–11] One advantage of PDT as compared to antibiotics is that bacteria do not develop resistance to oxygen species. As compared to chlorhexidine, PDT does not cause the reported side-effects.

An ideal PS should be nontoxic and should display local toxicity only after activation by illumination.[12] Curcumin, a compound isolated from *Curcuma longa* L., has been used for centuries as a medicine, dietary pigment, and spice. The drug possesses a variety of traditional pharmaceutical applications for diseases, including wounds, liver diseases, microbial effects, and inflamed joints.[13] Curcumin has proved nontoxic in a number of cell culture and whole animal studies. It has a rather broad absorption peak in the range of 300–500 nm (maximum ~430 nm) and exerts potent phototoxic effects in micromolar amounts. Therefore, curcumin has potential as a PS for treatment of localized superficial infections in the mouth or skin.[14] In addition, this PS has economical advantages considering its low cost, simple manipulation, and great effectiveness.

The effectiveness of PDT against oral bacteria has been the subject of several studies.[15–20] Zanin et al.[18] showed the photodynamic activity of some PS on biofilms of *Streptococcus mutans*, *Streptococcus sobrinus*, and *Streptococcus sanguinis*. Zanin et al.[20] evaluated the phototoxic effect of toluidine blue O (TBO) on the viability of *S. mutans* biofilms and observed reductions up to 99.99%. Wood et al.[17] observed the successful photodynamic effects of erythrosine in the killing of *S. mutans* biofilms. Fontana et al.[15] showed the photodynamic action of methylene blue on human dental plaque microorganisms.

The efficacy of photodynamic action on microorganisms has been extensively investigated using various sensitizers. However, none of those studies used curcumin as a PS for oral decontamination.

In this study, we aim to investigate the effects of PDT on bacteria derived from human saliva. The goal of our research was to detect the susceptibility of pathogens of salivary flora to PDT after sensitization with curcumin and exposure to blue light at 450 nm.

Materials and Methods

Subjects

Samples of saliva were taken from 13 healthy subjects aged 25 through 50 years. The study group was composed of 7 female and 6 male participants. The criteria for exclusion from the study were age < 18 years, pregnancy, using partial or total dentures or orthodontic brackets, presence of systemic diseases, or smoking habit (Fig. 1). None of the subjects had used antibiotics or had undergone medical or dental treatment during the 3 months prior to sampling. The volunteers were not allowed to practice any oral hygiene technique (brushing or flossing) and followed a zero diet (no food) during the 12 h prior to sampling. Permission to collect saliva samples was authorized by the Ethics Committee of the University of Pernambuco (UPE), protocol number 033/11. All subjects also gave their informed consent.

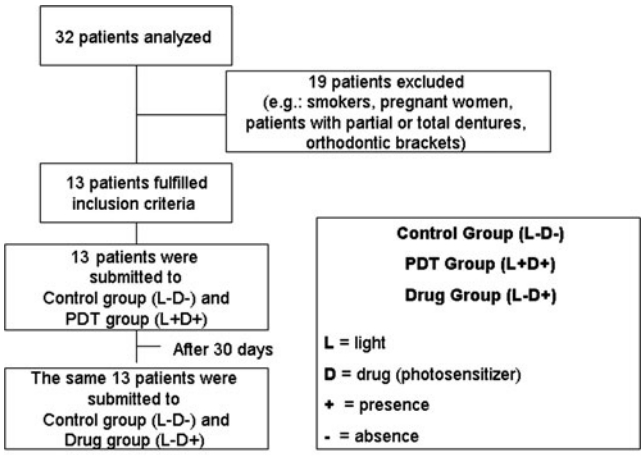

FIG. 1. Selection of patients and tested groups.

Preparation of blood agar culture plates

An enriched agar medium was prepared, containing 20 g/L of trypticase soy agar (Oxoid Ltd., Basingstoke, Hampshire, England), 26 g/L of brain – heart infusion agar (Oxoid Ltd., Basingstoke, Hampshire, England), 10 g/L of yeast extract (BBL), and 5 mg/L of hemin (Sigma Chemical Co., St. Louis, MO). The medium was autoclaved and cooled down to 50°C. Then, 5% defibrinated sheep blood (NewProv LTDA, Pinhais PR, Brazil) and 5 mg/mL of menadione (Sigma Chemical Co., St. Louis, MO) were added under aseptic conditions.

PS

Curcumin [1,7-bis-(4-hydroxy-3-methoxyphenyl)-1,6-heptadiene-3,5-dione] is an excellent lead compound for drug design and development on the basis of its explicit bioactivities, nontoxicity, and easy synthesis. Curcumin prepared by PDT–Pharma (Cravinhos SP, Brazil) was dissolved in sterile distilled water to give a solution at concentration of 1.5 g/L before use.

The ultraviolet-visible absorption spectra of this solution were recorded from 300 to 700 nm using quartz cuvettes with a 1-cm path length on a Cary 50 Bio UV-Vis spectrometer (Varian, Darmstadt, Germany), and were characterized by a long-wavelength maximum at 430 nm.

Light source

A blue light-emitting diode (Prototype, Project Finep/Gnatus LED Edixeon®, Edison Opto Corporation, New Taipei City, Taiwan) with an intensity of 67 mW/cm^2, a central wavelength of 450 nm and an estimated average fluency of 20.1 J/cm^2 was used. The system delivered light by uniform diffusion, which formed a semi-hemispheric illumination within the mouth cavity (Figs. 2 and 3). This spot of light was able to irradiate the full mouth. The power density of

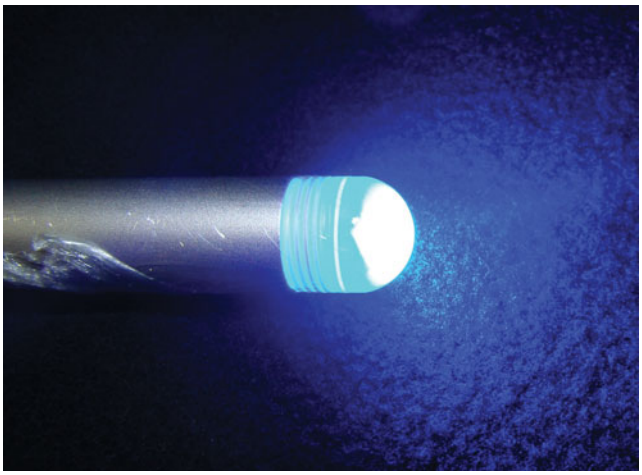

FIG. 2. Blue LED delivering light.

incident radiation was measured using a power meter (Coherent®, Santa Clara, CA).

The light parameters used in this study for saliva pathogen reduction were 67 mW/cm^2 (power density) and an estimated average fluency of 20.1 J/cm^2 (energy fluence).

Saliva samples and photodynamic treatment

Non-stimulated saliva (2 mL) was collected from each participant using the spitting method at two different periods of time and in three different situations.

Saliva samples for quantitative microbiological analysis at baseline were taken before any oral procedure (L-D-). For the group to which only the drug was administered (L-D+), samples were collected for microbiological analyses after mouth rinse with curcumin; for the group in whom the drug was used in association with light (L+D+), samples were collected after PDT (Fig. 1). The group L+D- (only light) was omitted based on previous experience of our group that detected unnoticeable variation with this level of light.

Subjects were instructed to rinse the oral cavity with 20 mL of curcumin solution (1.5 g/L) for 5 min. Then, for the PDT group (L+D+), the solution was expelled and a light source was introduced to activate the PS for 5 min. During this period, the temperature did not increase > 1.8°C.

The saliva samples of the participants, before and after oral cavity washing, with or without PDT, were collected in sterile containers. After illumination of the mouth, saliva samples underwent serial dilutions in brain–heart infusion broth, and 100-microliters aliquots were plated on blood agar plates and then incubated under microaerophilic conditions for 48 h at 36 ± 1°C. After incubation, the total number of colony-forming units (CFU) was determined.

Statistical analysis

The Statistical Package for Social Sciences (SPSS, Chicago, IL, 2006), version 13.0, was used for processing the data; $p < 0.05$ was used as a cutoff level for statistical significance. The data were analyzed for normality of distribution through the use of the Kolmogorov–Smirnov test. The statistical method used for correlating changes in bacterial counts was assessed by Student's t test.

Results

The action of PDT and curcumin for each subject was determined, verifying the reduction caused in each situation based on the following expression:

$$\text{Survival Fraction} = \frac{\text{Mean of test group} \cdot (100)}{\text{Mean of control group}}$$

Survival fractions were evaluated using repeated measures analysis of variance to compare treatment groups. Pairwise comparisons were performed using least significant difference tests.

Figures 4 and 5 and Table 1 show the obtained bacterial reduction for all subjects (L-D+, L+D+) and Fig. 6 shows the mean of survival fractions of saliva samples of the study groups. Each value represents the mean survival fraction from triplicate experiments. Whereas for drug alone (L-D+), a reduction of well below 40% was observed in most

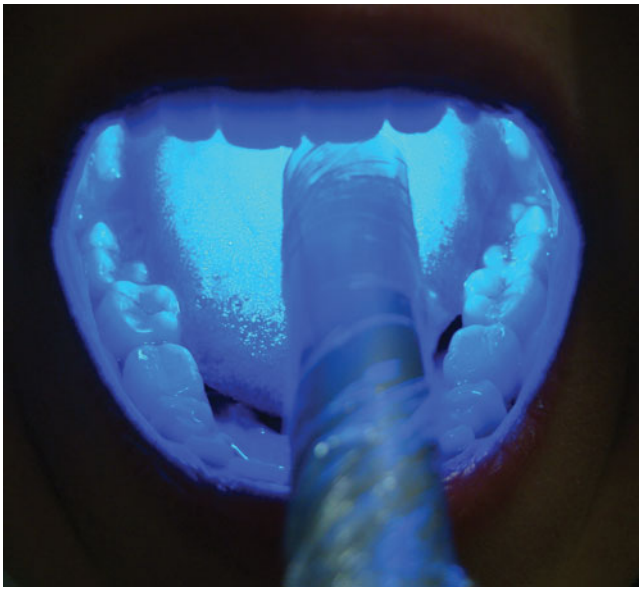

FIG. 3. System delivered light in the mouth cavity.

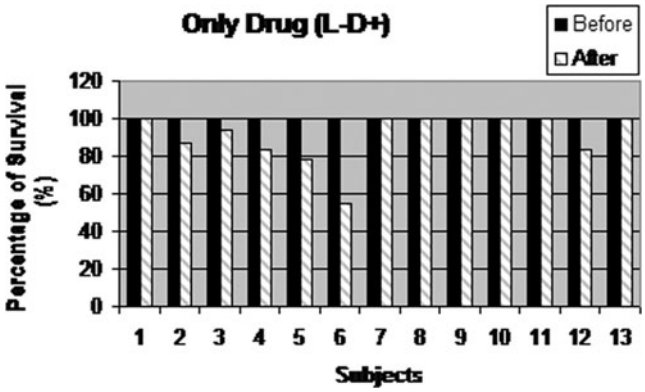

FIG. 4. Bacterial reduction for all subjects after drug mouth rinse (L-D+).

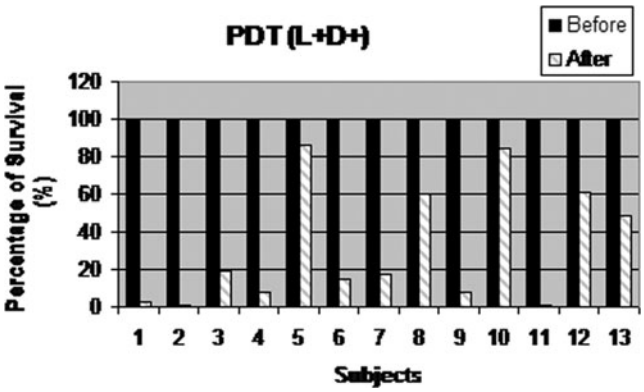

FIG. 5. Bacterial reduction for all subjects after drug mouth rinse followed by blue light (L+D+).

individuals (Fig. 4), for the group corresponding to PDT (L+D+), a large number of subjects with 90% reduction was exhibited. In fact, the PDT action caused a reduction of up to 99% in some subjects (Fig. 5).

In terms of averaging for all subjects (Fig. 6 and Table 1), a 9% reduction was obtained for the group L-D+, whereas a 68% reduction was obtained for the group L+D+. This indicates a significant effect on the reduction of the bacterial quantity in the mouth.

Pairwise comparisons using Student's *t* test (Table 2) indicated significant differences ($p<0.05$) between PDT (L+D+) and curcumin alone (L-D+). The photodynamic therapy group (L+D+) produced a statistically significant reduction in salivary bacterial counts in samples taken before PDT and those taken at the end of treatment ($p=0.004$), whereas the group treated only with drugs showed no influence in bacterial counts ($p=0.052$).

The synergism of light and curcumin is confirmed in our study: photodynamic therapy killed 68.3% of bacteria ($p<0.05$), whereas in the L-D+ group with the same volunteers, the effect of the drug alone did not result in an effective reduction of microorganisms.

Table 1. Bacterial Numbers (CFU) of Each Subject at Baseline and After Photodynamic Therapy (L+D+) or Mouth Rinse with Curcumin (L-D+)

	L+D+		*L-D+*	
Subjects	*Before*	*After*	*Before*	*After*
1	117	3	234	234
2	223	1	338	295
3	348	68	489	461
4	805	61	800	668
5	278	241	136	107
6	206	30	214	117
7	96	17	71	87
8	53	32	298	323
9	172	14	206	206
10	219	185	27	27
11	283	4	800	800
12	354	216	800	668
13	238	116	800	800
Mean	260.79	75.85	400.92	368.46

Discussion

The preoperative use of antiseptics in oral surgery is controversial. Many studies confirm that they reduce intraoral bacteria and decrease bacteremia during surgical procedures.[4,21–23] However, most surgeons are not convinced of their effect on reduction of postoperative infections.[24]

There is no generally accepted universal protocol for preoperative antimicrobial prophylaxis in oral surgery, but chlorhexidine gluconate is the most frequently used antiseptic solution and the most effective compound that shows pronounced antimicrobial effects both on Gram-positive and Gram-negative bacteria, as well as on fungi and some viruses.[5,25] However, it has not been recommended for use over long intervals because of the related side effects.[7,26]

Therefore, the study of new technologies for use in association with mouth rinse is very important. The technique of PDT may offer several advantages compared to traditional antimicrobial mouth rinses.

First, bacterial killing is fast, reducing the necessity for high concentrations of chemical substance. Second, as the death of the bacteria is linked to the mediation of reactive species, the development of bacterial resistance is unlikely. As demonstrated in our study, the PS by itself is not bactericidal, and bacterial reduction can be controlled by restricting the irradiated area.[27–30]

Therefore, PDT may be an interesting alternative to antibiotics and antiseptics used for oral bacteria reduction. Several studies have demonstrated the susceptibility of oral bacteria to PDT,[15–20] but despite studies that have shown the effectiveness of this procedure, some factors can influence the success of this treatment, such as type, concentration, and incubation time of the sensitizers; the microorganism species; the light source; and the given dose.

Most studies evaluating the efficacy of PDT on oral bacteria used TBO and methylene blue as PS, followed by irradiation with a red LED light.[11,31–35] Williams et al.[31] noted 100% death of *S. mutans* in a planktonic suspension, using an LED with TBO as the PS. Neither TBO dye nor light alone had a significant antibacterial effect under the experimental conditions used. These results and our findings highlight the need for dye–light conjugation to ensure the effectiveness of PDT. The photodynamic effects of the binomial dye–light were also confirmed by Giusti et al.[35] Photogem and TBO activated by red light caused bacterial reduction of *Lactobacillus acidophilus* and *S.mutans* in carious dentin.

The TBO dye is a common substance used in PDT[36]; however, its use in the mouth can change the color of tooth surfaces and restorations of resin-based composite.[35] In this article, a blue LED (450 nm) with an intensity of 67 mW/cm^2 was used together with a curcumin solution with a concentration of 1.5 g/L. The dyes work as optical absorption agents and are activated by irradiation with light of a specific wavelength, resulting in the generation of cytotoxic species, including singlet oxygen and free radicals, that exert a bactericidal effect but that are not toxic to host cells.[9,10]

As there is no published work, to our best knowledge, reporting the use of curcumin as a mouth rinse followed by illumination to promote oral cavity decontamination, it was our aim to perform a pilot study. Although this study has been conducted with only 13 patients, our intention was to show that the procedure using mouthwash is safe and that

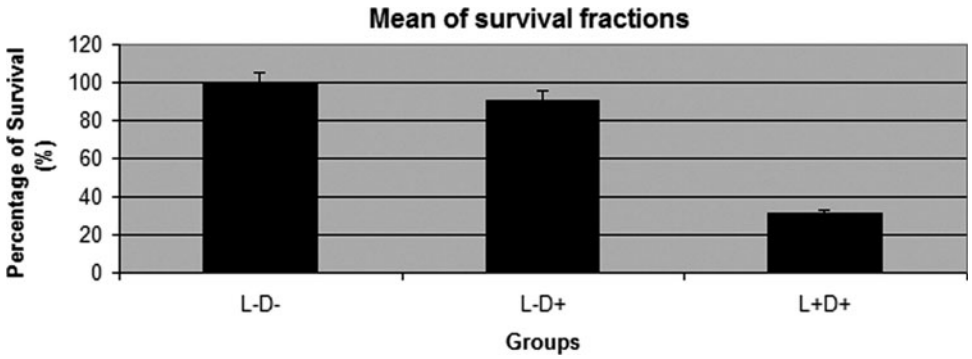

FIG. 6. Mean of microorganisms survival of studied groups – Same letter (A) means no significant difference ($p > 0.05$).

there is no dark toxicity effect. In this pilot study, the effective bacterial reduction provided by the photodynamic effect was significantly higher than that provided by other groups. These results are quite significant, encouraging us to perform more specific studies involving clinical periodontal parameters (i.e., pocket depth, bleeding on probing, and attachment level) with more patients and long-term observations.

Curcumin is shown to be a PS that is attached to the bacterial walls, drawing to itself the light at the time of irradiation with an essential antimicrobial action on oral bacteria. The concentration of curcumin was chosen based on another study that determined a safe concentration in terms of damage to the mucosa and of discoloration of the teeth.[37] The concentration of 1.5 g/L is in fact a very low concentration; even at such concentration, the results were surprisingly good. A reduction of >65% of microorganisms contained in saliva using a simple procedure is quite encouraging for a further development of the technique. The reduction is comparable to the results for rinsing with traditional oral solutions containing chlorhexidine and alcohol.[23] The great advantage to using curcumin is that it is a natural substance and harmless to the oral tissues.[14]

Neither a burning sensation, nor oral soreness, nor aphthous ulcers were reported by any subjects; however, oral itching was reported by a few volunteers. There was no significant difference for occurrence of adverse events between the two experimental groups (L-D+ and L+D+).

Overall, decontamination using this simple procedure is a desirable technique for general use in everyday dentistry practice. It should allow great improvement in avoiding complications during oral surgical procedures.

An important aspect of our demonstration is the very low price of curcumin (US $5/micrograms), making possible the production of a PS at affordable prices. That is an important requirement for making a PDT-type procedure a reality.

Table 2. Mean of Bacterial Numbers (CFU) at Baseline and After Performing Photodynamic Therapy (L+D+) or a Mouth Rinse with Curcumin (L-D+)

	Mean baseline	*Mean after*	p *Value*[a]
L+D+	260.79[a]	75.85[b]	0.004
L-D+	400.92[a]	368.46[a]	0.052

[a]*t* tests between groups (2-sided).
In rows, means with the same letter are not significantly different ($p > 0.05$).

Conclusions

In conclusion, in this study, the results indicate that PDT is a promising alternative for reducing the risk of postoperative infection by temporary reduction of intra-oral bacterial counts.

Acknowledgment

The authors thank all the volunteers who participated in this study. Financial support from Research Support Foundation of São Paulo State (FAPESP), Studies and Projects Financier (FINEP), Science and Technology Support Foundation of Pernambuco State (FACEPE), and Medical and Dental Equipment Gnatus was appreciated.

Author Disclosure Statement

No competing financial interests exist.

References

1. Polgárová, K., Behuliak, M., and Celec, P. (2010). Effect of saliva processing on bacterial DNA extraction. New Microbiol. 33, 373–379.
2. Summers, A.N., Larson, M.D., Edmiston, C.E., Gosain, A.K., Denny, A.D., and Radke, L. (2000). Efficacy of preoperative decontamination of the oral cavity. Plast. Reconstr. Surg. 106, 895–900.
3. Dar-Odeh, N.S., Abu-Hammad, O.A., Al-Omiri, M.K., Khraisat, A.S., and Shehabi, A.A. (2010). Antibiotic prescribing practices by dentists: a review. Ther. Clin. Risk Manag. 21, 301–306.
4. Pitten, F.A., and Kramer, A. (1999). Antimicrobial efficacy of antiseptic mouthrinse solutions. Eur. J. Clin. Pharmacol. 55, 95–100.
5. Gilbert, P., and Moore, L.E. (2005). Cationic antiseptics: diversity of action under a common epithet. J. Appl. Microbiol. 99, 703–715.
6. Maillard, J.Y. (2002). Bacterial target sites for biocide action. J. Appl. Microbiol. 92, Suppl., 16S–27S.
7. Arweiler, N.B., Auschill, T.M., Reich, E., and Netuschil, L. (2002). Substantivity of toothpaste slurries and their effects on reestablishment of the dental biofilm. J. Clin. Periodontol. 29, 615–621.
8. Huang, Z. (2005). A review of progress in clinical photodynamic therapy. Technol. Cancer Res. Treat. 4, 283–293.

9. Al-Watban, F.A., and Zhang, X.Y. (2005). Photodynamic therapy of human undifferentiated thyroid carcinoma-bearing nude mice using topical 5-aminolevulinic acid. Photomed. Laser Surg. 23, 206–211.
10. Komerik, N., and Wilson, M. (2002). Factors influencing the susceptibility of Gram-negative bacteria to toluidine blue O-mediated lethal photosensitization. J. Appl. Microbiol. 92, 618–623.
11. O'neill, J.F., Hope, C.K., and Wilson, M. (2002). Oral bacteria in multi-species biofilms can be killed by red light in the presence of toluidine blue. Lasers Surg. Med. 31, 86–90.
12. Meisel, P., and Kocher, T. (2005). Photodynamic therapy for periodontal diseases: state of the art. J. Photochem. Photobiol. B. 79, 159–170.
13. Aggarwal, B.B., Sundaram, C., Malani, N., and Ichikawa, H. (2007). Curcumin: the Indian solid gold. Adv. Exp. Med. Biol. 595, 1–75.
14. Haukvik, T., Bruzell, E., Kristensen, S., and Tønnesen, H.H. (2010). Photokilling of bacteria by curcumin in selected polyethylene glycol 400 (PEG 400) preparations. Studies on curcumin and curcuminoids, XLI. Pharmazie 65, 600–606.
15. Fontana, C.R., Abernethy, A.D., Som, S., et al. (2009). The antibacterial effect of photodynamic therapy in dental plaque-derived biofilms. J. Periodontal Res. 44, 751–759.
16. Metcalf, D., Robinson, C., Devine, D., and Wood, S. (2006). Enhancement of erythrosine-mediated photodynamic therapy of Streptococcus mutans biofilms by light fractionation. J. Antimicrob. Chemother. 58, 190–192.
17. Wood, S., Metcalf, D., Devine, D., and Robinson, C. (2006). Erythrosine is a potential photosensitizer for the photodynamic therapy of oral plaque biofilms. J. Antimicrob. Chemother. 57, 680–684.
18. Zanin, I. C., Lobo, M.M., Rodrigues, L.K., Pimenta, L.A., Höfling, J.F., and Gonçalves, R.B. (2006). Photosensitization of in vitro biofilms by toluidine blue O combined with a light-emitting diode. Eur. J. Oral Sci. 114, 64–69.
19. Komerik, N., and MacRobert, A.J. (2006). Photodynamic therapy as an alternative antimicrobial modality for oral infections. J. Environ. Pathol. Toxicol. Oncol. 25, 487–504.
20. Zanin, I. C., Gonçalves, R.B., Junior, A.B., Hope, C.K., and Pratten, J. (2005). Susceptibility of Streptococcus mutans biofilms to photodynamic therapy: an in vitro study. J. Antimicrob. Chemother. 56, 324–330.
21. Netuschil, L., Weiger, R., Preisler, R., and Brecx, M. (1995). Plaque bacteria counts and vitality during chlorhexidine, meridol and listerine mouthrinses. Eur. J. Oral Sci. 103, 355–361.
22. Tomás, I., Cousido, M.C., Tomás, M., Limeres, J., García–Caballero, L., and Diz, P. (2008). In vivo bactericidal effect of 0.2% chlorhexidine but not 0.12% on salivary obligate anaerobes. Arch. Oral Biol. 53, 1186–1191.
23. Herrera, D., Roldan, S., Santacruz, I., Santos, S., Masdevall, M., and Sanz, M. (2003). Differences in antimicrobial activity of four commercial 0.12% chlorhexidine mouthrinse formulations: an in vitro contact test and salivary bacterial counts study. J. Clin. Periodontol. 30, 307–314.
24. Heit, J.M., Farhood, V.W., and Edwards, R.C. (1991). Survey on antibiotic prophylaxis for intraoral orthognathic surgery. J. Oral Maxillofac. Surg. 49, 340–342.
25. McDonnell, G., and Russell, A.D. (1999). Antiseptics and disinfectants: activity, action, and resistance. Clin. Microbiol. Rev. 12, 147–179.
26. Owens, J., Addy, M., Faulkner, J., Lockwood, C., and Adair, R. (1997). A short-term clinical study design to investigate the chemical plaque inhibitory properties of mouthrinses when used as adjuncts to toothpastes applied to chlorhexidine. J. Clin. Periodontol. 24, 732–737.
27. Tamietti, B.F., Machado, A.H., Maftoum–Costa, M., Da Silva, N.S., Tedesco, A.C., and Pacheco–Soares, C. (2007). Analysis of mitochondrial activity related to cell death after PDT with AlPCS(4) . Photomed. Laser Surg. 25, 175–179.
28. Burns, T., Wilson, M., and Pearson, G.J. (1995). Effect of dentine and collagen on the lethal photosensitization of *Streptococcus mutans*. Caries Res. 29, 192–197.
29. Wilson, M., and Dobson, J. (1993). Lethal photosensitization of oral anaerobic bacteria. Clin. Infect. Dis. 16, S414–S415.
30. Wilson, M., Tracy, B., and Pratten, J. (1996). Killing of *Streptococcus sanguis* in biofilms using a light-activated antimicrobial agent. J. Antimicrob. Chemother. 37, 377–381.
31. Williams, J.A., Pearson G.J., Colles, M.J., and Wilson, M. (2003). The effect of variable energy input from a novel light source on the photoactivated bactericidal action of toluidine blue O on Streptococcus Mutans. Caries Res. 37, 190–193.
32. Wilson, M., Dobson, J., and Harvey, W. (1992). Sensitization of oral bacteria to killing by low-power laser radiation. Curr. Microbiol. 25, 77–81.
33. Wilson, M., Burns, T., and Pratten, J. (1996). Killing of Streptococcus sanguis in biofilms using a lightactivated antimicrobial agent. J. Antimicrob. Chemother. 37, 377–381.
34. Wilson, M., Burns, T., Pratten, J., and Pearson, G.J. (1995). Bacteria in supragingival plaque samples can be killed by low-power laser light in the presence of a photosensitizer. J. Appl. Bacteriol. 78, 569–574.
35. Giusti, J.S., Santos–Pinto, L., Pizzolito, A.C., et al. (2008). Antimicrobial photodynamic action on dentin using a light-emitting diode light source. Photomed. Laser Surg. 26, 281–287.
36. Usacheva, M.N., Teichert, M.C., and Biel, M.A. (2001). Comparison of the methylene blue and toluidine blue photobactericidal efficacy against gram-positive and gram-negative microorganisms. Lasers Surg. Med. 29, 165–173.
37. Sharma, R.A., Gescher, A.J., and Steward, W.P. (2005). Curcumin: the story so far. Eur. J. Cancer 41, 1955–1968.

Address correspondence to:
Natália Costa Araújo
57 Dom Sebastião Leme Street
Recife, PE
Brazil 52011-160

E-mail: nataliacosta84@yahoo.com.br

Photodiagnosis and Photodynamic Therapy (2012) 9, 60—68

Available online at www.sciencedirect.com

SciVerse ScienceDirect

journal homepage: www.elsevier.com/locate/pdpdt

Photodiagnosis and treatment of condyloma acuminatum using 5-aminolevulinic acid and homemade devices

Natalia Mayumi Inada PhD[a,*], Mardoqueu Martins da Costa[b], Orlando C.C. Guimarães[a], Elizeu da Silva Ribeiro[a], Cristina Kurachi[a], Silvana Maria Quintana[c], Wellington Lombardi[d], Vanderlei Salvador Bagnato[a]

[a] *Instituto de Física de São Carlos (IFSC/USP), Laboratório de Biofotônica, São Carlos, São Paulo, Brazil*
[b] *Escola de Engenharia de São Carlos (EESC/USP), São Carlos, São Paulo, Brazil*
[c] *Faculdade de Medicina de Ribeirão Preto (FMRP/USP), Ribeirão Preto, São Paulo, Brazil*
[d] *Faculdade de Medicina de Araraquara (UNIARA), Araraquara, São Paulo, Brazil*

Available online 20 October 2011

KEYWORDS
Human papillomavirus;
Condyloma;
Homemade device;
Photodiagnosis;
Photodynamic therapy

Summary *Background*: The objective of this study was to improve the feasibility of applying topic 5-aminolevulinic acid (ALA) in photodiagnosis (PD) and treatment of condyloma caused by human papillomavirus (HPV) using two homemade handheld devices and to discuss the photodynamic therapy (PDT) as a suitable alternative for each of the cases studied. Both, protoporphyrin IX production and photodegradation were analyzed, and the pain experienced during the illumination was correlated with the light intensities. *Methods*: A total of 40 women with different grades of lesions caused by HPV were chosen from patients of the School of Medicine of Ribeirão Preto (University of Sao Paulo) and of the Unit of Public Health of Araraquara, Sao Paulo. *Results*: We did not encounter any unexpected difficulties using our devices during the treatment. The existence of an easily observable reddish fluorescence with large intensity concentrated on the lesions is the clinical indication of the penetration and the selective concentration of protoporphyrin IX in the clinical and subclinical lesions rather than in the healthy tissue. The aesthetic results were much better than those obtained by conventional techniques as surgery or cryogenics, with no recurrence reported after two years of treatment. *Conclusions*: Our results are proof for the various advantages using ALA cream for the PD and PDT in many different cases of condyloma by HPV. This study will be continued to investigate the PpIX photobleaching and the irradiance and fluence rate to optimize conducting the clinical trials, to improve the devices and therefore increase the treatment response.

* Corresponding author at: Instituto de Física de São Carlos, Universidade de São Paulo, Grupo de Óptica, Laboratório de Biofotônica, Av. Trabalhador São-carlense, nº 400, Centro, 13566-590 São Carlos, SP, Brazil. Tel.: +55 16 3373 9810; fax: +55 16 3373 9811.
E-mail address: nataliainada@ursa.ifsc.usp.br (N.M. Inada).

1572-1000/$ — see front matter © 2011 Elsevier B.V. All rights reserved.
doi:10.1016/j.pdpdt.2011.09.001

Introduction

Condyloma acuminatum is an epidermal manifestation related to the epidermotropic human papillomaviruses (HPVs). A histological exam of the condyloma acuminata generally shows disruption of the epidermis with hyperkeratosis, coarse keratohyaline granules and the presence of koilocytes. The latter is the main characteristic cytological feature of HPV-infected cells with halo and clear cytoplasm. Although several medical treatments and also prevalence studies of type-specific HPV for immunization [1] and medications are known today, no single treatment can so far be considered effective to eliminate warty lesions and prevent them from recurring [2]. From another point of view, HPV vaccination is most beneficial in poorer countries lacking organized screening programs, where cervical cancer still remains a major cause of cancer-related female death [3]. The situation we face today in Brazil forces us to find new solutions: the development of new strategies to trace the infection, to fight its consequences and to help women with HPV.

Vulvar condyloma treatment using PDT was reported for the first time in 1996 [4], when it showed a clearance rate of 66% with a considerable better cosmetic result compared to other techniques. Still, many important points remain to be discussed with the aim to improve this technique. Another study reporting the Vulvar Intraepithelial Neoplasia (VIN) treatment using PDT was described by Martin-Hirsch et al. [5]. Low light doses of 50 J/cm^2 resulted in only 20% cure rate, while higher light doses of 100 J/cm^2 resulted in pain but also doubled the cure rate. The treatment of vulvar lichen sclerosus by PDT with ALA was also described [6].

It has now been proven that HPVs are an aetiological agent of many benign and malignant tumours arising from epidermal tissues. These are directly associated as the second most common cause of female cancer worldwide, cancer of the cervix, and is also strongly associated with several other ano-genital cancers such as: anal, penile, vulvar and vaginal carcinomas [7,8].

The risk of cervical cancer varies according to the HPV types: 16, 18, 31, 33, 35, 39, 45, 51, 52, 56, 58, 59, 68, 73 and 82 are considered to be high-risk HPV (HR-HPV) to cause cervical cancer while 6, 11, 42, 43 and 44 are low-risk HPV (LR-HPV) to cause cervical cancer [9,10]. The low-risk types primarily cause benign genital condylomas and low-grade squamous intraepithelial lesions. It is also known now that HPV-16 and persistent infections with other high oncogenic-risk HPV genotypes are more likely to progress toward cervical neoplasia [10,11]. Furthermore, women who smoke have an impaired immune response to HPV infections, increasing the likelihood of multiple HPV infections [12].

Among the techniques presently used to treat condyloma caused by HPV, the result of multiple surgical procedures can be vulval disfigurement and loss of sexual function [13]. The laser therapy has the advantage to preserve the vulval architecture but high recurrence rates have been observed [14].

Porphyrin-mediated photodynamic therapy (PDT) is a promising alternative method, which has already been used in the dermatological and recently also in the gynaecological field [15]. After application of a photosensitizer, dysplastic cells may be destroyed when light of a certain wavelength mediates local cytotoxic effects caused by reactive oxygen species, especially by singlet oxygen [16]. Whether to use PDT depends on many factors like cost, instrumentation, patient and the location of the lesions.

The 5-aminolevulinic acid (5-ALA) is a precursor for a protoporphyrin IX (PpIX), and it is the photosensitizer chosen in the presented work. It has already been widely used for the treatment of skin cancer. Due to its rapid kinetics and topical applicability, 5-ALA is a photosensitizer promising good results when used in diagnosis performed by fluorescence and photodynamic treatment [17]. 5-ALA is a precursor of heme formed by 5-ALA synthase from glycine and succinyl-CoA, the rate-limiting step of the heme biosynthesis [18]. Once this step is bypassed by exogenous administration of 5-ALA, porphyrins and heme accumulate mainly in the malignant or abnormal tissue, where the metabolic activity is different.

Our aim is to use two novel devices developed in our group and to compare the feasibility of PD and PDT with 20% 5-aminolevulinic acid (ALA)-cream applied topically on the following areas: the vulvar, vaginal, anal and perianal condyloma, comparing the results with existing conventional treatment and discussing improvements of the technique used.

We start by presenting the material and methods, then describe the conduction of the clinical trial and briefly describe also the developed devices. Finally, the results of the trial are presented and discussed on the basis of the follow up post-application.

Materials and methods

Chemicals

As a photosensitizer in our work we have chosen to use 5-aminolevulinic acid hydrochloride (pure) purchased from FSUE SSC ''NIOPIK'' (Moscow, Russia). Details of how cream was prepared before application are given below. (Ethylenedinitrilo)tetraacetic acid (EDTA) and dimethylsulphoxide (DMSO) were obtained from Sigma (St. Louis, MO, USA).

Protocol of the study

Selection of the patients and conduction of clinical trial
The women were selected from patients of existing ongoing studies at the School of Medicine of Ribeirão Preto (University of Sao Paulo) and at the Unit of Public Health of Araraquara, Sao Paulo. Approval of the University Ethical Committee was obtained as required by the Brazilian Registration for clinical experiments (Process HCRP 2079/2008, 04/30/2008 and CIEPesquisa/UNIARA 33/2008, 09/12/2008). All women received and signed the written information and consent following an approval of the Medical Ethics Committee of both institutions. The diagnosis of condyloma acuminatum was confirmed by either histo-pathological examination or HPV detection due to a polymerase chain reaction.

The study was realized from 2008 to 2010. Patients with a biopsy confirmed by HPV presence, were selected by the clinicians leading the research in a consecutive, non-random

manner. Written informed consent was obtained following approval of the Human Medical Ethics Committee of both institutions. Prior to the trial, serological ELISA HBsAg, ELISA Anti HCV, VDRL and ELISA Anti HIV were performed.

Preparation of the women for the PDT

Before the condyloma illumination, the full area covered by lesions was locally anesthetized with 2% xylocaine (infiltration anesthesia). If necessary, based on the women's reaction and pain report [19], the women received additionally an anti-inflammatory intravenous drug during the illumination.

The photosensitizer and the local topical application of ALA

5-Aminolevulinic acid ALA is a metabolic prodrug of the photosensitizer and its cream (20%; wt/wt) was prepared by dissolving ALA (FSUE SSC ''NIOPIK'' — Moscow, Russia) in a sterile NaCl solution (0.9%) immediately before the treatment and incorporating this mix in a emollient cream (oil-in-water emulsion containing 1 mM EDTA and 3% DMSO) before the application. The women were asked not to go to the toilet while waiting for the cream to take its effect. The photodynamic therapy was started 6 h after application of the 20% 5-aminolevulinic acid ALA cream. This protocol was standardized and used with all patients in this study.

Light device and illumination

We developed a device named ''PDT Flex Use'', optically based on 640 nm LED (Light Emitting Diodes) arrays. The illumination probes were anatomically designed for the specific applications: a cylinder measuring 30 mm in diameter and 115 mm in length for the intravaginal illumination, applying an average light intensity of 45 mW/cm^2. This device produces a uniform illumination on the surface, and it allows at the same time an interior illumination without creating shadows. A smaller circular probe for external illumination measuring 36 mm in diameter and an average light intensity of 150 mW/cm^2 is used to illuminate the small lesions localized at the perineum. Finally, a probe for external illumination measuring 74 mm in diameter and an average optical source of 60 mW/cm^2 was developed. This third probe is used for overall illumination.

An external water circulation device ensures that the temperature increase during illumination is kept at less than 2 °C. This device is placed in a small suitcase together with an electronic control (to allow control of both exposition time and light intensity, kept constant in this study).

Photodynamic therapy

The patient was asked to lie down on the operating table with their legs in stirrups. The clothing was removed and the previously applied ALA-cream was washed off using saline solution. Six hours after the ALA application the area to be treated was illuminated by the ''PDT Flex Use'' system at 640 nm and a total dose of 200 J/cm^2.

Fluorescence measurement

The fluorescence of the lesions was evaluated prior to and after the PDT using other homemade device (unpublished data) to achieve wide-field fluorescence images. That specific handheld unit has a compact light source, composed of two high-intensity Light-Emitting Diodes (LEDs), the emission being centered at 405 and 450 nm, a LED Concentrator Lens and five optical filters. The system was positioned in front of the lesions at a distance of approximately 5 cm to induce fluorescence. The use of fluorescence allows to measure the appropriate production of PpIX before the treatment as well verify that the photosensitizer has been fully used after the treatment. The PpIX production induced by the ALA can be proven by the red fluorescence observed in the image.

Clinical response analysis

Biopsies were collected for histological exams performed to diagnose condyloma by HPV before and after the treatment. Pictures of the full extension of the warts were taken using a digital camera Sony H50® coupled to a macro lens of 74 mm, and the images obtained before and after the PDT were compared.

Protoporphyrin IX photobleaching

Images were taken using a camera Sony H50® coupled to our homemade fluorescence imaging device. A sequence of fluorescence images (representing 30 sessions of PDT) taken during the treatment was stored and the PpIX fluorescence variation was plotted using an algorithm method (Matlab® 7.5 — The MathWorks, USA). For this experiment only the smaller probe was used for external illumination, with a 36 mm diameter and a light intensity of 150 mW/cm^2.

Results

The results of this study are presented in three parts: the ''PDT Flex Use'' device evaluation, the PpIX photobleaching results and the clinical outcome.

As for the ''PDT Flex Use'' device, it was developed in the Physics Institute of Sao Carlos, University of Sao Paulo, Brazil, and is optically based on 640 nm LED (Light Emitting Diodes) arrays (Fig. 1).

As for the condyloma treatment outcome using the ''PDT Flex Use'', a total of 40 women with different grades of warts caused by HPV participated in this study (Table 1). As expected, the women presented different responses according to varying characteristics: types of condyloma, age, immunological and nutritional conditions. Women ages ranged from 16 to 65 years. 29% of the women had small lesions and 71% had multiple long lesions. In our work in about 90% of the cases a complete clearance of the warts after less than three sessions was observed. Only in two cases we observed no response: one of them is the case of an immunosuppressed patient by HIV. The other patient, who did not show any results to the treatment presented condyloma with pigmented and hyperkeratinic lesions, which

Table 1 Patients main facts and outcome information.

Case	Vulva	Vagina	Anus	Perineum	Age	# of PDT sessions	Multicentric	Centric	Outcome
1	x	x			16	3	x		Clearance
2	x				56	1		x	Clearance
3		x	x	x	31	8	x		Remission
4			x	x	43	10	x		Clearance
5	x				44	4		x	Clearance
6	x				40	3		x	Clearance
7				x	41	6		x	Clearance
8	x				65	5		x	Remission
9			x		46	4	x		Clearance
10		x			55	4	x		Remission
11	x				18	7	x		Clearance
12			x		20	4	x		Clearance
13	x				30	5	x		Remission
14				x	18	3		x	Clearance
15	x				25	5		x	Clearance
16	x				65	10	x		Remission
17		x			30	5	x		Clearance
18				x	25	3		x	Clearance
19				x	18	2		x	Clearance
20	x			x	20	6	x		Clearance
21	x			x	25	3	x		Clearance
22			x		30	4		x	Clearance
23	x				32	2		x	Clearance
24	x				38	3	x		Remission
25	x				45	3		x	Clearance
26	x				65	3	x		Clearance
27	x				40	3		X	Clearance
28				x	41	2		x	Clearance
29	x				18	2		x	Clearance
30				x	22	2		x	Clearance
31				x	25	2		x	Clearance
32				x	30	1		x	Clearance
33	x				25	3	x		Clearance
34		x			27	2	x		Clearance
35				x	20	3	x		Clearance
36	x				45	2	x		Clearance
37				x	28	1		x	Clearance
38	x				35	5	x		Clearance
39			x		30	1		x	Clearance
40		x			32	1		x	Clearance

prove to be difficult to treat because of limitations of light penetration.

Nevertheless, all cases show very good elimination of lesions already after the first session. The efficiency of lesion-elimination in each application seems to be related to the lesion extension, thickness as well as other conditions like smoking and nutritional habits. The total numbers of sessions required for a complete removal of the lesions, depended mostly, on the extension, distribution and size of the lesions.

The three types of devices used clearly showed that the water cooling system was essential to avoid overheating. Only by avoiding overheating can the full photochemical action take place. The water cooling also collaborates/supports the thermal stability of the emitters, avoiding a possible change of the light intensity, which would decrease the required absorption from PpIX for the PDT action.

After 6 h of application of the ALA cream on the condylomas, the excess cream was removed and the fluorescence of the region was observed using our other homemade device. The easily observable reddish fluorescence mostly concentrated on the lesions is the clinical indication of the penetration and the selective concentration of protoporphyrin IX on the clinical and subclinical lesions rather than on the healthy tissue (Fig. 2A and B). We ensure that all patients reach this stage prior to performing the light application. At the end of the light-application, no fluorescence spots should still be detectable at all, which would indicate a photoreaction taking place, producing an appropriate quantity

Fig. 1 The homemade device ''*PDT Flex Use*''. This portable system consists of a briefcase containing three probes with different sizes: 1 — a cylinder for intravaginal illumination; 2 — a smaller circular device for external illumination of minor warts; 3 — a larger circular probe for illumination of lesions with an average diameter of 5 cm.

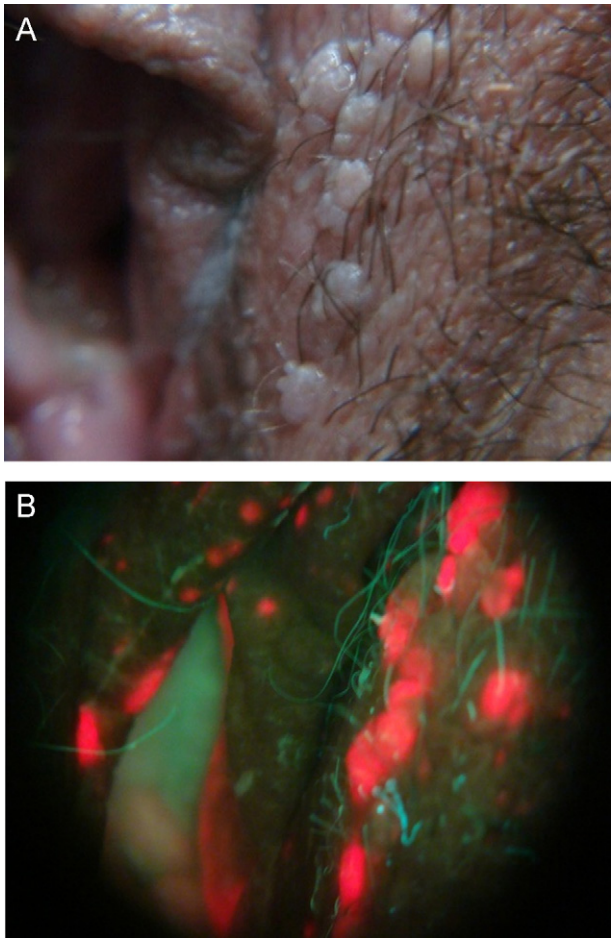

Fig. 2 Analysis of PpIX imaging fluorescence system. Condyloma by HPV was treated during 6 h with 20% ALA cream. Before and after this, the PpIX fluorescence was monitored using a homemade imaging fluorescence system. Panel A: original image before ALA application; panel B: 6 h after ALA application.

of free radicals, which actually also cause the degradation of the PpIX molecules. The disappearance of fluorescence spots is, however, a good indicator for the adequate coupling between light (at an appropriate dose) and the lesions.

To better illustrate the results of this study, Fig. 3 presents a sequence of pictures for one of the women presenting a large quantity of lesions inside the vagina as well as on the vulva. This is representative for cases with multiple lesions with sizes varying from on average of 4 mm to 5 mm diameter and from 2 mm to 4 mm thickness. Internal and external application of ALA-based cream is shown in Fig. 3B. Usually, an excess of cream is used to cover all lesions avoiding the possibility of missing any spot. The illumination is maintained at a defined time, assuming a final total dose of 200 J/cm^2 per area (Fig. 3C). In this specific case, the final result was obtained after 3 sessions of PDT (Fig. 3D). A complete elimination of all lesions is observed in both vagina and vulva, with even a complete absence of reminiscent scars from previous lesions. No recurrence was related two years after performing the PDT treatment.

It is in fact an important characteristic of PDT that it helps to obtain very good cosmetics aspects, much better than the alternative treatments previously reported [13,14].

Most cases have been quite similar to the one presented in Fig. 3. An interesting case is presented in Fig. 4. The perineum and anal region of the patient is fully covered with very old lesions by HPV, a situation completely reversed after 22 sessions of PDT, in a total of 22 weeks. In this case, the treatment was spread over many sessions in order to control evolution, pain and discomfort of the patient caused by an overall inflammation typically associated with PDT.

With the aim to illuminate correctly the gynaecological area, and to do a correlation study of the PpIX photodegradation and pain during illumination, we analyzed the lesions with our homemade fluorescence device just before the PDT. The images obtained showed red fluorescence, indicating the presence of the photosensitizer. These fluorescence images were calculated and monitored during the condylomas illumination. Two minutes after PDT at 150 mW/cm^2 and using the smaller circular device, this fluorescence had disappeared (approximately 80%) indicating a rapid photobleaching of the PpIX accompanied by a decrease in pain, and the color of the lesions turned white immediately after the PDT (Fig. 5). Before, during, and after the light illumination, the women were asked to define the pain or discomfort experienced using a scale ranging from 0 (no pain or discomfort) to 10 (unbearable pain necessitating immediate action). Pain was assessed every 1—2 min. If requested by the patient, the vulvar skin was rinsed with cool water.

Skin reaction was assessed and documented in photographs. During irradiation, women described pain as having a ''burning'' or ''stinging'' quality, which peaked at 3—4 min after begin of the treatment. The pain score average of the first 2 min was 8.0 ± 2.0. This score then decreased slowly to 4.0 ± 1.0 after a total dose of 200 J/cm^2. The epithelium recovered starting day 6—7. After processing and plotting all fluorescence images we observed that at lower intensities of 100 and 50 mW/cm^2, the PpIX photobleaching occurred slowly and the reported pain was lower than when using a higher intensity (Fig. 6).

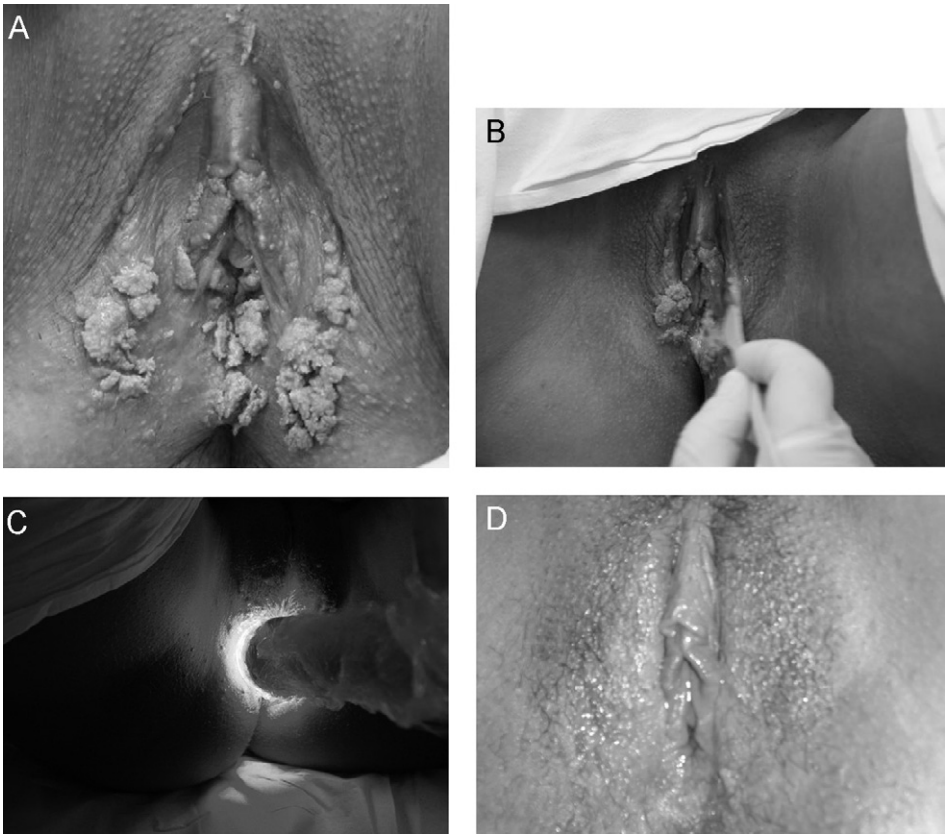

Fig. 3 First case of a condyloma-woman treated with PDT. Vulvar/vaginal condyloma was compared before, during and after PDT treatment with ALA and using the Brazilian homemade device ''PDT Flex Use''. Panel A: before the treatment; panel B: during ALA application; panel C: during condyloma illumination; panel D: after the treatment (three PDT sessions).

Discussion

The homemade device ''PDT Flex Use'' was successfully developed and we did not encounter any unexpected difficulties or system problems. Aminolevulinic acid application was chosen based on the following assessment: access to the area to be treated, photosensitizer production only in the clinical and subclinical condyloma, feasibility of the technique and the patient's acceptance to the treatment. We have seen the advantages of minimal tissue destruction, low side effects and excellent cosmetic results.

Inhibition of the ferrochelatase activity by chelators of iron has been found to enhance the accumulation of PpIX [20,21]. In this work we used the combination of DMSO and

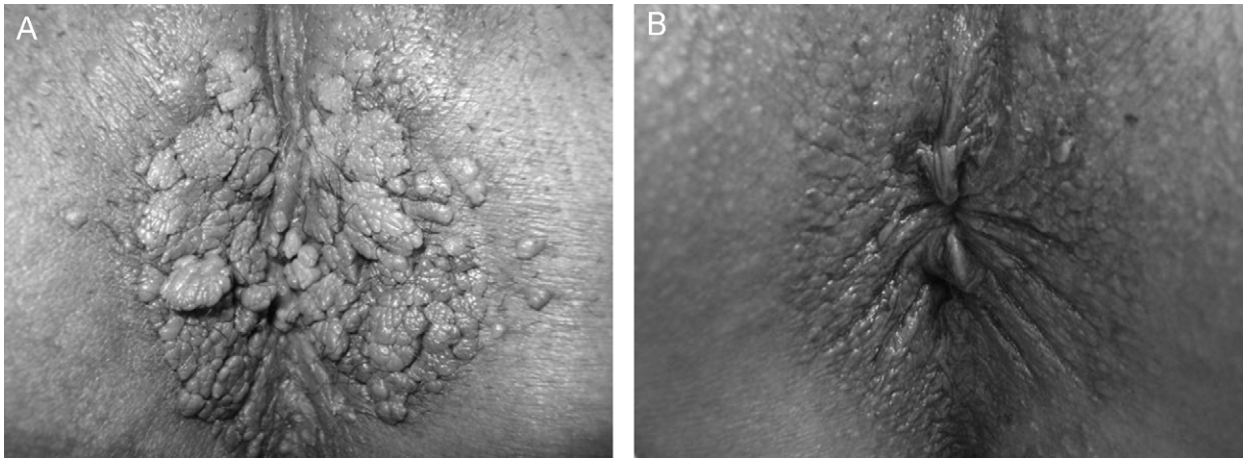

Fig. 4 A special case studied: the perineum and anal regions are fully covered by HPV-lesions. Panel A: before the treatment; panel B: after the treatment (twenty two PDT sessions).

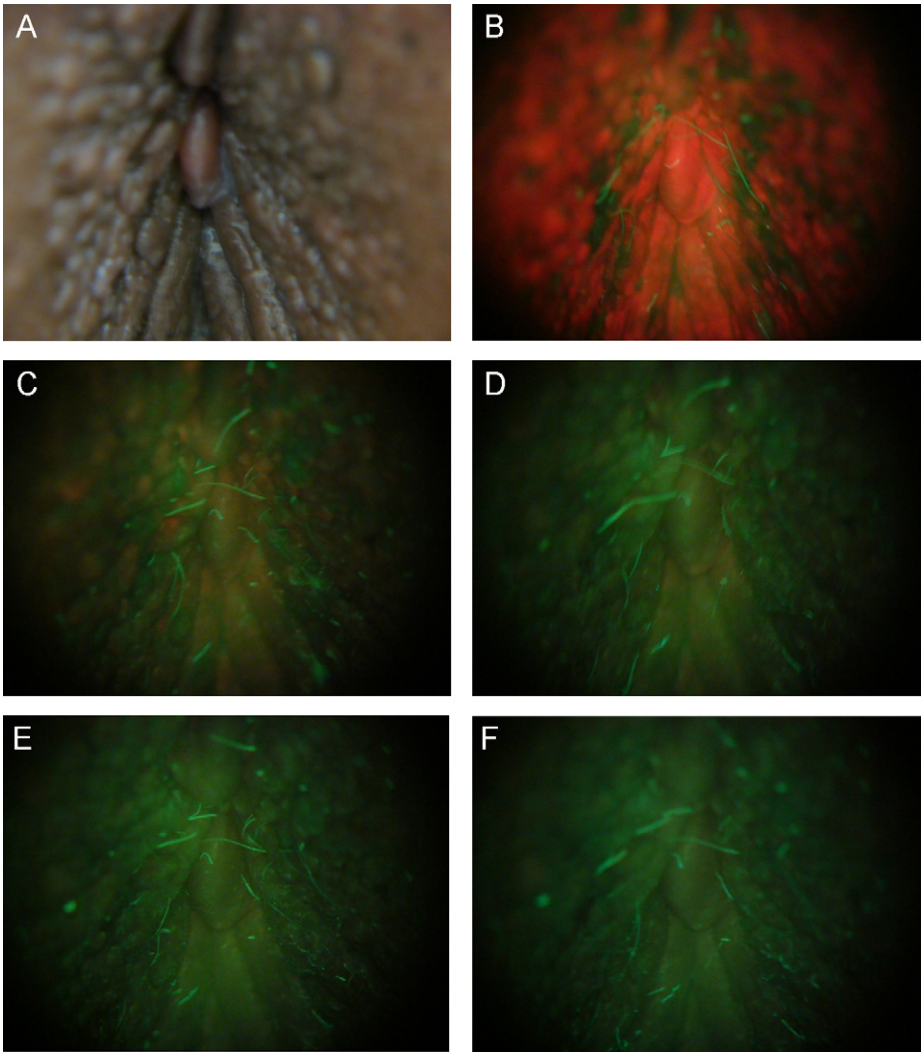

Fig. 5 PpIX photobleaching as a function of the illumination time. Panel A: white light image of the condylomas after ALA application; panel B: PpIX fluorescence image just before the PDT; panels C, D, E and F: PpIX fluorescence image after 2, 4, 6 and 8 min of PDT, respectively.

EDTA in the ALA cream formulation to enhance the ALA penetration (by the DMSO) and the PpIX production once EDTA inhibits the Fe-chelatase activity.

However, the main adverse effect with ALA treatment was pain, which was described by most women. This sensation can be a temporary discomfort or severe pain. The pain score used in this study was based on our experience asking patients to express pain according to a verbal scoring system and also according to the methods of others studies, where women marked the degree of pain on a scale of 0—10 [19].

The mechanism of ALA-PDT pain has been discussed for many years. The authors hypothesize that the basis for this could be that ALA and the non methyl ester-ALA (ALA-ME) is transported to the gamma-aminobutyric acid (GABA) receptors that are present in the peripheral nerve endings and may contribute to higher pain levels. Therefore, treatments which block GABA receptors may be beneficial [22—24]: still, as, the pain did not correlate with the level of PpIX produced, this suggests that the pain is not only caused by an activation of PpIX [22]. Other authors have also suggested that pain seems to be related to a PpIX fluorescence during illumination that was reduced using a lower fluence rate [25]. This discomfort could be prevented in many ways: using a lower optical intensity during PDT, using cold water and making breaks during the illumination [26].

Some of the women involved in this study had been subject to conventional treatment before. The conventional treatment often consists of repeated local excisions or laser ablation, techniques which can be painful and mutilating. Thus, it is clear that new forms of treatment are required for the elimination of condyloma and even more to avoid a recurrence of the lesions.

As the location of this treatment (lower female genital tract) can be reached by the topical drug used and by the light irradiation, PDT seems to be an attractive technique for the local treatment of this intraepithelial disease. All women showed a high acceptance of the treatment once first significant results appeared, usually after about a week's time. Furthermore, application was considered quite satisfying for the patients' comfort.

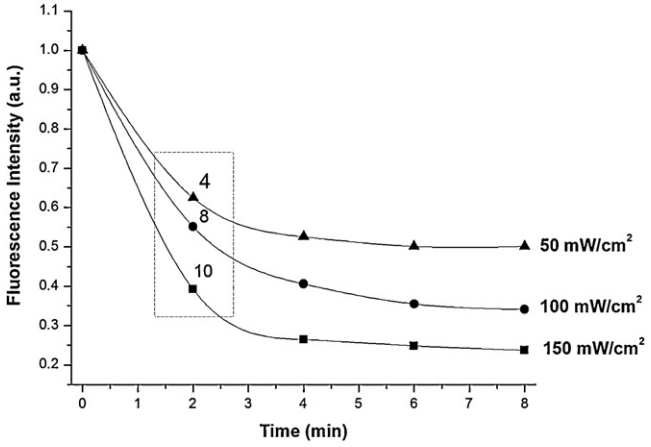

Fig. 6 Correlation between the PpIX photobleaching and pain score average: after processing and plotting all fluorescence images, we observed that the pain score average of the first 2 min and at a high fluence rate of 150 mW/cm^2 was 8.0 ± 2.0. This score then decreased slowly to 4.0 ± 1.0, after a total dose of 200 J/cm^2. At lower intensities of 100 and 50 mW/cm^2, the PpIX photobleaching occurred slowly and the reported pain was significantly lower than when a higher intensity was used.

Different types of therapies have been performed and have been compared to the photodynamic therapy. Some studies of photodynamic therapy (PDT) and imiquimod cream treatments have shown a certain degree of success and efficacy at least partly due to a stimulation of the local immune responses.

Studies have shown that nearly 80% of the squamous cancers of the anus contain HPV DNA [27]. Photodynamic therapy in dermatology offers the advantages of being non-invasive and well tolerated in slow healing sires, and the successful treatment of anogenital condylomata by ALA-PDT [28] was recently reported.

One of the known limitations for a PDT treatment of the vulvar/vaginal region is the irregularity due to many skin folds. These may create shadows of the light leading to a therapeutical under-dosage. These skin folds can also create limitations for the homogeneous distribution when photosensitizers are used, which then again will result in a lower cure rate. Contrary to spectroscopy, which performs a point-by-point analysis, fluorescence imaging may contribute to the detection of occult lesions and to delineation of lesion margins.

For these reasons and in order to warrant the correct area illumination, the lesions were analyzed before, during and after PDT using another homemade device (unpublished data), and the images showed red fluorescence, indicating presence of the PpIX. The appearance of photobleaching during the PDT application indicates a photodynamic reaction taking place. Photobleaching is directly related to the fluorescence, and therefore the decrease of fluorescence indicates the correct action of the light over the treated area.

In the conventional therapies the comparably high recurrence rate of genital warts can be attributed to the unsuccessful elimination of viruses in areas of subclinical and latent infection [29]. In this work and in all the cases studied, we established correlations between histopathologic examination and the aceto-whitening tests before and after the PDT. To check if the HPV is still present after the PDT, it is necessary to perform new biopsies and a new PCR analysis.

Finally, the conclusions underline the many advantages for the PD and PDT in the case of condyloma by HPV. The mortality rate of women for cervical cancer increases every year. It is therefore necessary to provide new alternatives for diagnosis and treatment, also with the goal of prevention.

This study is ongoing, e.g. to investigate the photobleaching of PpIX and the irradiance and fluence rate in order to optimize the treatment response.

Disclosure statement

NMI, MMC, OCCG, ESR, CK, SM, WL, and VSB report no conflicts of interest.

Contribution to authorship

NMI designed the study, obtained the ethics approval, performed all of the procedures, supervised the data collection, performed the data analyzed and wrote the paper. MMC worked together with NMI to obtain the results of the figures five and six. OCCG and ESR developed the device named ''PDT Flex Use''. SMQ and WL are the MDs (Obstetrics and Gynaecology) of all women treated. CK and VSB supervised the data collection and edited the paper.

Details of ethics approval

This study was approved by the Local Institutional Human Research Ethics Committee.

Acknowledgements

The authors would like to acknowledge Ms. Ana Paula da Silva for the technical assistance and Ms. Marilde Courteille for the linguistic revision of the manuscript. This work was supported by grants from Conselho Nacional de Desenvolvimento Científico e Tecnológico (CNPq; Grant No. 551201/2007-1), and from Fundação de Amparo à Pesquisa do Estado de São Paulo (FAPESP/CEPID-CEPOF; Grant No. 1998-14270-8). NMI was supported by a CNPq fellowship (Grant No. 381343/2008-1).

References

[1] Howell-Jones R, Bailey A, Beddows S, et al. Multi-site study of HPV type-specific prevalence in women with cervical cancer, intraepithelial neoplasia and normal cytology, in England. Br J Cancer 2010;103(2):209—16, doi:10.1038/sj.bjc.6605747.
[2] Kodner CM, Nasraty S. Management of genital warts. Am Fam Physician 2004;70(12):2335—42.
[3] Crosbie EJ, Brabin L. Cervical cancer: problem solved? Vaccinating girls against human papillomavirus. BJOG 2010;117(2):137—42.
[4] Fehr MK, Chapman CF, Krasieva T, et al. Selective photosensitizer distribution in vulvar condyloma acuminatum after

application of 5-aminolevulinic acid. Am J Obstst Gynecol 1996;174(3):951—7, doi:10.1016/S0002-9378(96)70332-0.
[5] Martin-Hirsch PL, Whitehurst C, Buckley CH, Moore JV, Kitchener HC. Photodynamic treatment for lower genital tract intraepithelial neoplasia. The Lancet 1998;351(9113):1403, doi:10.1016/S0140-6736(98)24019-0.
[6] Hillemanns P, Untch M, Pröve F, Baumgartner R, Hillemanns M, Korell M. Photodynamic therapy of vulvar lichen sclerosus with 5-aminolevulinic acid. Obstet Gynecol 1999;93(1):71—4.
[7] Bosch FX, Manos MM, Muñoz N, et al. Prevalence of human papillomavirus in cervical cancer: a worldwide perspective. International biological study on cervical cancer (IBSCC) Study Group. J Natl Cancer Inst 1995;87(11):796—802.
[8] Walboomers JM, Jacobs MV, Manos MM, et al. Human papillomavirus is a necessary cause of invasive cervical cancer worldwide. J Pathol 1999;189(1):12—9, doi:10.1002/(SICI)1096-9896(199909)189:1<12::AID-PATH431>3.0.CO;2-F.
[9] Franco E, Villa L, Rohan T, Ferenczy A, Petzl-Erler M, Matlashewski G. Design and methods of the Ludwig-McGill longitudinal study of the natural history of human papillomavirus infection and cervical neoplasia in Brazil. Ludwig-McGill Study Group. Rev Panam Salud Publica 1999;6(4):223—33.
[10] Trottier H, Mahmud S, Costa MC, et al. Human papillomavirus infections with multiple types and risk of cervical neoplasia. Cancer Epidemiol Biomarkers Prev 2006;15(7):1274—80, doi:10.1158/1055-9965.EPI-06-0129.
[11] Sasagawa T, Basha W, Yamazaki H, Inoue M. High-risk and multiple human papillomavirus infections associated with cervical abnormalities in Japanese women. Cancer Epidemiol Biomarkers Prev 2001;10(1):45—52.
[12] Simen-Kapeu A, Kataja V, Yliskoski M, et al. Smoking impairs human papillomavirus (HPV) type 16 and 18 capsids antibody response following natural HPV infection. Scand J Infect Dis 2008;40(9):745—51, doi:10.1080/00365540801995360.
[13] Andersen BL, Turnquist D, LaPolla J, Turner D. Sexual functioning after treatment of in situ vulvar cancer: preliminary report. Obstet Gynecol 1998;71(1):15—9.
[14] Herod JJ, Shafi MI, Rollason TP, Jordan JA, Luesley DM. Vulvar intraepithelial neoplasia: long term follow up of treated and untreated women. Br J Obstet Gynaecol 1996;103(5):446—52.
[15] Kennedy JC, Pottier RH, Pross DC. Photodynamic therapy with endogenous protoporphyrin IX: basic principles and present clinical experience. J Photochem Photobiol B 1990;6(1—2):143—8, doi:10.1016/1011-1344(90)85083-9.
[16] Henderson B, Dougherty T. How does photodynamic therapy work? Photochem Photobiol 1992;55(1):145—57, doi:10.1111/j.1751-1097.1992.tb04222.x.
[17] Kennedy JC, Pottier RH. Endogenous protoporphyrin IX, a clinically useful photosensitizer for photodynamic therapy. J Photochem Photobiol B 1992;14(4):275—92.
[18] Peng Q, Warloe T, Berg K, et al. 5-Aminolevulinic acid-based photodynamic therapy. Clinical research and future challenges. Cancer 1997;79(12):2282—308, doi:10.1002/(SICI)1097-0142(19970615)79:12<2282::AID-CNCR2>3.0.CO;2-O.
[19] Cottrell WJ, Paquette AD, Keymel KR, Foster TH, Oseroff AR. Irradiance-dependent photobleaching and pain in delta-aminolevulinic acid-photodynamic therapy of superficial basal cell carcinomas. Clin Cancer Res 2008;14(14):4475—83, doi:10.1158/1078-0432.CCR-07-5199.
[20] Liu HF, Xu SZ, Zhang CR. Influence of CaNa2 EDTA on topical 5-aminolaevulinic acid photodynamic therapy. Chin Med J (Engl) 2004;117(6):922—6.
[21] Casas A, Fukuda H, Di Venosa G, Batlle AM. The influence of the vehicle on the synthesis of porphyrins after topical application of 5-aminolaevulinic acid. Implications in cutaneous photodynamic sensitization. Br J Dermatol 2000;143(3):564—72, doi:10.1111/j.1365-2133.2000.03711.x.
[22] Wiegell SR, Stender IM, Na R, Wulf HC. Pain associated with photodynamic therapy using 5-aminolevulinic acid or 5-aminolevulinic acid methylester on tape-stripped normal skin. Arch Dermatol 2003;139(9):1173—7.
[23] Rud E, Gederaas O, Høgset A, Berg K. 5-Aminolevulinic acid, but not 5-aminolevulinic acid esters, is transported into adenocarcinoma cells by system BETA transporters. Photochem Photobiol 2000;71(5):640—7, doi:10.1562/0031-8655(2000)0710640AABNAA2.0.CO2.
[24] Warren CB, Karai LJ, Vidimos A, Maytin EV. Pain associated with aminolevulinic acid-photodynamic therapy of skin disease. J Am Acad Dermatol 2009;61(6):1033—43, doi:10.1016/j.jaad.2009.03.048.
[25] Wiegell SR, Skiveren J, Philipsen PA, Wulf HC. Pain during photodynamic therapy is associated with protoporphyrin IX fluorescence and fluence rate. Br J Dermatol 2008;158(4):727—33, doi:10.1111/j.1365-2133.2008.08451.x.
[26] Wiegell SR, Haedersdal M, Wulf HC. Cold water and pauses in illumination reduces pain during photodynamic therapy: a randomized clinical study. Acta Derm Venereol 2009;89(2):145—9, doi:10.2340/00015555-0568.
[27] Frisch M, Fenger C, van den Brule AJ, et al. Variants of squamous cell carcinoma of the anal canal and perianal skin and their relation to human papillomaviruses. Cancer Res 1999;59(3):753—7.
[28] Nucci V, Torchia D, Cappugi P. Treatment of anogenital condylomata acuminata with topical photodynamic therapy: report of 14 cases and review. Int J Infect Dis 2010;14S: e280—2.
[29] Wang HW, Wang XL, Zhang LL, Guo MX, Huang Z. Aminolevulinic acid (ALA)-assisted photodynamic diagnosis of subclinical and latent HPV infection of external genital region. Photodiagnosis Photodyn Ther 2008;5(4):251—5.

Lasers Med Sci (2012) 27:161–168
DOI 10.1007/s10103-011-0912-3

ORIGINAL ARTICLE

Photodynamic inactivation of microorganisms present on complete dentures. A clinical investigation

Photodynamic disinfection of complete dentures

Daniela Garcia Ribeiro · Ana Cláudia Pavarina · Lívia Nordi Dovigo · Ewerton Garcia de Oliveira Mima · Ana Lucia Machado · Vanderlei Salvador Bagnato · Carlos Eduardo Vergani

Received: 5 January 2011 / Accepted: 4 March 2011 / Published online: 12 April 2011

Abstract The aim of this study was to evaluate the effectiveness of photodynamic therapy (PDT) for the disinfection of complete dentures. Biofilm samples were collected from dentures of 60 denture users who were randomly divided into four experimental groups (n=15 each): subjects whose maxillary dentures were sprayed with 50 and 100 mg/l of Photogem® suspension (groups P50S and P100S) and patients whose maxillary dentures were treated with 50 and 100 mg/l of Photogem® gel (groups P50G and P100G). Dentures with photosensitizers were left in the dark for 30 min (pre-irradiation time) and then irradiated with blue LED light at 37.5 J/cm^2 (26 min). Denture samples were taken with sterile cotton swab before (left side surfaces) and after (right side surfaces) PDT. All microbial material was diluted and plated on selective media for *Candida* spp., *Staphylococcus mutans* spp., streptococci and a non-selective media. After incubation (48 h/37°C), the number of colony-forming units (cfu/ml) was counted. Microorganisms grown on selective media were identified using biochemical methods before and after PDT. The data were submitted to McNemar and Kruskal–Wallis tests (α=0.05). No growth after PDT was observed in 60, 53, 47, and 40% of dentures from P100G, P50G, P100S, and P50S groups, respectively. When evidence of microorganisms' growth was observed, PDT regimens eliminated over 90% of microorganisms on dentures. This clinical study showed that PDT was effective for disinfecting dentures.

Keywords Complete denture · Disinfection · Infection control · Photochemotherapy · Sterilization

D. G. Ribeiro
Department of Dentistry, Ponta Grossa State University,
Ponta Grossa, Paraná, Brazil

A. C. Pavarina (✉) · L. N. Dovigo · A. L. Machado · C. E. Vergani
Department of Dental Materials and Prosthodontics,
Araraquara Dental School, UNESP – Univ Estadual Paulista,
Humaitá Street, 1680, 14.801-903,
Araraquara, SP, Brazil
e-mail: pavarina@foar.unesp.br

E. G. de Oliveira Mima
Dentistry School, São Francisco University,
São Francisco de Assis Avenue, 218,
12916–900, Bragança Paulista, SP, Brazil

V. S. Bagnato
Physics Institute, USP – University of São Paulo,
Caixa Postal 369,
13560–970, São Carlos, SP, Brazil

Introduction

The potential risk of dentists acquiring or transmitting infectious diseases during clinical procedures has been a major concern in dental practice. A previous study demonstrated that all materials sent from dental offices to the dental laboratories, including prostheses, were contaminated with different species of microorganisms [27]. Therefore, prosthodontic patients can be considered a high-risk group for transmission of infectious diseases as well as being susceptible to acquiring them.

Dental prostheses can act as a potential source of infection because pathogenic microorganisms are capable of adhering to and surviving on acrylic resin surfaces,

promoting biofilm formation. Denture biofilms are complex structures similar to those found in dental plaque, except for the extensive presence of *Candida* spp. [23]. Different species of oral and non-oral pathogens are associated with denture plaque, including *Candida* spp., *Staphylococcus* spp., *Streptococcus* spp., *Lactobacillus* spp., *Pseudomonas* spp., *Enterobacter* spp. and *Actinomyces* spp. [15]. The presence of this microflora has been implicated in many local [44] and systemic pathologies [15], such as caries, periodontal disease, mucosa inflammation, urinary tract infections, conjunctivitis, pneumonia, meningitis, abscess, septicemia, and endocarditis.

The probable transmission of infectious agents between patients and dental staff has led to an effort to find methods for reducing the occurrence of cross-contamination in prosthodontic practice. Denture disinfection is an important procedure that must be performed before dentures are sent to the laboratory and before they are inserted in the patient. Chemical agents have been widely applied to reduce microbial contamination of dentures [22]. Nevertheless, some of the recommended denture-soaking solutions have been reported to change or damage the physical [32] and mechanical properties [1] of acrylic resins. Another alternative for denture disinfection may be microwave irradiation. Despite its effectiveness for inactivating microorganisms [28], many types of dentures cannot be disinfected by microwave, for example, removable partial dentures, because they are constructed with a metal framework. Bearing in mind that the denture materials should not be adversely affected by the disinfection process, many researchers have conducted studies to seek alternative therapies for denture decontamination.

Photodynamic therapy (PDT) seems to be a promising method for inactivating microorganisms. Until recently, the main application of PDT was to treat neoplasms [4] and non-neoplastic [22] disorders. However, the use of this technique for the treatment of microbial infection [39] is also gaining interest due to the growing resistance of microorganisms to conventional antimicrobial agents. Many studies have shown PDT to be highly effective for inactivating viruses [40], bacteria [16], and fungi [34]. The basic principle of this approach is based on the irradiation of a compound known as a photosensitizer (PS) with a light source, which causes cell death through the generation of reactive oxygen species (e.g., singlet oxygen). Several light sources have been applied to activate the PS. Although laser is the most commonly used light, another alternative light source for PDT is light-emitting diodes (LEDs). The LED device presents some advantages in comparison with laser light, such as: narrow-band non-coherent energy, lower cost and simple technology, being suitable for illuminating different targets. Moreover, there are different colors of LED light, which have radiations covering almost all the visible electromagnetic spectra.

Although the majority of studies have suggested antimicrobial PDT for the management of localized infections, this procedure may also emerge as a promising process for disinfection. Drinking water contaminated with a range of bacteria was disinfected using Rose Bengal, eosin, and methylene blue associated with a halogen lamp [21]. Furthermore, recent publications have reported the use of PDT in blood decontamination [41]. In dentistry, PDT can have important clinical applications such as the disinfection of root canals, periodontal pockets, and carious lesions [11, 42]. In the periodontal field, PDT has shown its efficacy for the treatment of periodontitis and peri-implantitis in animal models and clinical trials [9, 10].

Thus, this clinical study evaluated the effectiveness of PDT for disinfecting complete maxillary dentures worn by patients as a potential method to prevent cross-contamination. The hematoporphyrin derivative Photogem® was selected as PS and was associated with blue LED illumination.

Methods

Study population

Maxillary complete dentures of 60 patients, aged between 45–80 years, with a mean age 62.5 years, were included in this study. The patients, recruited from UNESP - São Paulo State University/ Araraquara Dental School, were invited by telephone to participate in the survey. They presented healthy oral mucosa, a good general health status and had been wearing their dentures for at least 6 months. Furthermore, one of the inclusion criteria was that the volunteers had not, or were not soaking dentures in a disinfectant solution. All the patients received verbal oral hygiene instructions. The examiners wore gloves, protective clothing, masks, and eye protection during all clinical and laboratory procedures. After attending each patient and performing microbial culture, the operator's gloves were discarded and replaced with sterile gloves. The research protocol was approved by the Ethics Committee of the Araraquara Dental School/ UNESP – São Paulo State University and each patient provided written consent to participate in this study.

Clinical procedures

The sixty patients were randomly divided into four experimental groups (P50S, P100S, P50G, and P100G) of 15 subjects each. Blind investigators were responsible for the clinical procedures such as: first denture biofilm collection, PDT procedures, and second denture biofilm collection. Microbiological procedures were carried out by one examiner. The first collection of biological material (control) of each denture was performed before PDT treatment. Control

samples were collected from the left half of all denture surfaces, which were vigorously rubbed for 1 min with a sterile cotton swab. Denture biofilm samples were placed in tubes containing 4.5 ml of sterile saline solution.

After the first collection, Photogem® (Photogem, Moscow, Russia) was used to photosensitize the denture biofilms. It is important to mention that Photogem® was the PS selected for the purposes of this investigation, because of its effectiveness in inactivating different types of microorganisms [12, 14, 16]. Furthermore, this PS is a hematoporphyrin derivative produced in Russia very similar to Photofrin II, which was the first authorized by the U.S. Food and Drug Administration for clinical use in PDT [14, 39]. Two preparations of Photogem® were used in this study: a liquid solution that was applied on dentures with a sparger to spray the PS; and a gel compound that was applied on dentures with a 5-ml syringe and carefully spread with a swab. Both preparations were made at two different concentrations according to the experimental groups: P50S and P100S patients had their maxillary denture sprayed with 5 ml of 50 and 100 mg/l of Photogem® suspension, respectively; P50G and P100G patients had their maxillary denture treated with 5 ml of 50 and 100 mg/l of Photogem® gel, respectively. After this, each denture was individually placed in a transparent plastic bag and left in the dark for 30 min (pre-irradiation). Next, all dentures were placed inside a LED device (Fig. 1) designed by the "Physics Institute" (University of São Paulo, USP, São Carlos, SP, Brazil). This system is composed of 24 royal blue LEDs (LXHL-PR09, Luxeon® III Emitter, Lumileds Lighting, San Jose, CA, USA) uniformly distributed throughout the device and contains three air coolers to avoid heating the samples. The LED device covered the wavelength range from 440–460 nm, with maximum emission at 455 nm. The intensity of light delivered was 24 mW/cm^2. The dentures were illuminated for 26 min (37.5 J/cm^2). After PDT procedures, a second collection (right side surfaces) of biological material from each of the 60 dentures was made as described for the first collection.

Microbiological analysis

The saline tubes prepared before and after PDT were first shaken for 1 min to dislodge the cells from the swab. All microbial material was diluted (10^{-1} to 10^{-3}) in saline solution and aliquots of each dilution (25 μl) were plated on selective media for *Candida* spp. (CHROMagar Candida, Probac do Brasil Produtos Bacteriológicos Ltda., São Paulo, SP, Brazil), *Staphylococcus* spp. (Mannitol Salt Agar, Acumedia Manufactures, Inc., Baltimore, MD), *mutans* streptococci (SB20) and a non-selective media (Mueller Hinton, Acumedia Manufactures, Inc., Baltimore, MD). The plates were incubated aerobically at 37°C for 48 h, except for mutans streptococci, which was incubated in candle jars. After incubation for 48 h, microbial colony counts of each plated denture were quantified using a digital colony counter (Phoenix CP 600 Plus, Phoenix Ind. e Com. de Equipamentos Científicos Ltd, Araraquara, SP, Brazil). Then, the colony-forming units per milliliter (cfu/ml) were determined.

Conventional biochemical methods were used to identify the microorganism cultures. *Candida* species were presumptively identified by CHROMagar Candida media and confirmed by biochemical tests (germ-tube tests, chlamydospore formation, assimilation and fermentation of sugars) [26, 29]. Moreover, an appropriate identification test was required to distinguish *Candida albicans* from *Candida dubliniensis* (thermotolerance test: growth at 42 and 45°C) [28]. Isolates of *C. albicans* grow well at 42 and 45°C while *C. dubliniensis* grow poorly or not at all these temperatures. *Staphylococcus* spp. isolates were subcultured

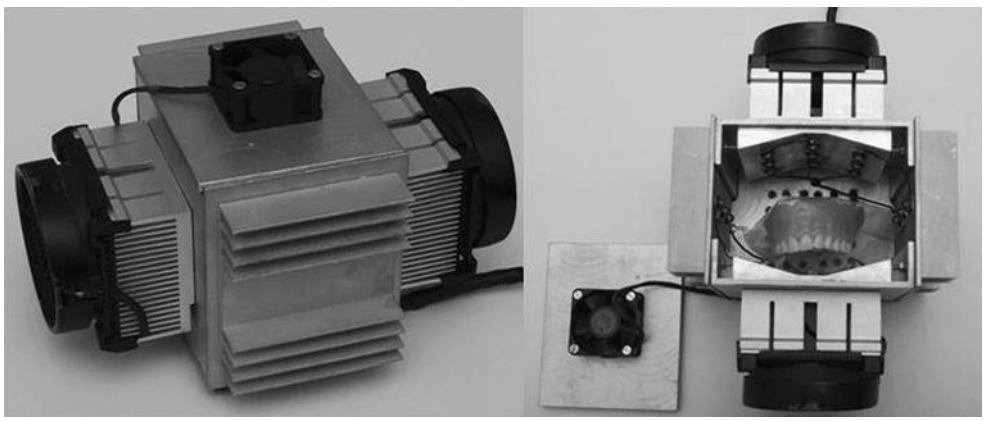

Fig. 1 Analysis of articular wash 3 and 6 h after induced inflammation. **a** Total number of leukocytes in articular lavage fluid after 3 h in the control group and after LLLT ($n = 6$ animals per group (*$p < 0.05$) (**$p < 0.001$). **b** Total number of leukocytes in articular lavage fluid after 6 h in the control group and after LLLT ($n = 6$ animals per group arthritis group (AT); the arthritis group treated with diclofenac (Diclof); the arthritis group treated with 1 J LLLT (AT+1 J); the arthritis group treated with 3 J LLLT (AT+3 J); the arthritis group treated with 6 J LLLT (AT+6 J); the arthritis group treated with 10 J LLLT (AT+10 J). Results are expressed as mean (± SEM)

onto Mannitol Salt Agar media. The isolate, which formed a yellow colony, referred to as *Staphylococcus aureus,* was plated on CHROMagar Staphylococcus (Probac do Brasil Produtos Bacteriológicos Ltda., São Paulo, SP, Brazil). For *S. aureus*, this culture media provides the growth of purple colonies. The *S. aureus* strains were identified by the coagulase test using rabbit plasma [13]. Mutans streptococci were identified by observing the physiological characteristics and using biochemical tests (fermentation of mannitol, sorbitol, melibiose and raffinose, hydrolysis of arginine, resistant to bacitracin and hydrogen peroxide) produced in accordance with Bergey's Manual [19].

Data analysis

The percentage of disinfected dentures in each experimental group was calculated. PDT was considered effective for disinfection when it resulted in at least 90% reduction of microorganisms on dentures. The percentage of reduction was calculated by subtracting the total cfu/ml value obtained on the second denture biofilm collection from the total cfu/ml value obtained on the first denture biofilm collection. The PDT effectiveness for denture disinfection was evaluated among the four experimental groups. The non-parametric Kruskal–Wallis test was applied to assess the statistical significance of differences among groups. Differences were considered statistically significant at $p<0.05$.

The inactivation of *Candida* spp., *Staphylococcus* spp. and mutans streptococci was recognized when no growth was observed on each selective media. These results were categorized and statistical analysis was performed by the McNemar test ($\alpha=0.05$) to verify whether the number of dentures with absence of each microorganism after PDT was significant in comparison with the number of dentures with the presence of the microorganism before PDT.

Results

Effectiveness of PDT

No microbial growth after PDT was observed in 60, 53, 47, and 40% of dentures, from groups P100G, P50G, P100S, and P50S, respectively. These values were calculated based on the number of dentures that showed no colony growth on all culture media after PDT.

When microbial growth was verified after PDT, the four PDT regimens eliminated over 90% of microorganisms from dentures. In addition, statistical analysis confirmed no significant difference in the cfu/ml values from the dentures among the four experimental groups. The *p* values obtained were $p=0.77$ for *Candida* spp., $p=0.82$ for *Staphylococcus* spp., $p=0.76$ for mutans streptococci and $p=0.95$ for microorganisms grown on non-selective media. For each experimental group, the cfu/ml values obtained before and after PDT in all culture media are presented in Table 1. Based on these values, the percentage of microbial reduction was calculated (Table 1).

Results of the McNemar's test showed that inactivation of microorganisms cultured on the selective media was significant. When the gel formulation of Photogem® was used at 100 mg/l (P100G) the inactivation of *Candida* spp. ($p=0.045$), *Staphylococcus* spp. ($p=0.014$) and mutans streptococci ($p=0.045$) was achieved. The liquid formulation of Photogem® at 100 mg/l (P100S) eliminated *Candida* spp. ($p=0.045$), *Staphylococcus* spp. ($p=0.045$) and mutans streptococci ($p=0.014$). The results of P50G showed that the gel formulation of Photogem® at 50 mg/l inactivated *Staphylococcus* spp. ($p=0.045$) and mutans streptococci ($p=0.025$) from dentures. When the liquid formulation of Photogem® was used at 50 mg/l (P50S), PDT treatment promoted inactivation of *Staphylococcus* spp. only ($p=0.045$).

Microbiological identification of isolates

Cultures from non-selective media showed substantial microbial growth for all dentures belonging to Groups P50S, P100S, P50G, and P100G before PDT procedures. The results obtained with selective media revealed that *Candida* spp. was the most frequent microorganism (60.0%) on dentures, followed by mutans streptococci (53.3%) and *Staphylococcus* spp. (48.3%). Among the dentures positive for *Candida* spp., three species were identified. *C. albicans* was the most frequent yeast isolated, occurring in 35 dentures, while *Candida glabrata* and *Candida tropicalis* were found in 09 and 02 dentures, respectively (Table 2). The species identified from dentures positive for *Staphylococcus* spp. were *Staphylococcus aureus* and non-aureus *Staphylococci* (Table 2). *Streptococcus mutans* was the only species identified among dentures colonized with mutans streptococci, which was found in 32 dentures (Table 2).

The identity of the various species recovered from each denture before and after PDT procedures is described in Table 3. The present study observed that dentures were not simultaneously colonized by all species identified.

Discussion

The present in vivo study demonstrated no microbial growth after PDT, using Photogem® in association with blue LED, in 60, 53, 47, and 40% of dentures from P100G, P50G, P100S, and P50S groups, respectively. These results from non-selective media showed that the absence of

Table 1 Mean of cfu/ml values obtained before and after PDT and percentage of reduction (%) obtained in each experimental group according to the culture media

Groups	Culture Media											
	CHROMagar			Mannitol Salt Agar			SB20			Mueller Hinton		
	Before PDT	After PDT	%	Before PDT	After PDT	%	Before PDT	After PDT	%	Before PDT	After PDT	%
P50S	3.16E+03	4.00E+01	98.7	1.04E+03	1.33E+01	98.7	8.53E+03	1.12E+02	98.6	3.46E+05	1.16E+03	99.6
P100S	8.37E+03	3.47E+01	99.5	2.85E+02	2.13E+01	92.5	3.92E+05	5.87E+01	99.9	2.67E+06	5.28E+02	99.9
P50G	1.57E+04	1.20E+02	99.2	3.95E+03	5.87E+01	98.5	6.79E+04	3.49E+02	99.4	5.45E+05	5.65E+02	99.8
P100G	2.96E+03	2.88E+02	90.2	4.59E+02	4.00E+01	91.2	1.17E+05	1.17E+02	99.9	6.22E+05	1.20E+03	99.8

microbial growth varied according to PDT regimes. The highest frequency of dentures with no growth (60 and 53%) was observed with the Photogem® in gel formulation, both at 100 and 50 mg/l, respectively. Experimental examinations [17, 24, 38] have revealed that the gel formulation can be more efficient than the liquid for disinfection purposes. Gomes et al. [17] showed that chlorhexidine gluconate gel was more efficient than the liquid presentation at equivalent concentrations against selected endodontic microorganisms. Another investigation [38] also proved that chlorhexidine in gel form eliminated *S. aureus* and *C. albicans* isolated from infected root canals. According to the research of Paolantonio et al. [24], filling the internal implant cavity with chlorhexidine gel resulted in a significant reduction in the total bacterial count and it proved to have a long-lasting antimicrobial effect when compared with chlorhexidine solution. The above-mentioned studies suggested that the higher effectiveness of the gel formulation was because the gel kept the chemical substance in contact with the microorganisms for a longer time than the liquid formulation did. Photogem® gel is capable of remaining on the denture surfaces throughout the pre-irradiation and illumination procedures, which may explain the better results obtained for Groups P100G and P50G. It is possible that the denture biofilm being kept in constant contact with the PS gel favored photosensitization of the microorganisms, and improved the effectiveness of PDT.

Table 2 Prevalence of the different species identified in 60 maxillary dentures before PDT procedures

Identified species	Dentures (n = 60)	
	Number	%
Candida spp.	36	60.0
C. albicans	35	58.3
C. glabrata	09	15.0
C. tropicalis	02	3.3
Staphylococcus spp.	29	48.3
Staphylococcus aureus	23	38.3
non-aureus *Staphylococci*	06	10.0
Mutans streptococci	32	53.3
Streptococcus mutans	32	53.3

PDT resulted in a substantial reduction in the viable microorganism counts from dentures. This disinfection was observed after the four PDT treatments, since they all significantly reduced over 90% of the microorganisms on the dentures. Although the present investigation was the first to describe the clinical use of PDT for denture disinfection, the results presented here can be compared to research that applied PDT for clinical disinfection in dentistry. Dörtbudak et al. [11] showed that the application of toluidine blue O (TBO) and laser for implant surface disinfection was capable of significantly reducing (2 log steps on an average) the initial values for the three bacteria groups tested. In another study, [30] the subgingival plaque samples from patients were exposed to laser in the presence of TBO and achieved significant reductions (over 90%) in the viability of aerobic and anaerobic organisms. Giusti et al. [14] evaluated the use of Photogem® in association with red LED light for decontaminating carious bovine dentin and observed that the initial number of bacteria was reduced by more than 90% after PDT treatment.

In addition to the studies already mentioned, the results are also corroborated by the findings of several in vitro studies [3, 25, 33, 36]. These aforementioned investigations showed that bacterial and yeast species are susceptible to PDT, including those found in dentures worn by edentulous patients. Soares et al. [33] obtained a significant reduction in the growth of planktonic *C. albicans*, *C. tropicalis* and *Candida parapsilosis* cultures after PDT mediated by TBO with LED light. Another in vitro study [3] demonstrated the possibility of photosensitizing *C. albicans* and *C. glabrata* with light-induced inactivation by using Photofrin® and an Hg arc lamp. According to Tegos et al. [36], the use of a chlorin(e6) conjugate in conjunction with a diode laser efficiently killed microbial suspensions of *S. aureus*. The susceptibility of one *S. mutans* strain was verified by using a dental light polymerizer in association with Rose Bengal dye [25]. The results of the above-mentioned studies are consistent with those of the present study, which also

Table 3 Summary of species from 60 dentures, identified before and after PDT procedures

Groups evaluated	Dentures from patients	Species recovered	
		Before PDT	After PDT
Group I	01	Sa	nd
	02	Ca, Cg, Sa, Ms	Ca, Cg, Sa, Ms
	03	nd	nd
	04	Ca	Ca
	05	Sa, Ms	Ms
	06	Ca, Ms	nd
	07	Ca	nd
	08	Ca, Ms	Ca, Ms
	09	Ca, Cg, Sa, Ms	Ca, Sa, Ms
	10	Sa, Ms	Ms
	11	nd	nd
	12	Ca, Sa, Ms	nd
	13	Ca, Sa, Ms	Ca, Sa, Ms
	14	nd	nd
	15	Ca	Ca
Group II	16	Ca, Ms	nd
	17	Ca, Ms	nd
	18	Ca, Ms	Ca
	19	Ms	nd
	20	Sa	nd
	21	Ca, Cg, Ms	Cg
	22	Sa	Sa
	23	Ca, Sa, Ms	Ca, Sa, Ms
	24	Ms	Ms
	25	nd	nd
	26	Ca, Sa	Ca, Sa
	27	Ca, n-Sa, Ms	Ca, Ms
	28	Cg	nd
	29	Sa, Ms	nd
	30	Ca, n-Sa	nd
Group III	31	Ca, Ms	nd
	32	nd	nd
	33	Ca, Sa	nd
	34	Ca, n-Sa, Ms	nd
	35	Ms	nd
	36	Ca, Cg, Sa, Ms	Ca, Cg, Ms
	37	Ca	Ca
	38	Ms	nd
	39	Ca, Sa, Ms	Ca, Sa, Ms
	40	nd	nd
	41	nd	nd
	42	Ca, n-Sa, Ms	Ca
	43	Sa	Sa
	44	Ca, Cg, Ms	Ca, Cg, Ms
	45	Ca, Sa	Ca, Sa
Group IV	46	Ca, Ct, Sa	Sa
	47	Ca, Cg, Sa, Ms	Ca, Cg, Ms
	48	Sa	nd
	49	Ca, Sa	Ca, Sa
	50	Ms	nd
	51	Ca, n-Sa	nd
	52	Ms	nd
	53	Ca, Ms	nd
	54	nd	nd
	55	Ca, Cg, Sa	Ca, Cg
	56	Ca, Cg, Ms	Ca, Cg, Ms
	57	n-Sa, Ms	nd
	58	Ca, Sa, Ms	Ca, Ms
	59	nd	nd
	60	Ca	nd

Ca= *C. albicans*, Cg= *C. glabrata*, Ct= *C. tropicalis*, Sa= *Staph. aureus*, n-Sa= non-aureus *Staph.*, Ms= Strep. mutans, nd= not detected.

observed that PDT caused significant reduction in microorganisms on dentures.

In order to simulate in vivo conditions, some investigations evaluated the photodynamic effects on in vitro biofilms. Research concerning biofilms provides relevant data since most of the microorganisms are found in nature living in microbial communities on different surfaces [7]. Recent studies showed that biofilms of *C. albicans* [5], *S. aureus* [31], and *S. mutans* [43] may be inactivated by using a variety of PS and light sources. In the present study, dentures colonized with microbial biofilm composed of different species (from non-selective media) were disinfected after PDT regimes. These results confirm the possibility of using PDT for inactivating microorganisms organized in biofilm communities. Nevertheless, microbial survival after PDT was observed in some dentures and one possible explanation for these findings could be the functional and structural characteristics of biofilm-grown cells [5, 7, 31], which may reduce their sensitivity to photodynamic damage. Developing biofilms have been associated mainly with the presence of extracellular matrix [5, 7, 31]. The latter is known to interact physically with antimicrobial agents and then contribute to the resistance to these drugs [6]. It has also been suggested that the production of extracellular material blocks the diffusion of the PS though the biofilm, thus reducing the susceptibility of the adhered organisms to photokilling [31]. It is also important to report that photodynamic inactivation is based on light-induced oxidation reactions that lead to cell death. Three critical elements are required for the photodynamic process to occur: a drug (PS) that can be activated by light and oxygen [20]. An activated PS can transfer energy directly to oxygen, generating the reactive singlet oxygen [18]. This molecule can react against a wide range of cell targets, including membrane lipids, cytoplasmic enzymes, and nucleic acids [20]. In PDT, the degree of photoinactivation will probably be equivalent to the amount of singlet oxygen produced. The use of high PS concentrations and light fluences can increase the amount of reactive oxygen formed and promote more oxidative damage in the biological targets. Demidova et al. [8] showed that a high amount of singlet oxygen is needed to kill a *Candida* cell. This fact has been attributed to the large size of the *Candida* cell and the presence of a nuclear membrane that may present an additional barrier to PS penetration [8, 45]. The results of the present study confirm that a high concentration of PS is required to inactivate *Candida* spp. since a significant inactivation was observed only after using 100 mg/l of Photogem® both gel (P100G) and liquid (P100S) formulation.

The results with regard to the microbiological identification of isolates from dentures revealed some species found on biofilm before and after PDT procedures. The initial collection showed that *Candida* species (60.0%) were the most frequent among the 60 dentures taken from healthy patients, followed by mutans streptococci (53.3%) and *Staphylococcus* spp. (48.3%). These results corroborate

those of Ribeiro et al., [28] who found the same three species in maxillary dentures, and *Candida* spp. appeared with the highest frequency of appearance (76.6%). Another study [2] reported the presence of *C. albicans*, *S. aureus*, and *S. mutans* on the inner surface of complete dentures taken from patients. *C. albicans* was isolated in 66.7% of the dentures, while *S. aureus* and *S. mutans* were isolated from 49.5% of the dentures. The present study observed that the yeast species isolated from dentures were *C. albicans*, *C. glabrata* and *C. tropicalis*. Vanden Abbeele et al. [37] confirmed that *C. albicans* (77.9%) was the commonest yeast found on patients' dentures, followed by *C. glabrata* (44.1%) and *C. tropicalis* (19.1%), respectively. After PDT treatments, the species were identified as *C. albicans*, *C. glabrata*, *S. aureus* and *S. mutans*. Some investigations [15, 35] have related the presence of *Candida*, *Staphylococcus*, and *Streptococcus* species on dentures to the development of systemic infections [35] such as pneumonia, and local infections such as denture-induced stomatitis [2]. Although the present research showed a reduction of more than 90% of microorganisms from all dentures, the persistence of pathogenic microorganisms on dentures after disinfection procedures may be cause for concern. Preferably, these procedures should be efficient for completely eliminating microorganisms, allowing denture sterilization and assuredly preventing cross-contamination between the dental office and dental laboratory personnel. Thus, further research is needed to determine an effective combination of PS concentration with light fluence for preventing cross-infection in dental practice.

In conclusion, this clinical study showed that PDT was effective in disinfecting dentures since the four treatments inactivated over 90% of microorganisms on the dentures. Gel formulation of Photogem® was more efficient for photosensitizing denture biofilm when compared with liquid form. Nevertheless, these results must be interpreted with caution because the survival of any microorganism on denture after PDT could be an infection hazard for dental staff and patients. Thus, to establish an effective infection-control program, it is important to not only decrease the number of microorganisms but also eliminate them from dentures. For this reason, a possible future direction in research to improve PDT effectiveness may be the investigation of higher Photogem® concentrations in order to achieve sterilization of dentures, as well as the evaluation of conventional disinfection methods to compare with PDT efficacy.

Acknowledgments This research was supported by São Paulo Council of Research (FAPESP Grant No. 2005/02192-8).

Conflict of interest The authors declare that they have no conflicts of interest.

References

1. Asad T, Watkinson AC, Huggett R (1992) The effect of disinfection procedures on flexural properties of denture base acrylic resins. J Prosthet Dent 68:191–195
2. Baena-Monroy T, Moreno-Maldonado V, Franco-Martínez F, Aldape-Barrios B, Quindós G, Sánchez-Vargas LO (2005) *Candida albicans*, *Staphylococcus aureus* and *Streptococcus mutans* colonization in patients wearing dental prosthesis. Med Oral Patol Oral Cir Bucal 10:E27–E29
3. Bliss JM, Bigelow CE, Foster TH, Haidaris CG (2004) Susceptibility of *Candida* species to photodynamic effects of Photofrin. Antimicrob Agents Chemother 48:2000–2006
4. Brow SB, Brown EA, Walker I (2004) The present and the future role of photodynamic therapy in cancer treatment. Lancet Oncol 5:497–508
5. Chabrier-Roselló Y, Foster TH, Pérez-Nazario N, Mitra S, Haidaris CG (2005) Sensitivity of *Candida albicans* germ tubes and biofilms to Photofrin-mediated phototoxicity. Antimicrob Agents Chemother 49:4288–4295
6. Chandra J, Kuhn DM, Mukherjee PK, Hoyer LL, McCormick T, Ghannoum MA (2001) Biofilm formation by the fungal pathogen *Candida albicans*: development, architecture, and drug resistance. J Bacteriol 183:5385–5394
7. Costerton JW, Lewandowski Z, Caldwell DE, Korber DR, Lappin-Scott HM (1995) Microbial biofilms. Annu Rev Microbiol 49:711–745
8. Demidova TN, Hamblin MR (2005) Effect of cell-photosensitizer binding and cell density on microbial photoinactivation. Antimicrob Agents Chemother 49:2329–2335
9. de Oliveira RR, Novaes AB Jr, Garlet GP, de Souza RF, Taba M Jr, Sato S, de Souza SL, Palioto DB, Grisi MF, Feres M (2010) The effect of a single episode of antimicrobial photodynamic therapy in the treatment of experimental periodontitis. Microbiological profile and cytokine pattern in the dog mandible. Lasers Med Sci. doi:10.1007/s10103-010-0864-z
10. de Paula EC, de Freitas PM, Esteves-Oliveira M, Aranha AC, Ramalho KM, Simões A, Bello-Silva MS, Tunér J (2010) Laser phototherapy in the treatment of periodontal disease. A review. Lasers Med Sci 25(6):781–792
11. Dörtbudak O, Haas R, Bernhart T, Mailath-Pokorny G (2001) Lethal photosensitization for decontamination of implant surfaces in the treatment of peri-implantitis. Clin Oral Implants Res 12:104–108
12. Dovigo LN, Pavarina AC, de Oliveira Mima EG, Vergani CE, Giampaolo ET, Bagnato VS (2011) Fungicidal effect of photodynamic therapy against fluconazoleresistant *Candida albicans* and *Candida glabrata*. Mycoses 54:123–30
13. Gaillot O, Wetsch M, Fortineau N, Berche P (2000) Evaluation of CHROMagar *Staph. aureus*, a new chromogenic medium, for isolation and presumptive identification of *Staphylococcus aureus* from human clinical specimens. J Clin Microbiol 38:1587–1591
14. Giusti JS, Santos-Pinto L, Pizzolito AC, Helmerson K, Carvalho-Filho E, Kurachi C et al (2008) Antimicrobial photodynamic action on dentin using a light-emitting diode light source. Photomed Laser Surg 26:281–287
15. Glass RT, Bullard JW, Hadley CS, Mix EW, Conrad RS (2001) Partial spectrum of microorganisms found in dentures and possible disease implications. J Am Osteopath Assoc 101:92–94
16. Gois MM, Kurachi C, Santana EJ, Mima EG, Spolidório DM, Pelino JE et al (2010) Susceptibility of *Staphylococcus aureus* to porphyrin-mediated photodynamic antimicrobial chemotherapy: an in vitro study. Lasers Med Sci 25(3):391–395
17. Gomes BPFA, Ferraz CCR, Zaia AA, Souza-Filho FJ (1999) Variations in the susceptibility of selected microorganisms to

endodontic irrigants (BES Spring Meeting Abstract). J Endod 25:299
18. Hamblin MR, Hasan T (2004) Photodynamic therapy: a new antimicrobial approach to infectious disease? Photochem Photobiol Sci 3:436–450
19. Hardie JM (1986) Oral streptococci. In: Bergey DH (ed) Bergey's manual of systematic bacteriology. Williams & Wilkins, Baltimore, pp 1054–1563
20. Henderson B, Dougherty TJ (1992) How does the photodynamic therapy work? Photochem Photobiol 55:145–157
21. Kuznetsova NA, Makarov DA, Kaliya OL, Vorozhtsov GN (2007) Photosensitized oxidation by dioxygen as the base for drinking water disinfection. J Hazard Mater 146:487–491
22. Mennel S, Barbazetto I, Meyer CH, Peter S, Stur M (2007) Ocular photodynamic therapy-standard applications and new indications (part 1). Review of the literature and personal experience. Ophthalmologica 221:216–226
23. Nikawa H, Hamada T, Yamamoto T (1998) Denture plaque-past and recent concerns. J Dent 26:299–304
24. Paolantonio M, Perinetti G, D'Ercole S, Graziani F, Catamo G, Sammartino G et al (2008) Internal decontamination of dental implants: an in vivo randomized microbiologic 6-month trial on the effects of a chlorhexidine gel. J Periodontol 79:1419–1425
25. Paulino TP, Ribeiro KF, Thedei G Jr, Tedesco AC, Ciancaglini P (2005) Use of hand-held photopolymerizer to photoinactivate *Streptococcus mutans*. Arch Oral Biol 50:353–359
26. Pfaller MA, Houston A, Coffmann S (1996) Application of CHROMagar Candida for rapid screening of clinical specimens for *Candida albicans*, *Candida tropicalis*, *Candida krusei*, and *Candida* (Torulopsis) *glabrata*. J Clin Microbiol 34:58–61
27. Powell GL, Runnells RD, Saxon BA, Whisenant BK (1990) The presence and identification of organisms transmitted to dental laboratories. J Prosthet Dent 64:235–237
28. Ribeiro DG, Pavarina AC, Dovigo LN, Spolidorio DM, Giampaolo ET, Vergani CE (2009) Denture disinfection by microwave irradiation: a randomized clinical study. J Dent 37:666–672
29. Sandven P (1990) Laboratory identification and sensitivity testing of yeast isolates. Acta Odontol Scand 48:27–36
30. Sarkar S, Wilson M (1993) Lethal photosensitization of bacteria in subgingival plaque from patients with chronic periodontitis. J Periodontal Res 28:204–210
31. Sharma M, Visai L, Bragheri F, Cristiani I, Gupta PK, Speziale P (2008) Toluidine blue-mediated photodynamic effects on staphylococcal biofilms. Antimicrob Agents Chemother 52:299–305
32. Shen C, Javid NS, Colaizzi FA (1989) The effect of glutaraldehyde base disinfectants on denture base resins. J Prosthet Dent 61:583–589
33. Soares BM, da Silva DL, Sousa GR, Amorim JC, de Resende MA, Pinotti M et al (2009) In vitro photodynamic inactivation of *Candida* spp. growth and adhesion to buccal epithelial cells. J Photochem Photobiol B 94:65–70
34. Souza RC, Junqueira JC, Rossoni RD, Pereira CA, Munin E, Jorge AO (2010) Comparison of the photodynamic fungicidal efficacy of methylene blue, toluidine blue, malachite green and low-power laser irradiation alone against *Candida albicans*. Lasers Med Sci 25(3):385–389
35. Sumi Y, Kagami H, Ohtsuka Y, Kakinoki Y, Haruguchi Y, Miyamoto H (2003) High correlation between the bacterial species in denture plaque and pharyngeal microflora. Gerodontology 20:84–87
36. Tegos GP, Anbe M, Yang C, Demidova TN, Satti M, Mroz P et al (2006) Protease-stable polycationic photosensitizer conjugates between polyethyleneimine and chlorine(e6) for broad-spectrum antimicrobial photoinactivation. Antimicrob Agents Chemother 50:1402–1410
37. Vanden Abbeele A, De Meel H, Ahariz M, Perraudin JP, Beyer I, Courtois P (2008) Denture contamination by yeasts in the elderly. Gerodontology 25:222–228
38. Vianna ME, Gomes BPFA, Berber VB, Zaia AA, Ferraz CCR, Souza-Filho FJ (2004) In vitro evaluation of the antimicrobial activity of chlorhexidine and sodium hypochlorite. Oral Surg Oral Med Oral Pathol 97:79–84
39. Wainwright M (1998) Photodynamic antimicrobial chemotherapy (PACT). J Antimicrob Chemother 42:13–28
40. Wainwright M (2004) Photoinactivation of viruses. Photochem Photobiol Sci 3:406–411
41. Wainwright M, Mohr H, Walker WH (2007) Phenothiazinium derivatives for pathogen inactivation in blood products. J Photochem Photobiol B 86:45–58
42. Walsh LJ (2003) The current status of laser applications in dentistry. Aust Dent J 48:146–155
43. Zanin IC, Gonçalves RB, Junior AB, Hope CK, Pratten J (2005) Susceptibility of *Streptococcus mutans* biofilms to photodynamic therapy: an in vitro study. J Antimicrob Chemother 56:324–330
44. Zarb GA, Mackay HF (1980) The partially edentulous patient. I. The biologic price of prosthodontic intervention. Aust Dent J 25:63–68
45. Zeina B, Greenman J, Purcell WM, Das B (2001) Killing of cutaneous microbial species by photodynamic therapy. Br J Dermatol 144:274–278

Usefulness of tissue autofluorescence imaging in actinic cheilitis diagnosis

Ademar Takahama Junior,[a] Cristina Kurachi,[b] Alessandro Cosci,[b] Isabel Schausltz Pereira Faustino,[a] Danielle Resende Camisasca,[a] Karla Bianca Fernandes da Costa Fontes,[a] Fábio Ramôa Pires,[c] and Rebeca Souza Azevedo[a]
[a]Fluminense Federal University, Oral Pathology, School of Dentistry, Nova Friburgo, Rio de Janeiro 28625-650, Brazil
[b]University of São Paulo, Institute of Physics of São Carlos, São Carlos, São Paulo 13566-590, Brazil
[c]State University of Rio de Janeiro, Oral Pathology, School of Dentistry, Rio de Janeiro 21550-030, Brazil

Abstract. Actinic cheilitis (AC) is a potentially malignant disorder of the lips. Because of its heterogeneous clinical aspect, it is difficult to indicate representative biopsy area. The purpose of this study was to evaluate the usefulness of tissue autofluorescence in AC diagnosis. The system was composed of a 405-nm light-emitting diode, sent to the sample by a dichroic, that allows the fluorescence signal to reach a camera directly plugged in the system. Fifty-seven patients with clinical diagnosis of AC and 45 normal volunteers were selected. According to clinical and fluorescence features, one or more areas were selected for biopsies in the AC group and epithelial dysplasia (ED) grades were established. The autofluorescence images were processed by a clustering algorithm for AC automated diagnosis. The tissue autofluorescence image revealed a heterogeneous pattern of loss and increase of fluorescence in patients with AC. ED was found in 93% of the cases, and most of the areas graded as moderate or severe ED were chosen with the aid of autofluorescence. The processed autofluorescence images from AC patients showed a higher number of spots in an irregular pattern. Tissue autofluorescence image system is a useful technique in association with clinical examination for AC diagnosis. [DOI: 10.1117/1.JBO.18.7.076023]

Keywords: actinic cheilitis; autofluorescence; epithelial dysplasia; diagnosis.

Paper 130062R received Feb. 1, 2013; revised manuscript received Jun. 2, 2013; accepted for publication Jun. 27, 2013; published online Jul. 25, 2013.

1 Introduction

Actinic cheilitis (AC), or solar cheilosis, is a potentially malignant disorder that mostly affects the vermilion border of the lower lip.[1–4] It usually involves fair-skinned, middle-aged or older patients with a history of prolonged sun exposure, especially in outdoors workers.[5] Some studies have identified the prevalence of AC in some different groups of Brazilian population, such as Junqueira et al.,[6] who found 39% of AC among agricultural workers; Martins-Filho et al.,[7] who found 16.7% of AC among farmers in a semi-arid northeastern; and de Souza Lucena et al.,[8] who found about 15% of AC among beach workers.

The solar ultraviolet (UV) radiation is considered the main risk factor for AC and lip squamous cell carcinoma (SCC),[9–11] but tobacco has also been associated with these lesions and with AC progression to SCC.[11] Lip SCC is one of the most common malignancies of the oral cavity[11] and almost all lip SCCs are associated with clinical areas of AC.[12,13]

AC is a heterogeneous clinical entity that may be localized or, more commonly, presented as a diffuse lesion, including atrophy, dryness, scaly areas, swelling, erythema, ulceration, loss of vermilion border definition, transverse fissures, white plaques, erosion, crusting, blotchiness, and tissue pallor as the main clinical features.[2,3,5,11] Histopathological changes vary from hyperkeratosis to SCC in the presence of solar elastosis.[4,11,13] Epithelial dysplasia (ED), which is still the most important predictor of malignant development,[14,15] is described in up to 100% of AC cases.[1–3,5] Additionally, although the precise AC malignant transformation rate is unknown,[4] lip SCC is described to have a high metastatic potential when compared to skin SCC, turning the assessment of ED degree in AC a critical diagnosis step.[5,11]

AC diagnosis is mainly based on demographic, clinical, and histopathological findings,[1–3] but as clinical appearance is sometimes subtle and may not correspond to the severity of tissue damage,[1,11,13,16] most authors consider biopsy mandatory to establish AC definitive diagnosis and treatment planning.[2,11] Recurrent ulceration, red and white blotchy areas with loss of the vermilion border, persistent crusting, generalized atrophy, and induration are clinical signs that may indicate high-grade epithelial dysplastic changes or even a malignant transformation.[5,11] Nonetheless, due to the fact that AC is characterized by multifocal and heterogeneous lesions, it is not easy to predict which area will exhibit representative histopathological changes to define the biopsy site[3] and an SCC may be misdiagnosed if the biopsy is not performed at a proper site.[13]

Some noninvasive clinical methods, such as the tissue autofluorescence widefield imaging system, have been reported as complementary approaches to discriminate malignant/dysplastic areas from normal tissue.[17] Direct tissue fluorescence visualization or tissue autofluorescence widefield imaging systems are becoming attractive noninvasive diagnostic tools to identify oral ED, because they have been used to identify biochemical and morphological alterations in tissues that are not easily

Address all correspondence to: Ademar Takahama Junior, Fluminense Federal University–Rua Doutor Silvio Henrique Braune, Oral Pathology, School of Dentistry, Nova Friburgo, 22-Centro—CEP: 28625-650, Nova Friburgo, Rio de Janeiro 21550-030, Brazil. Tel: + 55 22 25287168; Fax: + 55 22 25287166; E-mail: ademartjr@yahoo.com.br

0091-3286/2013/$25.00 © 2013 SPIE

discriminated under white light illumination.[18,19] This technique is based on the use of an illumination under UV-blue spectrum to excite native tissue fluorophores, like metabolic markers as nicotinamide adenine dinucleotide (NADH) and flavin adenine dinucleotide (FAD), and proteins as collagen, elastin, and keratin.[20] The emitted fluorescence by the excited tissue can be visualized by the observer[21] and provides information about metabolic and biochemical status of the resident cells.[22] Changes in this fluorescence may be related to malignant progression[23,24] and loss of normal tissue autofluorescence is described as a sign of malignant changes in the oral cavity.[20,25–28] Several widefield optical imaging systems have been reported with good results in the oral and oropharyngeal regions,[21,23,24] and some authors have presented a handheld device for widefield fluorescence imaging for oral tissue fluorescence direct visualization.[21] In this way, this optical technique seems to have a potential to improve visual evaluation of AC heterogeneity, helping the decision of biopsy sites and, as a consequence, assisting the detection of possible premalignant changes. Accordingly, the purpose of this study was to evaluate the usefulness of the tissue autofluorescence widefield imaging system in the clinical diagnosis of AC, using the histopathological examination as gold standard.

2 Material and Methods

Fifty-seven patients with clinical diagnosis of AC assisted at School of Dentistry of Fluminense Federal University (Nova Friburgo, Rio de Janeiro, Brazil) from March 2011 to March 2012 were included in this study. The study population was composed of 27 males (47.4%) and 30 females (52.6%), with ages ranging from 23 to 82 years (mean of 58.3 years) and having only fair-skin types (phototypes I, II, or III). A control group including 45 normal volunteers with similar sex and age distribution [23 males (51.1%) and 22 females (48.9%); age ranging from 30 to 88 years; mean of 50.6 years), most having fair-skin types (75.6%), and without any clinical signs of AC were also included for clinical and autofluorescence exams. Study and control groups did not include patients with any other lip disease. This study was carried out with the approval of the Research Ethics Committee (Medical School, Antonio Pedro School Hospital, Fluminense Federal University).

All patients were examined under white light by two oral medicine specialists who performed a detailed lip evaluation considering dryness, blurred vermilion border demarcation, swelling, hardness, red or white lesions, pigmented and pallor areas, vertical fissures, erosion, ulceration, and crusts. Ulceration, erosion, crust, and red and white areas were considered the main regions prone to malignant changes and were selected as elected biopsy sites. After clinical examination, the lip was evaluated using the tissue autofluorescence widefield imaging in a dark room. A homemade handheld device was assembled with a light-emitting diode (LED) array emitting at the violet-blue range. The light source was an LED (Edison, EDEV-3LA1) emitting at 405 nm, 40 nm bandwidth, and 350 mW output power. The emission peak was cleaned by a custom-made bandpass filter (Proteon, SP, Brazil) having a center wavelength of 430 nm and a bandwidth of 40 nm. A dichroic beam splitter (FF483/639-Di01, Semrock, NY), with a cutting wavelength of 460 nm, deflected the excitation light to the sample and allowed the fluorescence signal to reach the detector. Furthermore, a custom-made longpass filter (Proteon), with a cutting wavelength of 475 nm, was placed in front of the camera objective in order to block the backscattered excitation light. Autofluorescence features were evaluated, and areas with loss of fluorescence (LOF) were considered the main regions prone to malignant changes and were selected as elected biopsy sites. All clinical and autofluorescence characteristics observed were noted in a chart sketch of the lip divided into 19 sites. Biopsies using a 5-mm punch biopsy were performed in all AC patients, and the specimens were taken from the biopsy site selected under white light and under fluorescence. If these sites were coincident, only one site was biopsied; if these sites were not coincident, each elected site was biopsied. In cases of absence of a biopsy site selected by one of the exams, the biopsy was taken from the site selected by the other exam. Tissue specimens identified by clinical and/or fluorescence indications were processed for histopathological analysis. Hematoxylin and eosin stained slides were evaluated by three oral pathologists to score ED grade as mild, moderate, or severe according to the World Health Organization criteria and classification.

Fluorescence images were obtained always with the same exposure time using a Canon EOS Obj.18–55 3.5–5.6 IS with 100 mm 2.8 AF USM Macro Lens and Macro Ring Lite (Canon Inc., Tokyo, Japan) connected with the widefield fluorescence system; and they were processed by a clustering algorithm for AC automated diagnosis. The lower lip was hand-selected from the fluorescence images and placed on a new image with a black background for an easy recognition of the lip by the program. Among the three color channels, only the green one was selected for the analysis since it showed the highest intensity variation. A Gaussian blur filter was applied for noise reduction and K-means algorithm was used to assign pixel with similar intensity value to the same classification cluster. After this procedure, from a starting image of 256 grayscale intensity levels, a new image was obtained with only four intensity values (clusters). In order to evaluate the intensity distribution, the number of clustering areas was determined for each lip, in both study and control groups, and it was chosen as score for AC diagnosis. A 10-fold cross-validation with J48 decision tree algorithm[29] was used to create a model to classify lip images. Briefly, this algorithm randomly divides the whole data set of scores into two groups: 90% of the scores were used to find the threshold value, according to the J48 decision tree classifier, and the remaining 10% were used for validation to determine the sensitivity and the specificity rates. This procedure was repeated 10 times.

In order to understand whether AC diagnostic methods would be associated with ED upon histopathological analysis, chi-square tests were performed. The chi-square test is designed to analyze categorical data and tests the null hypothesis that the variables are independent. The association between diagnostic method, whether clinical, tissue autofluorescence widefield imaging system, or both, and ED was verified.

3 Results

AC affected the lower lip of all patients and also affected the upper lip of nine patients, four men and five women. Clinically, AC was diffuse and heterogeneous and it was mainly observed as an area of blurred vermilion border demarcation associated with a wide swelling, focal hypopigmentation, and/or red lesions [Table 1 and Fig. 1(a) and 1(b)]. Likewise, autofluorescence analysis showed that patients with AC exhibited a heterogeneous pattern of fluorescence, mixing areas of loss and increased emission intensity, in comparison with the normal autofluorescence (NF) observed in the control group

Table 1 Summary data of clinical features from 57 cases of AC.

Clinical findings	N	%
Blurred vermilion border demarcation	56	98.3
Hypopigmentation	51	89.5
Swelling	46	80.7
Red macule	44	77.2
Hyperpigmentation	28	49.1
Dryness	27	47.4
Induration	24	42.1
Crust	17	29.8
Fissures	15	26.3
White plaque	14	24.6
Erosion/Ulceration	3	3.5

lips. In AC, LOF was clinically characterized mainly as red or pigmented areas and increase of autofluorescence (IOF) as hypopigmented, whitish or hyperkeratotic areas. IOF pattern was not the same in all cases, but usually exhibited a greater intensity in the hypopigmented regions than in the white plaques. In some areas, there was also a fluorescence emission similar to the NF, and these areas were examples of transverse fissures, hypopigmentation, hyperpigmentation, red macules, and a white plaque. It is noteworthy that there were cases without any clinical alteration that exhibited LOF or IOF (16 cases; 28.1%). In this way, the region close to lip commissure was mainly characterized as an LOF area (49 cases; 86.0%) and the border between lip semi-mucosa and lip skin as an IOF area (46 cases; 80.7%) [Table 2 and Fig. 1(d) and 1(e)].

Considering the control group, patients had no evidence of AC [Fig. 1(c)], but it was possible to observe areas of focal hyperpigmentation (18 cases; 40.0%), transverse fissures (13 cases; 28.9%), hypopigmentation (10 cases; 22.2%), dryness (7 cases; 15.6%), telangiectatic vessels (3 cases; 6.7%), and an area of focal crust (1 case; 2.2%). Autofluorescence analysis of this group revealed a general homogeneous fluorescence appearance [Fig. 1(f)], with cases exhibiting an NF pattern (38 cases; 84.4%) or an IOF pattern (7 cases; 15.6%). In many of these cases, focal areas of LOF were simultaneously observed (30 cases; 66.7%). LOF areas were clinically characterized as hyperpigmentation (16 cases), hypopigmentation (8 cases), fissures (3 cases), or telangiectatic vessels (3 cases); and IOF areas were clinically characterized as a fissure (1 case) or as a crust (1 case). As observed in AC, the region adjacent to lip commissure was mainly identified as an LOF area (28 cases; 62.2%) and the vermillion border as an IOF area (17 cases; 37.8%).

A total of 113 areas were biopsied, ranging from 1 to 4 areas, with an average number of 1.98 biopsied areas per patient. Clinical assessment was used as the single clinical procedure to choose the biopsy site in 22 cases (19.5%), autofluorescence visualization alone was used in 45 cases (39.8%), and the combination of both techniques was used in 46 cases (40.7%). ED was found in 105 biopsies (93%) and they were graded as mild in 55 cases, moderate in 41 cases, and severe in 9 cases (Fig. 2). Mild and moderate ED were mainly detected at the biopsy sites chosen by the combination of both clinical and autofluorescence exams (45.4 and 41.5%, respectively), while the widefield autofluorescence imaging exam alone was the diagnostic technique that resulted in the highest detection of areas of severe ED (55.6%). Among the eight biopsy sites without ED, three were indicated by both clinical and autofluorescence exams, one by clinical exam only, and four by autofluorescence exam only. In addition, 20 patients had at least two biopsy sites separately chosen by clinical or autofluorescence indication. In seven of them, the autofluorescence exam revealed a higher grade of ED, while in four of these cases, the clinical exam revealed a higher grade of ED; in the remaining nine cases, both exams revealed the same grade of ED. However, chi-square tests revealed no statistically significant association between any diagnostic method and the presence or the degree of ED ($p > 0.05$, Table 3).

In this study, the resultant number of clustering areas was used to score the lip images. A scatter plot of the number of

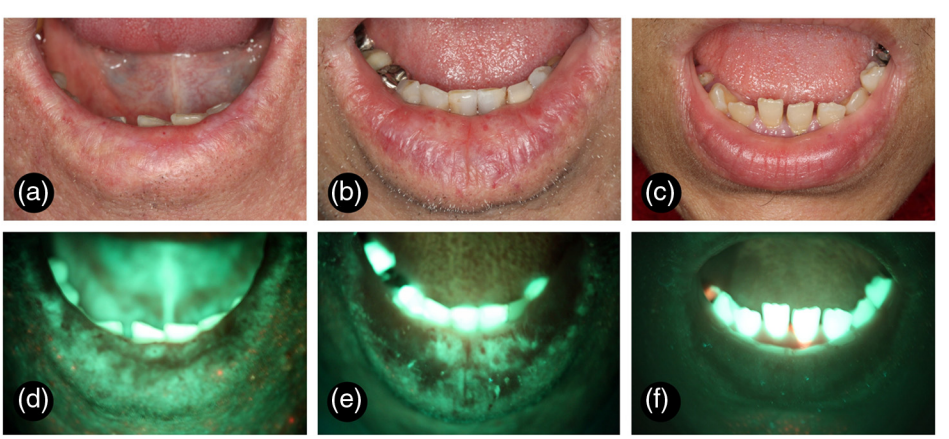

Fig. 1 Clinical and autofluorescence appearance of lower lip from AC and normal volunteer patients. (a) Clinical aspect of an AC patient presenting blurred vermilion border demarcation associated with areas of focal hypopigmentation and red and white lesions in the lower lip. (b) Clinical aspect of another AC patient showing a swollen lip with hypopigmented areas and some red spots. (c) Clinical aspect of a normal patient presenting some subtle transverse fissures. (d) Autofluorescence view of the same patient on (a), showing a heterogeneous pattern mixing areas of LOF and IOF. (e) Autofluorescence view of the same patient on (b), also showing a heterogeneous pattern. (f) Autofluorescence view of the same patient on (c), showing a homogeneous pattern of NF.

Table 2 Summary data of autofluorescence features from 57 cases of AC.

Clinical characteristics	Loss *n* (%)	Increase *n* (%)	Retention *n* (%)
Hypopigmentation[a]	3 (5.3)	51 (89.5)	3 (5.3)
Red macule[b]	43 (75.4)	0	2 (3.5)
Hyperpigmentation[c]	29 (50.9)	0	2 (3.5)
Crust	9 (15.8)	8 (14.0)	0
Fissure[d]	11 (19.3)	0	5 (8.8)
White plaque	1 (1.8)	12 (21.1)	1 (1.8)
Erosion/Ulceration	3 (5.3)	0	0
Vascular abnormalities[e]	6 (10.5)	0	0
Apparently normal lip semi-mucosa	13 (22.8)	3 (5.3)	0

[a]In two patients, some pallor areas were observed as IOF and others as LOF; and in three patients, some pallor areas were observed as IOF and others as ROF.
[b]In one patient, some red areas were observed as LOF and others as ROF.
[c]In one patient, some brown spots were observed as LOF and others as as ROF.
[d]In one patient, some fissured areas were observed as LOF and others as ROF.
[e]Varicose and telangiectatic veins.

areas for each group, both for control and AC, is presented in Fig. 3(a). Using a 10-fold cross-validation with J48 decision tree algorithm, a threshold value of 25 areas was found. K-means images with a number of areas above the threshold value was classified as AC lip and the ones with a lower number as normal lip. Using this image processing analysis, values of 80.7% of sensitivity and 78.3% of specificity were obtained. An example of a control and an AC fluorescence image processed with the K-means algorithm is shown in Fig. 3(b) and 3(c). Control normal lip had a more homogeneous fluorescence intensity distribution, with clustering areas showing regular shapes. It was possible to notice that, in cases of lower-lip AC, images were fragmented, showing a higher number of areas with an irregular pattern.

4 Discussion

AC is considered a potentially malignant disorder resulting from cumulative and long-term exposure to UV radiation.[4,5,11] Population from tropic countries near to the Equator latitude, like Brazil, have a greater risk to develop AC and lip SCC,[30] and progression to SCC may take decades.[11,12] AC clinical presentation is variable and includes early changes, such as indistinct vermilion border and dryness, and late changes, such as ulceration, induration, white and red lesions.[2,3] Nonetheless, these clinical features do not necessarily correlate with the severity of histological findings and may also include an unnoticed SCC;[1,3,13] thus, AC definitive diagnosis and treatment decision should be made taking into account the histopathological assessment.[5,11]

The present study group was clinically characterized by the presence of many different clinical findings in a single lower lip,

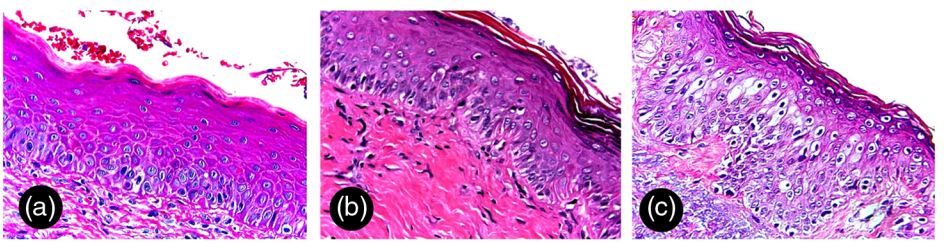

Fig. 2 ED grading of biopsies from AC patients (hematoxylin and eosin, 20×). (a) Mild ED—architectural disturbance and cytological atypia limited to the lower third of the epithelium. (b) Moderate ED—architecture disturbance and cytological atypia extending into the middle third of the epithelium. (c) Severe ED—architecture disturbance and cytological atypia above the middle third of the epithelium.

Table 3 Summary data of the diagnostic methods used to indicate 113 areas of biopsy from 57 cases of AC.

	Epithelial dysplasia				
Diagnostic methods	Absence *n* (%)	Mild *n* (%)	Moderate *n* (%)	Severe *n* (%)	Total *n* (%)
Clinical exam	1 (12.5)	10 (18.2)	8 (19.5)	3 (33.3)	22 (19.5)
Fluorescence visualization	4 (50.0)	20 (36.4)	16 (39.0)	5 (55.6)	45 (39.8)
Clinical exam and fluorescence visualization	3 (37.5)	25 (45.4)	17 (41.5)	1 (11.1)	46 (40.7)
Total	8 (7.0)	55 (48.7)	41 (36.3)	9 (8.0)	113 (100)

$p = 0.631$.

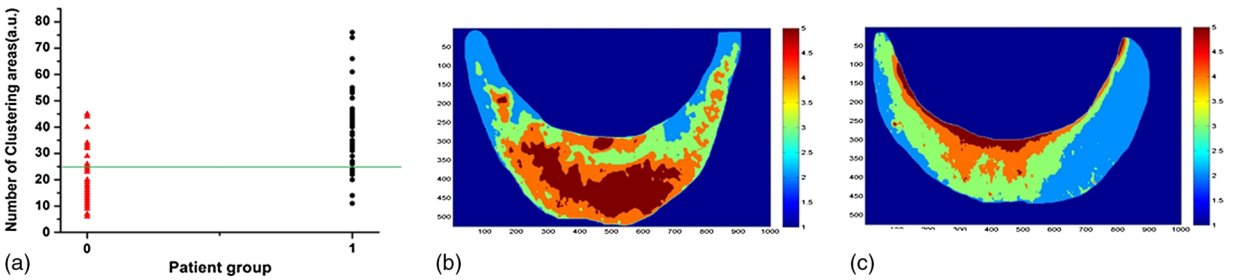

Fig. 3 Autofluorescence images processed by a clustering algorithm for automated AC diagnosis. (a) Scatter plot of number of clustering areas for control group (represented as 0 in red) and for AC group (represented as 1 in black). In green, the threshold line obtained using 10-fold cross-validation with J48 decision tree algorithm. All images with a number of areas higher than the threshold value were classified as AC. (b) and (c) K-means images obtained by processing the green channel of fluorescence images from a AC patient (b) and normal volunteer (c). Color scale is common for both images: light blue for lower-intensity pixel values and magenta for higher-intensity pixel values.

rendering a heterogeneous appearance that sometimes turn it difficult to select the best area to perform the biopsy to establish the definitive diagnosis and to identify and grade ED. In these cases, a clinician can use an adjuvant tool, as the tissue autofluorescence widefield imaging system, which has already been used to investigate oral potentially malignant disorders, and also oral SCC, oral SCC tumor margins, and high-risk oral SCC patients.[17,19,21,22,28,31–33] Autofluorescence image techniques are also described as an important adjuvant tool to choose the most appropriate region for biopsy, especially on superficial non-homogeneous oral lesions.[33] Hence, we decide to ascertain the usefulness of a tissue autofluorescence widefield imaging system in AC diagnosis.

Direct oral autofluorescence visualization is obtained by the excitation of natural biofluorophores existing in the epithelial and connective tissue in a suitable wavelength between 400 and 440 nm of light source,[34–36] and it is influenced by clinic and microscopic morphology and tissue biochemistry.[19] Oral normal mucosal sites have an almost identical autofluorescence spectral intensity, except for the lateral border of the tongue and vermillion border of the lips that have the lowest total intensities.[37] In general, pathologic tissues usually emit a lower fluorescence because of modified distribution of the native biofluorophores or have a lack of emission because of molecular or environment changes, such as collagen matrix breakdown in tissue remodeling, increased hemoglobin absorption in high-vascularized areas, epithelial thickening in malignant progression, and decreased flavin adenine dinucleotide concentration in metabolic functions.[19,21,33,36]

The qualitative evaluation of tissue autofluorescence widefield imaging system performed in this series revealed that while normal lip has a general homogeneous dark green autofluorescence appearance, AC lip has a clear heterogeneous appearance containing areas of both LOF and IOF. LOF areas observed in AC may be explained by the constant finding of solar elastosis that is characterized by the replacement of the normal collagen fibers by an amorphous basophilic granular material and deformation of superficial elastic fibers.[1–3,38] Vasodilatation is also a constant finding in AC[3] and may be responsible for maintaining a high local hemoglobin concentration and, consequently, be associated with LOF areas. Similarly, IOF areas observed in AC may be the result of hyperkeratinization[1–3] that probably increases the emitted fluorescence. Inflammation is also a common finding in AC, but its influence on tissue autofluorescence is controversial,[32,35] although it is known that oxidative phosphorylation and glycolysis may be altered during inflammation and inflammatory disorders may be characterized as both clinic and microscopic LOF.[20,22,32,33]

Interestingly, it was possible to notice that the autofluorescence heterogeneous pattern of AC reproduces its clinical heterogeneity. Red macule, hyperpigmentation, fissure, crust, vascular abnormalities, erosion, and ulceration were mainly visualized as an IOF area. Red benign, premalignant, and malignant lesions and superficial blood vessels were already described as an LOF image.[22,32,33,36] Reactive inflammatory ulceration was considered as a negative autofluorescence in a study performed by Onizawa et al.[17] using filters absorbing fluorescence below 390, 480, and 520 nm. The three cases clinically characterized as erosion and ulceration in the present study were visualized as LOF areas, but associated crust in two of these cases has an IOF appearance. The LOF visualized in our study as a hyperpigmentation was already described in the oral mucosa of three dark-skinned patients in a spectroscopy autofluorescence study, and this finding probably occurs because melanin absorbs excitation and emission fluorescence.[39] On the other hand, hypopigmentation and white plaques were mainly visualized as an IOF area. White lesions, including leukoplakias and frictional keratosis, may have LOF and IOF appearance,[28,36] and it can also show absence of autofluorescence abnormality as a case of hyperkeratotic SCC described by Koch et al.[32] Finally, it is noteworthy that some apparently normal lip vermilion also presented LOF (22.8%) or IOF (5.3%) areas, especially because clinically occult high-risk lesions will probably be visualized as an LOF area.[19,31]

There are many studies using direct autofluorescence imaging systems devices to differentiate benign from potentially malignant and malignant lesions,[17,21,22,31,33,40] but, to the best of our knowledge, there are no studies using these autofluorescence methods in AC diagnosis. The use of the tissue autofluorescence widefield imaging system in this group of AC patients was useful in the clinical differentiation of AC lip from healthy lip and in the selection of the best area for incisional biopsy. Autofluorescence general appearance was reasonably heterogeneous in AC even in cases having a subtle clinical presentation and it was especially important in the identification of light red macules. Also, the autofluorescence imaging system, alone or combined with clinical exam, was used to detect most of the areas histopathologically classified as moderate and severe ED (39 cases; 78% of only moderate and severe ED), which are considered high-risk grades for malignant transformation.[14,15,41] Nevertheless, the autofluorescence exam, with or without the

use of clinical exam in the diagnostic approach, indicates most cases with mild or no ED (52 cases; 82.5%). The aforementioned findings reinforce the impression that this device may be helpful in confirming the diagnosis of premalignant and malignant conditions, but it is not helpful in discriminating low-risk lesions from high-risk lesions without the clinical interpretation.[21,22,28,32,33,36] Yet, the value of this technology is remarkable in cases of apparently normal mucosa or semi-mucosa having an LOF appearance in patients with AC and other potentially malignant disorders or a previous history of oral cancer.[19,22,28,31]

Promising results were obtained by this study for an operator-independent classification by means of an automated algorithm. Using K-means clustering algorithm, fluorescence images were processed, improving the discrimination of the heterogeneous fluorescence of AC patients. Due to the inherent curvature of the lower lip, the central part of the illuminated area received a higher excitation intensity, resulting, in general, in a higher fluorescence intensity in this region and a lower resolution contrast at the image borders. Even with this nonuniform illumination condition, present in all cases of normal and AC lips, the proposed image processing showed relevant results. The heterogeneous fluorescence intensity distribution was the main feature observed in AC lips; so a threshold value of number of clustering areas was defined in this diagnostic algorithm. Misclassified lips showed, in the clinical assessment, hyperpigmentation, ulceration, and dryness. These false results reinforce the fact that fluorescence imaging is an auxiliary diagnostic tool and does not replace clinical examination. Tissue autofluorescence visualization presents additional information for the clinician to improve diagnostic resolution, as also stated by some authors when reporting that LOF is not useful in diagnosing premalignant and malignant conditions if the associated clinical interpretation is not performed with caution.[22,33]

The values of sensitivity and specificity for the tissue autofluorescence imaging system in the identification of oral dysplastic or malignant lesions vary in the literature. Studies evaluating patients at risk for oral cancer revealed sensitivity values varying from 98 to 100% and specificity values varying from 80.8 to 100% when discriminating normal mucosa and benign lesion from ED and cancer,[21,28,33] but these values vary from 30 to 84% of sensitivity and from 15.3 to 63% of specificity in the identification of ED.[22,36] A study using the autofluorescence imaging system coupled with an objective imaging analysis, similar to the present study, found 100% of sensitivity and 91.4% of specificity in the discrimination of normal tissue from ED and malignancy.[40] Our results of 80.7% sensitivity and 78.3% specificity show the potential of autofluorescence imaging as an auxiliary tool to discriminate AC in lower lip. This lower diagnostic resolution was already expected, since the AC tissue condition is more similar to the normal tissue, than the alterations observed at a carcinoma. In addition, as the present results showed, even a normal lip may present clinical variations, such as areas of hyperpigmentation, fissures, hypopigmentation, dryness, and punctiform red spots. Therefore, the autofluorescence from an AC lip will not be as distinct as the one from a normal lip, when compared to the autofluorescence seen in an SCC lip. The use of more complex algorithms and the addition of other fluorescence features may result in higher sensitivity and specificity.

Tissue autofluorescence widefield imaging system seems to be a valuable technique for assisting AC diagnosis, mainly in the identification of suspicious areas for incisional biopsy. However, it does not substitute clinical examination because LOF may represent benign variations that do not indicate a propensity to malignant development. As a result, the association of the autofluorescence technique with the physical exam may contribute to enhance our naked eye visualization in the identification of potentially malignant changes in this clinically heterogeneous lesion.

Acknowledgments

We would like to thank Fundação Carlos Chagas Filho de Amparo à Pesquisa do Estado do Rio de Janeiro (FAPERJ), Fundação de Amparo à Pesquisa do Estado de São Paulo (FAPESP), and Conselho Nacional de Desenvolvimento Científico e Tecnológico (CNPq) for the financial support.

References

1. G. E. Kaugars et al., "Actinic cheilitis: a review of 152 cases," *Oral Surg. Oral Med. Oral Pathol. Oral Radiol. Endod.* **88**(2), 181–186 (1999).
2. A. Markopoulos, E. Albanidou-Farmaki, and I. Kayavis, "Actinic cheilitis: clinical and pathologic characteristics in 65 cases," *Oral Dis.* **10**(4), 212–216 (2004).
3. A. S. R. Cavalcante, A. L. Anbinder, and Y. R. Carvalho, "Actinic cheilitis: clinical and histological features," *J. Oral Maxillofac. Surg.* **66**(3), 498–503 (2008).
4. I. van der Waal, "Potentially malignant disorders of the oral and oropharyngeal mucosa; terminology, classification and present concepts of management," *Oral Oncol.* **45**(4–5), 317–323 (2009).
5. N. W. Savage, C. McKay, and C. Faulkner, "Actinic cheilitis in dental practice," *Australian Dental J.* **55**(Suppl 1), 78–84 (2010).
6. J. L. Junqueira et al., "Actinic cheilitis among agricultural workers in Campinas, Brazil," *Community Dent. Health* **28**(1), 60–63 (2011).
7. P. R. Martins-Filho, L. C. Da Silva, and M. R. Piva, "The prevalence of actinic cheilitis in farmers in a semi-arid northeastern region of Brazil," *Int. J. Dermatol.* **50**(9) 1109–1114 (2011).
8. E. E. de Souza Lucena et al., "Prevalence and factors associated to actinic cheilitis in beach workers," *Oral Dis.* **18**(6), 575–579 (2012).
9. D. D. Picascia and J. K. Robinson, "Actinic cheilitis: a review of the etiology, differential diagnosis, and treatment," *J. Am. Acad. Dermatol.* **17**(2 Pt 1), 255–264 (1987).
10. J. G. de Visscher and I. van der Waal, "Etiology of cancer of the lip. A review," *Int. J. Oral Maxillofac. Surg.* **27**(3), 199–203 (1998).
11. Y. T. Jadotte and R. A. Schwartz, "Solar cheilosis: an ominous precursor: part I. Diagnostic insights," *J. Am. Acad. Dermatol.* **66**(2), 173–184 (2012).
12. J. H. Main and M. Pavone, "Actinic cheilitis and carcinoma of the lip," *J. Can. Dent. Assoc.* **60**(2), 113–116 (1994).
13. M. M. S. Nico, E. A. Rivitti, and S. V. Lourenco, "Actinic cheilitis: histologic study of the entire vermilion and comparison with previous biopsy," *J. Cutan. Pathol.* **34**(4), 309–314 (2007).
14. P. M. Speight, "Update on oral epithelial dysplasia and progression to cancer," *Head Neck Pathol.* **1**(1), 61–66 (2007).
15. S. Warnakulasuriya et al., "Oral epithelial dysplasia classification systems: predictive value, utility, weaknesses and scope for improvement," *J. Oral Pathol. Med.* **37**(3), 127–133 (2008).
16. F. C. Xavier et al., "WNT-5A, but not matrix metalloproteinase 3 or beta-catenin protein, expression is related to early stages of lip carcinogenesis," *J. Oral Pathol. Med.* **38**(9), 708–715 (2009).
17. K. Onizawa et al., "Usefulness of fluorescence photography for diagnosis of oral cancer," *Int. J. Oral Maxillofac. Surg.* **28**(3), 206–210 (1999).
18. W. H. Westra and D. Sidransky, "Fluorescence visualization in oral neoplasia: shedding light on an old problem," *Clin. Cancer Res.* **12**(22), 6594–6597 (2006).
19. C. F. Poh et al., "Direct fluorescence visualization of clinically occult high-risk oral premalignant disease using a simple hand-held device," *Head Neck* **29**(1), 71–76 (2007).

20. I. Pavlova et al., "Understanding the biological basis of autofluorescence imaging for oral cancer detection: high-resolution fluorescence microscopy in viable tissue," *Clin. Cancer Res.* **14**(8), 2396–2404 (2008).
21. P. Lane et al., "Simple device for the direct visualization of oral cavity tissue fluorescence," *J. Biomed. Opt.* **11**(2), 024006 (2006).
22. C. S. Farah et al., "Efficacy of tissue autofluorescence imaging (VELScope) in the visualization of oral mucosal lesions," *Head Neck* **34**(6), 856–862 (2012).
23. D. C. de Veld et al., "The status of in vivo autofluorescence spectroscopy and imaging for oral oncology," *Oral Oncol.* **41**(2), 117–131 (2005).
24. D. Roblyer et al., "Multispectral optical imaging device for in vivo detection of oral neoplasia," *J. Biomed. Opt.* **13**(2), 024019 (2008).
25. S. P. Schantz et al., "In vivo native cellular fluorescence and histological characteristics of head and neck cancer," *Clin. Cancer Res.* **4**(5), 1177–1182 (1998).
26. A. Gillenwater et al., "Noninvasive diagnosis of oral neoplasia based on fluorescence spectroscopy and native tissue autofluorescence," *Arch. Otolaryngol. Head Neck Surg.* **124**(11), 1251–1258 (1998).
27. N. Ramanujam, "Fluorescence spectroscopy of neoplastic and non-neoplastic tissues," *Neoplasia* **2**(1–2), 89–117 (2000).
28. A. Moro et al., "Autofluorescence and early detection of mucosal lesions in patients at risk for oral cancer," *J. Craniofac. Surg.* **21**(6), 1899–1903 (2010).
29. R. Quinlan, *C4.5: Programs for Machine Learning*, Morgan Kaufmann Publishers, San Mateo, CA (1993).
30. E. Kornevs et al., "5 year experience with lower lip cancer," *Stomatologija* **7**(3), 95–98 (2005).
31. C. F. Poh et al., "Fluorescence visualization detection of field alterations in tumor margins of oral cancer patients," *Clin. Cancer Res.* **12**(22), 6716–6722 (2006).
32. F. P. Koch et al., "Effectiveness of autofluorescence to identify suspicious oral lesions—a prospective, blinded clinical trial," *Clin. Oral Investig.* **15**(6), 975–982 (2011).
33. M. Scheer et al., "Autofluorescence imaging of potentially malignant mucosa lesions," *Oral Surg. Oral Med. Oral Pathol. Oral Radiol. Endod.* **111**(5), 568–577 (2011).
34. C. S. Betz et al., "Autofluorescence imaging and spectroscopy of normal and malignant mucosa in patients with head and neck cancer," *Lasers Surg. Med.* **25**(4), 323–334 (1999).
35. E. Svistun et al., "Vision enhancement system for detection of oral cavity neoplasia based on autofluorescence," *Head Neck* **26**(3), 205–215 (2004).
36. K. H. Awan, P. R. Morgan, and S. Warnakulasuriya, "Evaluation of an autofluorescence based imaging system (VELscope™) in the detection of oral potentially malignant disorders and benign keratosis," *Oral Oncol.* **47**(4), 274–277 (2011).
37. D. C. de Veld et al., "Autofluorescence characteristics of healthy oral mucosa at different anatomical sites," *Lasers Surg. Med.* **32**(5), 367–376 (2003).
38. S. Imayama et al., "Ultraviolet-B irradiation deforms the configuration of elastic fibers during the induction of actinic elastosis in rats," *J. Dermatol. Sci.* **7**(1), 32–38 (1994).
39. D. C. de Veld et al., "Effects of individual characteristics on healthy oral mucosa autofluorescence spectra," *Oral Oncol.* **40**(8), 815–823 (2004).
40. D. Roblyer et al., "Objective detection and delineation of oral neoplasia using autofluorescence imaging," *Cancer Prev. Res.* **2**(5), 423–431 (2009).
41. O. Kujan et al., "Evaluation of a new binary system of grading oral epithelial dysplasia for prediction of malignant transformation," *Oral Oncol.* **42**(10), 987–993 (2006).

Photodiagnosis and Photodynamic Therapy (2013) 10, 328–330

Available online at www.sciencedirect.com

SciVerse ScienceDirect

journal homepage: www.elsevier.com/locate/pdpdt

CASE REPORT/RESEARCH LETTER

Fast elimination of onychomycosis by hematoporphyrin derivative-photodynamic therapy

Ana Paula da Silva, Cristina Kurachi, Vanderlei Salvador Bagnato, Natalia Mayumi Inada PhD*

University of Sao Paulo, Physics Institute of Sao Carlos, 13566-590 Sao Carlos, SP, Brazil

Available online 12 February 2013

KEYWORDS
Photodynamic inactivation;
Photodynamic therapy;
Onychomycosis;
Photosensitizer;
Photogem®

Summary Onychomycosis is a fungal nail disease and is one of the major onychopathy worldwide. Topical or oral antifungal therapies are used to treat this disease, but often they are inefficient and oral medications can even cause several side effects. Photodynamic therapy (PDT) is a well established technique and hence, may represent an alternative non invasive technique for the treatment of onychomycosis. In this work, we present a case of onychomycosis that was completely cured by using the porphyrin–photodynamic therapy. A 59-year-old patient, who had two nails with onychomycosis (the right and the left hallux, with more than thirty and ten years, respectively) caused by fungi was treated once a week for a period of six weeks. The nails were first treated and prepared by a specialist. An hour after the photosensitization, the nail was illuminated using a light source based on light emitting diodes (LEDs) in the red wavelength (630 nm, at a total dose of 54 J/cm^2).

Background

The drugs usually indicated to treat ringworm of the nails are topical ointments, solutions or glazes. More difficult cases require treatment using oral tablets, and once the organisms become resistant, due to the slow growth of the nails, improvement is then slow. Nails can take up to 12 months to completely renovate and any treatment should be maintained throughout this whole period of time [1]. Persistence is key to conventional treatment which requires a long follow-up, and the type of treatment will depend on the extent of the ringworm. However, limitations of many possible treatments are: inadequate spectrum of activity and pharmacokinetics, drug interactions, high cost, recurrence, long duration and potential toxicity, among others. The only solution to this problem may be the use of photodynamic reactions.

Photodynamic therapy (PDT) has also promising potential in the treatment of superficial fungal skin infections caused by dermatophytes. *Trichophyton rubrum* is responsible for tinea pedis (athelete's foot), fungal folliculitis, onychomycosis, and dermatophytosis (tinea or ringworm) [2].

Knowledge of epidemiology, trends of dermatophytoses and correct understanding of the causes can lead to the

* Corresponding author at: Instituto de Física de São Carlos, Universidade de São Paulo, Grupo de Óptica, Laboratório de Biofotônica, Av. Trabalhador São-carlense, No. 400, Centro, 13566-590 São Carlos, SP, Brazil. Fax: +55 16 3373 9811.
E-mail addresses: nataliainada@ursa.ifsc.usp.br, nataliainada@gmail.com (N.M. Inada).

1572-1000/$ – see front matter © 2013 Elsevier B.V. All rights reserved.
http://dx.doi.org/10.1016/j.pdpdt.2013.01.001

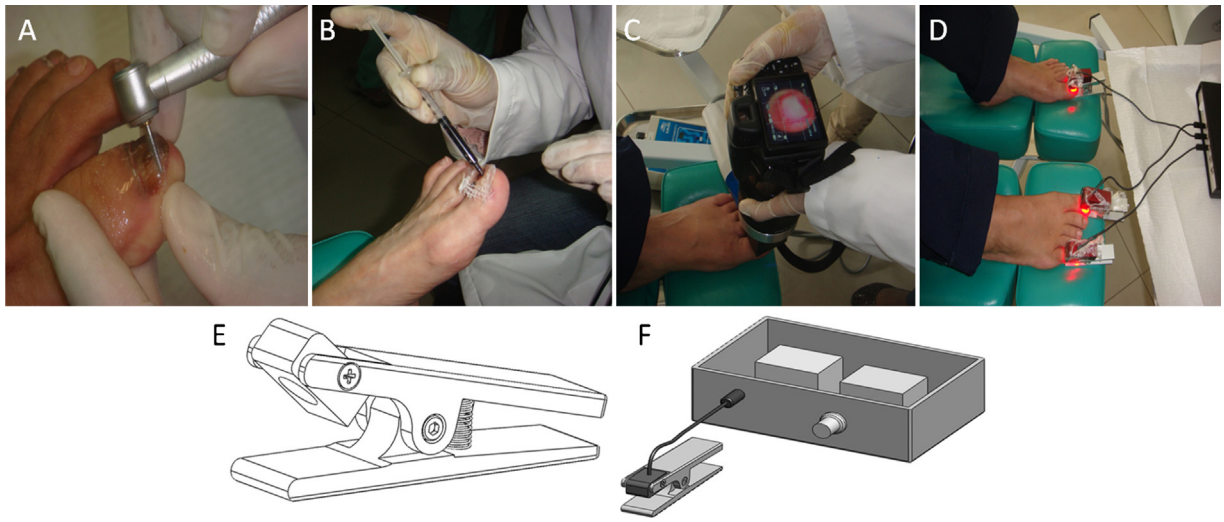

Fig. 1 Clinical trial for the photodynamic inactivation of the onychomycosis. Panel A: polishment of the nails that favors the photo sensitizer absorption. Panel B: Photogem® application. Panel C: after 1 h the photosensitizer fluorescence is checked using a digital camera coupled at a homemade device emitting at 405 nm. Panel D: irradiation of the nails using a homemade device like a staple that fits perfectly to the nails. Panel E: details of the staple. Panel F: design of the device registered in National Institute of Industrial Property (INPI Protocol No. 18110047225, 05th December 2011).

implementation of public health measures for Photodynamic therapy to reduce the growth of this type of infections. PDT is a relatively new form of treatment of fungal and bacterial infections, providing several advantages over traditional methods, using antibiotics. Advantages are: selectivity of the treatment, possibility to repeat the procedure several times if necessary, and the side effects are controlled and less adverse, minimizing the possibility of bacterial resistance [3].

This technique is based on the phototoxicity of target cells or microorganisms and involves a photosensitizing agent, the light source and molecular oxygen. The success of photodynamic therapy depends on several factors such as the amount of the drug present, the illumination of the tissue, and the photoactivation. Is a promising alternative method, which has already been used in the dermatological and recently also in the gynecological field [4,5].

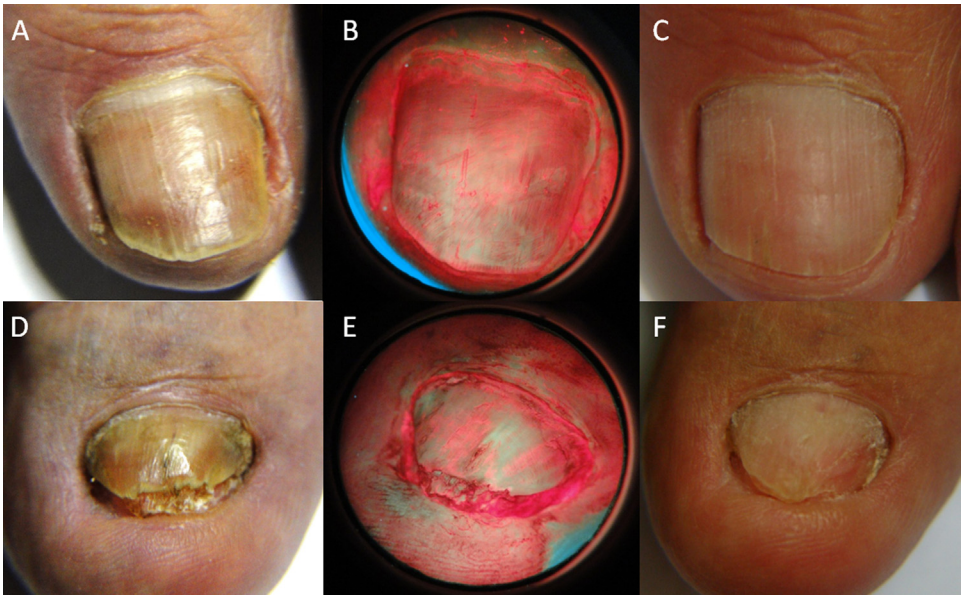

Fig. 2 Treatment of two nails of the same patient with onychomycosis. Panel A: left hallux with 10 years of injury, before PDT. Panel B: Photogem® fluorescence indicating total photosensitization of nail and adjacent tissue. Panel C: onychomycosis elimination after six weeks (six PDT sessions). Panel D: right hallux with 30 years of injury, before PDT. Panel E: photo sensitizer fluorescence. Panel E: clinical result after six PDT sessions.

In this study we analyze the efficiency of a hematoporphyrin derivative compound (Photogem®, Limited Liability Company Photogem, Moscow, Russia) applied topically, followed by PDT using a portable homemade device and anatomic based on LEDs.

Case study

We conducted this study with a patient (male, 59 years old) with nail diseases caused by fungus. This patient had the lesions for approximately 30 (right hallux) and 10 (left hallux) years and was treated with the solution Photogem®. Approval of the University Ethical Committee was obtained as required (79th Ethics Committee Meeting on November 16, 2010). The patient had not responded to oral treatment with fluconazole, and was positive for the laboratory cultures indicating the presence of fungi, has been invited to participate in this study. The patiente signed a written informed consent form.

An emollient solution of 20% urea is applied for 10 min, and approximately 0.5 mm thick of nails is removed by a micro motor with pneumatic diamond drill. The photosensitizer Photogem® (1 ml, 5 mg/ml) was applied topically to the nails (Fig. 1, panels A and B). After a period of 1 h protected from light the presence of the photosensitizer was checked using a digital camera Sony H50® coupled at other homemade device based on LEDs emitting at 405 nm (Fig. 1, panel C and Fig. 2, panels B and E). Then the region was illuminated for 9 min (total fluence of 54 J/cm^2) using a homemade light source containing one LED each anatomically staple emitting at 630 nm, with an intensity measured at the nail surface of 100 mW/cm^2 (Fig. 1, panels D—F).

Seven days after the illumination, there was a clinical evaluation to confirm the response to the treatment. The follow-up treatment was done. The process was documented using images (photographs weekly clinical cases).

The patient reported no pain, neither during the irradiation nor later. The sessions were repeated once a week, with a total of six sessions of PDT. Complete healing was reported after an irradiation over six weeks (Fig. 2, panels A—F) and in addition, the microorganism culture indicated negative for fungi.

Discussion and conclusion

In this work we are presenting a new clinical trial using porphyrin and a homemade device anatomically designed for the treatment of the onychomycosis. This work represents part of a complete research that compares two different photosensitizers and involves around 90 patients. Other compound photoactivated at 450 nm is being evaluated and we are working to present the results soon. The *in vitro* studies such as confocal microscopy are ongoing to understand the photodynamic inactivation mechanisms.

Acknowledgements

This work has been supported by grants from Fundação de Amparo à Pesquisa do Estado de São Paulo (FAPESP; CEPOF Grant No. 98/14270-8) and Financiadora de Estudos e Projeto FINEP-Gnatus (Grant No. 554339/2010-2). APS was supported by a Conselho Nacional de Desenvolvimento Científico e Tecnológico fellowship (CNPq FINEP-Gnatus; Grant No. 381132/2010-2).

References

[1] Gupta AK, Ryder JE, Johnson AM. Cumulative meta-analysis of systemic antifungal agents for the treatment of onychomycosis. British Journal of Dermatology 2004;150(3):537—44, doi:10.1046/j.1365-2133.2003.05728.x.

[2] Dai T, Fuchs BB, Coleman JJ, Prates RA, Astrakas C, St Denis TG, et al. Concepts and principles of photodynamic therapy as an alternative antifungal discovery platform. Front Microbiology 2012;3:120, doi:10.3389/fmicb.2012.00120.

[3] Gonzales FP, Maisch T. Photodynamic inactivation for controlling *Candida albicans* infections. Fungal Biology 2012;116(1):1—10, http://dx.doi.org/10.1016/j.funbio.2011.10.001

[4] Inada NM, Costa MM, Guimarães OC, Ribeiro Eda S, Kurachi C, Quintana SM, et al. Photodiagnosis and treatment of condyloma acuminatum using 5-aminolevulinic acid and homemade devices. Photodiagnosis Photodynamic Theraphy 2012;9(1):60—8, doi:10.1016/j.pdpdt.2011.09.001.

[5] Allison RR, Bagnato VS, Sibata CH. Future of oncologic photodynamic therapy. Future Oncology 2010;6(6):929—40, doi:10.2217/fon.10.51.

Oral Oncology 50 (2014) 593–599

Contents lists available at ScienceDirect

Oral Oncology

journal homepage: www.elsevier.com/locate/oraloncology

Analysis of surgical margins in oral cancer using *in situ* fluorescence spectroscopy

Ana Lucia Noronha Francisco [a], Wagner Rafael Correr [b], Clóvis Antônio Lopes Pinto [c], João Gonçalves Filho [d,e], Thiago Celestino Chulam [d,e], Cristina Kurachi [b], Luiz Paulo Kowalski [d,e,*]

[a] Department of Oral Diagnosis, School of Dentistry of Piracicaba, University of Campinas (UNICAMP), Av. Limeira, 901, Piracicaba 13414-018, São Paulo, Brazil
[b] Department of Physics and Materials Science, São Carlos Institute of Physics, University of São Paulo (USP), Av. Trabalhador São-Carlense, 400, São Carlos 13566-590, São Paulo, Brazil
[c] Department of Pathology, A.C. Camargo Cancer Center, Rua Prof. Antonio Prudente, 211, São Paulo 01509-900, São Paulo, Brazil
[d] Department of Head and Neck Surgery and Otorhinolaryngology, A.C. Camargo Cancer Center, Rua Prof. Antonio Prudente, 211, São Paulo 01509-900, São Paulo, Brazil
[e] National Institute of Science and Technology in Oncogenomics (INCITO), Rua Prof. Antonio Prudente, 211, São Paulo 01509-900, São Paulo, Brazil

ARTICLE INFO

Article history:
Received 2 July 2013
Received in revised form 10 February 2014
Accepted 11 February 2014
Available online 13 March 2014

Keywords:
Squamous cell carcinoma
Fluorescence spectroscopy
Surgical margins
Diagnosis
Oral cavity

SUMMARY

Oral cancer is a public health problem with high prevalence in the population. Local tumor control is best achieved by complete surgical resection with adequate margins. A disease-free surgical margin correlates with a lower rate of local recurrence and a higher rate of disease-free survival. Fluorescence spectroscopy is a noninvasive diagnostic tool that can aid in real-time cancer detection. The technique, which evaluates the biochemical composition and structure of tissue fluorescence, is relatively simple, fast and, accurate.

Objectives: This study aimed to compare oral squamous cell carcinoma lesions to surgical margins and the mucosa of healthy volunteers by fluorescence spectroscopy.

Materials and methods: The sample consisted of 56 individuals, 28 with oral squamous cell carcinoma and 28 healthy volunteers with normal oral mucosa. Thirty six cases (64.3%) were male and the mean age was 60.9 years old. The spectra were classified and compared to histopathology to determine fluorescence efficiency for diagnostic discrimination of tumors.

Results: In the analysis of the other cases we observed discrimination between normal mucosa, injury and margins. At two-year follow up, three individuals had local recurrence, and in two cases investigation fluorescence in the corresponding area showed qualitative differences in spectra between the recurrence area and the area without recurrence at the same anatomical site in the same patient.

Conclusion: In situ analysis of oral mucosa showed the potential of fluorescence spectroscopy as a diagnostic tool that can aid in discrimination of altered mucosa and normal mucosa.

Introduction

The options for curative treatment of oral cavity squamous cell carcinoma have not changed significantly in the last decades [1], and include surgery, radiation therapy, chemotherapy, or combinations of these modalities [2]. The choice of treatment depends mainly on the site and size of the primary lesion, in addition to the patient's age and general health [3]. Local tumor control is best achieved by complete surgical resection with adequate margins [4]. Moreover, several studies have shown the significance of positive surgical margins [5]. The clear margins status during resection is an important predictor to reduce the risk of local recurrence and a higher rate of survival [6,7]. Some conflicting results may have been due to lack of standardization of the acceptable margin distance and different clinical discrimination between margins containing small alterations or dysplasia or carcinoma *in situ* [7]. A better standardization is important because the rate of five-year overall survival of oral squamous cell carcinoma (OSCC) ranges from 50% to 60% [7,8].

Intraoperative frozen-section pathology evaluation of surgical margins in head and neck cancer resection is a common procedure that involves a close interaction between the operating room and pathologist [9]. The procedure is performed at localized selected areas and the specific margins reported by the surgeon are considered. However, in addition to its high cost and the entire margin extension is not evaluated [10].

* Corresponding author at: Department of Head and Neck Surgery and Otorhinolaryngology, A.C. Camargo Cancer Center, Rua Prof. Antonio Prudente, 211, 01509-900 São Paulo, Brazil. Tel.: +55 11 2189 5172; fax: +55 11 5541 3341/5541 0326.
E-mail address: lp_kowalski@uol.com.br (L.P. Kowalski).

http://dx.doi.org/10.1016/j.oraloncology.2014.02.008
1368-8375/

Fluorescence spectra superficially collected differ depending on the excitation wavelength, investigated oral site, biochemical composition, and tissue architecture. The excitation wavelength affects the final fluorescence spectrum, as various endogenous fluorophores may be excited. The oral mucosa presents distinct structural characteristics according to the anatomic sites investigated. More keratinized areas, as gingival and hard palate, show distinct fluorescence spectra when compared to buccal mucosa and inner lower lip, for example. Also, the tongue shows different fluorescence patterns depending on its interrogated site, lateral border, ventral or dorsum. Indeed, the use of optical techniques for analysis of biological tissues has shown good results in the diagnosis and evaluation of cellular changes by anatomical sites [11–13]. Additionally, optical tools are fast, accurate, and noninvasive procedures [14]. Using fluorescence spectroscopy, we compared OSCC lesions to surgical margins and the mucosa of healthy volunteers, with the aim to investigate whether the optical technique could provide information similar to that obtained with the pathologist report and being a diagnostic aid *in situ*.

Materials and methods

A total of 56 subjects were enrolled in the study, 20 (35.7%) women and 36 (64.3%) men. The average age was 60.9 years old (range 34–82); the average age of women was 62.8 years old and that of men was 59.9 years. Seventeen subjects (60.7%) were smokers and 19 (67.8%) reported either chronic or social alcohol consumption.

All subjects were interviewed and filled in a standardized anamnesis form regarding habits associated with the risk of oral cancer (tobacco and alcohol) and family history. A clinical examination was performed and participants signed an informed consent form (Table 1).

Twenty-eight healthy volunteers with normal oral mucosa and no signs of airway and upper digestive tract tumors and 28 patients with OSCC at various stages of development were investigated. The patients with OSCC underwent surgery under general anesthesia and had at least one safety margin area in the same oral site of the tumor. They were approached in cancer prevention campaigns that occur at the hospital AC Camargo Cancer Center (see Tables 2–4).

Patients were identified by a numerical code and underwent biopsy of the oral cavity with histopathology diagnosis, which is considered the gold standard for diagnosis of OSCC. Qualitative fluorescence patterns were determined to identify potential spectroscopic signatures for each mucosal class evaluated: OSCC (B), margin (M), and normal mucosa (N). The spectra were mathematically processed using different multivariate analysis as principal component analysis (PCA), K-nearest neighbor (KNN), and intra-spectral analysis using emission ratio at specific spectral regions to, whenever possible, define discrimination algorithms to establish the difference from normal *versus* carcinoma.

In healthy volunteers, fluorescence examination was performed in the same anatomical sites of the cancer of the case corresponding and a cytology sample was collected taken from these areas. In individuals with cancer of the oral cavity, site interrogation was performed in the operating room at the hospital AC Camargo Cancer Center, in São Paulo, Brazil. Surgical margins were defined by the head and neck surgeon after induction of general anesthesia with in minimum 10 mm of the distance of the limit of the lesion.

A homemade fluorescence spectroscopy system composed of excitation light, investigation probe, portable USB 2000 spectrophotometer (Ocean Optics, USA), and laptop computer was assembled and a solid-state laser diode emitting at 406 nm was employed, at a maximum emission of 8 mWA Y-type probe (Ocean Optics, USA) with one end connected to the laser and the other to the spectrophotometer was used. Two optical fibers of 600 μm diameter were positioned side by side, one to conduct the excitation light and the other to collect the re-emitted light from the tissue. The collection fiber is connected to the spectrometer, and a longpass filter at 420 nm is placed to reject the excitation light. The interrogation area diameter of the metallic probe is of 1.6 mm and the overall diameter in contact with the tissue surface was 3.2 mm. The fluorescence measurements are collected and recorded using the spectrometer manufacturer's software (OOIBase32, Ocean Optics, USA).

The clinical characteristics, oral cancer site, and lesion measurements from OSCC patients were recorded. The spectroscopic measurements were carried out at the border of the lesion; superficial heterogeneities, as erythroplakia, leukoplasia or granulomatous region, were identified and representative regions were chosen to correlate with different clinical patterns; necrotic areas were

Table 1
Clinicopathological characteristics of the individuals.

Characteristic	Options	Number	Percentage (%)
Tobacco consumption			
OSCC	Yes	17	60.7
	No	11	39.3
Normal	Yes	9	32.2
	No	19	67.8
Alcohol consumption			
OSCC	Yes	19	67.8
	No	9	32.2
Normal	Yes	15	53.6
	No	13	46.4
Clinical tumor status	T*is*	2	7.1
	T1	1	3.6
	T2	9	32.1
	T3	12	42.9
	T4	4	14.3
Site	Border of the tongue	10	35.8
	Floor of the mouth	4	14.3
	Retromolar	4	14.3
	Buccal mucosa	3	10.7
	Labial mucosa	3	10.7
	Hard palate	2	7.1
	Gingiva	2	7.1
Pathological degree	*In situ*	2	7.1
	I	3	10.7
	II	15	53.6
	III	8	28.6

Table 2
Comparison of means between NB and each N1, N2, N3, N4 e N5 and B1, B2, B3, B4 e B5 in anatomical site floor of the mouth ($n = 4$ cases).

Variable	Mean	Standard deviation	*p*-value
Nb	50189.67	9644.14	
N1	38167.67	27342.01	0.418
N2	37028.33	25394.99	0.350
N3	37512.00	26221.05	0.379
N4	37185.00	26232.37	0.371
N5	32956.00	23807.27	0.212
B1	32640.33	29456.1	
B2	31482.00	30621.48	0.423
B3	31948.67	30141.33	0.422
B4	31702.33	34152.08	0.366
B5	29741.22	33677.89	0.656

p-value obtained by paired *t* Student test.
Table 2 shows the mean comparison between NB and each measures of N of the floor of the mouth. There are not statistical significance difference between the mean of the NB and each N.
Also no difference was observed for B1 and the other Bs.

Table 3
Comparison of means between NB and each N1, N2, N3, N4 e N5 and B1, B2, B3, B4 e B5 in anatomical site border of the tongue ($n = 10$ cases).

Variable	Mean	Standard deviation	p-value
Nb	83803.89	22504.67	
N1	53472.67	9960.63	0.110
N2	52624.22	10250.91	0.116
N3	51831.33	10628.39	0.122
N4	61305.89	18415.09	0.215
N5	61778.11	18202.44	0.214
B1	44599.73	17171.81	
B2	44532.38	17744.42	0.979
B3	44552.73	17752.12	0.986
B4	38297.83	16045.12	0.472
B5	39053.26	15781.38	0.544

p-value obtained by paired t Student test.
Table 3 shows the mean comparison between NB and each measures of N in border of the tongue. There are not statistical significance difference between the mean of the NB and each N.
Also no difference was observed for B1 and the other Bs.

Table 4
Comparison of means between NB and each N1, N2, N3, N4 e N5 and B1, B2, B3, B4 e B5 in anatomical site retromolar ($n = 4$ cases).

Variable	Mean	Standard deviation	p-value
Nb	64803.79	12504.31	
N1	63725.77	10196.64	0.412
N2	52624.23	10261.97	0.316
N3	59431.36	10783.47	0.223
N4	63105.89	14435.23	0.226
N5	64678.17	14902.55	0.216
B1	54576.79	18541.93	
B2	52539.36	22784.45	0.875
B3	52551.81	23252.99	0.886
B4	53295.29	23046.18	0.573
B5	53604.22	25719.33	0.415

p-value obtained by paired t Student test.
Table 4 shows the mean comparison between NB and each measures of N in retromolar area. There are not statistical significance difference between the mean of the NB and each N.
Also no difference was observed for B1 and the other Bs.

avoided. At least five spectroscopic measurements were performed in each chosen area at a wavelength of 406 nm. Surgical margins were analyzed in a concentric manner in clockwise direction (3, 6, 9 and 12 o'clock). Whenever possible, all subjects with OSCC had at least one border of the lesion and the surgical margin analyzed in the same anatomical site.

A 3 mm punch biopsy was performed in OSCC patients at the time of surgery. All biopsies were performed on sites that had spectroscopic measurements taken according to the heterogeneity of the border of the lesion, and in the four margin points more distant of the tumor, always in the cases with the corresponding anatomical site of the tumor border and margin. The specimens were placed in plastic vials containing 10% formalin for later processing.

The spectra collected were analyzed according to the different tumor site locations and the spectra of the altered tissue injury compared to that of normal tissue and surgical margins. The results of the spectra were correlated with the histopathological diagnosis and we conducted a descriptive analyzes to better discriminate between normal tissue and neoplastic tissue.

The spectral processing was performed using MATLAB. An algorithm was developed to import the data from the data sheet. Some spectral data were excluded due to saturated emission intensity and/or detected outliers. All data from the dorsum of the tongue were excluded due to variable fluorescence emission, mainly resulting from the presence of porphyrins produced by bacteria

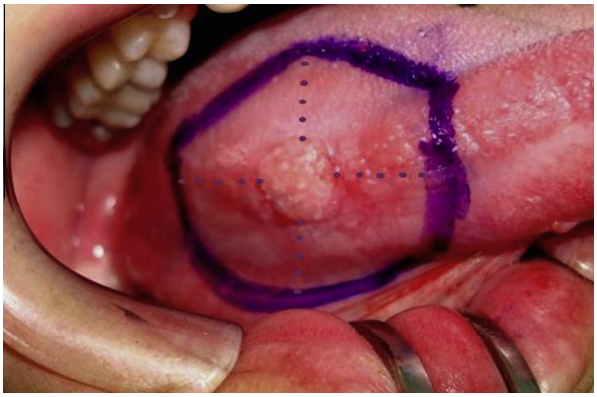

Fig. 1. Measures of the margins, moving away from the tumor, as from the border of the lesion until surgical margin determined clinically free of disease.

present in this region, even after oral asepsis. This fact not observed in other anatomical sites evaluated.

The groups proposed for classification of spectra were: normal (N), squamous cell carcinoma (B), and surgical margins (M). The measures of the margins were numbered, in ascending order of the 1–5, moving away from the tumor, as from the border of the lesion until surgical margin determined clinically free of disease (Fig. 1). First, an overall assessment was performed regardless of oral tumor site. Then, a subsequent analysis was performed according to group and anatomical site.

It was observed that some spectra presented a high ratio between peaks around 495 nm and 515 nm. A MATLAB algorithm was written to calculate this ratio for spectra from each group (Normal, Border, and Margins) in each anatomical site, according to the following equation and diagram (Fig. 2): Areas 1 and 2 were randomly chosen within the total area most representatives of the spectra.

$$R = \frac{A_1}{A_2} = \frac{\int_{491}^{501} Id\lambda}{\int_{511}^{521} Id\lambda}$$

The boxplot was used for data visualization. Briefly, this type of graph is used in descriptive statistics for side-by-side visualization of data from different experiments or distinct groups in same experiment. In this paper, we used box plot to observe the differences between normal group (N), border of lesion (B), and margins (M1 to M5). The whiskers extend to the most variable data point, and the outliers are plotted individually as asterisks.

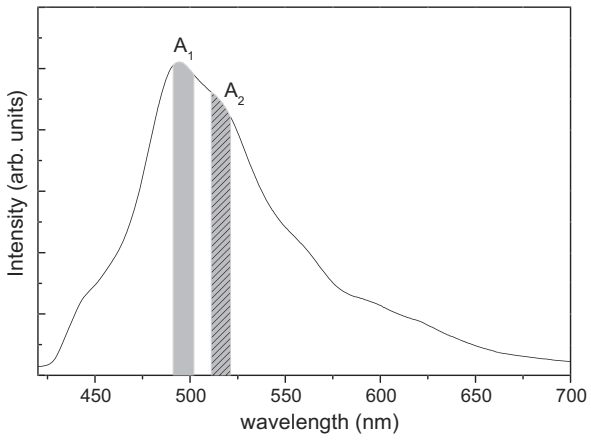

Fig. 2. The ratio parameter was calculated according to the above diagram.

Results

In this study, we found that the most affected oral site was the border of the tongue (BOT) with 10 lesions (35.7%) followed by the floor of the mouth (FOM) and retromolar region (RM), with four cases (14.3%) each. The predominant pathology was invasive carcinoma (25 cases, 89.3%), and grade 2 tumors were the most prevalent ones (15 cases, 53.6%). There were 12 T3 (42.8%), nine T2 (32.1%), and four T4 cases (14.3%), and of these, 11 (39.3%) patients had positive neck lymph nodes (Table 1).

A total of 1024 spectra at 406 nm excitation were evaluated: 610 spectra of normal mucosa from healthy volunteers, 214 spectra of tumor margins from OSCC lesions, and 200 spectra of (clinically normal) surgical margins from OSCC lesions.

In healthy volunteers, oral mucosa at gingiva, BOT, and FOM showed low spectra intensity at 406 nm excitation. The tongue and FOM are highly vascularized tissues, and hemoglobin is the main absorber component, whereas the oxyhemoglobin and methemoglobin have their absorption regions in the wavelength of 540 nm and 630 nm, respectively. The spectra of normal mucosa from healthy volunteers followed a similar pattern in each oral site variation that could be observed was the emission intensities. In the cytology analysis all cells were free of malignant changes could include keratosis, hyperplasia and inflammation cells as long as there was no dysplasia or carcinoma cells.

The cancer interrogation sites collected were in the clinically detected borders. The central region of the lesions was not interrogated to avoid necrotic tissue commonly present at ulcerated tumors.

Initially, the spectral analysis was based on qualitative differences between spectra of the border of OSCC tumors, surgical margins, and/or normal mucosa at the same anatomical site. In general, the margins of the tumor showed fluorescence emission patterns ranging from the tumor border to normal mucosa. All surgical margins microscopically examined resulted in free disease tissues, with some changes such as the presence of inflammation, hyperplasia, acanthosis and/or mild dysplasia.

Of the 28 subjects with OSCC that had been operated on, three patients exhibited two-year local recurrence, and only two of them exhibited local recurrence where fluorescence measurements were taken. The spectra were investigated in each patient to check if there were detectable changes in the fluorescence pattern. Two patterns were observed in margins clinically defined as normal. The spectra of the anterior margins were qualitatively similar to the spectra of normal mucosa whereas the spectra of the posterior margins were more similar to the spectra of the border of the tumor. We also observed changes in the red region (600–650 nm) of posterior margins and lesions (Figs. 3 and 4). In pathological reviewing was not observed some data of tissue change that justifies tumor recurrence in these two cases.

Spectral analysis could not be performed in samples from the third individual with local recurrence in the hard palate because there was no fluorescence interrogation in the same area of recurrence. In this case, no margins were taken from the hard palate in the primary resected tumor.

The qualitative analysis of the spectra showed major differences between the border of the cancerous lesion and normal mucosa and surgical margins.

The box plot in Fig. 5 shows a clear differentiation in the ratio of spectra between B and N to M. For instance, there were differences in spectra in border of the tongue between B and N and M, but no difference between M and N or N and M5 measurements ($p = 0.276$) (Fig. 5C). Conversely, there were no differences between equidistant points M1, M2, M3, M4 and M5.

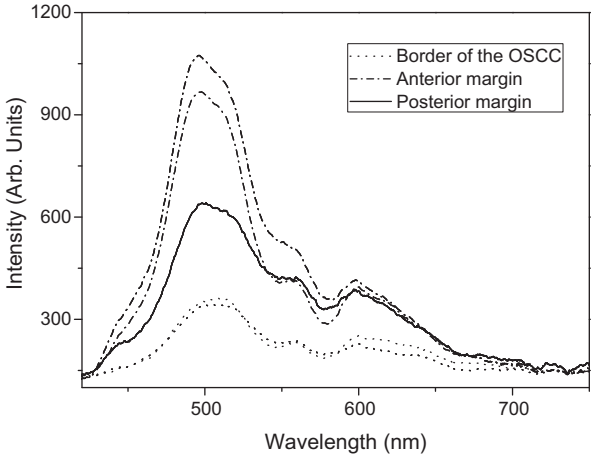

Fig. 3. Qualitative analysis of spectra of the border of the tongue from subject 1, who had local recurrence in the posterior limit.

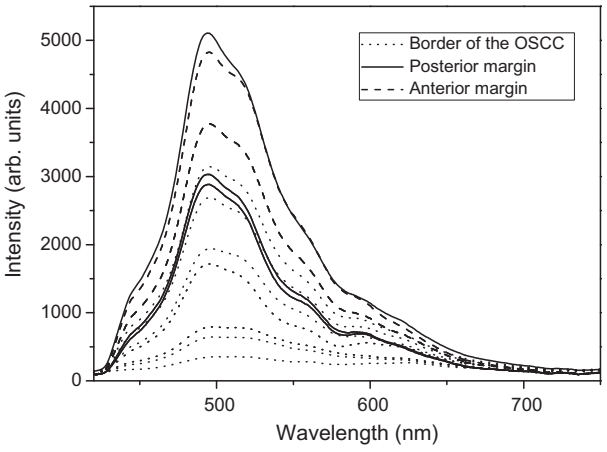

Fig. 4. Qualitative analysis of spectra of the border of the tongue from subject 2, who had local recurrence in the posterior margin.

After normalization by the maximum, mean of the degree of similarity of the spectra were calculated for each patient compared with a volunteer, in each anatomical site, using the comparison by calculating the Euclidean distance. The graph in Fig. 6 is the calculations similarity between the spectra of B and N, n1, n2, n3, n4 and n5 are the calculations between N and M, B1, B2, B3, B4 and B5 are the calculations between spectra M and C.

It was expected that the values of *n* series were lower and b values were higher, but this was not observed in all patients, which can be justified by the presence of subclinical changes in the oral mucosa of surgical margins.

Global survival of patients with T1–T2 and T3–T4 stage tumors after two-year follow-up was 91% and 78%, respectively, and specific disease-free survival after 2 years was 91.7% for T1–T2 and 66% for T3–T4 stages. In addition, individuals under primary treatment for lymph node metastasis had 44.5% of specific disease-free survival after 2 years ($p = 0.008$).

Of the 28 cases, six (21.4%) cases had recurrence within 2 years, three (10.7%) cases had local recurrence specifically in the primary site, and the other three cases were lymph node or distant metastasis. In all three cases of local recurrence, fluorescence had previously identified spectra that were similar to the primary tumor (Fig. 7). The two recurrent cases had grade II OSCC and free surgical margins of tumor in the primary surgery.

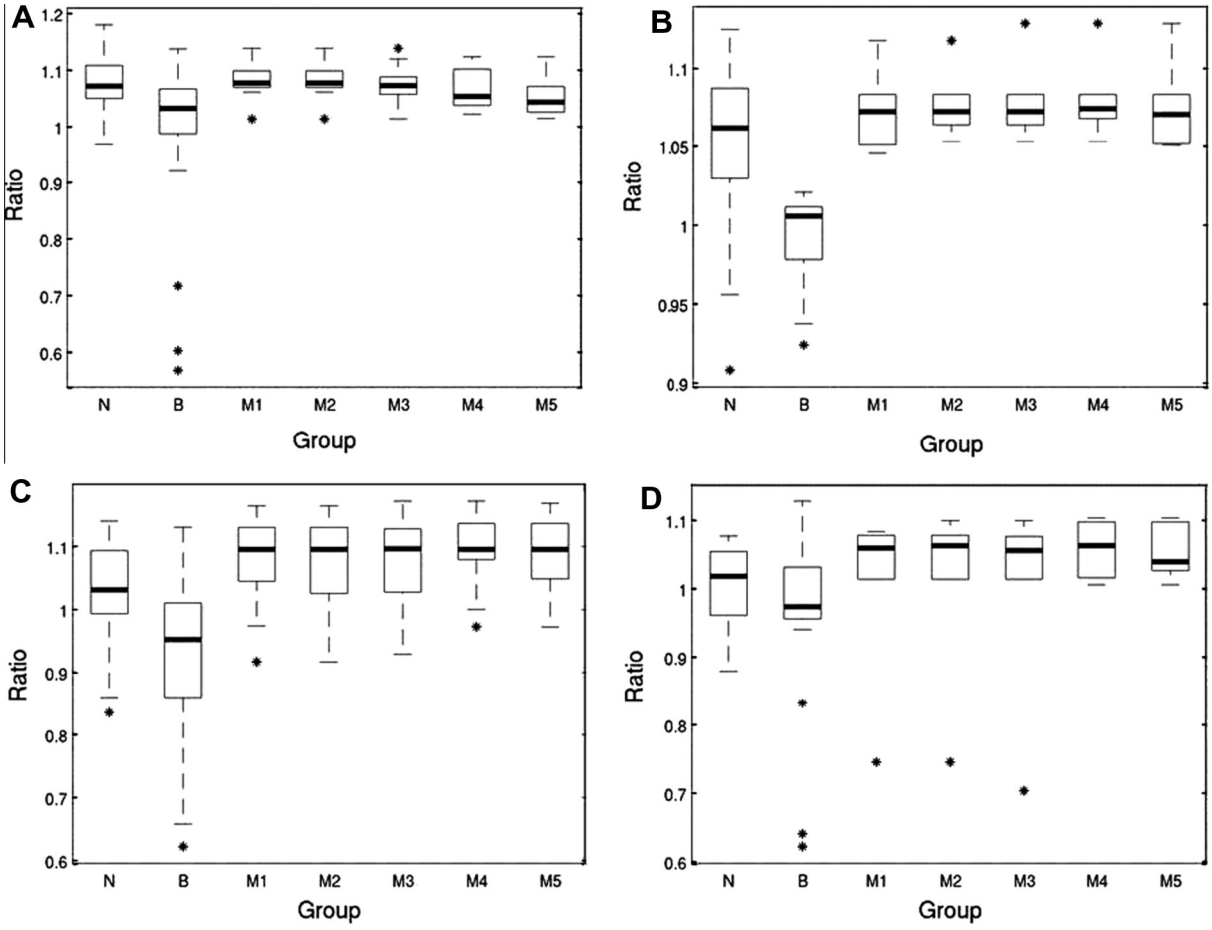

Fig. 5. Box plots of the ratio of spectra mensuration in normal mucosa (N), border of lesion (B) and surgical margins (M) of the different anatomical sites. A – Floor of the mouth; B – buccal mucosa; C – border of the tongue; and D – lip.

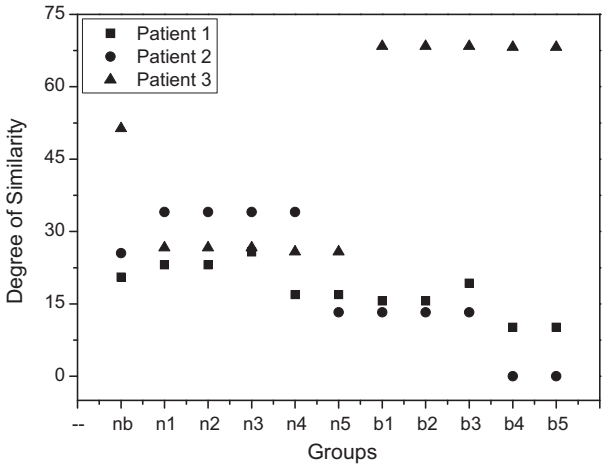

Fig. 6. Analysis of degree of similarity of three patients with OSCC in floor of the mouth.

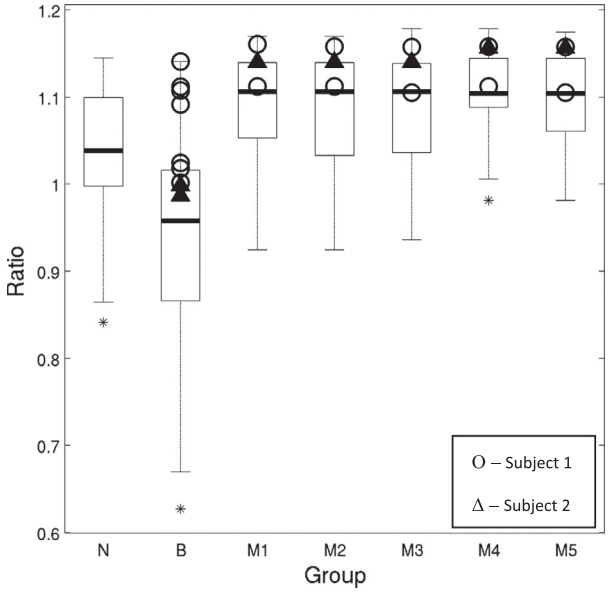

Fig. 7. Box plot with recurrence patients highlighted.

Discussion

The definition of surgical margins is a critical step in radical surgery for OSCC because there is no consensus on the surgical extension, which strongly depends on surgeon's and pathologist's decisions [4]. Ideally, the definition of safety margin resection should consider several factors about the tumor and oral site, and the three-dimensional aspects of tumor extension and pathological factors such as the pattern of invasion should be analyzed [8,15,16].

Frozen section of surgical margins is an accepted practice in OSCC surgery and a pathological method for providing rapid

consultation during surgery [9]. The accuracy of frozen section diagnosis is very close to the final diagnosis (>90%) and the usefulness of the procedure is well established [10,17]. The report of negative surgical margins is a prognostic factor of extreme importance. The retreatment for positive margins after initial surgery is an effective form of treatment, but it is undesirable, and often not possible. Moreover, frozen sections are high priority, costly procedures that require multiple well-trained professionals [10]. In this study, all cases had surgical margins frozen and their pathology reports were free of neoplasia.

Evidence suggests that an occult disease often extends beyond the extent of the visible tumor and is responsible for the high rate of recurrence of carcinoma at the primary site (~10–30%) [18]. There is great need to develop new approaches that can be easily used in clinical practice to facilitate detection of this field cancerization, and optical techniques represent an attractive tool to assess tissue changes [11,19–21]. These optical techniques are advantageous due to their fast response and use of noninvasive and *in situ* interrogation. Moreover, patient investigation can usually be performed in preoperative and intraoperative settings for better delineation of tissue changes. This study did not aim to exclude the conventional procedure of frozen section and pathologic evaluation, but test the fluorescence spectroscopy as an auxiliary tool for better delineation of surgical margins *in situ* in an attempt to prevent a rapprochement.

Some studies have shown an association between the loss of fluorescence cancer development and in normal tissues corroborating with the present study. For instance, direct fluorescence visualization has been used in different tissues and organs and successfully distinguished premalignant and malignant lesions that cannot be detected by naked eye [22–26]. In our study, spectroscopy satisfactorily discriminated normal tissue and slightly altered mucosa from cancerous lesions. However, discrimination between normal and altered mucosa showed low accuracy.

Several studies have demonstrated that the analysis of the light/tissue interaction can result in the discrimination of changes in tissue structure and metabolic activity such as the breakdown of the collagen matrix and the change in concentration of nicotinamide adenine dinucleotide in its reduced form (NADH), tryptophan, tyrosine, phenylalanine, and flavin adenine dinucleotide (FAD) [27–30]. In addition, some of the epithelium of the oral cavity is covered with a layer of keratin, which scatters some of the incoming excitation light and reduces its penetration depth, a fact confirmed in our study. It has also been shown that collagenase enzymes responsible for the degradation of collagen are usually present in tissue areas undergoing significant architectural changes, resulting in the observed changes in NADH and collagen contributions to the tissue fluorescence spectrum with progression of disease [31].

In an *in vitro* study, Ingrams et al. showed that the differences between normal and abnormal mucosa were most marked at 410 nm excitation and observed increased fluorescence above 600 nm in the dysplastic tissue comparable to histopathology [11]. Similarly, Gillenwater et al. used autofluorescence at neoplastic and non-neoplastic oral mucosa and showed that the alterations in areas of disease were seen more in the ratio of 600 nm to 455–490 nm [32]. Different from our study that uses the technique of fluorescence spectroscopy for *in situ* evaluation, but also resulted in higher uptake of changes in the ratio of 450–600 nm.

De Veld et al. and Richards-Kortum et al. reported that several studies using autofluorescence spectroscopy and imaging successfully distinguished normal and altered oral mucosa (dysplasia and cancer). Thus, autofluorescence spectroscopy and imaging are helpful in diagnosis of lesions of the oral mucosa and has shown great promise for enhancing visualization of neoplastic areas. These studies assessed the limits of the lesions is clinically visible or not, however, few studies have evaluated the surgical margins of cancer lesions of the oral cavity [33,34], be a difference in our study.

The decision on the length of clinically normal tissue that should be removed beyond the tumor is highly controversial. Typically, surgeons arbitrarily remove 10 mm or more of normal mucosal margin if anatomically feasible. However, this approach does not completely remove all the abnormal tissue in all individuals. Poh et al. and Svistun et al. showed that most tumors have occult changes and that the width for subclinical extension ranges between 4 and 25 mm, often extending in at least one direction by over 10 mm with some potentially malignant disorder, thus increasing the chance of tumor recurrence [21,23]. In this study, all surgical margins were clinically normal and had negative results for malignancy, but subclinical alterations showed mild spectral changes confirming the need for further investigation at the molecular level.

Fluorescence techniques are advantageous over frozen section histopathology because they are noninvasive and provide information on microscopic diagnosis and lesion margins. In fact, some studies using fluorescence techniques have reported high sensitivity and specificity in the diagnosis of dysplasia and invasive carcinoma during surgery [4,21,36]. In study of Poh et al. confirmed that the development of new optical techniques that enable us to visualize spectral alterations associated with oral cancer could add a further dimension to these developing paradigms regarding the concept of cancer/risk field [21].

Poh et al. had great results with the protocol of optically-guided approach for oral lesions surgical and has demonstrated interest in continuing the study doing a follow-up of individuals monitoring the changes in the mucosa in surgery sites both in the clinical evaluation and by fluorescence [35]. The risk of recurrence or development of a new primary tumor warrant long-term follow-up for all patients treated for cancer of the oral cavity, and regular monitoring is indicated for a minimum 5 years. Finally, high-risk patients should be monitored more frequently than low-risk ones [1,8,37]. We continue doing clinical follow-up of the subjects of the research, as well as other hospital patients, and until the present moment only two cases recurred. Find difficulty making the following fluorescence seen that cases who received radiotherapy had changed spectra when compared with individuals without radiotherapy and fluorescence exams performed in surgery.

Conclusion

Our results demonstrate the potential of the system to detect tissue changes. Fluorescence spectroscopy is a noninvasive method that must be further explored as a tool for detection of surgical margins. The accuracy of this technique for the detection of positive margins and field cancerization should be investigated in a large number of patients.

Conflict of interest statement

None declared.

Acknowledgments

The authors thank FAPESP (CEPOF-CEPID Program, proc. no 98/14270-8, aid research proc. no 07/57126-5 and no 11/10802-1), CNPq (proc. no 477439/2007-1 and ALNF scholarship no 140493/2011-5), and INCITO for financial support.

References

[1] Genden EM, Ferlito A, Silver CE, Takes RP, Suárez C, Owen RP, et al. Contemporary management of cancer of the oral cavity. Eur Arch Otorhinolaryngol 2010;267:1001–17.

[2] Jerjes W, Upile T, Petrie A, Riskalla A, Hamdoon Z, Vourvachis M, et al. Clinicopathological parameters, recurrence, locoregional and distant metastasis in 115 T1–T2 oral squamous cell carcinoma patients. Head Neck Oncol 2010 April 20:2–9.

[3] El-Husseiny G et al. Squamous cell carcinoma of the oral tongue: an analysis of prognostic factors. Br J Oral Maxillofac Surg 2000;38:193–9.

[4] Hinni ML Ferlito A, Brandwein-Gensler MS, Takes RP, Silver CE, Westra WH, Seethala RR, et al. Surgical margins in head and neck câncer: a contemporary review. Head and Neck 2012.

[5] Looser KG, Shah JP, Strong EW. The significance of "positive" margins in surgically resected epidermoid carcinomas. Head Neck Surg 1978;1:107–11.

[6] Batsakis JG. Surgical excision margins: a pathologist's perspective. Adv Anat Pathol 1999;6:140–8.

[7] Meier JD, Oliver DA, Varvares MA. Surgical Margin determination in head and neck oncology: current clinical pratice. The results of an international american head and neck society member survey. Head Neck 2005;27:952–8.

[8] Kademani D, Bell RB, Bagheri S, et al. Prognostic factors in intraoral squamous cell carcinoma: the influence of histologic grade. J Oral Maxilofac Surg 2005;63:1599–605.

[9] Wick MR, Mills SE. Evaluation of margins in anatomic pathology: technical, conceptual and clinical considerations. Semin Diagn Pathol 2002;19:207–18.

[10] Black C, Marotti J, Zarovnaya E, Paydarfar J. Critical evaluation of frozen section margins in head and neck cancer resections. Cancer 2006;107. 2792–800.

[11] Ingrams DR, Dhingra JK, Roy K, Perrault Jr DF, Bottrill ID, Kabani S, et al. Autofluorescence characteristics of oral mucosa. Head Neck 1997;19(1):27–32.

[12] de Veld DCG, Skurichina M, Witjes MJH, Duin RPW, Sterenborg DJCM, Star WM. Autofluorescence characteristcis of healthy oral mucosa at different anatomical sites. Lasers Surg Med 2003;32:367–76.

[13] Pavlova I, Weber CR, Schwarz RA, Williams M, Gillenwater A, Richards-Kortum R. Fluorescence spectroscopy of oral tissue: monte carlo modeling with site-specific tissue properties. J Biomed Opt 2009;14(1):014009.

[14] Pavlova I, Williams M, El-Naggar A, Richards-Kortum R, Gillenwater A. Understanding the biological basis of autofluorescence imaging for oral cancer detection: high-resolution fluorescence microscopy in viable tissue. Clin Cancer Res 2008;14:2396–404.

[15] Beitler JJ, Smith RV, Silver CE, et al. Close or positive margins after surgical resection for the head and neck câncer patient: the addition of brachytherapy improves local control. Int J Radiat Oncol Biol Phys 1998;40(2):313–7.

[16] Sparano A, Weinstein G, Chalian A, Yodul M, Weber R. Multivariate predictors of occult neck metastasis in early oral tongue cancer. Otolaryngol Head Neck Surg 2004;131:472–6.

[17] Zarbo RJ, Hoffman GG, Howanitz PJ. Interinstitutional comparison of frozen section consultation. Arch Pathol Lab Med 1991;115:1187–94.

[18] Leemans CR, Tiwari R, Nauta JJ, van der Waal I, Snow GB. Recurrence at the primary site in head and neck cancer and the significance of neck lymph node metastases as a prognostic factor. Cancer 1994;73:187–90.

[19] Lam S, MacAulay C, Hung J, LeRiche J, Profio AE, Palcic B. Detection of dysplasia and carcinoma *in situ* with a lung imaging fluorescence endoscope device. J Thorac Cardiovasc Surg 1993;105:1035–40.

[20] Ramanujam N, Mitchell MF, Mahadevan A, et al. In vivo diagnosis of cervical intraepithelial neoplasia using 337-nm-excited laser-induced fluorescence. Proc Natl Acad Sci USA 1994;91:10193–7.

[21] Poh CF, Zhang L, Anderson DW, Durham JS, Williams PM, Priddy RW, et al. Fluorescence visualization detection of field alterations in tumor margins of oral cancer patients. Clin Cancer Res 2006 November 15;12(22):6716–22.

[22] Gillenwater A, Jacob R, Ganeshappa R, Kemp B, El-Naggar AK, Palmer L, et al. Noninvasive diagnosis of oral neoplasia based on fluorescence spectroscopy and native tissue autofluorescence. Arch Otolaryngol Head Neck Surg 1998;124:1251–8.

[23] Svistun E, Alizadeh-Naderi R, El-Naggar A, Jacob R, Gillenwater A, Richards-Kortum R. Vision enhancement system for detection of oral cavity neoplasia based on autofluorescence. Head Neck 2004;26:205–15.

[24] Meyer LE, Lademann J. Application of laser spectroscopic methods for in vivo diagnostics in dermatology. Laser Phys Lett 2007;4:754–60.

[25] AlSalhi MS, Masilamani V, Atif M, Farhat K, Rabah D, Al Turki MR. Fluorescence spectra of benign and malignant prostate tissues. Laser Phys Lett 2012;9:631–5.

[26] Poh CF, Ng SP, Williams PM, et al. Direct fluorescence visualization of clinically occult high-risk oral premalignant disease using a simple hand-held device. Head Neck 2006 September 18. on-line publication.

[27] Ganesan S, Sacks PG, Yang Y, Katz A, Al-Rawi M, Savage HE, et al. Native fluorescence spectroscopy of normal and malignant epithelial cells. Cancer Biochem Biophys 1998;16:365–73.

[28] Schantz SP, Kolli V, Savage HE, et al. In vivo native cellular fluorescence and histological characteristics of head and neck cancer. Clin Cancer Res 1998;4:1177–82.

[29] Chu SC, Hsiao T-CR, Lin JK, Wang C-Y, Chiang HK. Camparison of performance of linear multivariate analysis methods for normal and dysplasia tissues differentiation using autofluorescence spectroscopy. IEEE Trans Biomed Eng 2006;53:2265–73.

[30] Swinson B, Jerjes W, El-Maaytah M, Norris P, Hopper C. Optical techniques in diagnosis of head and neck Malignancy. Oral Oncol 2006;42:221–8.

[31] Badizadegan K, Backman V, Boone CW, Crum CP, Dasari RR, Georgakoudi I, et al. Spectroscopic diagnosis and imaging of invisible pre-cancer. Faraday Discuss 2004;126:265–79.

[32] Gillenwater A, Jacob R, Richards-Kortum R. Fluorescence spectroscopy; a technique with potiential to improve the early detection of aerodigestive tract neoplasia. Head Neck 1998;20(6):556–62.

[33] De Veld DCG, Witjes MJH, Sterenborgb HJCM, Roodenburg JLN. The status of in vivo autofluorescence spectroscopy and imaging for oral oncology. Oral Oncol 2005;41:117–31.

[34] Roblyer D, Kurachi C, Stepanek V, Williams MD, El-Naggar AK, Lee JJ, et al. Objective detection and delineation of oral neoplasia using autofluorescence imagingobjective detection and delineation of oral neoplasia using autofluorescence imaging. Cancer Prev Res (Phila) 2009 May;2(5):423–31.

[35] Poh CF, Durham JS, Brasher PM, Anderson DW, Berean KW, MacAulay CE, et al. Canadian Optically-guided approach for Oral Lesions Surgical (COOLS) trial: study protocol for a randomized controlled trial. BMC Cancer 2011;11:462.

[36] Hughes OR, Stone N, Kraft M, Arens C, Birchall MA. Optical and molecular techniques to identify tumor margins within the larynx. Head Neck 2010 November;32(11):1544–53.

[37] Dissanayaka WL, Pitiyage G, Kumarasiri PV, Liyanage RL, Dias KD, Tilakaratne WM. Clinical and histopathologic parameters in survival of oral squamous cell carcinoma. Oral Surg Oral Med Oral Pathol Oral Radiol 2012 April;113(4):518–25.

Photomedicine and Laser Surgery
Volume 32, Number 11, 2014

Pp. 627–632
DOI: 10.1089/pho.2014.3805

Effects of Photodynamic Therapy with Blue Light and Curcumin as Mouth Rinse for Oral Disinfection: A Randomized Controlled Trial

Diego Portes Vieira Leite, DS,[1,2] Fernanda Rossi Paolillo, PhD,[2] Thiago Nogueira Parmesano,[2] Carla Raquel Fontana, PhD,[3] and Vanderlei Salvador Bagnato, PhD[2]

Abstract

Objective: The purpose of this study was to evaluate the effects of the antimicrobial photodynamic therapy (a-PDT) with blue light and curcumin on oral disinfection during the 2 h after treatment. ***Background data:*** a-PDT is a technique that can potentially affect the viability of bacterial cells, with selective action targeting only areas with photosensitizer accumulation. ***Materials and methods:*** A randomized controlled trial was undertaken. Twenty-seven adults were randomly divided into three groups: (1) the PDT group, which was treated with the drug, curcumin, and blue light ($n=9$); (2) the light group, which was treated only with the blue light, and no drug ($n=9$) and; (3) the curcumin group, which was treated only with the drug, curcumin, and no light ($n=9$). The irradiation parameters were: blue light-emitting diode (LED) illumination (455 ± 30 nm), 400 mW of average optical power, 5 min of application, illumination area of 0.6 cm^2, 600 mW/cm^2 of intensity, and 200 J/cm^2 of fluence. A curcumin concentration of 30 mg/L was used. The saliva samples were collected for bacterial counts at baseline and after the experimental phases (immediately after treatment, and 1 and 2 h after treatment). Serial dilutions were performed, and the resulting samples were cultured on blood agar plates in microaerophilic conditions. The number of colony-forming units (CFU) was determined. ***Results:*** The PDT group showed a significant reduction of CFU immediately after treatment (post-treatment) with PDT (5.71 ± 0.48, $p=0.001$), and 1 h (5.14 ± 0.92, $p=0.001$) and 2 h (5.35 ± 0.76, $p=0.001$) after treatment, compared with pretreatment (6.61 ± 0.82). There were no significant changes for the light group. The curcumin group showed a significant increase of CFU 1 h after treatment (6.77 ± 0.40, $p=0.02$) compared with pretreatment (5.57 ± 0.91) falling to baseline values at 2 h after treatment (5.58 ± 0.70). ***Conclusions:*** The PDT group showed significant difference in microbial reduction ($p<0.05$) compared with both the light and curcumin groups until 2 h post-treatment. The new blue LED device for PDT using curcumin may be used for reduction of salivary microorganisms, leading to overall disinfection of the mouth (e.g., mucosa, tongue, and saliva), but new protocols should be explored.

Introduction

The normal mouth has a large number of bacteria. It results in increased risk of infection when many types of surgical procedures are performed, mainly intraoral surgery. In these cases, prophylactic systemic antibiotics are used, but these drugs may be associated with unfavorable side effects. Oral antiseptics (for example, chlorhexidine) can also be used in these cases, but the reduction of intraoral bacterial counts is temporary.[1] In this context, new procedures for oral disinfection should be investigated.

Blue light (405–470 nm) without the addition of exogenous photosensitizers (PS) has intrinsic antimicrobial effect and shows fewer deleterious effects to mammalian cells than ultraviolet irradiation.[2] According Soukos et al.,[3] the amount of endogenous porphyrin and/or other cell pigments produced in *Prevotella intermedia*, *Porphyromonas gingivalis*, *Prevotella melaninogenica*, and *Prevotella nigrescens* can explain a susceptibility to blue light resulting in oral disinfection.

Moreover, curcumin [1,7-bis(4-hydroxy-3-methoxyphenyl)-1,6-heptadiene-3,5,-dione] shows antimicrobial activity as

[1]Department of Biomedical Engineering from University of Camilo Castelo Branco (UNICASTELO) São José dos Campos, SP, Brazil.
[2]Optics Group from Physics Institute of São Carlos (IFSC), University of São Paulo (USP), São Carlos, SP, Brazil.
[3]Department of Clinical Analysis, School of Pharmaceutical Sciences, Universidade Estadual Paulista (UNESP), Araraquara, SP, Brazil.

well. Curcumin is the principal yellow pigment isolated from turmeric (*Curcuma longa Linn*).[4] Several pharmacological properties of curcumin have been reported, such as antioxidant and anti-inflammatory,[4,5] antibacterial,[6] antifungal,[7] and anticarcinogenic[5] effects, mainly with high doses of curcumin alone.[8] Because of the extended antimicrobial activity of curcumin and its safety assessed by clinical trials in humans,[9] it was used as a structural sample to design the new antimicrobial agents with modified and increased antimicrobial activities through the synthesis of various derivatives related to curcumin.[10] Moreover, curcumin-mediated antimicrobial photodynamic therapy (a-PDT) can be used at low doses in combination with light exposure, with considerable antibacterial effect. In this context, curcumin has a rather broad absorption peak (range 300–500 nm), with a maximum absorption band at wavelength 430 nm, and it can be used as PS in a-PDT.[11]

PDT uses a nontoxic drug called a PS, which is activated by exposure to light of a specific wavelength in the presence of oxygen. This results in the production of reactive oxygen species (ROS), which can potentially affect the viability of bacterial cells with selective action targeting only areas with PS accumulation.[12,13] In this context, PDT has no side effects, and bacteria do not develop resistance to ROS.[1]

Several *in vitro* studies and clinical trials were performed to investigate bactericidal action and oral disinfection using blue light[3,14,15] or curcumin,[16,17] or by performing PDT with blue light and curcumin.[18–22] In dentistry, a-PDT may reduce both dental plaque and the risk of developing caries, as well as contributing to treating gingivitis, periodontitis, peri-implantitis and endodontic diseases.[23]

Previous clinical trials from our group have found that PDT with blue light and curcumin significantly reduced salivary microorganisms pre- and post-treatment.[1] However, oral disinfection as a function of time, to our knowledge, has not been investigated. Therefore, the aim of this study was to evaluate the effects of the PDT with blue light and curcumin on oral disinfection during 2 h after treatment. Our target was overall oral flora (mucosa, tongue, saliva), conducting analyses of salivary pathogens before and after antimicrobial photodynamic therapy. Our hypothesis was that blue light with or without curcumin, as well as only curcumin, could reduce colony-forming units (CFU).

Materials and Methods

The current research has been approved by the Ethics Committee of the Federal University of São Carlos (UFSCar) in São Carlos, Brazil (N. 258.461). The study was registered with the National Institutes of Health (NIH) ClinicalTrials (NCT02152475). All subjects signed written informed consent forms before their participation in the study.

A randomized controlled trial was undertaken. The inclusion criteria were healthy adults not using any antibiotic therapy who did not perform any oral hygiene, such as flossing, brushing, or use of antiseptic mouthwash, and who had fasted for 12 h prior the treatment and measurements. The exclusion criteria were having had oral cancer, smoking, pregnancy, or wearing partial or total dentures or orthodontic brackets. We performed simple randomization by a computer program. Twenty-seven healthy adult females and males between 20 and 35 years of age were randomly divided into three groups: (1) the PDT group, which was treated with the drug, curcumin, and blue light ($n=9$); (2) the light group, which was treated only with the blue light, and no drug ($n=9$); and (3) the curcumin group, which was treated only with the drug, curcumin, and no light ($n=9$).

Instrumentation to perform PDT

In order to perform PDT on the oral cavity, a device based on blue light-emitting diode (LED) (455 ± 30 nm) with transparent acrylic diffuser tip and cylindrical shape (89 mm length and 6.73 mm diameter) was developed by researchers of the industry (MM Optics, São Carlos, SP, Brazil) and the Optics Group of the Physics Institute of São Carlos (IFSC), University of São Paulo (USP). An optical power meter model FieldMaster TO-II (Coherent Inc., Santa Clara, CA) linked to a photodetector was used to calibrate this device, and to reveal a 400 mW average optical power, a 0.6 cm^2 illumination area, and a 600 mW/cm^2 intensity. The light was applied for 5 min, which led to an energy density (radiation dose) delivered of $\sim$200 J/cm^2. We considered a total energy per unit of area reaching the surface as the delivered dose, but this was not necessarily uniformly absorbed. The dose delivery was approximated, because different areas and several distances were irradiated. The new blue LED device in the oral cavity can be seen in Fig. 1. Although we applied the blue LED for 5 min as in the clinical trial of Araújo and collaborators,[1] the device

FIG. 1. New blue light-emitting diode (LED) device for photodynamic therapy (PDT) in the oral cavity.

TABLE 1. EFFECTS OF THE BLUE LED ILLUMINATION WITH OR WITHOUT CURCUMIN

	Pretreatment	*Post-treatment*	*Post 1 h*	*Post 2 h*
PDT group	6.61 ± 0.82	5.71 ± 0.48[a]	5.14 ± 0.92[a]	5.35 ± 0.76[a]
Light group	5.67 ± 0.82	6.10 ± 0.62	5.51 ± 0.93	5.84 ± 0.65
Curcumin group	5.57 ± 0.91	6.21 ± 0.58	6.77 ± 0.40[a]	5.58 ± 0.70[b]

Data represent the $\log_{10}$ CFU/mL.
[a]Significant intragroup difference compared with pretreatment (two way ANOVA with post-hoc Tukey, $p < 0.01$).
[b]Significant intragroup difference compared with period immediately before (two way ANOVA with post-hoc Tukey, $p < 0.05$).
LED, light-emitting diode; PDT, photodynamic therapy; CFU, colony-forming units.

geometry used in our study was different; therefore, the parameters also were different.

Curcumin

A stock solution (1.5 g/L) of curcumin (PDT Pharma, Cravinhos, SP, Brazil) was prepared in dimethylsulfoxide (DMSO) (0.1%) and then diluted in autoclaved distilled water (980 mL) to obtain the concentration used (30 mg/L). The literature explores different concentrations.[18–20,22] In the clinical trial of Araújo and collaborators,[1] the curcumin salt used had 1 g of salt containing 0.654 g of the cucumin plus curcuminoid, but in our study, natural curcumin (curcumin 53.4% and curcuminoid 46.16%) was used.

Treatment for oral disinfection

The volunteers in the PDT group used mouthwash with 20 mL of curcumin solution for 5 min, after which the solution was expelled and a blue light was introduced to activate the curcumin for 5 min. In the same way, the oral cavity of the light group was illuminated with blue light for 5 min and the curcumin group used mouthwash with 20 mL of curcumin solution for 5 min.[1] We did not use similar parameters of the blue illumination and curcumin concentration to those applied in *in vitro* studies, because *in vivo* studies show complexity regarding variety of biological tissues in the oral cavity and in immunological response.

Microbiological analyses

Two saliva samples from each volunteer were collected at each time point (pretreatment, post-treatment, post 1 h, and post 2 h) and stored in sterile containers. The saliva samples underwent serial dilutions and 100 μL aliquots were plated on Brain Heart Infusion Agar (BHIA) with 10% Sheep Blood (Difco Laboratories, Detroit, MI) plates (in duplicate) and then incubated under microaerophilic conditions for 48 h at ~36°C. After incubation, the total number of CFUs was determined.[1]

Statistical analysis

The data were expressed as means and standard deviations. In order to assess the effect of the treatments, CFU/mL values were transformed to logarithm ($\log_{10}$). The Shapiro–Wilk test was used to analyze data normality and the homogeneity of variances using Levene's test. Two way repeated measures ANOVA with post-hoc Tukey tests were used to compare changes in CFUs as a function of time. The independent factors were group (with three levels: PDT, light, and curcumin groups) and time (with four levels: pretreatment, post-treatment, post 1 h, and post 2 h), which was also considered a repeated measurement (intragroup differences). The survival fraction normalized and the delta CFU between the situations before and after the treatments (post-treatment, post 1 h, and post 2 h) was performed for intergroup comparisons using a one-way ANOVA with post-hoc Tukey tests. The Statistica for Windows Release 7 software (Statsoft Inc., Tulsa, OK) was used for the statistical analysis, and the significance level was set at 5% ($p < 0.05$).

Results

The PDT group showed a significant reduction in CFUs (1 log reduction) at post-treatment, post 1 h, and post 2 h ($p < 0.01$) compared with instance pretreatment. There were no significant changes for the light group. The curcumin group showed a significant increase in CFUs at post 1 h ($p < 0.05$) compared with pretreatment, falling to baseline values at post 2 h. These intragroup differences can be seen in the Table 1. The PDT group showed a significant difference ($p < 0.05$) in both normalized CFUs (Fig. 2) and microbial reduction (Fig. 3) compared with both the light and curcumin groups.

Discussion

The main finding of this study was that the PDT group showed reduction in CFUs immediately post-treatment.

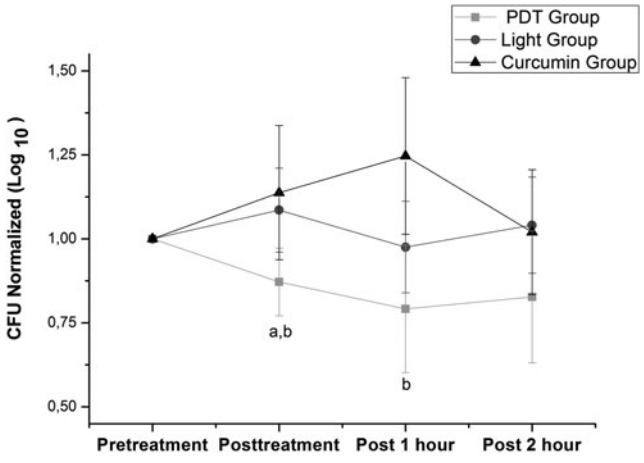

FIG. 2. Normalized colony-forming units (CFU). [a]Significant intergroup difference compared with light group (one way ANOVA with post-hoc Tukey, $p < 0.05$). [b]Significant intergroup difference compared with curcumin group (one way ANOVA with post-hoc Tukey, $p < 0.01$).

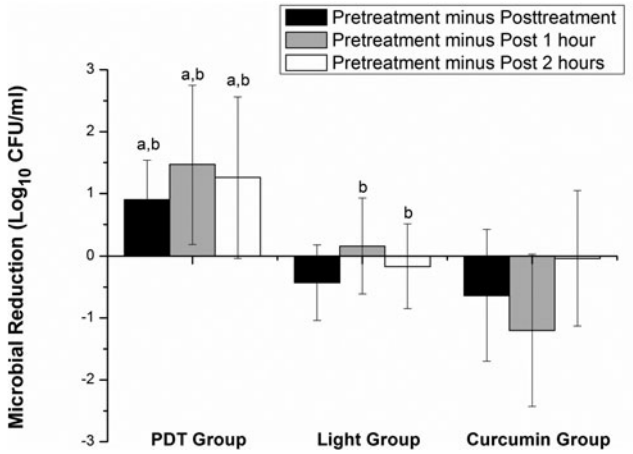

FIG. 3. Viable counts of colony-forming units (CFU) between pretreatment and after treatment. Significant intergroup difference (one way ANOVA with post-hoc Tukey, $p<0.05$). The photodynamic therapy (PDT) group showed significant microbial reduction compared with both the light[a] and curcumin[b] groups at pretreatment minus posttreatment ($p=0.02$ and $p=0.03$), pretreatment minus post 1 h ($p=0.01$ and $p=0.04$), and pretreatment minus post 2 h ($p=0.04$ and $p=0.03$). The light group showed significant difference compared with the curcumin[b] group ($p=0.01$).

Surprisingly, this antimicrobial effect was observed for 1 h after PDT (~1 log reduction). These findings corroborate study of Araújo et al.,[1] which investigated the immediate effects of PDT with blue light and curcumin in a clinical trial. Other studies also showed the positive effects of a-PDT. However, these studies used first and second generation photosensitizers such as porphyrin derivative,[24] phthalocyanines,[13] chlorine,[25] toluidine blue,[26] and methylene blue,[27] which may target both gram-negative and gram-positive bacteria.

Regarding a-PDT with curcumin and blue light, several *in vitro* studies were performed. Dovigo et al.[18,19] showed that low curcumin concentrations were effective for inactivating *Candida albicans* when associated with blue LED (450 nm) excitation. In similar studies, Araújo et al.[22,28] found reduction of *Streptococcus mutans* and *Lactobacillus acidophilus* on planktonic cultures,[28] and this reduction was more effective in biofilm compared with carious dentine conditions.[22] In a recent study, Pileggi et al.[20] showed that curcumin associated with a dental quartz-tungsten-halogen light source, emitting blue light (380–500 nm) inactivated *Enterococcus faecalis* on planktonic cultures or in biofilm cultures. In another recent study, Panhóca et al.[29] performed PDT with blue LED and curcumin associated with surfactant (sodium dodecyl sulfate 0.1%), and showed inactivation of *S. mutans* in biofilm, optimizing a-PDT. In the same line, Paschoal et al.[21] showed that a low concentration of curcumin associated with white light (400–700 nm with a central wavelength of 550 nm) illumination lead to inactivation of *S. mutans*.

These results with regard to a-PDT are limited to an *in vitro* model; however, they may support our clinical trial results. Moreover, these *in vitro* model results also showed that blue light irradiation alone or curcumin alone did not reduce CFU.

Unlike other *in vitro* studies, the work of Lipovsky et al.[30] showed bacterial reduction (*Staphylococcus aureus* and *Escherichia coli*) with blue light (415 and 455 nm) alone, mainly at higher fluences (120 J/cm^2); however, at low fluences, blue light enhanced bacterial proliferation.[31] In addition, Feuerstein et al.[14] showed bacterial reduction (*P. gingivalis* and *Fusobacterium nucleaturn*) with blue light (450 nm) at fluences of 62, 78, and 94 J/cm^2 under aerobic condition; however, this phototoxic effect was not observed when the bacteria were exposed to light under anaerobic conditions. Considering blue LED applications, several clinical trials for treatment of acne showed positive effects of this wavelength.[31,32] It is also evidenced by decrease numbers of *Propionibacterium acnes in vitro*.[32] Therefore, the antibacterial effect of blue light is dose dependent as well as dependent upon the response of an organism to O_2 in its environment.

Regarding use of curcumin alone, our study showed that CFU increased significantly, suggesting that curcumin probably caused disaggregation of dental plaque clumps on tooth enamel leading to saliva. Curcumin has been tested as a compound to inhibit fibril formation. Rabbie et al.[33] observed disaggregation of preformed fibrils upon addition of curcumin. Overall, this compound appears to be able to interact with native, intermediate, and fibrillar forms.[34,35] There is a fair amount of support from oral research to suggest that bacteria fibrils are made of protein, and some evidence that suggests that some are even made of glycoprotein. They are difficult to remove, and some strains of oral streptococci have tufts of fibrils (that were grouped together into a new species and given the name ''*Streptococcus cristae*'').[36] There is evidence that fibril tufts and coaggregation may also be involved in adhesion, this time to rod-shaped bacteria, to make the structures commonly found in mature dental plaque called ''corncob-configuration.''[37]

Considering the action on adhesion, our result in which curcumin alone increased CFUs significantly, suggests that this mouth rinse disrupts coaggregation bacteria attachment to a tooth surface, leading bacteria to saliva. However, several studies have shown that curcumin and other oral disinfectants reduced CFU. Curcumin mouth rinse may be dependent upon several factors, including duration of fasting[28] and time of mouth rinse.[38] Although there is a growing number of publications about the effect of curcumin on bacterial reduction,[16,18,28,39,41] few publications[28,39] such as this study observed the magnitude of curcumin as a mouth rinse.

In an *in vitro* model, Hegde and Kesaria[17] showed that curcumin reduced only *C. albicans*, and that sodium hypochlorite and neem (*Azadirachta indica*) were more effective in microbial inactivation, because it reduced both *E. faecalis* and *C. albicans*. In a clinical trial, Bhat et al.[16] showed that the antimicrobial efficacy of neem (3%) was highest, followed by cetylpyridinium chloride (0.5%), curcumin (5%), and chlorhexidine gluconate (0.2%) when the CFU (*S. mutans*) reduction was measured. Chlorhexidine is widely used in dentistry for decontamination. In the study by Hayek et al.,[41] *Prevotella sp.*, *Fusobacterium sp.*, and *Streptococcus beta-haemolyticus* were significantly reduced in ligature-induced peri-implantitis in dogs; however, no significant differences were observed between chlorhexidine and PDT with paste-based azulene and GaAlAs laser ($\lambda=660$ nm).

The action of curcumin alone as mouth rinse is quite encouraging for a further development of the technique, as prewash plaque remover and the reduction of 1 log for 2 h after PDT is an excellent result, considering the advantages of curcumin being a natural substance and harmless to the oral tissues. Overall, decontamination using a simple procedure is desirable for general use in dentistry. In this context, the reduction of bacterial counts and its maintenance during 2 h are important for several intraoral surgical procedures during a single session. Moreover, bacterial reduction is initiated on superficial surfaces of the oral environment, and after multiples sessions of PDT, deeper layers can be achieved. PDT is cumulatively bactericidal.[42] However, some limitations of our study were the small sample size per group, and not having used different procedures for optimizing a-PDT. Future studies should explore these aspects.

Conclusions

In conclusion, in this study, the results indicate that curcumin has a potential to disaggregate oral plaque, and the new blue LED device for PDT-curcumin may be used for reduction of salivary microorganisms lasting 2 h, leading to overall disinfection of the mouth for several intraoral surgical procedures during a single session of dentistry. However, new protocols should be explored to optimize a-PDT.

Acknowledgments

The authors thank the National Council for Scientific and Technological Development (CNPq) - grant no. 573587/2008 and the São Paulo Research Foundation (FAPESP) - grant nos. 2013/07276-1 and 2013/14001-9 for financial support. The authors also acknowledge scientific contributions and helpful advice from Hérica Ricci and Vitor Hugo Panhóca.

Author Disclosure Statement

No competing financial interests exist.

References

1. Araújo, N.C., Fontana, C.R., Gerbi, M.E., and Bagnato, V.S. (2012). Overall-mouth disinfection by photodynamic therapy using curcumin. Photomed. Laser Surg. 30, 96–101.
2. Dai, T., Gupta, A., Murray, C.K., Vrahas, M.S., Tegos, G.P., and Hamblin, M.R. (2012). Blue light for infectious diseases: Propionibacterium acnes, Helicobacter pylori, and beyond? Drug Resist. Updat. 15, 223–236.
3. Soukos, N.S., Som, S., Abernethy, A.D., Ruggiero, K., Dunham, J., Lee, C, Doukas, A.G., and Goodson, J.M. (2005). Phototargeting oral black-pigmented bacteria. Antimicrob. Agents Chemother. 49, 1391–1396.
4. Somparn, P., Phisalaphong, C., Nakornchai, S., Unchern, S., and Morales, N.P. (2007). Comparative antioxidant activities of curcumin and its demethoxy and hydrogenated derivatives. Biol. Pharm. Bull. 30, 74–78.
5. Aggarwal, B.B., Kumar, A., and Bharti, A.C. (2003). Anticancer potential of curcumin: preclinical and clinical studies. Anticancer Res. 23, 363–398.
6. Tajbakhsh, S., Mohammadi, K., Deilami, I., Keivan, Z., Fouladvand, M., Ramedani, E., and Asayesh, G. (2008). Antibacterial activity of indium curcumin and indium diacetylcurcumin. Afr. J. Biotechnol. 7, 3832–3835.
7. Martins, C.V., da Silva, D.L., Neres, A.T., Magalhães, T.F., Watanabe, G.A., Modolo, L.V., Sabino, A.A., de Fátima, A., and de Resende, M.A. (2009). Curcumin as a promising antifungal of clinical interest. J. Antimicrob. Chemother. 63, 337–339.
8. Moghadamtousi, S.Z., Kadir, H.A., Hassandarvish, P., Tajik, H., Abubakar, S., and Zandi, K. (2014). A review on antibacterial, antiviral, and antifungal activity of curcumin. Biomed. Res. Int. 2014:186864.
9. Hatcher, H., Planalp, R., Cho, J., Torti, F.M., and Torti, S.V. (2008). Curcumin: from ancient medicine to current clinical trials. Cell Mol. Life Sci. 65, 1631–1652.
10. Anand, P., Kunnumakkara, A.B., Newman, R.A., and Aggarwal, B.B. (2007). Bioavailability of curcumin: problems and promises. Mol Pharm. 4, 807–818.
11. Haukvik, T., Bruzell, E., Kristensen, S., and Tønnesen, H.H. (2010). Photokilling of bacteria by curcumin in selected polyethylene glycol 400 (PEG 400) preparations. Studies on curcumin and curcuminoids, XLI. Pharmazie 65, 600–606.
12. Dai, T., Huang, Y.Y., and Hamblin, M.R. (2009). Photodynamic therapy for localized infections state of the art. Photodiagnosis Photodyn Ther. 6, 170–188.
13. Longo, J.P., Leal, S.C., Simioni, A.R., de Fátima, M.M.A.S., Tedesco, A.C., and Azevedo, R.B. (2012). Photodynamic therapy disinfection of carious tissue mediated by aluminum-chloride-phthalocyanine entrapped in cationic liposomes: an in vitro and clinical study. Lasers Med. Sci. 27, 575–584.
14. Feuerstein, O., Ginsburg, I., Dayan, E., Veler, D., and Weiss, E.I. (2005). Mechanism of visible light phototoxicity on Porphyromonas gingivalis and Fusobacterium nucleatum. Photochem. Photobiol. Photochem. Photobiol. 81, 1186–1189.
15. Bumah, V.V., Masson–Meyers, D.S., Cashin, S.E., and Enwemeka, C.S. (2013). Wavelength and bacterial density influence the bactericidal effect of blue light on methicillin-resistant Staphylococcus aureus (MRSA). Photomed. Laser Surg. 31, 547–553.
16. Bhat, P.K., Badiyani, B.K., Sarkar, S., Chengappa, S., and Bhaskar, N.N. (2012). Effectiveness of antimicrobial solutions on Streptococcus mutans in used toothbrushes. World J. Dent. 3, 6–10.
17. Hegde, V., and Kesaria, D.P. (2013). Comparative evaluation of antimicrobial activity of neem, propolis, turmeric, liquorice and sodium hypochlorite as root canal irrigants against E. Faecalis and C. Albicans – An in vitro study. Endodontology 25, 38–45.
18. Dovigo, L.N., Pavarina, A.C., Carmello, J.C., Machado, A.L., Brunetti, I.L., and Bagnato, V.S. (2011). Susceptibility of clinical isolates of Candida to photodynamic effects of curcumin. Lasers Surg. Med. 43, 927–934.
19. Dovigo, L.N., Pavarina, A.C., Ribeiro, A.P., Brunetti, I.L., Costa, C.A., Jacomassi, D.P., Bagnato, V.S., and Kurachi, C. (2011). Investigation of the photodynamic effects of curcumin against Candida albicans. Photochem. Photobiol. 87, 895–903.
20. Pileggi, G., Wataha, J.C., Girard, M., Grad, I., Schrenzel, J., Lange, N., and Bouillaguet, S. (2013). Blue light-mediated inactivation of Enterococcus faecalis in vitro. Photodiagnosis Photodyn. Ther. 10, 134–140.
21. Paschoal, M.A., Santos–Pinto, L., Lin, M., and Duarte, S. (2014). Streptococcus mutans photoinactivation by combination of short exposure of a broad-spectrum visible light

and low concentrations of photosensitizers. Photomed. Laser Surg. 32, 175–180.
22. Araújo, N.C., Fontana, C.R., Bagnato, V.S., and Gerbi, M.E. (2014). Photodynamic antimicrobial therapy of curcumin in biofilms and carious dentine. Lasers Med. Sci. 29, 629–635.
23. Gursoy, H., Ozcakir–Tomruk, C., Tanalp, J., and Yilmaz, S. (2013). Photodynamic therapy in dentistry: a literature review. Clin. Oral Investig. 17, 1113–1125.
24. Fontana, C.R., Lerman, M.A., Patel, N., Grecco, C., Costa, C.A., Amiji, M.M., Bagnato, V.S., and Soukos, N.S. (2013). Safety assessment of oral photodynamic therapy in rats. Lasers Med. Sci. 28, 479–486.
25. Fekrazad, R., Bargrizan, M., Sajadi, S., and Sajadi, S. (2011). Evaluation of the effect of photoactivated disinfection with Radachlorin® against Streptococcus mutans (an in vitro study). Photodiagnosis Photodyn. Ther. 8, 249–253.
26. Kömerik, N., Nakanishi, H., MacRobert, A.J., Henderson, B., Speight, P., and Wilson, M. (2003). In vivo killing of Porphyromonas gingivalis by toluidine blue-mediated photosensitization in an animal model. Antimicrob. Agents Chemother. 47, 932–940.
27. Soukos, N.S., Chen, P.S., Morris, J.T., Ruggiero, K., Abernethy, A.D., Som, S., Foschi, F., Doucette, S., Bammann, L.L., Fontana, C.R., Doukas, A.G., and Stashenko, P.P. (2006). Photodynamic therapy for endodontic disinfection. J. Endod. 32, 979–984.
28. Araújo, N.C., Fontana, C.R., Bagnato, V.S., and Gerbi, M.E. (2012). Photodynamic effects of curcumin against cariogenic pathogens. Photomed. Laser Surg. 30, 393–399.
29. Panhóca, V.H., Geralde, M.C., Corrêa, T.Q., Carvalho, M.T., Souza, C.W.O.S., and Bagnato, V.S. (2014). Enhancement of the photodynamic therapy effects on Streptococcus Mutans biofilm. J. Phys. Sci. Applic. 4, 107–114.
30. Lipovsky, A., Nitzan, Y., Gedanken, A., and Lubart, R. (2010). Visible light-induced killing of bacteria as a function of wavelength: implication for wound healing. Lasers Surg. Med. 42, 467–472.
31. Wheeland, R.G., and Koreck, A. (2012). Safety and effectiveness of a new blue light device for the self-treatment of mild-to-moderate acne. J. Clin. Aesthet. Dermatol. 5, 25–31.
32. Kawada, A., Aragane, Y., Kameyama, H., Sangen, Y., and Tezuka, T. (2002). Acne phototherapy with a high–intensity, enhanced, narrow-band, blue light source: an open study and in vitro investigation. J. Dermatol. Sci. 30, 129–135.
33. Rabiee, A., Ebrahim–Habibi, A., Ghasemi, A., and Nemat–Gorgani, M. (2013). How curcumin affords effective protection against amyloid fibrillation in insulin. Food Funct. 4, 1474–1480.
34. Palmal, S., Maity, A.R., Singh, B.K., Basu, S., Jana, N.R., and Jana, N.R. (2014). Inhibition of amyloid fibril growth and dissolution of amyloid fibrils by curcumin-gold nanoparticles. Chemistry 20, 6184–6191.
35. Marchiani, A., Rozzo, C., Fadda, A., Delogu, G., and Ruzza, P. (2014). Curcumin and curcumin-like molecules: from spice to drugs. Curr. Med. Chem. 21, 204–222.
36. Handley, P.S., Correia, F.F., Russell, K., Rosan, B., and DiRienzo, J.M. (2005). Association of a novel high molecular weight, serine-rich protein (SrpA) with fibril-mediated adhesion of the oral biofilm bacterium Streptococcus cristatus. Oral Microbiol. Immunol. 20, 131–140.
37. Lévesque, C., Lamothe, J., and Frenette, M. (2003). Coaggregation of Streptococcus salivarius with periodontopathogens: evidence for involvement of fimbriae in the interaction with Prevotella intermedia. Oral Microbiol. Immunol. 18, 333–337.
38. Muglikar, S., Patil, K.C., Shivswami, S., and Hegde, R. (2013). Efficacy of curcumin in the treatment of chronic gingivitis: a pilot study. Oral Health Prev. Dent. 11, 81–86.
39. Bhawana, Basniwal, R.K., Buttar, H.S., Jain, V.K., and Jain, N. (2011). Curcumin nanoparticles: preparation, characterization, and antimicrobial study. J Agric Food Chem. 59, 2056–2061.
40. Vimala, K., Varaprasad, K., Sadiku, R., Ramam, K., and Kanny, K. (2013). Development of novel protein-Ag nanocomposite for drug delivery and inactivation of bacterial applications. Int. J. Biol. Macromol. 63, 75–82.
41. Hayek, R.R., Araújo, N.S., Gioso, M.A., Ferreira, J., Baptista–Sobrinho, C.A., Yamada, A.M., and Ribeiro, M.S. (2005). Comparative study between the effects of photodynamic therapy and conventional therapy on microbial reduction in ligature-induced peri-implantitis in dogs. J. Periodontol. 76, 1275–1281.
42. Müller Campanile, V.S., Giannopoulou, C., Campanile, G., Cancela, J.A., and Mombelli, A. (2013). Single or repeated antimicrobial photodynamic therapy as adjunct to ultrasonic debridement in residual periodontal pockets: clinical, microbiological, and local biological effects. Lasers Med. Sci. 2013 May 10. [Epub ahead of print].

Address correspondence to:
Fernanda Rossi Paolillo
University of São Paulo (USP)
Av. Trabalhador Sãocarlense
400 – Centro, CEP 13560-970
São Carlos, SP
Brazil

E-mail: fer.nanda.rp@hotmail.com

IOP Publishing | Astro Ltd Laser Physics

Laser Phys. **24** (2014) 015701 (8pp) doi:10.1088/1054-660X/24/1/015701

Fluorescence spectroscopy for the detection of potentially malignant disorders of the oral cavity: analysis of 30 cases

A L N Francisco[1], W R Correr[2], L H Azevedo[3], V K Galletta[3], C A L Pinto[4], L P Kowalski[5] and C Kurachi[2]

[1] Department of Oral Diagnosis, School of Dentistry of Piracicaba, University of Campinas (UNICAMP), Avenida Limeira, 901, Piracicaba, 13414-018, São Paulo, Brazil
[2] Department of Physics and Materials Science, Physics Institute of São Carlos, University of São Paulo (USP), Avenida Trabalhador São-Carlense, 400, São Carlos, 13566-590, São Paulo, Brazil
[3] Special Laboratory of Laser in Dentistry, School of Dentistry of São Paulo, University of São Paulo (USP), Avenida Professor Lineu Prestes, Cidade Universitária, São Paulo, 05508-000, São Paulo, Brazil
[4] Department of Pathology, A C Camargo Hospital, Rua Professor Antonio Prudente, 211, São Paulo, 01509-900, São Paulo, Brazil
[5] Department of Head and Neck Surgery and Otorhinolaryngology, A C Camargo Hospital and National of Science and Technology Institute in Oncogenomics (INCITO), Rua Professor Antonio Prudente, 211, São Paulo, 01509-900, São Paulo, Brazil

E-mail: lp_kowalski@uol.com.br and cristina@ifsc.usp.br

Received 26 February 2013, revised 4 November 2013
Accepted for publication 4 November 2013
Published 10 December 2013

Abstract

Oral cancer is a major health problem worldwide and although early diagnosis of potentially malignant and malignant diseases is associated with better treatment results, a large number of cancers are initially misdiagnosed, with unfortunate consequences for long-term survival. Fluorescence spectroscopy is a noninvasive modality of diagnostic approach using induced fluorescence emission in tumors that can improve diagnostic accuracy. The objective of this study was to determine the ability to discriminate between normal oral mucosa and potentially malignant disorders by fluorescence spectroscopy. Fluorescence investigation under 408 and 532 nm excitation wavelengths was performed on 60 subjects, 30 with potentially malignant disorders and 30 volunteers with normal mucosa. Data was analyzed to correlate fluorescence patterns with clinical and histopathological diagnostics. Fluorescence spectroscopy used as a point measurement technique resulted in a great variety of spectral information. In a qualitative analysis of the fluorescence spectral characteristics of each type of injury evaluated, it was possible to discriminate between normal and abnormal oral mucosa. The results show the potential use of fluorescence spectroscopy for an improved discrimination of oral disorders.

Keywords: squamous cell carcinoma, fluorescence spectroscopy, early diagnosis, potentially malignant disorders, oral cavity

(Some figures may appear in colour only in the online journal)

1. Introduction

Squamous cell carcinoma is the most frequent cancer type of the oral cavity, corresponding to over 90% of all malignant tumors [1, 2]. Unfortunately, most potentially malignant disorders and initial oral cancers are usually missed or misdiagnosed and not treated until they are at advanced stages. At advanced stages, the effectiveness of therapeutic modalities are low and result in high mortality and morbidity rates [3]. Moreover, the long-term results of oral cancer therapy have

been significantly hindered by the development of second primary tumors. Therefore, early detection of neoplastic changes in the oral cavity is essential to improve survival rates [4].

In clinical practice, an accurate clinical examination and biopsy of a suspect lesion must be done to determine the diagnosis [5]. However, most oral cavity squamous cell carcinomas do not originate from potentially malignant disorders nor from other noticeable clinical changes in the oral mucosa [6, 7]. Most potentially malignant disorders are clinically present as leukoplakia or erythroplakia, but histologically they may have a wide range of phenotypes such as hyperkeratosis or dysplasia [8]. On the other hand, similar clinical features of carcinomas at the initial stage and benign lesions are major factors making early cancer diagnosis a difficult task. Incisional biopsy remains as the gold standard diagnostic method for the detection of oral neoplasia, but the choice of a proper biopsy site in a large non-homogeneous potentially malignant disorder or malignant lesion is not simple and can result in misdiagnosis. Recently, optical techniques have been developed, aiming to became auxiliary tools to address these challenges [9–12]. Due to its sensitivity to tissue alterations, optical diagnosis has been indicated, not only for cancer detection, but also for other diagnostic applications, such as dental calculus and demineralization [13, 14]. Among those techniques, fluorescence spectroscopy is a noninvasive, accurate and fast diagnostic method that can be potentially used for the early detection and diagnosis of cancer in real time [15]. Its principal feature relies on the fact that several changes taking place along tumorigenesis alter light/tissue interactions, including tissue fluorescence, and these normal oral mucosa and potentially malignant or malignant lesions present distinct fluorescence spectra [16, 17].

Pavlova *et al* studied a Monte Carlo model that showed variations in optical parameters associated with neoplastic development that influence the intensity and shape of the fluorescence spectra. Changes associated with dysplastic progression were associated with a decreased fluorescence intensity and an emission shift to longer wavelengths [17]. Several *in vitro* and *in vivo* studies have shown the efficiency of fluorescence spectroscopy for oral cancer discrimination with high rates of sensitivity and specificity [10, 16]. Clinical studies have also presented the potential of this technique to improve cancer diagnosis, even though the discrimination of potentially malignant disorders versus cancer is still contradictory in the literature [18, 10].

In this study, we report the results obtained using a double excitation fluorescence spectroscopy system in 30 patients presenting oral leukoplakia and/or erythroplakia and in 30 volunteers with normal oral mucosa. Spectral analysis was performed using principal component analysis combined with clinical impression and histopathological diagnosis.

2. Patients and methods

The subjects included in this prospective clinical study were 30 volunteers with normal oral mucosa and no history of malignancy in the upper digestive tract, and 30 patients with potentially malignant disorders clinically detectable at various stages of development. All subjects were over 18 years old, both genders, smokers and nonsmokers. The investigated lesions were located in the oral cavity and a biopsy was taken for histological diagnosis. The biopsy site was chosen based only on clinical examination. All patients were investigated at the Special Laboratory of Laser in Dentistry, University of São Paulo (LELO-USP) and Hospital A C Camargo, São Paulo, after a written informed consent was signed.

A homemade fluorescence spectroscopy system was used in this study. The system is composed of two excitation lasers (408 nm diode laser and 532 nm frequency-doubled Nd:YAG laser), a Y-type probe (Ocean Optics, USA), a USB-spectrometer (USB-4000-Ocean Optics, USA) and a laptop. The Y-type probe with two 600 μm optical fibers is connected on one end to the excitation laser and the other end to the spectrometer, and the investigation tip is enclosed in an aluminum handpiece. The external diameter of the interrogation tip is 2.5 mm.

All subjects answered an anamnestic form with medical information about habits associated with the etiology of cancer (smoking and alcohol), family history, among others. A detailed clinical examination was carried out, resulting in a clinical diagnosis following the classification in normal mucosa and abnormal mucosa (erythroplakia, leukoplakia or erythroleukoplakia) and the definition of the biopsy site.

A mouth washing with saline solution was performed just before optical measurements to minimize possible contaminants in the mucosa, such as food scraps. The subjects had fasted for at least 1 h before the examination to prevent dye intake and alteration of the fluorescence pattern of the investigated mucosa.

Each measurement site was assessed using excitation wavelengths at 408 and 532 nm. For patients with a clinically detectable lesion with a diameter of less than 1 cm, the entire altered area was screened with the needed points to cover the lesion surface. In patients with lesions greater than 1 cm in diameter, and in the case of identification of surface heterogeneity, representative regions were chosen to correlate with different clinical patterns, avoiding any area of necrosis. In each chosen site, at least five spectra, for each excitation wavelength, were taken to check the variability on measurement performance. All the optical measurements were taken by a single operator (ALNF).

Four-mm punch biopsies were taken after the previous dentist/physician decision based on clinical impression, and the correlated fluorescence spectrum identified. The tissue sample was stained for HE analysis and the slides were evaluated by certified pathologists blinded to the clinical impression and fluorescence spectra (figure 1).

Normal volunteers were investigated at distinct oral sites: lateral border of the tongue, dorsum of the tongue, floor of the mouth, lower lip mucosa, buccal mucosa, gingiva and hard palate, with five optical measurements per excitation wavelength for each site. Cytological material was collected from all investigated sites using Oral CDX brush biopsy and fixed with 95% ethanol for the smear slide.

Figure 1. Comparative clinical pathology (a) erythroleukoplakia disorder in the buccal mucosa and (b) histopathological results of moderate dysplasia.

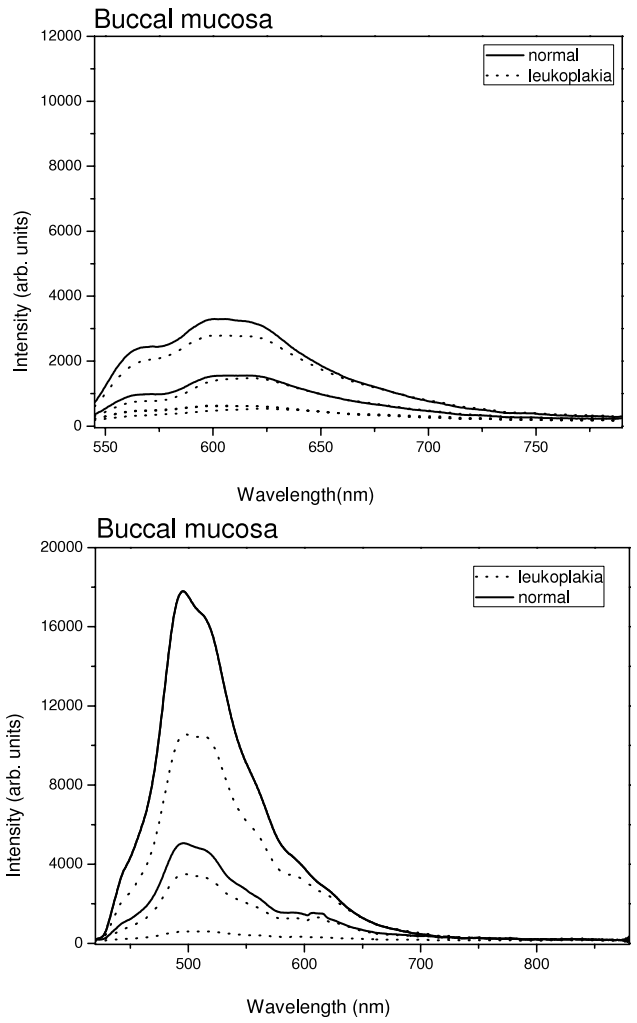

Figure 2. Comparison in the buccal mucosa of spectra in sites of normal mucosa and leukoplakia, at wavelengths of 532 nm and 406 nm, respectively.

Fluorescence spectra were classified using histopathology, the gold standard for diagnostics, in normal epithelium and epithelial dysplasia. For normal volunteers, clinical impressions and cytological results were used for classification. Principal component analysis (PCA) was used for evaluation of the diagnostic resolution of the training set.

3. Results

Thirty patients, 15 female and 15 male, with potentially malignant disorders were investigated in the period of May of 2009 and June of 2010. Table 1 summarizes the clinical features and pathology diagnostics of the study population. The most prevalent disorder type concerning clinical diagnosis was leukoplakia, and the oral sites were tongue and buccal mucosa. The most frequent histopathological classifications were mild and moderate dysplasia. For erythroplakia (4) and erythroleukoplakia (1) lesion dysplasia was graded as moderate or severe. With a minimum follow-up of two years, 20% of cases progressed to cancer, four *in situ* and two moderately differentiated oral squamous cell carcinoma.

Fluorescence spectra showed distinct behaviors considering oral site, clinical diagnosis, and pathological findings. Oral mucosa at different oral sites present distinct fluorescence spectra for each excitation wavelength; in this sense, the discrimination was better achieved when the comparison between normal and altered mucosa was performed individually for each site. At the same time, due to the small sample number, statistical analysis could not be performed for each site, but only in general for the oral cavity.

Leukoplakia and erythroplakia showed different autofluorescence patterns even for the same histological result. Figure 2 shows the fluorescence spectra for both excitation wavelengths in the buccal mucosa. As can be noted for leukoplakia, tissue discrimination is not obtained for the used excitation wavelengths. On the other hand, for erythroplakia, fluorescence spectra under both excitations provided a good discrimination for the suspect lesions (figure 3).

Figures 3, 4 and 5 also show some examples of the discrimination obtained for erythroplakia in the buccal mucosa, leukoplakia on the floor of the mouth, and erythroplakia on the border of the tongue, respectively. Other oral sites as palate, gingival, dorsum of the tongue, and inner mucosa of the lip also presented some lesions, but the analysis is difficult due to the low number of cases. Changes on emission intensity and on spectra shape could be noted at

Table 1. Clinical features and histopathology diagnosis of the study population. (Note: one of the erythroplakia was *in situ* carcinoma. BOT = border of the tongue, DOT = dorsum of the tongue, FOM = floor of the mouth, BM = buccal mucosa.)

								Pathology diagnosis			
	Oral sites								Epithelial dysplasia		
Clinical impression	BOT	DOT	FOM	Gingiva	Palate	Lip mucosa	BM	Epithelial hyperplasia	Mild	Moderate	Severe
Leukoplakia	9	1	3	4	0	2	8	5	13	8	1
Erythroplakia	0	0	1	0	1	0	3	0	0	2	2
Leukoerythroplakia	1	0	0	0	0	0	0	0	0	0	1

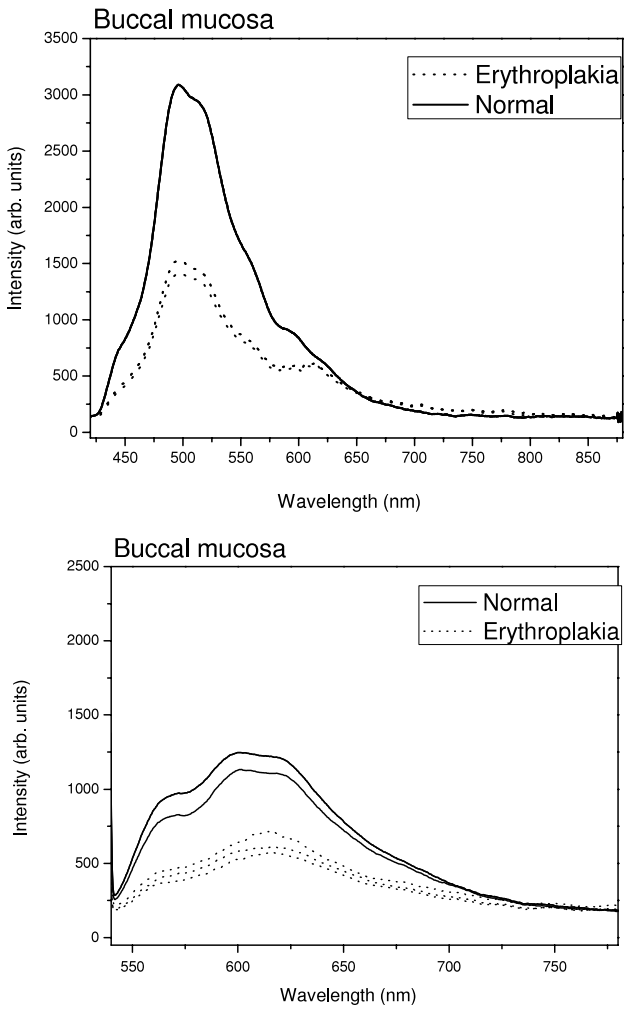

Figure 3. Comparison in the buccal mucosa of spectra in sites of normal mucosa and erythroplakia, at wavelengths of 406 nm and 532 nm, respectively.

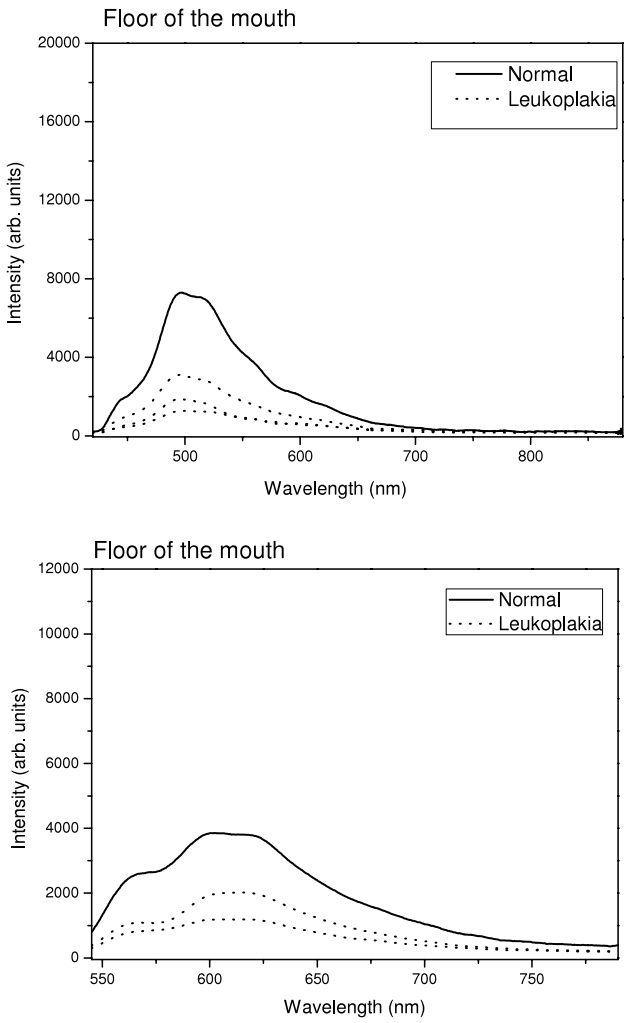

Figure 4. Comparison in the floor of the mouth of spectra in sites of normal mucosa and leukoplakia, at wavelengths of 406 nm and 532 nm, respectively.

some lesion regions, but in other areas the fluorescence spectra were quite similar to the clinically normal contralateral area. The fluorescence spectra varied according to the anatomical site, even for the same clinical characteristics of the lesion, as well as for distinct histopathological diagnosis. Another observation that should be pointed out is that, for the subjects in this study, the normal mucosa of the patients showed distinct patterns when compared to the oral mucosa of the normal volunteers. This behavior should be further investigated, also in comparison with clinically non-malignant mucosa of oral cancer patients. In PCA analysis of the sensitivity and specificity weighted were 0.874 and 0.776, respectively.

4. Discussion

The prognosis of patients with squamous cell carcinoma of the oral cavity involves several demographic, clinical, pathological and therapeutic variables. The most significant prognostic factors are the tumor site and size and the variables related to regional metastases. These factors significantly influence the probability of disease locoregional control and survival rates. Primary and secondary prevention seems to be the best chance to improve long-term survival results and there is a need for the development of diagnosis tools aiming to aid in the diagnosis of potentially malignant disorders and early stage cancers [3, 19].

Point spectroscopy is a potential diagnostic tool that can investigate only superficial lesions, since its response is dependent on the excitation light penetration into the tissue and on the collection of the fluorescence exiting from the tissue surface. The volume of the investigated tissue and the origin of the emitted fluorescence are mainly dependent on excitation wavelength and tissue composition. Also, the amount of keratinized layer or vascularization influences the collected fluorescence. Keratinization causes a higher light scattering, and vascularization a higher absorption, modifying the fluorescence evaluated [20, 21].

The variation in tissue architecture alters the pattern of the fluorescence spectrum collected, since the coupling of excitation light and the optical path of photons at different wavelengths is influenced by the organization

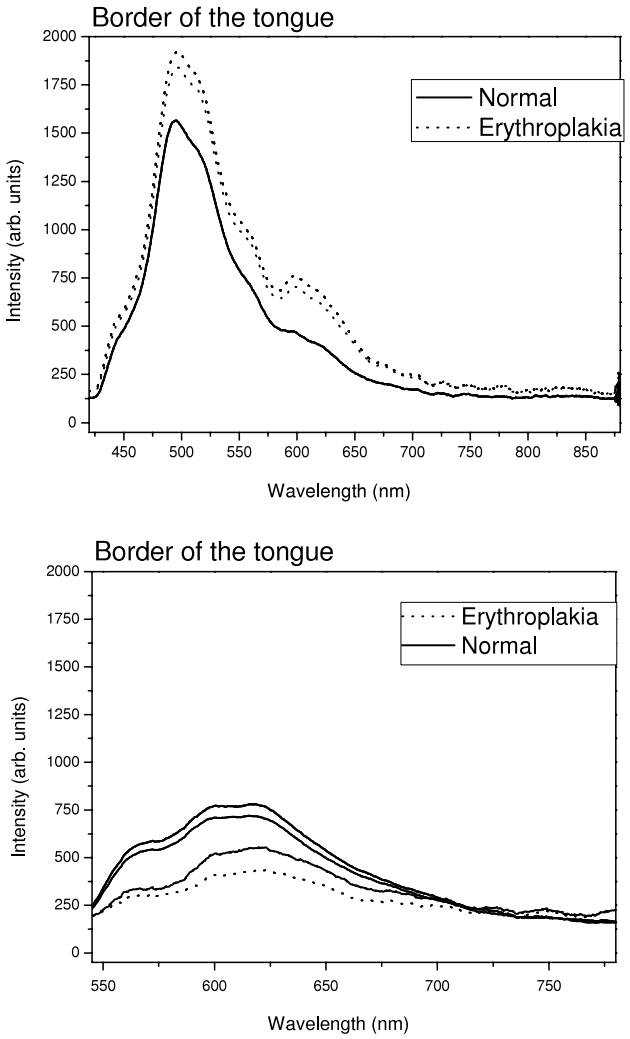

Figure 5. Comparison in the border of the tongue of spectra in sites of normal mucosa and erythroplakia, at wavelengths of 406 nm and 532 nm, respectively.

of biomolecules. The biochemical composition, especially the concentration of absorbers, scatterers and fluorescent biomolecules defines the final emission collected by the system. Monochromatic light is used because it provides a more selective excitation of fluorophores, scatterers or absorbers, improving the efficacy of the method [22]. The analysis of each spectrum was performed according to the histopathological diagnosis without taking other tissue features into account. This clearly reduces diagnostic resolution, since distinct spectral patterns can be found in cases with the same histological phenotype.

Normal mucosa at distinct oral sites shows a distinct histological architecture, composition and fluorescence spectrum. Ramanujam and Chu *et al* have previously discussed this spectral difference at oral sites [23, 24]. Schwarz *et al* also observed spectral differences between oral sites, especially when considering keratinized and non-keratinized oral mucosa. Veld *et al* reported differences between the autofluorescence spectra of normal oral mucosa in a group of 96 volunteers. The most important factor raised by the authors was ethnicity. Based on our results, oral site must be considered when investigating normal versus altered mucosa at different oral sites [25, 26].

Westra and Sidransky have shown that the observed correlation of pathologic features and some genetic alterations indicate that fluorescence visualization is superior to clinical judgment alone in gauging the delimitation of the cancer field. Indeed, the field of optical changes seemed to be more accurate in the diagnosis of the field of genetic changes than traditional light microscopy [27].

Currently, fluorescence techniques have been used as a diagnostic tool in a number of clinical situations and in different medical specialties, aiming not only at the identification of early stage lesions, but also at fluorescence guided biopsy and even fluorescence guided local cancer therapy [28, 29]. Optical diagnosis of the head and neck is a rapidly developing area of clinical research that can be translated to patient treatment [30].

The main problem using point spectroscopy analyses is that only a small tissue volume interacts with the laser. The depth of laser penetration in the region between green and violet is restricted to surface layers of tissue and the intensity of fluorescence emitted is very low. This represents a limitation of this technique, especially when considering heterogeneous lesions, such as most of the potentially malignant disorders of the oral cavity. It was found that fluorescence spectra collected in the same tissue show different patterns depending on the excitation used. This variation occurs because the penetration depth and the fluorophores excited at each wavelength are distinct. Laser excitation at 532 nm shows a higher penetration depth compared to excitation at 408 nm [20], so the contribution of fluorophores of deeper layers may be more important at the collected fluorescence. Furthermore, some of the characteristics of the tissue in which the endogenous fluorophores are present have a great influence. Hemoglobin that is present in vascular structures absorbs a portion of the emitted fluorescence, particularly visible in the excitation at 408 nm. Epithelial fluorophores such as NADH also play a major role in the characteristics of the spectra of shallow depths and stromal fluorophores because collagen contributes to the measured signal from deeper regions [16, 31, 32].

Schwarz *et al* suggest that the short wavelengths may be more sensitive for the detection of initial changes in the epithelium, such as nuclear size and nucleus/cytoplasm ratio, and in the superficial stroma region where the early tissue changes during malignant transformation occur. In non-keratinized tissue, diagnostic performance was achieved using optical spectra only at superficial and medium depths. The discrimination of the spectra of normal and abnormal sites is somewhat better when used with shorter excitation wavelengths, which are heavily constrained to the epithelial layer and minimize the effects of absorption of hemoglobin [32].

High-resolution fluorescence and confocal microscopy have elucidated variable oral tissue autofluorescence and the dispersion characteristics of the layers of the epithelium and stroma under conditions of normal tissues, benign diseases and dysplasia. Pavlova *et al* suggest that

the oral epithelium can be divided into three layers with different optical properties. The oral epithelium is composed of a superficial layer of keratin, which varies in thickness depending on the anatomical location. The main fluorophore of the superficial epithelium is keratin, which is above the non-keratinized epithelium occupied by intermediate and basal cells. The fluorescence from the non-keratinized epithelium is associated with metabolic fluorophores NADH and FAD, which increase in samples of oral dysplasias [16, 33].

The carcinogenic process involves a biochemical signaling between the epithelium and the extracellular matrix, with greater alterations in the optical properties in the superficial stroma than those in the deep stroma by disease progression. The fluorescence related to collagen, elastin and angiogenesis is significantly reduced in oral dysplastic lesions and inflammatory lesions, especially in the stromal layer underneath the dysplastic epithelium. The progression of dysplasia in oral mucosa results in a decrease in the volume fraction of collagen, decreased dispersion of the stroma, and angiogenesis that may also be more prominent in the superficial stroma [10, 33].

The presence of inflammation may be another complicating factor for spectroscopic diagnosis of oral lesions. Autofluorescence of inflammatory conditions and cancer may be difficult to distinguish, since both are correlated to reduced emission. As inflammation mainly affects the stroma with concomitant changes in the dysplastic epithelium, depth-sensitive spectral data, in particular the data derived from the more superficial layers, may furnish more useful information for the discrimination of benign lesions from malignant or dysplastic lesions [32].

Erythematous lesions show lower fluorescence intensity when compared to leukoplakia lesions, likely due to a higher concentration of hemoglobin, the most important endogenous absorber, which absorbs excitation light in both spectral regions of violet and green as well as the emitted fluorescence in the tissue. Leukoplakic lesions behave differently in re-emission of light because they are rich in keratin, which has a prominent role in the phenomena of scattering, absorption and fluorescence intensity re-emitted [18].

We also observed distinct spectral features at the fluorescence emission between 500 and 560 nm. This emission region has been correlated with the endogenous fluorophores NADH and FAD, both present at the epithelial cells and relevant for metabolic evaluation. Our optical setup does not discriminate at what tissue layer the emission originates. The collected fluorescence spectrum is a result of the emission from the epithelium and superficial stroma. Possibly an excitation/collection setup as described by Schwarz *et al* would improve the diagnostic resolution [32].

Pavlova *et al* studied the fluorescence emission under UV excitation from four different locations in the tongue of a single patient. One of the four sites was clinically and histologically normal; the other three sites were oral lesions that were histologically diagnosed as inflammation, dysplasia and cancer, respectively. The normal oral tissue was characterized by strong epithelial and stromal autofluorescence. In contrast, the lesion diagnosed with severe inflammation showed a relevant decrease in the fluorescence of both epithelium and stroma. Moreover, while the fluorescence of normal tissue stroma originated from collagen fibers, the changes observed at the inflammatory condition was due to the inflammatory cells in the stroma. The oral lesion diagnosed with dysplasia was characterized by increased epithelial thickness with fluorescent cells throughout the epithelium and a decrease in fluorescence of the superficial stroma. A diagnostic technique with a fast response can provide important information to clinicians, helping in the classification of the lesion, the scanning of large areas, border delineation of the lesion, and also the choice of biopsy site [17, 18, 10, 19, 20, 33].

Distinguishing clinical features were observed in different behaviors of the fluorescence spectra. The violet excitation showed better discrimination of normal versus malignant potential in comparison with excitation at 532 nm. The results show the potential use of fluorescence spectroscopy on the discrimination of oral lesions. When there is a progression from the normal state to an altered state, this is reflected in the spectral characteristics of fluorescence of tissues, which may be correlated with the histopathological examination of tissues. Our results demonstrate the potential of fluorescence spectroscopy to diagnose objectively and noninvasively distinguishing sites of dysplastic oral mucosa. Moreover, these results support the use of depth-sensitive optical spectroscopy to improve performance in the diagnosis.

Acknowledgments

The financial support provided by FAPESP (CEPOF-CEPID Program, proc. no. 07/57126-5 and ALNF scholarship no. 09/12938-8), CNPq (proc. no. 477439/2007-1), INCITO and Professors Dr Dante Antônio Migliare and Carlos de Paula Eduardo.

References

[1] Mashberg A *et al* 1993 Tobacco smoking, alcohol drinking, and cancer of the oral cavity and oropharynx among US veterans *Cancer* **72** 1369–75

[2] Andre K *et al* 1995 Role of alcohol and tobacco in the aetiology of head and neck cancer: a case—control study in the Doubs region of France *Eur. J. Cancer Oral Oncol.* **31b** 301–9

[3] Kowalski L P, Parise O and Lehn C 2008 *Diagnóstico e Tratamento—Câncer de Cabeça e Pescoço* 1st edn (São Paulo: Revisada Ed Âmbito) pp 93–141, Parte II

[4] Nayak G S *et al* 2006 Principal component analysis and artificial neural network analysis of oral tissue fluorescence spectra: classification of normal premalignant and malignant pathological conditions *Biopolymers* **82** 152–66

[5] Gillenwater A *et al* 1998 Noninvasive diagnosis of oral neoplasia based on fluorescence spectroscopy and native tissue autofluorescence *Arch. Otolaryngol. Head Neck Surg.* **124** 1251–8

[6] Silverman S Jr, Gorsky M and Lozada F 1984 Oral leukoplakia and malignant transformation: a follow-up study of 257 patients *Cancer* **53** 563–8

[7] Silverman S Jr 1968 Observations on the clinical characteristics and natural history of oral leukoplakia *J. Am. Dent. Assoc.* **76** 772–7

[8] Kademani D 2007 Symp. on solid tumors *Oral Cancer Mayo Clin. Proc.* **82** 878–87
[9] Tsai T, Chen H M, Wang C Y, Tsai J C, Chen C T and Chiang C P 2003 *In vivo* autofluorescence spectroscopy of oral premalignant and malignant lesions: distortion of fluorescence intensity by submucous fibrosis *Lasers Surg. Med.* **33** 40–7
[10] Veld D C G, Witjes M J H, Sterenborg H J C M and Roodenburg J L N 2005 The status of *in vivo* autofluorescence spectroscopy and imaging for oral oncology *Oral Oncol.* **41** 117–31
[11] Dietterle S *et al* 2008 *In vivo* diagnosis and non-inasive monitoring of Imiquimod 5% cream for non-melanoma skin cancer using confocal laser scanning microscopy *Laser Phys. Lett.* **5** 752–9
[12] Meyer L E and Lademann J 2007 Application of laser spectroscopic methods for *in vivo* diagnostics in dermatology *Laser Phys. Lett.* **4** 754–60
[13] Gonchukov S, Biryukova T, Sukhinina A and Vdovin Yu 2010 Fluorescence detection of dental calculus *Laser Phys. Lett.* **7** 812–6
[14] Chen Q G, Lin B, Chen Z B, Zhu H H and Chen H 2010 Pilot study on early detection of dental demineralization based on laser induced fluorescence *Laser Phys. Lett.* **7** 752–6
[15] AlSalhi M S, Masilamani V, Atif M, Farhat K, Rabah D and Al Turki M R 2012 Fluorescence spectra of benign and malignant prostate tissues *Laser Phys. Lett.* **9** 631–5
[16] Pavlova I *et al* 2008 Monte Carlo model to describe depth selective fluorescence spectra of epithelial tissue: applications for diagnosis of oral precancer *J. Biomed. Opt.* **13** 064012
[17] Pavlova I, Weber C R, Schwarz R A, Williams M D, Gillenwater A M and Richards-Kortum R 2009 Fluorescence spectroscopy of oral tissue: Monte Carlo modeling with site-specific tissue properties *J. Biomed. Opt.* **14** 014009
[18] van Staveren H J, van Veen R L P, Speelman O C, Witjes M J H, Star W M and Roodenburg J L N 2000 Classification of clinical autofluorescence spectra of oral leukoplakia using a artificial neural network: a pilot study *Oral Oncol.* **36** 286–93
[19] Reibel J 2003 Prognosis of oral pre-malignant lesions: significance of clinical, histopathological, and molecular biological characteristics *Crit. Rev. Oral Biol. Med.* **14** 47–62
[20] Kurachi C, Bagnato V S, Fontana C R and Rosa L E B 2008 Fluorescence spectroscopy for the detection of tongue carcinoma—validation in an animal model *J. Biomed. Opt.* **13** 034018
[21] Rahman M S *et al* 2010 Evaluation of a low-cost, portable imaging system for early detection of oral cancer *Head Neck Oncol.* **22** 10
[22] Welch A J *et al* 1997 Propagation of fluorescent light *Lasers Surg. Med.* **21** 166–78
[23] Ramanujam N 2000 Fluorescence spectroscopy of neoplastic and non-neoplastic tissues *Neoplasia* **2** 89–117
[24] Chu S C, Hsiao T-C R, Lin J K, Wang C-Y and Chiang H K 2006 Comparison of performance of linear multivariate analysis methods for normal and dysplasia tissues differentiation using autofluorescence spectroscopy *IEEE Trans. Biomed. Eng.* **53** 2265–73
[25] Schwarz R A *et al* 2009 Noninvasive evaluation of oral lesions using depth-sensitive optical spectroscopy *Cancer* **115** 1669–79
[26] Veld D C G, Skurichina M, Witjes M J H, Duin R P W, Sterenborg D J C M and Star W M 2003 Autofluorescence characteristcis of healthy oral mucosa at different anatomical sites *Lasers Surg. Med.* **32** 367–76
[27] Westra W H and Sidransky D 2006 Fluorescence visualization in oral neoplasia: shedding light on an old problem *Clin. Cancer Res.* **12** 6594–7
[28] Moghissi K, Stringer M R and Hons K D B A 2008 Fluorescence photodiagnosis in clinical practice *Photodiagn. Photodyn. Ther.* **5** 235–7
[29] Bedard N, Pierce M, El-Nagger A, Anandasabapathy S, Gillenwater A and Richards-Kortum R 2010 Emerging roles for multimodal optical imaging in early cancer detection: a global challenge *Technol. Cancer Res. Treat.* **9** 211–7
[30] Upile T *et al* 2009 Head & neck optical diagnostics: vision of the future of surgery *Head Neck Oncol.* **1** 25
[31] Heintzelman D L *et al* 2000 Optimal excitation wavelengths for *in vivo* detection of oral neoplasia using fluorescence spectroscopy *Photochem. Photobiol.* **72** 103–13
[32] Schwarz R A, Gao W, Daye D, Williams M D, Richards-Kortum R and Gillenwater A M 2008 Autofluorescence and diffuse reflectance spectroscopy of oral epithelial tissue using a depth-sensitive fiber-optic probe *Appl. Opt.* **47** 825–34
[33] Pavlova I, Williams M, El-Naggar A, Richards-Kortum R and Gillenwater A 2008 Understanding the biological basis of autofluorescence imaging for oral cancer detection: high-resolution fluorescence microscopy in viable tissue *Clin. Cancer Res.* **14** 2396–404

Photodiagnosis and Photodynamic Therapy (2014) 11, 22—26

Available online at www.sciencedirect.com

ScienceDirect

journal homepage: www.elsevier.com/locate/pdpdt

Experience and BCC subtypes as determinants of MAL-PDT response: Preliminary results of a national Brazilian project

Dora P. Ramirez MD, MSc[a,*], Cristina Kurachi[a], Natalia M. Inada[a], Lilian T. Moriyama[a], Ana G. Salvio[b], José D. Vollet Filho[a], Layla Pires[a], Hilde H. Buzzá[a], Cintia Teles de Andrade[a], Clovis Greco[a], Vanderlei S. Bagnato[a]

[a] *Biophotonics Laboratory, São Carlos Institute of Physics, University of São Paulo (USP), 13566-590 São Carlos, São Paulo, Brazil*
[b] *Skin Department, Amaral Carvalho Foundation, Brazil*

Available online 8 January 2014

KEYWORDS
Non-melanoma skin cancer;
Photodynamic therapy;
National Brazilian project;
BCC subtypes;
Doctor experience;
Determinants

Summary Non-melanoma skin cancer is the most prevalent cancer type in Brazil and worldwide. Photodynamic therapy (PDT) is a noninvasive technique with excellent cosmetic outcome and good curative results, when used for the initial stages of skin cancer. A Brazilian program was established to determine the efficacy of methyl aminolevulinate (MAL)-PDT, using Brazilian device and drug. The equipment is a dual device that combines the photodiagnosis, based on widefield fluorescence, and the treatment at 630 nm. A protocol was defined for the treatment of basal cell carcinoma with 20% MAL cream application. The program also involves the training of the medical teams at different Brazilian regions, and with distinct facilities and previous PDT education. In this report we present the partial results of 27 centers with 366 treated BCC lesions in 294 patients. A complete response (CR) was observed in 76.5% (280/366). The better response was observed for superficial BCC, with CR 160 lesions (80.4%), when compared with nodular or pigmented BCC. Experienced centers presented CR of 85.8% and 90.6% for superficial and nodular BCC respectively. A high influence of the previous doctor experience on the CR values was observed, especially due to a better tumor selection.

Introduction

The non-melanoma skin cancer (NMSC) represents the most common type of cancer worldwide. In the United States, it accounts for more than 2 million cases per year and, in Brazil, more than 130,000 new cases were estimated

* Corresponding author. Tel.: +55 1688029300; fax: +55 1633739810.
E-mail addresses: dorapatriciaramirez@gmail.com, patykobucara@hotmail.com (D.P. Ramirez).

1572-1000/$ — see front matter © 2013 Elsevier B.V. All rights reserved.
http://dx.doi.org/10.1016/j.pdpdt.2013.11.001

for 2012, with the basal cell carcinoma (BCC) representing approximately to 80% of all NMSC lesions [1].

PDT has been investigated for several applications, being widely used for the treatment of NMSC [2,3]. Three elements are fundamental in PDT: the presence of a photosensitizer (PS), a molecule which absorbs light to initiate a series of photochemical reactions; light at a specific wavelength to be absorbed by the PS; and the availability of molecular oxygen in the tissue to be treated [3,4]. The combination of drug, light and oxygen leads to the production of oxidative cytotoxic agents, leading the treated tissue to death by inducing necrosis, apoptosis or autophagy, when a irreversible damage is achieved [4]. Methyl aminolevulinate (MAL) is topically administered to the patient, using a transdermal delivery cream. MAL penetrates in the cells and the aminolevulinic acid induces in the mitochondria, the protoporphyrin IX (PpIX) production [4].

For a decade, our group has been introducing PDT as an experimental therapeutic option in Brazil [5]. After several years of local experience, we have organized a national initiative with the main goal of installing about 100 centers and treatment of approximately 2000 lesions to evaluate the efficacy of the proposed protocol and a new device that combines the fluorescence visualization and treatment.

The low accessibility to imported drug and equipment, mainly due to the high costs, prevents a large clinical implementation of PDT among Brazilian dermatologists. Brazil is a country with a large territorial area; the patient access to specialized facilities is difficult and inefficient considering the long distances and waiting list, which in some regions can achieve 12 months.

With the disponibility of Brazilian drug and equipment, the costs of a PDT procedure decrease significantly, allowing a high technique implementation. First of all, these components must be tested before its disponibilization by the public health system. This program has as a major aim to evaluate all these at different medical levels, from simple general facility to highly qualified cancer centers, and Brazilian regions. For the validity of the program, as well as to promote adjustments that guarantees a full success, it is necessary the analysis of different response aspects. Therefore in this communication, we present some aspects concerning the PDT clinical outcome based on partial results (with about 20% of the expected number of patients) already collected. The complete response depending on a previous professional experience and the BCC subtypes is presented.

Materials and methods

Training the centers

This is a multicenter prospective study involving 27 dermatological centers in Brazil. Each center was classified as experienced (EC) or not experienced center (NEC) according to the spontaneous physicians report, regarding their own previous knowledge and/or practice with PDT for more than one year.

Regardless of this experience, all teams received the same training, lasting 8 h, which included a lecture with the concepts of photodynamic therapy, pharmacology and all clinical protocol followed by training with practical application of the protocol in patients previously scheduled. A training team was composed of doctors, pharmacists, physicists and related fields toward a more comprehensive approach to the concepts involved.

The presented data are from 14 EC and 13 NCE. The study was approved by local Internal Review Board, and by the Brazilian Federal Council on Ethics. All patients provided a written informed consent before enrollment into the study.

Clinical protocol

Eligible patients were subjects of both genders, over 18 years old with primary superficial (sBCC), nodular (nBCC) and pigmented (pBCC) BCC with diameter less than of 20 mm, estimated clinically immediately prior to treatment. The maximum thickness of the tumor was 2 mm. This evaluation was done for histopathological or clinical analysis. Pregnant women and subjects presenting porphyria or any type of photosensitivity were excluded.

All lesions were measured and photographed. Then, the lesion was investigated using the fluorescence visor — (LINCE®, MMOptics, Brazil) that emits an ultraviolet-blue light centered at 400 ± 10 nm, from an LED array and with irradiance of 40 ± 8 mW/cm^2. Autofluorescence visualization improves the physician ability on discrimination of altered tissues, by highlighting lesion structures. Superficial BCC lesions were prepared by surface debridement to remove scales and crusts and to facilitate penetration of the MAL cream. For nBCC, a curettage without local anesthesia was performed to reduce the tumor thickness, resulting in a flat surface. Was used MAL 200 mg/g cream containing: methylparaben, propylene glycol, EDTA (ethylenediaminetetraacetic acid), DMSO (dimethyl sulfoxide), BHT (butylated hydroxytoluene), imidazolidinyl urea, water, Polawax, decila oleate, Nipasol (PDT-Pharma, Cravinhos, SP, Brazil) was placed over the lesion, including an extension to 5 mm of normal surrounding skin, with at least 1 mm thickness. An occlusive dressing, using plastic film and aluminum foil was placed for 3 h. After that, the dressing was removed, the cream was washed off with saline solution. The presence of PpIX, a highly fluorescent molecule, was verified by using the fluorescence visor to observe the characteristic red fluorescence under 405 nm excitation. The uniformity and intensity of the red fluorescence give indication to evaluate the PpIX production. If there is lack or dimmed red emission, the photodynamic response will not take place. If there is a non-uniform PpIX distribution, the PDT will not properly occur, potentially resulting in remaining untreated cancer cells. After checking the PpIX, the lesion was immediately illuminated with a red (630 ± 10 nm) LED light source (LINCE®, MMOptics, Brazil), with irradiance of 125 mW/cm^2, and fluence of 150 J/cm^2. Subsequently to treatment, PpIX photobleaching was verified by fluorescence imaging in order to evaluate consumption of PS and certification of an expected photodynamic reaction. We believe that a fluorescence visor is a relevant device to enable an improved lesion examination, and analysis of the PDT steps, giving clinical information to predict the individual response.

The same protocol was repeated, with an interval of 1 week between sessions.

Table 1 Clinical characteristics of the patients and lesion.

Clinical characteristics	Number or percent
Male/female	144/222 lesions
Lesion location, no. (%)	
Head and neck	80.8%
Upper and lower extremities	6.5%
Trunk	12.5%
Histological subtypes	
Superficial BCC	199 lesions
Nodular BCC	151 lesions
Pigmented BCC	16 lesions

Evaluation of response

Thirty days after the second PDT session, the patient was clinically evaluated by the physicians with digital pictures to help the macroscopic analysis and a punch biopsy was performed for histological analysis. The final response, based on the clinical and histological analyses, was classified as complete response (CR), partial response (PR) or interrupted treatment (IT).

CR was used to classify results when no lesion was observed in clinical and/or histological analysis. PR was used for lesions that have regressed, but not enough to eradicate the lesion. IT was used when there were external causes for the patient. There was no reported allergic reaction.

Statistical analysis

Statistically, data were reported as numbers and/or percentages. The chi-square statistic was used to assess predetermined bivariate comparisons, and the equal proportions hypothesis was rejected when the *P* values were less than 0.05.

Results

In this multicenter study, 294 patients with a total of 366 BCC lesions were treated in 27 different centers. The skin type, I—VI rated according to the Fitzpatrick's classification, of each patient was recorded. From all lesions, 296 (80.8%) were located at the head and neck, 24 (6.5%) at upper and lower extremities, and 46 (12.5%) at the trunk. Two hundred and twenty-two lesions (60.6%) were diagnosed in women, and 144 lesions (39.3%) in men. CR was observed in 76.5% (280/366), PR in 20.2% (74/366), IT in 3.2% (12/366) of the cases (Table 1). The better response was observed for sBCC, with 160 CR (80.4%), 29 PR (14.5%), and 10 IT (5%) of treated lesions ($P < 0.01$). For nBCC, the results were: CR at 112 lesions (74.1%), PR at 37 (24.5%), and IT at 2 (1.3%) ($P < 0.01$). Only 16 pBCC lesions were included in the present study, showing CR at 50%, and PR at 50% of the cases (Fig. 1). In Fig. 2, a comparison between the results obtained at experienced centers (EC) and non-experienced centers (NEC) is presented. EC corresponds to centers where the professionals self-related previous experience in PDT, while NECs are those introduced to PDT. There is an evident higher CR rates

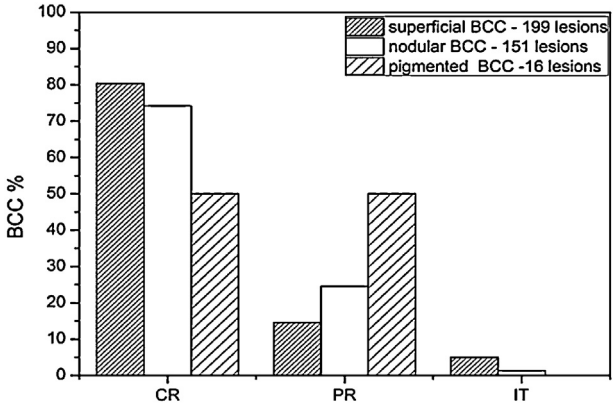

Figure 1 Response of lesion to PDT. The complete response (CR), partial response (PR) and discontinued treatment (IT). Also, the lesions were divided into subtypes: superficial BCC, BCC nodular BCC pigmented. It can be observed better response to superficial BCC, followed by CBC nodular pigmented BCC.

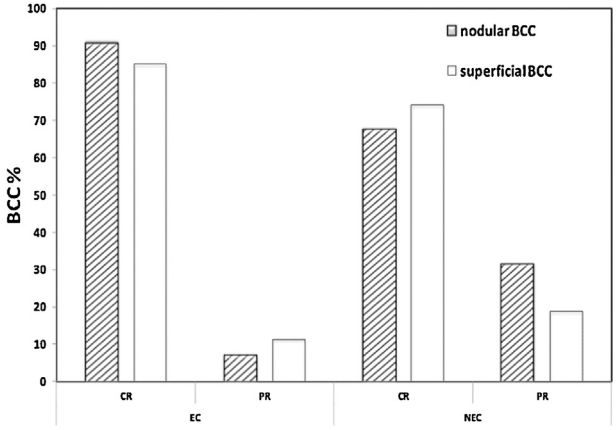

Figure 2 Comparison of results obtained for the center with photodynamic experience in photodynamic therapy (EC) and without previous experience (CNE). Additionally, the figure shows the results obtained for a subtype of lesion superficial BCC or nodular BCC.

for the EC, showing the importance of the previous education and experience of the professionals on the therapy. In general, for BCC lesions, a CR of 86% was observed at ECs, when compared to 69.2% of the NECs. For sBCC, was no statistically significant association between CR for ECs and NECs (85.8% *versus* 74.1%) respectively ($P = 0.053$). Nodular lesions showed CR of 90.6% (39/43), and PR of 6.9% (3/43) ($P < 0.01$) for ECs, and NECs obtained CR of 67.5% (73/108), and PR of 31.4% (34/108) ($P < 0.01$).

Discussion

This report showed the preliminary results of a multicenter clinical study that included 27 dermatological centers in different regions of the Brazilian territory. One of the main aims of this project is to evaluate the proposed PDT protocol in facilities of different levels, and with medical professionals of distinct training and educational. A treatment technique for cancer to be diffusely implemented in Brazil must first be

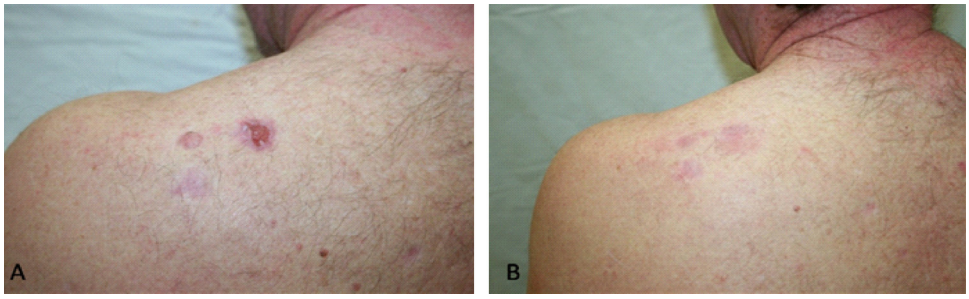

Figure 3 Response to MAL-PDT in a patient after two sessions. (A) Untreated lesion(s) and (B) response 30 days after treatment.

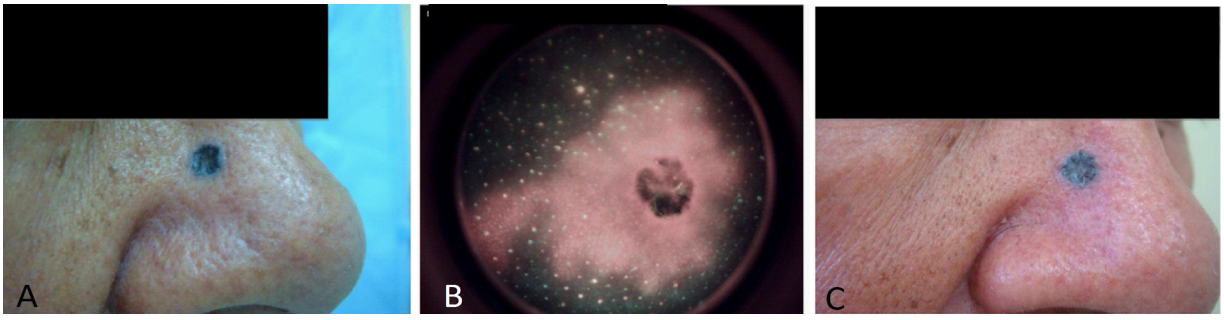

Figure 4 (A) Pigmented BCC prior to treatment; (B) fluorescence image of the formation of PpIX and (C) 30 days after treatment.

tested and show satisfactory results in all levels of Medicine services. In this study, it was possible to verify the influence of the previous experience on PDT in the treatment response. A CR was observed in 76.5% of the treated cases (Fig. 3), which is in the range of the rates reported in scientific literature, from 52.2% to 100% [2,6—8]. Horn et al. in 2003 observed that for BCC lesions a better response was observed for superficial lesions when compared to nodular lesions (85% *versus* 75%) of 47 and 51 respectively investigated cases [9]. In our study, sBCC responded better to PDT when compared to nodular lesions, with CR rates of 80.4%, 74.1%, respectively but it was no statistically significant ($P = 0.053$) (Fig. 1). In BCC, different factors can affect the response to the technique [10—13]. BCC lesions thicker than 2 mm present limited response to topical PDT [14], with efficacy decreasing as thickness increased. In our study, a limit of 2 mm of thickness was set; however, in some cases, especially at centers not specialized in Oncology the definition of the lesion thickness could not be properly accessed. A limited penetration depth of MAL cream and of visible light into the deeper layers of the tissue also explains the resulted response rates. Pigmented lesions are evidently more difficult to be treated with PDT due to higher light absorption at the presence of melanin, preventing deeper illumination with enough energy, resulting in lack of PDT response at tumor bottom margin.

Fig. 4 shows PpIX fluorescence in the photosensitized tissue. It is possible to observe that the pigmented region absorbs both the excitation and the fluorescence emission from PpIX. In the same way, these absorbing regions produce shield effect during irradiation, avoiding that all the lesion receive the proper amount of light, reducing PDT efficacy [15].

Pre-PDT curettage and/or debulking of nBCC are procedures proven to increase the success of the technique. Christensen et al., in 2009, attempted to use curettage only to remove the superficial layers of epidermis, and have observed that it contributed to high success rates in their results [16]. However, the execution of these procedures depends on the skills of the physician. In our study, we have observed that ECs presented better results when compared to the NECs. Even though, PDT is a simpler treatment procedure that requires less complex training, when compared to surgery, the resulted response may derive from the fact that an EC do not require an adjustment period to properly treat these lesions using PDT. This experience reflects in an improved selection of the indicated lesions, and also in their ability in performing proper lesion curettage for PDT. An example of that is that the lowest number of nodular BCC lesions was observed at the ECs.

Conclusion

MAL-PDT is a noninvasive, safe, moderately effective, and well-tolerated option for treating superficial BCC lesion. Moreover, we can anticipate that the BCC subtype and medical experience influence the final result. The fact that the lack of previous knowledge on PDT results in a lower degree of success, indicates that a closer interaction of the professionals involved in the multicenter study should provide an improved education on the PDT principles and clinical case discussions. As the study progress, we expected that the acquire experience will improve considerable outcome results.

Acknowledgments

The authors acknowledge the financial support by BNDES (09.2.1458.1) and MMOptics. We appreciate support from FAPESP (Program CEPID-INCT), CNPq, CAPES and FINEP.

References

[1] Kim RH, Armstrong AW. Nonmelanoma skin cancer. Dermatologic Clinics 2012;30(1):125—39, ix.
[2] Lehmann P. Methyl aminolaevulinate-photodynamic therapy: a review of clinical trials in the treatment of actinic keratoses and nonmelanoma skin cancer. British Journal of Dermatology 2007;156(5):793—801.
[3] Moseley H, et al. Clinical and research applications of photodynamic therapy in dermatology: experience of the Scottish PDT Centre. Lasers in Surgery and Medicine 2006;38(5):403—16.
[4] Agostinis P, et al. Photodynamic therapy of cancer: an update. CA: A Cancer Journal for Clinicians 2011;61(4):250—81.
[5] Bagnato VS, et al. PDT experience in Brazil: a regional profile. Photodiagnosis and Photodynamic Therapy 2005;2(2): 107—18.
[6] Calzavarapinton PG. Repetitive photodynamic therapy with topical delta-aminolevulinic-acid as an appropriate approach to the routine treatment of superficial nonmelanoma skin tumors. Journal of Photochemistry and Photobiology B: Biology 1995;29(1):53—7.
[7] Surrenti T, et al. Efficacy of photodynamic therapy with methyl aminolevulinate in the treatment of superficial and nodular basal cell carcinoma: an open-label trial. European Journal of Dermatology 2007;17(5):412—5.
[8] Lindberg-Larsen R, Solvsten H, Kragballe K. Evaluation of recurrence after photodynamic therapy with topical methylaminolaevulinate for 157 basal cell carcinomas in 90 patients. Acta Dermato-Venereologica 2012;92(2):144—7.
[9] Horn M, et al. Topical methyl aminolaevulinate photodynamic therapy in patients with basal cell carcinoma prone to complications and poor cosmetic outcome with conventional treatment. British Journal of Dermatology 2003;149(6):1242—9.
[10] Christensen E, et al. Pre-treatment evaluation of basal cell carcinoma for photodynamic therapy: comparative measurement of tumour thickness in punch biopsy and excision specimens. Acta Dermato-Venereologica 2011;91(6):651—5.
[11] Fink-Puches R, et al. Long-term follow-up and histological changes of superficial nonmelanoma skin cancers treated with topical delta-aminolevulinic acid photodynamic therapy. Archives of Dermatology 1998;134(7):821—6.
[12] Christensen E, Mørk C, Skogvoll E. High and sustained efficacy after two sessions of topical 5-aminolaevulinic acid photodynamic therapy for basal cell carcinoma: a prospective, clinical and histological 10-year follow-up study. British Journal of Dermatology 2012;166(6):1342—8.
[13] Vinciullo C, et al. Photodynamic therapy with topical methyl aminolaevulinate for 'difficult-to-treat' basal cell carcinoma. British Journal of Dermatology 2005;152(4):765—72.
[14] Morton CA, et al. Photodynamic therapy for basal cell carcinoma: effect of tumor thickness and duration of photosensitizer application on response. Archives of Dermatology 1998;134(2):248—9.
[15] Szeimies RM. Methyl aminolevulinate-photodynamic therapy for basal cell carcinoma. Dermatologic Clinics 2007;25(1):89—94.
[16] Christensen E, et al. Photodynamic therapy with 5-aminolaevulinic acid, dimethylsulfoxide and curettage in basal cell carcinoma: a 6-year clinical and histological follow-up. Journal of the European Academy of Dermatology and Venereology 2009;23(1):58—66.

Int J Diabetes Dev Ctries (January–March 2014) 34(1):32–39
DOI 10.1007/s13410-013-0132-4

Impact of fat distribution on metabolic, cardiovascular and symptomatic aspects in postmenopausal women

Fernanda Rossi Paolillo · Juliana Cristina Milan · Alessandra Rossi Paolillo · Sérgio Luiz Brasileiro Lopes · Cristina Kurachi · Vanderlei Salvador Bagnato · Audrey Borghi-Silva

Received: 10 July 2012 / Accepted: 21 May 2013 / Published online: 27 September 2013

Abstract The aim of this study was to investigate the anthropometric, metabolic, cardiovascular and symptomatic profile in gynoid and android postmenopausal women. Forty five postmenopausal women aged 50 to 60 years were divided into two groups according to fat distribution [waist-to-hip ratio (WHR)]: gynoid group (WHR between 0.68 and 0.8; $N=13$) and android group (WHR>0.8; $N=32$). Body composition, skinfold thickness, serum/plasma estradiol, creatinine, urea, lipid profile, glucose and insulin, maximal exercise testing and menopause rating scale (MRS) were evaluated. The android group when compared to the gynoid group showed ($P<0.05$): (i) higher values of body mass, BMI, waist circumference, body fat, lean mass and skinfold thickness; (ii) higher values of estradiol, triglycerides, very low-density lipoprotein (VLDL) and insulin levels with lower insulin sensitivity (%S) and greater insulin resistance (%IR) index; (iii) higher blood pressure (BP) during rest and lower maximal heart rate (HRmax) during maximal exercise testing and; (iv) higher scores of the somatic and urogenital-sexual symptoms. This study suggests that android postmenopausal women develop features that can lead to metabolic syndrome (MetS) and future cardiovascular disease (CVD), and these women may present higher scores of somatic and urogenital-sexual symptoms.

Keywords Postmenopausal women · Body composition · Metabolic syndrome · Menopause symptoms

F. R. Paolillo · C. Kurachi · V. S. Bagnato
Optics Group from Instituto de Física de São Carlos (IFSC), University of São Paulo (USP), Av. Trabalhador Sãocarlense, 400 - Centro, CEP 13560-970, São Carlos, SP, Brazil

C. Kurachi
e-mail: cristina@ifsc.usp.br

V. S. Bagnato
e-mail: vander@ifsc.usp.br

F. R. Paolillo · C. Kurachi · V. S. Bagnato
Biotechnology Program, Federal University of São Carlos (UFSCar), São Carlos, Brazil

J. C. Milan · A. Borghi-Silva
Cardiopulmonary Physiotherapy Laboratory, Department of Physical Therapy, Federal University of São Carlos (UFSCar), Rodovia Washington Luiz, Km. 235, Caixa Postal 676, CEP 13565-905, São Carlos, SP, Brazil

J. C. Milan
e-mail: juliana_milan10@hotmail.com

A. Borghi-Silva
e-mail: audrey@ufscar.br

A. R. Paolillo
Bioengineer Program, University of São Paulo (USP), Av. Trabalhador Sãocarlense, 400 - Centro, CEP 13560-970, São Carlos, SP, Brazil
e-mail: arpaolillo@yahoo.com.br

S. L. B. Lopes
Department of Medicine, Federal University of São Carlos (UFSCar), Rodovia Washington Luiz, Km. 235, Caixa Postal 676, CEP 13565-905, São Carlos, SP, Brazil
e-mail: slblopes@ufscar.br

F. R. Paolillo (✉)
University of São Paulo (USP), Av. Trabalhador Sãocarlense, 400 - Centro, CEP 13560-970, São Carlos, SP, Brazil
e-mail: fer.nanda.rp@hotmail.com

Introduction

Changes in body composition have been observed in postmenopausal women, due to hormonal changes [1]. After the menopause, the gynoid fat distribution gradually changes to an android distribution with an increased upper body fat, in the abdominal region [2]. These are associated with decreased aerobic capacity and reduced total energy expenditure [3] and may lead to the metabolic syndrome (MetS), as evidenced by androgenic obesity, insulin resistance, diabetes melittus (type II), hypertension and dyslipidemia [4, 5]. According to the National Cholesterol Education Program/Adult Treatment Panel III (NCEP/ATP III) definition [6], MetS is diagnosed when three of the above mentioned criteria are met, and CVD is the leading cause of mortality and morbidity in postmenopausal woman [2].

It is not clear whether the transition to menopause increases the CVD risk for all women or only for those who develop features of the MetS [7]. Studies [8, 9] have identified the menopausal transition a trigger for changes in the body fat distribution in healthy middle-aged women. Moreover, the type of body fat distribution is related to the possibility of developing metabolic disorder, mainly as androgenic obesity plays an important role in MetS [5, 10].

The objective of our study was to investigate anthropometric, metabolic, cardiovascular and symptomatic profiles in gynoid and android postmenopausal women. The hypothesis of the present study was that postmenopausal androgenic obesity increases both the risk of developing MetS and CVD, as well as the magnitude of the postmenopausal symptoms, when compared to gynecoid obesity.

Materials and methods

The study research has been approved by the Ethics Committee of the Federal University of São Carlos (UFSCar) in São Carlos, Brazil (no. 159/2010). All participants signed a written consent form before starting the first testing session. The study was registered with NIH Clinical Trials (NCT01745042).

Participants

A cross-sectional survey was conducted. Inclusion criteria were healthy postmenopausal Caucasian women, Brazilians, between 50 and 60 years of age. The postmenopausal period was defined by an absence of menstruation for more than 12 months. Exclusion criteria were symptoms and signs of any neurological, metabolic, inflammatory and/or cardiologic disease as well as cigarette smoking and use of any mediators, including hormone replacement therapy (HRT). The women were divided according to the fat distribution [waist-to-hip ratio (WHR)] [11] into two groups:

1) Gynoid (WHR between 0.68 and 0.8; $N=13$)
2) Android (WHR>0.8; $N=32$)

Assessment of body composition and skinfolds

Anthropometric data were used to determine the body mass index [BMI: body weight (in kg) divided by height (in m) squared] and the WHR [waist circumference (in cm) divided by hip circumference (in cm)]. The anatomical landmarks to measure the circumference (cm), in the upright position of the body were: 1) waist: measured at the above the iliac crest; 2) hip: measured at the largest protuberance of the buttocks [12]. The body fat and lean mass were measured by the bipolar electrical bioimpedance of the upper limbs (OMRON®, Kyoto, Japan) [13]. The measurements of the skinfolds (in mm) were performed in the upright position, the caliper was placed at specific locations on the right side of the body, which was relaxed and dry. Three measurements were reformed at each location to obtain an average. The anatomic locations for these measurements were: triceps, subscapular, suprailiac, abdominal, anterior thigh, medial calf [14, 15].

Assessment of biochemical exams

Blood was collected after a 12-hour fasting according to standard laboratory procedures of the Medical School Hospital of our Institution. Serum level of estradiol, urea, creatinine, triglycerides, total cholesterol, high-density lipoprotein (HDL) cholesterol, low-density lipoprotein (LDL) cholesterol, very low-density lipoprotein (VLDL) cholesterol, insulin and glucose were measured. Low-density lipoprotein (LDL) cholesterol was calculated according to Friedewald's formula [LDL=colesterol total−(HDL+VLDL)]. Very low-density lipoprotein (VLDL) cholesterol was calculated according to: triglycerides divided by 5.

According to the Castelli Index, higher LDL levels and lower HDL levels result in greater risk [16, 17]: (i) Castelli Index I: total cholesterol/HDL, (ii) Castelli index II: LDL/HDL.

The Homeostasis Model Assessment (HOMA) β, which estimates the functioning of pancreatic β cells, the HOMA %S, which estimates insulin sensitivity and HOMA %IR, which estimates insulin resistance were calculated [18]. The reference values for some of the parameters are: glucose≤ 100 mg/dL, insulin from 2.6 to 24.9 uUI/ml, triglycerides≤ 150 mg/dL, total cholesterol≤200 mg/dl and HDL≥50 mg/dL, LDL≤130 mg/dL and VLDL up to 40 mg/dL [5, 19, 20].

Assessment of cardiovascular responses during rest and maximal exercise testing

The subjects had a 12-lead conventional ECG recording (Ergo, HeartWare Ltda, Belo Horizonte, MG, Brazil) under rest and an ergometric test. For the incremental exercise testing on a treadmill we used the Modified Bruce Protocol [21]. The systolic blood pressure (SBP) and the diastolic blood pressure (DBP) were measured at rest and at each step of the test using the auscultatory sphygmomanometer. Estimated maximum oxygen consumption (VO_2max) achieved at peak exercise [22] was determined using the method described by the American Heart Association [23]. The metabolic equivalents (METs) were determined by the formula: VO_2 / 3.5 [23].

Assessment of menopause symptoms

Symptoms of menopause were assessed by the Menopause Rating Scale (MRS) of Hauser et al. [24], translated into Portuguese and was previously used in a descriptive study [25]. The MRS questionnaire is composed of 11 items divided into three subscales: (1) somatic symptoms such as hot flashes, heart discomfort, sleeping problems, and muscle and joint problems (items 1–3 and 11); (2) psychological symptoms such as depressive mood, irritability, anxiety, and physical and mental exhaustion (items 4–7); and (3) urogenital-sexual problems such as bladder problems and vaginal dryness (items 8–10). The total score per each subscale (somatic, psychological, and urogenital-sexual) is the sum of each graded item contained in that subscale. The total MRS score is the sum of the scores obtained for each subscale. The scores were also obtained by averaging the items. The magnitude of the symptoms can be categorized according to the severity of the symptoms for each domain of the MRS: absent or occasional (0–4 points), mild (5–8 points), moderate (9–15 points) or severe (≥16 points). Higher scores obtained by the MRS point toward severe symptoms and a poor quality of life [25].

Statistical analysis

Measurements were expressed as mean and standard deviations. The Shapiro-Wilk test was used to analyze the data normality. Comparisons between the gynoid and android groups were made using the unpaired Student's t test. To investigate the relationship between the key variables, we used the Pearson product–moment correlation coefficients. The level of statistical significance was 5 % ($P<0.05$). For the statistical analysis the software Statistica for Windows Release 7 (Statsoft Inc., Tulsa, OK) was used.

Results

The clinical characteristics can be seen in Table 1. The android group showed significantly higher values for body mass, BMI, waist circumference, body fat, lean mass and skinfolds ($P<0.05$). Compared to gynoid group, android women had significantly higher values of estradiol, triglycerides, VLDL, Castelli index I and insulin with lower insulin sensitivity and greater insulin resistance. The SBP and DBP values during rest were significantly higher, and the maximal heart rate (HRmax) during maximal exercise testing showed lower values for the android group ($P<0.05$) (Table 2). There were no significant differences ($P\geq0.05$) in the estimated VO_2max (Table 2). The magnitude of the somatic and urogenital-sexual symptoms was significantly higher for the android group compared to the gynoid group (Table 3).

There were lower but significant correlations between estradiol and body fat ($r=0.41$, $P<0.01$) as well as WHR for both triglycerides ($r=0.42$, $P<0.01$) and insulin ($r=0.34$, $P<0.05$). There were also significant correlations between waist circumference with Castelli index I ($r=0.43$, $P<0.01$, Fig. 1a). SBP during rest was moderately correlated to subscapular skinfold ($r=0.56$, $P<0.001$, Fig. 1b), suprailiac skinfold ($r=0.47$, $P<0.01$), triceps skinfold ($r=0.32$, $P<0.05$), abdominal skinfold ($r=0.39$, $P<0.01$), body fat ($r=0.51$, $P<0.001$), triglycerides ($r=0.32$, $P<0.05$) and glucose ($r=0.51$, $P<0.001$). Regarding the menopause symptoms, there were lower but significant inverse correlations between the HOMA %β-cell and the somatic symptoms ($r=-0.39$, $P<0.05$) as well as positive correlations between urogenital-sexual symptoms and circumference of waist ($r=0.37$, $P<0.05$, Fig. 1c).

Discussion

This study shows that android postmenopausal women develop features that can lead to MetS, and that they have higher scores of somatic and urogenital-sexual symptoms. Estradiol levels had positive correlations with body fat. In abdominal fat stores, androgens are converted to estrogen [12] which stimulates lipogenesis [26] and can explain that higher BMI, body fat percentage and subcutaneous fat in the android group. A mobilization of fat from the adipocytes to the visceral region is related to changes in the glucose utilization that leading to insulin resistance, increased lipid accumulation and increased production of triglycerides. Hyperinsulinemia results in enhanced sodium reabsorption and increased sympathetic nervous system activity, which may contribute to hypertension, and to increased levels of free fatty acids [27].

Table 1 Values of mean and standard deviation and statistical results of clinical characteristics of the women

	Gynoid group (*N*=13)	Android group (*N*=32)	P value
Anthropometric characteristics			
Age (years)	56±2	55±2	NS
Duration of menopause (years)	8±4	8±6	NS
Body composition and skinfold thickness			
Body mass (Kg)	62±10	76±13	<0.05
Height (cm)	155±7	157±6	NS
BMI (Kg/m^2)	26±4	31±5	<0.05
Waist (cm)	83±9	101±10	<0.01
Hip (cm)	104±9	109±10	NS
W/H (cm/cm)	0.79±0.03	0.92±0.05	<0.01
Body fat (%)	36±4	41±4	<0.01
Fat mass (Kg)	22±6	31±8	<0.01
Lean mass (Kg)	40±6	45±5	<0.05
Triciptal (mm)	28±7	34±6	<0.01
Subescapular (mm)	26±8	37±6	<0.01
Suprailiac (mm)	23±9	33±7	<0.01
Abdominal (mm)	30±6	38±5	<0.01
Anterior thigh (mm)	38±8	44±6	<0.05
Medial calf (mm)	31±9	35±8	NS
Σ6 skinfolds (mm)	174±44	224±34	<0.01
Biochemical exams			
Estradiol (pg/ml)	14±11	20±11	<0.05
Creatinine (mg/dl)	0.8±0.09	0.78±0.12	NS
Urea (mg/dl)	31±9	33±7	NS
Triglycerides (mg/dl)	117±106	177±85	<0.01
Total cholesterol (mg/dl)	225±39	233±49	NS
HDL(mg/dl)	55±12	50±10	NS
LDL (mg/dl)	146±29	147±41	NS
VLDL (mg/dl)	23±19	36±17	<0.01
Castelli index I	4±1.6	4.8±1.4	<0.05
Castelli index II	2.6±1.3	2.9±0.9	NS
Glucose (mg/dl)	93±15	98±21	NS
Insulin (μUl/ml)	4±3	8±5	<0.01
HOMA %β-cell	76±23	94±45	NS
HOMA %S	155±67	76±61	<0.05
HOMA %IR	0.8±0.35	1.6±1.3	<0.05

NS No significant difference was found between the groups, *W/H* Waist-to-hip ratio, *6 skinfolds* sum of six skinfolds, *HDL* high-density lipoprotein, *LDL* low-density lipoprotein, *VLDL* very low-density lipoprotein, *HOMA* homeostasis model assessment, *S* insulin sensitivity, *IR* insulin resistance

The accumulation of abdominal fat (android pattern), dyslipidemia and hypertension have a higher incidence in women after menopause compared to those with irregular menstrual cycles (perimenopause) and with regular cycles [4]. Thus, MetS risk factors are increased during the post menopause. Our study also identified that the android group showed higher values of triglycerides, VLDL and insulin with an increase of the HOMA %IR and a reduction of the HOMA %S compared to the gynoid group. Still, both triglycerides and insulin had positive correlations with WHR.

The increase of the insulin can lead to an increased blood glucose (compensatory mechanism) mainly because there was greater insulin resistance, which indicates an increased risk of developing type 2 diabetes mellitus [27]. Moreover, our data suggest that android postmenopausal women developed features of the MetS with an increased risk of CVD, as evidenced by insulin resistance, Castelli index and hypertension [5, 6, 8, 10].

The increased CVD risk among postmenopausal women may be associated with a progressive decrease in insulin sensitivity as a consequence of increased visceral adipose

Table 2 Values of mean and standard deviation and statistical results of the cardiovascular parameters during rest and maximal exercise testing

	Gynoid group (N=13)	Android group (N=32)	P value
Rest			
HR (beats/min)	69±7	73±9	NS
SBP (mmHg)	118±15	134±19	<0.01
DBP (mmHg)	76±8	80±10	<0.01
Exercise peak			
HR max (beats/min)	163±10	138±35	<0.05
SBP (mmHg)	162±19	164±20	NS
DBP (mmHg)	77±8	79±10	NS
VO_2 max (ml/kg/min)	28.1±7.9	27.7±7.1	NS
METs reaching	8.1±4.2	7.9±2.1	NS
Bruce (stage)	2.5±0.7	2.4±0.6	NS

NS No significant difference was found between the groups, *HR* Heart rate, *SBP* systolic blood pressure, *DBP* diastolic blood pressure, *VO_2max* maximal oxygen consumption, *METs* equivalent metabolic

tissue mass, emphasizing the importance of considering body fat distribution [28]. However, this study showed that HRT protects against the negative effects of increased visceral adiposity in postmenopausal women [28].

Both chronological age and ovarian age contributed to substantial changes in body composition, increasing the fat mass and the waist circumference over a 6 years period for premenopausal or perimenopausal women. These changes have important implications by establishing a metabolic environment which can be considered healthy or unhealthy [29], mainly for postmenopausal women. The recent study of Goss et al. [30] showed that the endocrine environment (i.e., circulating estrogen, free testosterone, cortisol and sex-hormone-binding globulin status) is associated with fat distribution in healthy postmenopausal women. This study suggests that the HRT generates a higher level of circulating estradiol which limits the lipid deposition in the intra-abdominal cavity. On the other hand, high proportion of weak estrogens may promote a gain of intra-abdominal adipose tissue over time. Moreover, postmenopausal women not using HRT may limit intra-abdominal adipose tissue accrual due to the higher circulating free testosterone [30]. Another study showed conflicting results, demonstrating that after menopause, an abdominal yet not gluteofemoral fat distribution is associated with high levels of free estradiol and free testosterone and with low levels of sex hormone-binding globulin [31]. Further studies are therefore needed to elucidate the mechanism by which sex hormones profiles regulate a lipid deposition in postmenopausal women and the extent to which HRT may affects these relationships.

Table 3 Values of mean and standard deviation of menopause symptoms by Menopause Rating Scale (MRS)

	Gynoid group (N=13)	Android group (N=32)	P value
Somatic symptoms score			
Sum	4.3±2.5	6.4±2.3	<0.05
Mean	1.1±0.6	1.5±0.8	<0.05
Psychological symptoms score			
Sum	5.6±0.7	6.3±0.5	NS
Mean	1.4±0.7	1.6±0.9	NS
Urogenital-sexual symptoms score			
Sum	2.7±1.8	4.6±1.9	<0.05
Mean	0.9±0.8	1.6±0.9	<0.05
Total score			
Sum	14.6±6.9	16.4±5.6	NS
Mean	1.3±0.6	1.5±0.5	NS

A significant difference was found between the groups for the sum and mean of the somatic and urogenital-sexual symptoms (P<0.05)

NS No significant difference was found between the groups

The sample size limitations in the gynoid group seen in the our study may be explained by the changes in the body composition with a gain of upper body fat and abdominal fat (subcutaneous and visceral) possibly due to hormonal decline observed during the postmenopausal period. This fat distribution is similar to that reported previously [28–31], reflecting the contribution of sex hormone profiles to the accumulation of abdominal fat.

No significant difference between the groups was found for the estimated VO_{2max} which indicates that women in both groups showed similar levels of aerobic fitness. However, the android group showed higher values of SPB and DPB during rest as well as lower HRmax. The lower HRmax for the android group may indicate a compensatory mechanism of depressed chronotropic responses [32]. In this context, autonomic nervous control of the heart rate could be analyzed in the future, as depressed autonomic responses have been observed in arterial hypertension [33].

Our results showed that the upper body subcutaneous fat (triceps, subescapular and suprailiac), serum triglycerides and blood glucose had a positive correlation with SPB. This indicates that women with a higher fat percentage, mainly android postmenopausal women, can develop hypertension

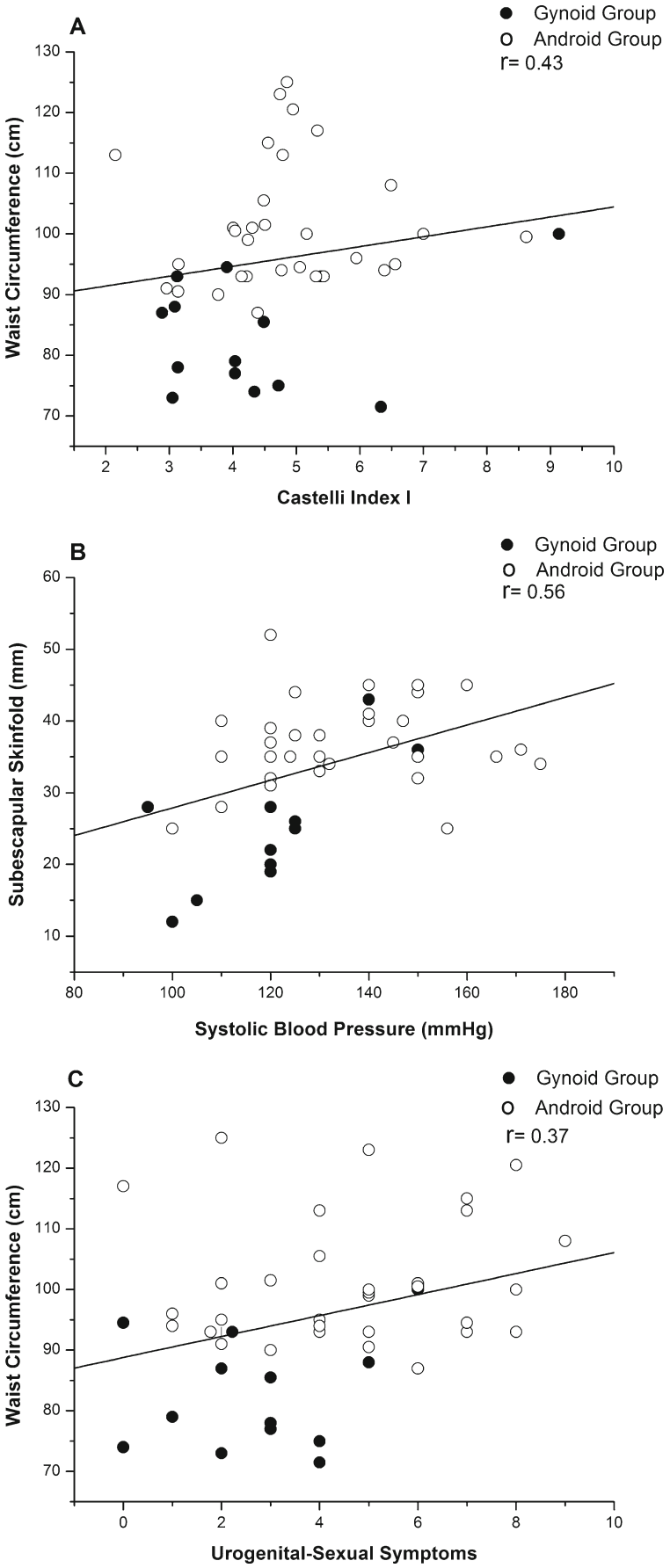

Fig. 1 Correlations between variables in gynoid (N=13) and android (N=32) postmenopausal women. Waist circumference as a function of Castelli index: the regression line represents both the average of the waist circumference and the Castelli index; the regression (r=0.43) was statistically significant at P=0.01 (**a**). Subescapular skinfold as a function of systolic pressure: the regression line represents both the average of the subescapular skinfold and the systolic blood pressure; the regression (r=0.56) was statistically significant at P=0.000 (**b**). Waist circumference as a function of urogenital-sexual symptoms: the regression line represents both the average of the waist circumference and the urogenital-sexual symptoms; the regression (r=0.37) was statistically significant at P=0.02 (**c**)

associated with dyslipidemia and insulin resistance with attendant complications [19]. These findings were corroborated by a longitudinal study, where even in adolescents (12–18 years) the increase in blood pressure was associated with an increased BMI, abdominal fat and upper body subcutaneous fat [15]. Moreover, in another study, Lee et al. [34] observed that postmenopausal women with MetS showed a higher total score of MRS and a higher subscale score for the somatic symptoms.

Higher somatic symptoms were observed in the android group. Hot flush, sweating, insomnia, dizziness and heart discomfort, palpitations and, muscle and, joint problems occur with a higher frequency in postmenopausal women, mainly for those with an increased body mass. Android fat distribution and a higher BMI can result in a poor quality of life during menopause [11].

Weakness and fatigue of the lower abdominal and pelvic floor muscles in postmenopausal women can result in urinary incontinence. Higher BMI can result in a higher intra-abdominal pressure and in development and recurrence of urinary incontinence [35]. Lower levels of sexual desire and lower frequency of penile–vaginal intercourse were associated with more body fat and larger waist or hip circumference as well as lower arousal, orgasm, and lubrication, when associated with MetS during the premenopausal state [36, 37]. Moreover, sexual pain and orgasmic disorder also occur due to hypoestrogenemia [38].

However, in our study, the psychological symptoms were similar for the both groups, being commonly encountered by women in this period of life [39] and they were not influenced by the type of fat distribution. A descriptive study in Brazil showed that perimenopausal women, but not postmenopausal women, were at greater risk to undergo minor psychiatric disorders [40]. A low level of education, memory loss, irritability, and the menopausal transition were risk factors which may lead to positive findings in a screening for minor psychiatric disorders [40]. However, the magnitude of all symptoms estimated by MRS for the gynoid and android group ranged from occasional to moderate. This may be due to the fact that, probably, a higher magnitude of these symptoms occurs in the menopausal transition.

However, an advantage for the android group observed in the current study is the larger muscle mass compared to the gynoid group. This is important since the aging process induces a loss of muscle mass due to atrophy and neuromuscular degeneration [41]. The bigger muscle mass in the obese postmenopausal women can be influenced by weight-bearing effects, which improves muscular function [22].

Several strategies have been developed to reduce MetS and CVD risk factors, for example, medication use [42], diet programs [43], physical exercise program [44] and phototherapeutic technologies such as treatments using laser [45] or light-emitting diodes (LED) [46].

The limitations of this study were: we only used anthropometric parameters and electrical bioimpedance to measure body composition and these do not distinguish between accumulations of visceral and subcutaneous abdominal fat. In this context, imaging techniques (e.g., computed tomography, magnetic resonance and ultrasonography), which can distinguish fat from other tissues should be used in future studies.

In conclusion, postmenopausal women with central obesity present a greater risk to develop MetS and CVD, because these women showed higher rates of hypertension, dyslipidemia, insulin resistance and hyperinsulinemia, leaving them prone to the development of a higher magnitude of somatic and urogenital-sexual symptoms. Moreover, the association of androgenic obesity with hypertension, hipertriglyceridemia and insulin resistance can also amplify the occurrence of MetS and future CVD during the postmenopausal period. Finally, the somatic and urogenital-sexual dysfunction could also occurs more often in these women than in those presenting the gynoid pattern.

Acknowledgments We thank the participants without whom this study would not have been possible. We acknowledge the support from Fundação de Amparo à Pesquisa do Estado de São Paulo (FAPESP) – Grant no. 98/14270-8 and 09/01842-0; Conselho Nacional de Desenvolvimento Científico e Tecnológico (CNPq) – Grant no. 150949/2011-1 and 151008/2012-4; Coordenação de Aperfeiçoamento de Pessoal de Nível Superior (CAPES).

Conflicts of interest None

References

1. Messier V, Karelis AD, Lavoie ME, Brochu M, Faraj M, Strychar I, et al. Metabolic profile and quality of life in class I sarcopenic overweight and obese postmenopausal women: a MONET study. Appl Physiol Nutr Metab. 2009;34:18–24.
2. Gorodeski GI. Update on cardiovascular disease in post-menopausal women. Best Pract Res Clin Obstet Gynaecol. 2002;16:329–55.
3. Lovejoy JC, Champagne CM, Jonge L, Xie H, Smith SR. Increased visceral fat and decreased energy expenditure during the menopausal transition. Int J Obes (Lond). 2008;32:949–58.
4. Ebrahimpour P, Fakhrzadeh H, Heshmat R, Ghodsi M, Bandarian F, Larijani B. Metabolic syndrome and menopause: a population-based study. Diab Metab Syndr Clin Res Rev. 2010;4:5–9.
5. Blümel JE, Legorreta D, Chedraui P, Ayala F, Bencosme A, Danckers L, et al. Optimal waist circumference cutoff value for defining the metabolic syndrome in postmenopausal Latin American women. Menopause J N Am Menopause Soc. 2012. doi:10.1097/gme.0b013e318231fc79.
6. Corona G, Mannucci E, Petrone L, Schulman C, Balercia G, Fisher AD, et al. A comparison of NCEP-ATPIII and IDF metabolic syndrome definitions with relation to metabolic syndrome-associated sexual dysfunction. J Sex Med. 2007;4:789–96.
7. Misso ML, Jang C, Adams J, Tran J, Murata Y, Bell R, et al. Differential expression of factors involved in fat metabolism with age and the menopause transition. Maturitas. 2005;51:299–306.

8. Feng Y, Hong X, Wilker E, Li Z, Zhang W, Jin D, et al. Effects of age at menarche, reproductive years, and menopause on metabolic risk factors for cardiovascular diseases. Atherosclerosis. 2008;196:590–7.
9. Toth MJ, Tchernof A, Sites CK, Poehlman ET. Effect of menopausal status on body composition and abdominal fat distribution. Int J Obes. 2000;24:226–31.
10. Després JP, Lemieux I. Abdominal obesity and metabolic syndrome. Nature. 2006;44:881–7.
11. Castelo-Branco C, Palacios S, Ferrer-Barriendos J, Cancelo MJ, Quereda F, Alberich X. Impact of anthropometric parameters on quality of life during menopause. Fertil Steril. 2009;96:1947–52.
12. Li S, Wagner R, Holm K, Lehotsky J, Zinaman MJ. Relationship between soft tissue body composition and bone mass in perimenopausal women. Maturitas Eur Menopause J. 2004;47:99–105.
13. Fujibayashi M, Hamada T, Matsumoto T, Kiyohara N, Tanaka S, Kotani K, et al. Thermoregulatory sympathetic nervous system activity and diet-induced waist-circumference reduction in obese Japanese women. Am J Hum Biol. 2009;21:828–35.
14. Moreno LA, Mesana MI, González-Gross M, Gil CM, Fleta J, Wärnberg J, et al. Anthropometric body fat composition reference values in Spanish adolescents. The AVENA Study. Eur J Clin Nutr. 2006;60:191–6.
15. Maximova K, O'Loughlin J, Paradis G, Hanley JA, Lynch J. Changes in anthropometric characteristics and blood pressure during adolescence. Epidemiology. 2010;21:324–31.
16. Bagnoli VR, Fonseca AM, Halbe HW, Sauerbronn AVD, Pinotti JA. Como diagnosticar e tratar a síndrome do climatério. Rev Bras Med. 2007;64:99–109.
17. Wilson PWF, Anderson KM, Harris T, Kannel WB, Castelli WP. Determinants of change in total cholesterol and HDL-C with age: the Framingham Study. J Gerontol Med Sci. 1994;49:M252–7.
18. HOMA Calculator. University of Oxford: Diabetes Trials Unit. www.dtu.ox.ac.uk/homacalculator/index.php.
19. Gorodeski EZ, Gorodeski GI. Epidemiology and risk factors of cardiovascular disease in postmenopausal women. In: Lobo RA, editor. Treatment of the menopausal women: basic and clinical aspects. 3rd ed. San Diego: Academic; 2007. p. 405–52.
20. Romaguera J, Ortiz AP, Roca FJ, Colón G, Suárez E. Factors associated with metabolic syndrome in a sample of women in Puerto Rico. Menopause J N Am Menopause Soc. 2010;17:388–92.
21. Johnson PH, Cowley AJ, Kinnear WJM. A randomized controlled trial of inspiratory muscle training in stable chronic heart failure. Eur Heart J. 1998;19:1249–53.
22. Paolillo FR, Milan JC, Bueno PG, Paolillo AR, Borghi-Silva A, Parizotto NA, et al. Effects of excess body mass on strength and fatigability of quadriceps in postmenopausal women. Menopause J N Am Menopause Soc. 2012. doi:10.1097/gme.0b013e3182364e80.
23. Haskell WL, Lee IM, Pate RR. Physical activity and public health: updated recommendation for adults from the American College of Sports Medicine and the American Heart Association. Med Sci Sports Exerc. 2007;39:1423–34.
24. Hauser GA, Huber IC, Keller PJ, Lauritzen C, Schneider H. Evaluation of climacteric symptoms (Menopause Rating Scale). Zentralbl Gynakol. 1994;116:16–23.
25. De Lorenzi D, Catan LB, Cusin T, Feline R, Bassani F, Arpini AC. Caracterização da qualidade de vida segundo o estado menopausal entre as mulheres da região sul do Brasil. Rev Bras Saúde Matern Infant. 2009;9:459–66.
26. Rossi ABR, Vergnanini AL. Cellulite: a review. Eur Acad Dermatol Venereol. 2000;14:251–62.
27. Eckel R, Grundy S, Zimmet. The metabolic syndrome. Lancet. 2005;365:1415–28.
28. Munoz J, Derstine A, Gower BA. Fat distribution and insulin sensitivity in postmenopausal women: influence of hormone replacement. Obes Res. 2002;10:424–31.
29. Sowers MF, Zheng H, Tomey K, Karvonen-Gutierrez C, Jannausch M, Li X, et al. Changes in body composition in women over six years at midlife: ovarian and chronological aging. J Clin Endocrinol Metab. 2007;92:895–901.
30. Goss AM, Darnell BE, Brown MA, Oster RA, Gower BA. Longitudinal associations of the endocrine environment on fat partitioning in postmenopausal women. Obesity (Silver Spring). 2012;20:939–44.
31. Liedtke S, Schmidt ME, Vrieling A, Lukanova A, Becker S, Kaaks R, et al. Postmenopausal sex hormones in relation to body fat distribution. Obesity (Silver Spring). 2012;20:1088–95.
32. Lauer MS, Okin PM, Larson MG, Evans JC, Levy D. Impaired heart rate response to graded exercise: prognostic implications of chronotropic incompetence in the Framingham Heart Study. Circulation. 1996;93:1520–6.
33. Pal GK, Pal P, Nanda N, Amudharaj D, Karthik S. Spectral analysis of heart rate variability (HRV) may predict the future development of essential hypertension. Med Hypotheses. 2009;72:183–5.
34. Lee SW, Jo HH, Kim MR, Kwon DJ, You YO, Kim JH. Association between menopausal symptoms and metabolic syndrome in postmenopausal women. Arch Gynecol Obstet. 2011;285:541–8.
35. Noblett KL, Jesen JK, Ostergard DR. The relationship of body mass index to intra-abdominal pressure as measured by multichannel cystometry. Int Urogynecol J. 1997;8:323–6.
36. Esposito K, Ciotola M, Marfella R, Di Tommaso D, Cobellis L, Giugliano D. The metabolic syndrome: a cause of sexual dysfunction in women. Int J Impot Res. 2005;17:224–6.
37. Esposito K, Giuliano D. Obesity, the metabolic syndrome, and sexual dysfunction. Int J Impot Res. 2005;17:391–8.
38. Tan O, Bradshaw K, Carr BR. Management of vulvovaginal atrophy related sexual dysfunction in postmenopausal women: an up-to-date review. Menopause J N Am Menopause Soc. 2012. doi:10.1097/gme.0b013e31821f92df.
39. Timur S, Sahyn NH. The prevalence of depression symptoms and influencing factors among perimenopausal and postmenopausal women. Menopause J N Am Menopause Soc. 2010;17:545–51.
40. Oppermann K, Fuchs SC, Donato G, Bastos CA, Spritzer PM. Physical, psychological, and menopause-related symptoms and minor psychiatric disorders in a community-based sample of Brazilian premenopausal, perimenopausal, and postmenopausal women. Menopause J N Am Menopause Soc. 2012. doi:10.1097/gme.0b013e31822ba026.
41. Messier V, Rabasa-Lhoret R, Barbat-Artigas S, Elisha B, Karelisc AD, Aubertin-Leheudre M. Menopause and sarcopenia: a potential role for sex hormones. Maturitas. 2011;68:331–6.
42. Koh Y, Ben-Ezra V, Biggerstaff KD, Nichols DL. Responses of blood lipids and lipoproteins to extended-release niacin and exercise in sedentary postmenopausal women. J Gerontol A Biol Sci Med Sci. 2010;65A:924–32.
43. Nicklas BJ, Katzel LI, Bunyard LB, Dennis KE, Goldberg AP. Effects of an American Heart Association diet and weight loss on lipoprotein lipids in obese, postmenopausal women. Am J Clin Nuir. 1997;66:853–9.
44. Hagner W, Hagner-Derengowska M, Wiacek M, Zubrzycki IZ. Changes in level of VO_2max, blood lipids, and waist circumference in the response to moderate endurance training as a function of ovarian aging. Menopause J N Am Menopause Soc. 2009;16:1009–13.
45. Rushdi TA. Effect of low-level laser therapy on cholesterol and triglyceride serum levels in ICU patients: a controlled, randomized study. EJCTA. 2010;4:95–9.
46. Paolillo FR, Milan JC, Aniceto IV, Barreto SG, Rebelatto JR, Borghi-Silva A, et al. Effects of infrared-LED illumination applied during high-intensity treadmill training in postmenopausal women. Photomed Laser Surg. 2011;29:639–45.

Journal of Pharmacy and Pharmacology 3 (2015) 434-437
doi: 10.17265/2328-2150/2015.09.005

A Promising Strategy for the Treatment of Onychomycosis with Curcumin and Photodynamic Therapy

Ana Paula da Silva, Fernanda M. Carbinatto, Vanderlei S. Bagnato and Natalia M. Inada
University of Sao Paulo, Physics Institute of Sao Carlos, 13566-590 Sao Carlos, SP, Brazil

Abstract: Onychomycosis is a disease of high incidence in the nail plate and responsible for approximately half of the cases of nail infections. Conventionally, dermatologists prescribe antibiotics and antifungals for long periods for its treatment. The high incidence of this type of infection and the increase of microbial strains resistant to the available drugs have justified the importance of the development of new technologies and treatments. This paper presents the photodynamic therapy as an alternative treatment of onychomycosis. New strategies for the use of curcumin as a photosensitizer and its therapeutic response were investigated in different formulations (gel and emulsion). Photodynamic therapy is a promising technique by which microorganisms are eliminated by a photosensitizing compound , light and oxygen. It was evaluated in two patients who had developed lesions in the fingernails caused by onychomycosis for approximately 10 years. The lesions were treated by photodynamic therapy with curcumin. The therapeutic efficacy was observed after a maximum of six photodynamic therapy sessions without any other adjuvant therapy. Curcumin has become more promising than the therapeutic standard as it is a natural and versatible drug for incorporation in different formulations, at low cost and low probability of side effects.

Key words: Onychomycosis, photodynamic therapy, curcumin, formulations.

1. Introduction

Onychomycosis is a nail fungal infection caused by dermatophytes, yeasts or nondermatophytes. Systemic and topical antifungal agents can be used in its conventional treatment [1, 2]. However, oral antifungals may cause adverse effects. The topical formulation with antifungal agents may have low therapeutic efficacy because of their limited ability to penetrate the nail plate and reach the affected area [3].These factors and the high incidence of this infection are important parameters for the analyses of new formulations associated with other techniques to ensure the success of the therapy.

PDT (photodynamic therapy) is a noninvasive simple technique, therefore it is an interesting therapy for the treatment of onychomycosis. It is characterized by the association of a photosensitizing agent and a light source of suitable wavelength. When this photosensitizer is activated by light in the presence of oxygen, it produces reactive oxygen species that inactivate the fungi and cause onychomycosis [4].

Curcumin is a component obtained from the rizoma of *Curcuma* Longa Linn and investigated as a potential PS (photosensitizing compound) in PDT for the inactivation of microorganisms. Besides its use as a PS, it can act on localized superficial infections. Initially, curcumin was used mainly in the food industry, but its application is not limited to the food area. It has shown several biological effects, such as suppression of carcinogenesis by avoiding the

Corresponding author: Natalia M. Inada, Ph.D., doctor of medical pathophysiology, post-doctorate by the physics institute of USP in São Carlos (IFSC), researcher, research fields: biology, medicine, pharmacy, chemistry and physics, with a background in biochemistry (metabolism and bioenergetics), operates mainly in: mitochondrial bioenergetics, tumor cells, reactive oxygen species, cell death mechanisms, basic photodynamic therapy (*in vitro* and *in vivo*) and applied (clinical research), optical devices applied in health. E-mail: nataliainada@gmail.com.

proliferation of a wide variety of tumor cells (skin, lung, stomach, colon and breast), anti-inflammatory, antioxidant and bactericidal activitivies. Pharmacological actions can be intensified when curcumin is irradiated with blue light [5-7].

Silva, A. P. et al reported some promising results regarding the use of curcumin solutions for onychomycosis treatments in patients that had showed unsatisfactory results in conventional therapies and had been affected by the disease for more than 5 years. The patients nail plates were applied a curcumin solution and then illuminated with LED (light emitting diode) 450 nm [8]. However, curcumin in solution does not remain long in contact with the lesion due to the limitation of its standard formulation. As the nail plate is composed mainly of keratin, a low content of lipids and water, it works as a hydrophilic barrier. Lipids may represent an important route of transportation mainly for hydrophobic substances [9]. As the nail plate hampers the permeation of the PS, we have studied new formulations to improve the success of the therapy with curcumin.

Due to the structural characteristics of the nail plate, curcumin was used in different formulations (hydrophilic gel and water/oil emulsion) for the analysis of the success of the therapy.

2. Material and Methods

2.1 Patient Selection

The patients with onychomycosis were selected with a clinical diagnosis confirmed by podiatrist.

The experiments were approved by the Ethics Committee of Anhembi Morumbi University (79th Ethics Committee Meeting on November 16, 2010) and patients signed an informed consent.

2.2 Formulation with PS

Curcumin was solubilize with 1% alcohol and 0,1% dimethyl sulfoxide after Curcumin was incorporated in the 1.5% concentration in two different formulation, in carbopol gel and emulsion W/O.

2.3 PDT for Treatment Onycomycosis

Patients with Onychomycosis were treated for 20 min by an LED (450 nm, 100 mW/cm^2) system developed in the Laboratory of Technological Support and anatomically designed for fingernails and Toenails (total fluence of 120 J/cm^2) (Fig. 1).

Patients had their nail plate prepared with a solution of 40% urea emollient two hours before the treatment. Urea was in contact with the nail for one hour and after this period its excess was removed and PS was applied for one hour before illumination.

Curcumin in the 1.5% concentration was topically applied in gel or emulsion and subjected to illumination. After a seven-day treatment, a new evaluation was conducted for the analysis of the clinical response to the treatment. The follow-up treatment was performed by a clinical evaluation and documented by photographic images weekly.

For a comparative analysis of different formulations, the treatment was performed in two patients (case 1: male, aged 27 and case 2: female, 65 years old) with

Fig. 1 Design of the device registered in the National Institute of Industrial Property (INPI Protocol No. 18110047225, December 5th, 2011).

fingernail diseases caused by fungi. Both patients had had the lesions for approximately 10 years. The results were positive for the laboratory cultures, which indicated the presence of fungi.

3. Results

3.1 Patient 1: Treatment of Onychomycosis with Gel Curcumin

Gel curcumin (1.5%) was topically applied to the fingernail (Fig. 2) in case 1. The nail was then protected from light for 1h. Only 6 PDT sessions were applied and a complete healing was achieved (Fig. 2b) and evidenced by the negative culture of microorganisms for fungi that cause onychomycosis.

3.2 Patient 2: Treatment of Onychomycosis with Emulsion Curcumin

Curcumin incorporated in emulsion (1.5%) was topically applied to the fingernail (Fig. 3) in case 2. The nail was then protected from light for 1h. Only 5 PDT sessions were necessary and a complete healing was achieved (Fig. 3b) and evidenced by the negative culture of microorganisms for fungi that cause onychomycosis.

Fig. 2 Male patient, 10 years of lesion, (a) before treatment and (b) after 6 sessions of PDT with curcumin (PDT pharma gel 1.5%).

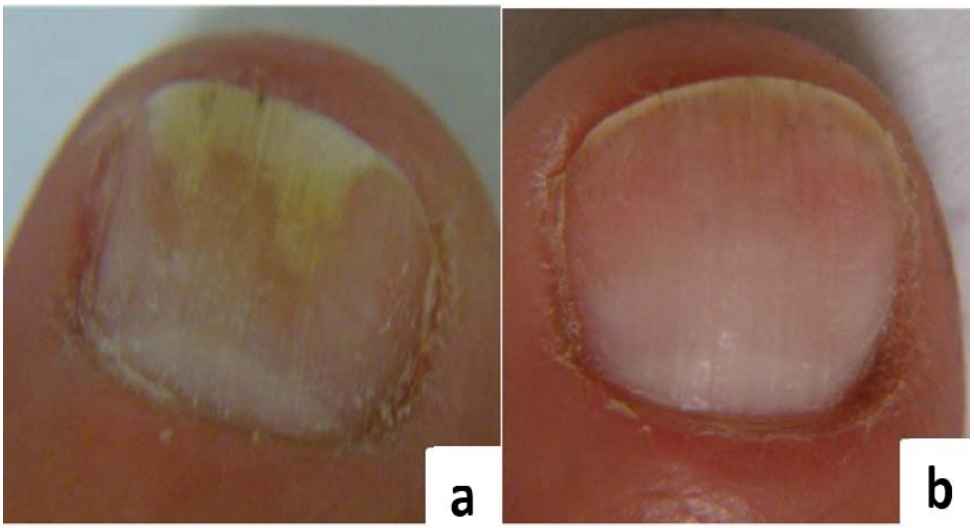

Fig. 3 Female patient, 10 years of lesion, (a) before treatment and (b) after 5 sessions of PDT with curcumin (PDT Pharma Emulsion 1.5%).

4. Discussions

This study has demonstrated the efficacy of PDT with curcumin as a photosensitizer agent in the treatment of onychomycosis. The possibility of using vehicular curcumin in different formulations (gel and emulsion) can be a positive aspect for this approach.

The new formulation combined with the pre-treatment of the nail bed, can favor the penetration of curcumin in the lesion. The patients reported no pain during and after the treatment and the sessions were repeated weekly.

The satisfactory results achieved with few treatment sessions have proven the differential of this new approach to treat onychomycosis in comparison to conventional treatments, which require a higher number of sessions and may cause discontinuity of the treatment.

5. Conclusion

Photodynamic therapy has shown increased potential to aid in microbial and fungal reductions . It was possible to reach a favorable setting for commercial viability of the formulations developed for clinical research, which should help to expedite the availability of this technique to the national and international clinical reality. PDT using different formulation with curcumin is a technique with great potential and low-cost treatment of onychomycosis.

Acknowledgements

This research has been supported by grants from Fundacão de Amparo à Pesquisa do Estado de São Paulo (FAPESP; CEPOF Grant No. 98/14270-8) and Financiadora de Estudos e Projeto FINEP-Gnatus (Grant No. 554339/2010-2). APS was supported by Conselho Nacional de Desenvolvimento Científico e Tecnológico (CNPq FINEP-Gnatus; GrantNo. 381132/2010-2).

References

[1] Naumann, S., Meyer J. P., Kiesow, A., Mrestani, Y., Wohlrab, J., and Neubert, R. H. 2014. “Controlled Nail Delivery of a Novel Lipophilic Antifungal Agent Using Various Modern Drug Carrier Systems as well as *in Vitro* and *ex Vivo* Model Systems.” *J. Control Rel*. 180: 60-70.

[2] Laborde, S. V., and Scher, R. K. 2000. “Developments in the Treatment of Nail Psoriasis, Melanonychia striata, and Onychomycosis.” *Dermatol. Clin.* 18: 37-46.

[3] Lim, E. H., Kim, H. R., Park, Y. O., Lee, Y., Seo, Y. J., Kim, C. D., Lee, J. H., and Im, M. 2014. “Toenail Onychomycosis Treated with a Fractional Carbon-Dioxide Laser and Topical Antifungal Cream.” *J. Amer. Acad. Dermatol*. 70: 918-23.

[4] Pavarina, A. C., Ribeiro, A. P. D., Dovigo, L. N. Andrade, C. R. Costa, C. A. S. and Vergani, C. E. 2012. “Photodynamic Therapy to Eradicate Tumor Cells.” In: *Cell Metabolism-Cell Homeostasis and Stress Response,* edited by Dr. Paula Bubulya, InTech, 149-62.

[5] Bruzell, E. M., Morisbak, E., and Tønnesenet, H. H. 2005. “Studies on Curcumin and Curcuminoids. XXIX. Photoinduced Cytotoxicity of Curcumin in Selected Aqueous Preparations.” *Photochem. Photobiol*. Sci. 4: 523-30.

[6] Wikene, K. O., Hegge, A. B., Bruzell, E., and Tønnesen, H. H. 2014. “Formulation and Characterization of Lyophilized Curcumin Solid Dispersions for Antimicrobial Photodynamic Therapy (aPDT): Studies on Curcumin and Curcuminoids LII.” *Drug Dev. Ind. Pharm*. 1-9.

[7] Khalil, O. A. K., Oliveira, O. M., Vellosa, J. C., Quadros, A. U., Dalposso, L. M., Karam, T. K., Mainardes, R. M., and Khalil, K. M. 2012. “Curcumin Antifungal and Antioxidant Activities Are Increased in the Presence of Ascorbic Acid.” *Food Chem*. 133: 1001-5.

[8] Silva, A. P., Chianfrone, D. J., Tinta, J. W. R., Kurachi, C., Inada, N. M., Bagnato, V. S. 2015. “Development and Comparison of Two Devices for Treatment of Onychomycosis by Photodynamic Therapy.” *J. Biomed. Opt.* 20 (6): 061109.

[9] Murdan, S. 2002. “Drug Delivery to the Nail Following Topical Application.” *Int. J. Pharm.* 236: 1-26.

Journal of Photochemistry & Photobiology, B: Biology 153 (2015) 103–110

Contents lists available at ScienceDirect

Journal of Photochemistry & Photobiology, B: Biology

journal homepage: www.elsevier.com/locate/jpb

Can low-level laser therapy (LLLT) associated with an aerobic plus resistance training change the cardiometabolic risk in obese women? A placebo-controlled clinical trial

Fernanda Oliveira Duarte [a,*], Marcela Sene-Fiorese [b], Antonio Eduardo de Aquino Junior [a,c], Raquel Munhoz da Silveira Campos [d], Deborah Cristina Landi Masquio [d], Lian Tock [e], Ana Claudia Garcia de Oliveira Duarte [f], Ana Raimunda Dâmaso [d], Vanderlei Salvador Bagnato [b,c], Nivaldo Antonio Parizotto [a,c]

[a] Therapeutic Resources Laboratory, Department of Physiotherapy, Federal University of São Carlos (UFSCar), Rodovia Washington Luis, Km 235, 13565-905 São Carlos, São Paulo, Brazil
[b] São Carlos Institute of Physics, University of São Paulo (USP), Avenida Trabalhador Sãocarlense, 400, PO Box 369, 13560-970 São Carlos, São Paulo, Brazil
[c] Post-Graduated Program of Biotechnology, Federal University of São Carlos (UFSCar), Rodovia Washington Luis, Km 235, 13565-905 São Carlos, São Paulo, Brazil
[d] Post-Graduated Program of Nutrition, Federal University of São Paulo (UNIFESP), Rua Marselhesa, 650, 04021-001 São Paulo, São Paulo, Brazil
[e] Weight Science, rua Teodoro Sampaio, 744, Cj. 98, 05406-000 São Paulo, São Paulo, Brazil
[f] Nutrition and Metabolism Applied to Exercise Laboratory, Department of Physical Education, Federal University of São Carlos (UFSCar), Rodovia Washington Luis, Km 235, 13565-905 São Carlos, São Paulo, Brazil

ARTICLE INFO

Article history:
Received 12 May 2015
Received in revised form 28 August 2015
Accepted 31 August 2015
Available online 2 September 2015

Keywords:
Obesity
Low-level laser therapy (LLLT)
Aerobic exercise
Resistance exercise
Inflammation
Cardiometabolic risk

ABSTRACT

Introduction: Obesity is one of the most important link factors to coronary artery disease development mainly due to the pro-inflammatory and pro-thrombotic states favoring atherosclerosis progression. The LLLT acts in the cellular metabolism and it is highly effective to improve inflammation. The same occur in response to different kinds of exercise. However, we have not known the associate effects using LLLT therapies with aerobic plus resistance training as strategy specifically with target at human obesity control and its comorbidities.
Objective: Investigate the effects of the LLLT associated with aerobic plus resistance training on cardiometabolic risk factors in obese women.
Methodology: Women aged 20–40 years (BMI ≥ 30 kg/m^2), were divided into 2 groups: Phototherapy (PHOTO) and Placebo. They were trained aerobic plus resistance exercises (in a concurrent mode), 1 h, 3 times/week during 16 weeks. Phototherapy was applied after each exercise session for 16 min, with infrared laser, wavelength 808 nm, continuous output, power 100 mW, and energy delivery 50 J. The body composition was measured with bioimpedance. Inflammatory mark concentrations were measured using a commercially available multiplex.
Results: LLLT associated with aerobic plus resistance training was effective in decrease neck ($P = 0.0003$) and waist circumferences ($P = 0.02$); percentual of fat ($P = 0.04$); visceral fat area ($P = 0.02$); HOMA-IR ($P = 0.0009$); Leptin ($P = 0.03$) and ICAM ($P = 0.03$). Also, the reduction in leptin ($P = 0.008$) and ICAM-1 (0, 05) was much more expressive in the phototherapy group in comparison to placebo group when analyzed by delta values.
Conclusion: LLLT associated with concurrent exercise (aerobic plus resistance training) potentiates the exercise effects of decreasing the cardiometabolic risk factors in obese woman. These results suggest the LLLT associated with exercises as a new therapeutic tool in the control of obesity and its comorbidities for obese people, targeting to optimize the strategies to control the cardiometabolic risk factors in these populations.

1. Introduction

Obesity is a complex disease and its pathogenesis is multifactorial, resulting mainly from sedentary behaviors coupled with inadequate eating habits [1,2]. It is strongly associated with subclinical inflammation, metabolic syndrome, type 2 diabetes and an elevated risk of cardiovascular diseases [3]. Some cytokines with higher concentrations in obesity promote the development of cardiovascular disease, mainly pro-inflammatory proteins such as leptin, plasminogen activator inhibitor (PAI-1), interleukin-6 (IL-6), tumor necrosis factors alpha (TNF-α), intracellular adhesion molecule 1 (ICAM-1) and vascular cell adhesion molecule 1 (VCAM-1), among others [4,5].

* Corresponding author at: Therapeutic Resourses Laboratory, Department of Physiotherapy, Federal University of São Carlos (UFSCar), Rodovia Washington Luis, Km 235, 13565-905 São Carlos, São Paulo, Brazil. Tel.: +55 16 3351 8985.
E-mail address: fefa.duarte74@gmail.com (F.O. Duarte).

http://dx.doi.org/10.1016/j.jphotobiol.2015.08.026
1011-1344/

In this context, the obesity, mainly the visceral fat, is directly associated with major risk for cardiovascular and metabolic diseases and is a feature of systemic inflammation [6]. The hyperleptinemia and hyperinsulinemia configure the profile of most obese individuals and appear to be the key factors of the metabolic abnormalities, providing inadequate response to weight loss therapy [7]. Furthermore, the PAI-1 increase in plasma of the obese individuals leads to a hyperthrombotic state by hypofibrinolysis, hypercoagulability and platelets activation that leads to the development of atherosclerotic plaques formation, main predictor for myocardial infarction [8,9].

Data supports that the interdisciplinary intervention model associated to aerobic plus resistance training was more effective in improving the visceral adiposity, inflammatory markers and metabolic profile in obese adolescents [10,11]. In addition, Jackson and colleagues [12] find changes in the body composition as in circumferential measurements across waist, hips, and thighs compared to placebo subjects after LLLT treatment, with a total of six treatments across 2-weeks. The authors suggest that change in the adipose tissue occurs due to adaptations in the membrane permeability of adipocytes, releasing fatty acids in blood circulation, but their removal and metabolism mechanisms still remain unclear [12].

Actually the advance in studies involved low-level laser therapy (LLLT) or light-emitting diode (LED) therapy has allowed a better understanding of their mechanisms in the biologic tissues. Therefore, the use of light in different applications like LLLT as ancillary non-invasive treatment has been disseminated in recent years, mainly in controlling pain, inflammation, mucositis, tissue repairs besides the muscle performance and also in the aesthetic treatments [13–16].

Although, recently a pioneer study of our research group demonstrated that phototherapy when associated with swimming training was efficient to potentiate the weight loss, as well as ameliorate the lipid profile in exogenous obese rats [17]. Nonetheless, we did not find studies using the association between LLLT therapies with aerobic plus resistance training as strategy specifically with target at human obesity control and its comorbidities.

This way, we hypothesized that the LLLT associated with aerobic plus resistance training may promote a reduction in pro-inflammatory and prothrombotic markers, contributing to reduce cardiometabolic risk factors in obese women in a placebo-controlled clinical trial.

2. Material and Methods

The details about experimental design are shown in Fig. 1.

2.1. Subjects

For this study, a total of 64 adult obese women, with the age of 20–40 years were involved in this randomized double blind controlled clinical trial. The volunteers were recruited by impress and electronic media, TV and radio. The inclusion criteria were: 1) primary obesity, body mass index (BMI) between 30 and 40 kg/m^2 and 2) age between 20 and 40 years old. Exclusion criteria were: 1) the use of cortisone, anti-epileptic drugs; 2) history of renal disease; 3) alcohol intake; 4) smoking and 5) secondary obesity due to endocrine disorders.

The study was conducted in accordance with the principles of the Declaration of Helsinki and was approved by the ethics committee on human research at Universidade Federal de São Carlos — UFSCar (#237.050) and registered at Clinical Trial: 231.286. All procedures were made clear to the volunteers and consent for research was agreed. The evaluations were performed at different times: in the beginning and the end of therapy; and in the middle (4 months) of interdisciplinary intervention. The main reasons for dropping out (n = 12) in our study were pregnancy, family problems and job opportunities.

The volunteers were randomly assigned between two groups through the sample randomization program (www.randomization.com): placebo group and phototherapy group (PHOTO). The treatment consisted in physical exercise intervention – moderate aerobic plus resistance training – and the individually application of phototherapy immediately after the end of the training. The same interventions of phototherapy group were applied for placebo group voluntaries however, during the application of phototherapy the placebo group did not received the incidence of laser light, characterizing the study as a placebo-controlled clinical trial. This one is the blind analyzer and the other is the person that analyzed the data, without the knowledge of the treated group. The voluntaries do not know which group they belonged. During the experimental

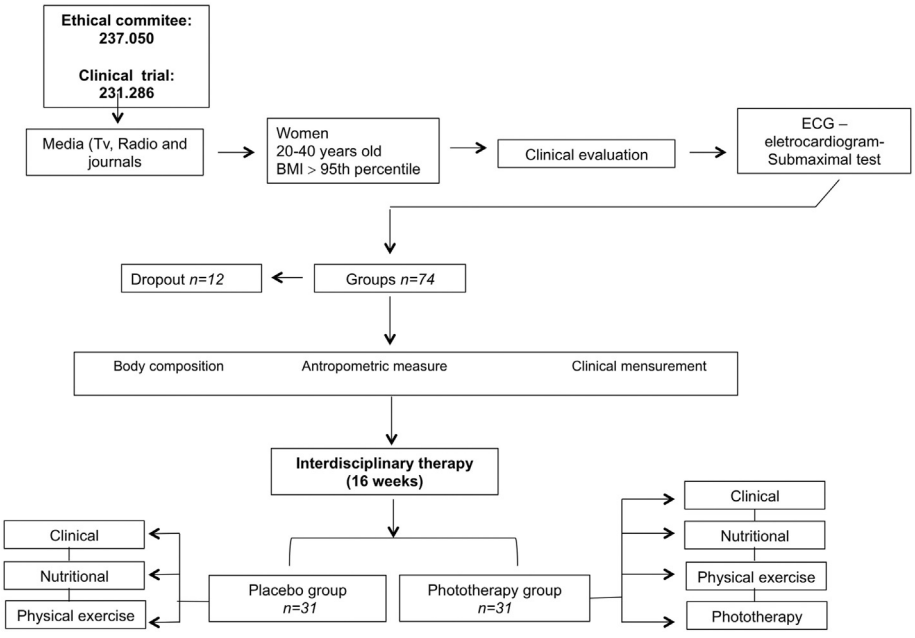

Fig. 1. Methodological description.

protocol, all volunteers received nutritional counseling. The only one that differs among groups was the presence of the light.

2.2. Anthropometric and Body Composition Measurements

Volunteers were measured for weight and height using light clothes and no shoes using an electronic scale. The parameters used in this study were: body mass (kg); total body fat (kg and %) and visceral body fat (cm^2). We used the bioelectrical impedance analysis (BIA) devices to measure the change in impedance in body tissues by sending detectable electrical signals through the body. The BIA device used in this study was the InBody® 720 (Biospace Co. Ltd.; Seol, Korea), which uses 6 frequencies (1, 5, 50, 250, 500, and 1000 kHz). The body mass index (BMI) was calculated as body mass (kg) dividing stature $(m)^2$.

Neck circumference (NC) was measured at the base of the neck, below the cricothyroid cartilage with the volunteer's head positioned in the Frankfurt horizontal plane, keeping in inspiratory apnea with an inelastic tape. Values above 34 cm for women and 37 cm for men indicate an increased risk for the occurrence of cardiovascular risk [18].

Waist circumference (WC) was determined at the end of normal expiration at the midpoint between the iliac crest and the last rib using a flexible and inelastic tape without compressing the skin. Values above 80 cm for women and above 94 cm for men indicate a risk for cardiovascular disease [19].

Hip circumference (HC) was measured at the most salient point between the waist and the thigh, using an inelastic tape. The waist–hip ratio was calculated [19].

2.3. Serum Analysis

Blood samples were collected after 12 h of overnight fast at approximately 8:00 am in the outpatient clinic.

Insulin sensitivity was assessed using the homeostasis model assessment IR (insulin resistance) index (HOMA-IR). HOMA-IR was calculated using the following formula:

$$\text{HOMA-IR}\left[\text{fasting blood glucose}\left(\frac{\text{mg}}{\text{dL}}\right)\times\text{fasting insulin}\left(\frac{\mu\text{U}}{\text{mL}}\right)\div 405\right].$$

The cut-off value determined for Brazilian population is HOMA-IR ≤ 2.71 for classified the subjects with IR [20].

The leptin, PAI-1, VCAM and ICAM-1 concentrations were measured using a commercially available multiplex assay (EMD Millipore; HMHMAG-34 K). Manufacture-supplied controls were included to measure assay variation and all samples were analyzed on the same day to minimize day-to-day variation. A minimum of 100 beads were collected for each analyzed using a Luminex MagPix System (Austin, Texas), which was calibrated and verified prior to sample analysis. Unknown sample values were calculated offline using Milliplex Analyst Software (EMD Millipore) [21].

2.4. Therapy

Three times during the intervention period (4 months) at Unidade de Saúde Escola (USE)/Universidade Federal de São Carlos — UFSCar, all voluntaries were monitored and evaluated by clinical tests. These evaluations were done by the team of health professionals including endocrinologist, nutritionist and physical educator. The medical follow-up included the initial medical history and a physical examination of blood pressure, cardiac frequency and body composition were checked (Fig. 1).

2.5. Physical Exercise Intervention — Moderate Aerobic Plus Resistance Training (M-Rt)

During the 4 months period, the voluntaries followed a combined exercise training therapy. The protocol was performed three times per week and included 30 min of aerobic training and 30 min of resistance training per session. The aerobic training consisted of running on a motor-driven treadmill (Movement®) between 70–85% of a maximal cardiac frequency (FC) intensity, which was previously determined by treadmill submaximal test. The physical exercise intervention was based on the guidelines from the American College of Sports Medicine (ACSM) [22]. Resistance training was also designed based on ACSM recommendations [23] (Fig. 1).

2.6. Phototherapy Intervention

The device prototype used was composed of 4 plates with 16 infrared laser emitters. The characteristics of phototherapy equipment are described below (Table 1).

The phototherapy equipment (Table 1 and Fig. 2) was developed by the Laboratory Technology Support-LAT, Center for Research in Optics and Photonics Institute of Physics in São Carlos city at Universidade de São Paulo — USP. For phototherapy intervention, the plates were placed in abdominal, gluteal and lower limbs in the quadriceps and biceps femoral region. The positioning of the plates in each region is demonstrated in Fig. 2. The emitters are disposed perpendicularly (90°) to the skin. The total application time was 16 min (8 min per side) and the application was performed after each exercise session, in accordance with the previous study of our research group [24,25] (Fig. 2).

2.7. Statistical Analysis

Statistical analysis was performed using the program STATISTICA version 7.0 for Windows (StatSoft Inc., Tulsa, OK, USA). The significance level

Table 1
Device information, irradiation and treatment parameters.

Type	Ga-Al-As semiconductor diode laser
Wavelength	808 nm
Operating mode	Continuous wave
Number of Emitters	16 (per plate)
Number of Plate	4
Number of electronic control box	2
	Per emitter
Spot diameter (elliptical shape)	Horizontal 0.3692/vertical 0.0582 cm
Spot area	0.0169 cm^2
Output power	100 mW
Irradiance	6.0 W/cm^2
Radiant energy	96 J
	Characteristic of the application
Application technique	Plates over the following perpendicularly to the skin in the regions: anterior region: abdominal and quadriceps simultaneously during 8 min. Change the position to irradiate the posterior region: gluteus and biceps femoral during 8 min totalizing 16 min
Number of points irradiated	64 (per position)/128 (total)
Total radiant energy delivered	Per session (16 min): 6,144 J/all sessions (48): 294,912 J
Number and frequency of treatment sessions	Three times per week after physical exercise, totalizing 48 sessions of treatment

Fig. 2. Illustrative places of phototherapy application. Volunteer receiving phototherapy after physical exercise — A. In ventral decubitus — 8 min of phototherapy application per session; B. In dorsal decubitus — 8 min of phototherapy application per session; C. Prototype phototherapy equipment.

was set up at $p < 0.05$. The Kolmogorov–Smirnov test was applied to assess the assumption of normality for the data. Parametric data were expressed as mean ± standard deviation (SD). To analyze the effects intervention and difference between the groups, a two-way ANOVA was applied followed by Tukey post hoc test. Comparing the delta values was performed by t test independent by groups.

Table 2
Effect of LLLT associated aerobic plus resistance training on body composition and anthropometric measurements.

Placebo group				Phototherapy group		
Variables	Baseline	End	Δ value (%)	Baseline	End	Δ value (%)Δ
Age	33.954 ± 4.805	__ ± __	__ ± __	32.20 ± 4.969	__ ± __	__ ± __
Height (m)	1.63 ± 0.04	__ ± __	__ ± __	1.65 ± 0.06	__ ± __	__ ± __
Body mass (Kg)	97.212 ± 13.002*	94.487 ± 12.795 P = 0.0000001**	−4.743 ± 2.180	94.487 ± 12.79	89.293 ± 12.834 P = 0.000001**	−5.546 ± 2.051 P = 0.3916
Body mass index (Kg/m^2)	36.083 ± 4.137	33.886 ± 4.278 P = 0.0000001**	−6.181 ± 2.722	34.396 ± 4.036	32.629 ± 3.921 P = 0.000001**	−5.480 ± 2.589 P = 0.4520
Waist circumference (cm)	113.225 ± 13.825	110.562 ± 13.02 P = 0.000006**	−2.309 ± 1.139	107.687 ± 10.024	103.812 ± 9.07 P = 0.00001**	−3.554 ± 0.708 P = 0.02***
Neck circumference (cm)	36.983 ± 2.109	36.583 ± 1.942 P = 0.0361**	−1.044 ± 1.939	38.093 ± 2.265	36.266 ± 1.869 P = 0.00009**	−4.711 ± 3.202 P = 0.00031***
Fat mass %	40.886 ± 3.159	39.113 ± 3.0507 P = 0.0000001**	−4.332 ± 1.504	40.950 ± 2.467	38.833 ± 2.4473 P = 0.000007**	−5.608 ± 1.599 P = 0.048***
Visceral fat (cm^2)	160.891 ± 21.449	154.400 ± 22.228 P = 0.00004**	−4.425 ± 2.824	150.480 ± 19.938	140.710 ± 19.982 P = 0.0000001**	−7.094 ± 2.001 P = 0.0209***
Hip (cm)	119.8 ± 6.2	118.2 ± 5.6	1.28 ± 1.9	118.2 ± 7.7	112.8 ± 7.7	4.56 ± 3.3 P = 0.0073***

Values expressed by mean ± SD. References values: body mass index: ≤24.9 Kg/m^2; waist circumference: ≤80 cm for women and ≤94 cm for men; neck circumference: ≤34 for women and ≤37 for men; fat mass%: 18 to 28% for females; visceral fat: ≤100 cm^2. Kg: kilogram, m^2: square meter, %: percentage, cm: centimeter, cm^2: square centimeter.

* Statistical difference between baseline values.

** Statistical difference between baseline vs after therapy values.

*** Statistical difference between delta values.

The delta values were obtained from the formula: $\Delta = \frac{\text{final value} - \text{initial value}}{\text{initial value}} \times 100$.

3. Results

3.1. Effects of Phototherapy Associated With Aerobic Plus Resistance Training on Anthropometric Measures and Body Composition

In initial treatment, there are no differences between the group placebo and phototherapy for all anthropometric and body composition parameters — body weight (Kg), height (cm), BMI (Kg/m2), hip, waist and neck circumferences (cm), percentage of total fat mass (%), visceral fat (cm^2), and waist–hip ratio.

At the end of treatment in relation to initial treatment, placebo and phototherapy groups had decrease in body mass, BMI, waist and neck circumferences, percentage of total fat mass, visceral fat, hip and waist–hip ratio. Furthermore, those decreases were greater in the phototherapy group than in the placebo group with exception for body mass and BMI that had no differences between groups (Table 2).

3.2. Effects of Phototherapy Intervention Associated With Aerobic Plus Resistance Training on Metabolic Profile

In initial of treatment, there are no differences between the group placebo and phototherapy for glucose (mg/dl), insulin (uU/ml), HOMA-IR and platelets plasma concentration (K/uL). After interdisciplinary intervention, an improvement was observed on the metabolic profile with reduction in the insulin, HOMA-IR and platelets in plasma concentration in both groups. Interestingly, once again the phototherapy intervention potentiated the effects on those parameters when compared to placebo group. Glucose concentration didn't change with treatment (Table 3).

3.3. Effects of Phototherapy Intervention Associated With Aerobic Plus Resistance Training on Inflammatory Markers

In this study, it didn't have any differences in PAI-1 (ng/ml), leptin (ng/ml), SCAM-1 (pg/ml) and ICAM-1 (pg/ml) concentrations in initial of treatment in both groups. Significant reduction in the PAI-1, leptin and ICAM-1 was shown only in the phototherapy group. The reduction in leptin, PAI-1 and ICAM-1 was much more expressive in the phototherapy group in comparison with the placebo group when analyzed by delta values (Table 4, Fig. 3). The VCAM-1 delta showed no statistical difference between the groups.

4. Discussion

The aim of the present investigation is to analyze the possible mechanism linking the effects of the LLLT associated with aerobic plus resistance training on cardiometabolic risk in obese women. Therefore, the most important finding in this clinical approach was to know that the LLLT associated with physical exercise was effective in reducing some cardiometabolic risk factors in the analyzed population, including a reduction on hyperleptinemia state, PAI-1, HOMA-IR, ICAM and visceral adiposity. LLLT is highly effective to relieve pain, inflammation and edema as well as to prevent death tissue and stimulate tissue regeneration, treating different pathologies even in cellulite treatment [26–28]. But we do not found in the literature clinical studies that could relate to phototherapy with aerobic plus resistance training specifically targeting the treatment of obesity and obesity-correlated disease.

Interdisciplinary intervention (nutrition, psychology, physical exercise and clinical therapy) has been used with success for obesity treatment, without the use of the agent pharmacological or surgery [10,11]. In fact, in our study, the application of lifestyle intervention was effective in reducing all parameters of body composition, metabolic profile and inflammatory marks in obese women confirming to be necessary in the union of different professionals working together to treat obesity.

However, interestingly, the highlight findings of our study demonstrated that when we associated the phototherapy with aerobic plus resistance training intervention in obese women, all the beneficial effects promoted by lifestyle intervention were potentiated, mainly the improvement in inflammatory markers, platelets and HOMA, and besides it promote greater reduction in the visceral fat and in the percentage of body fat.

We know that the adipose tissue produces and releases different hormones, peptides, and cytokines. Thus, this tissue participates in food intake regulation, in the metabolism of glucose and lipid, inflammation, coagulation, and blood pressure control, may affect cardiovascular function through the mechanism endocrine, paracrine and autocrine [29]. The increase in size of adipocytes leads to a dysfunction of adipose tissue that pass to release increased amounts of free fat acids (FFAs) that inhibit insulin's antilipolytic action and exert pro-atherogenic effects, contributing to the development of atherosclerosis. Besides that, these excess of released FFAs establish a paracrine continuous cycle that leads to the development of chronic low-grade inflammatory state of the adipose tissue due to the increase in the TNF-α production and secretion by adipose tissue and macrophages [30,31]. Indeed, enlarged adipose tissue also increases vascular endothelial cell damage with increase in VCAM-1 and ICAM-1 by endothelium, contributing for release in pro-inflammatory cytokines [5]. So, obesity is accompanied by many adverse health effects for instance hypertension, insulin resistance, diabetes, dyslipidemia and subclinical inflammation, all factors leading to atherosclerosis [3,32].

In accordance with recent studies, the phototherapy promotes photobiomodulation characterized by a change in physiological processes inside the tissues triggered by specific wavelengths of light. Some body systems like circulatory, musculoskeletal and adipose tissue

Table 3
Effect of LLLT associated aerobic plus resistance training on metabolic profile.

	Placebo group			Phototherapy group		
Variables	Initial	End	Δ value (%)	Initial	End	Δ value (%)
Glucose (mg/dl)	91.000 ± 5.621	91.750 ± 6.255 P = 0.573	0.943 ± 5.633	93.866 ± 7.586	93.133 ± 7.954 P = 0.476	−0.725 ± 4.099 P = 0.355
Insulin (μU/ml)	18.212 ± 7.148*	14.156 ± 4.737 P = 0.002**	−19.915 ± 13.718	20.192 ± 13.651	12.476 ± 7.644 P = 0.0008**	−36.151 ± 9.277 P = 0.0011***
HOMA-IR	4.219 ± 1.797	3.273 ± 1.419 P = 0.002**	−20.913 ± 14.421	4.683 ± 2.887	2.836 ± 1.701 P = 0.0002**	−38.080 ± 9.230 P = 0.00094***

Values expressed by mean ± SD. References values: baseline glycaemia: 70 to 100 mg/dl; baseline insulin: ≤29.1 uU/ml; HOMA-IR ≤ 2.71. mg/dl: milligram/deciliter, μU/ml: microunits/milliliter.

* Statistical difference between baseline values.

** Statistical difference between baseline vs after therapy values.

*** Statistical difference between delta values.

Table 4
Effect of LLLT associated aerobic plus resistance training on inflammatory marks.

	Placebo group			Phototherapy group		
Variable	Initial	End	Δ value (%)	Initial	End	Δ value (%)
PAI-1 (ng/ml)	16.77 ± 6.51*	15.24 ± 13.23	−2.148 ± 18.21	24.24 ± 13.24	20.28 ± 10.77 P = 0.05**	−14.79 ± 6.48
sICAM-1 (pg/ml)	243.57 ± 47.65	243.28 ± 47.88	−1.7209 ± 8.929	230.0 ± 57.11	206.2 ± 75.57 P = 0.03**	−11.911 ± 12.862 P = 0.05***
sVCAM-1 (pg/ml)	347.42 ± 103.54	336.0 ± 89.99	2.270 ± 17.513	344.40 ± 38.42	319.0 ± 76.84	−4.040 ± 16.125
Leptina (ng/ml)	36.949 ± 12.058	35.650 ± 15.657	−4.493 ± 17.905	27.682 ± 8.370	19.767 ± 7.786 P = 0.0039**	−28.958 ± 14.722 P = 0.008***
Platelet (K/uL)	292.78 ± 52.99	287.0 ± 50,08 P = 0.01**	−1.89 ± 1.66	270.0 ± 22.24	249.80 ± 23.77 P = 0.05**	−7.53 ± 2.89 P = 0.00008***

Values expressed by mean ± SD. Leptin values: between 4.9 and 24 ng/ml for females. PAI-1: plasminogen activator inhibitor, ICAM-1: intracellular adhesion molecule 1, VCAM-1: vascular cell adhesion molecule 1, pg/ml: picogram/milliliter and ng/ml: nanogram/milliliter, K/uL:thousands/microliter.
* Statistical difference between baseline values.
** Statistical difference between baseline vs after therapy values.
*** Statistical difference between delta values.

have chromophores (light-absorbing molecules) that are capable of absorbing photons, for example hemoglobin, myoglobin, cell membranes and mitochondria [27,33]. In fact, we observed in the current study that the LLLT treatment associated with aerobic plus resistance training promoted improvement in cardiometabolic risk factors in obese women, first due to the decrease of visceral fat then for the decrease of inflammatory markers. It is well established in the literature that chromophores, present in the respiratory chain of the cellular mitochondria, including in adipocytes, absorb red and near-infrared photons, increase of membrane potential, oxygen consumption and ATP (adenosine triphosphate), a transient rise in ROS (reactive oxygen species), and release of NO (nitric oxide) leading to an up regulation's cAMP (cyclic protein adenosine monophosphate). The cAMP increased, in turn activates PKA (protein kinase) and phosphorylates HSL (hormone sensitive lipase) that cause degradation of TG (triacylglycerol) and diglycerides to monoglycerides that are further degraded to fatty acid (FA) and glycerol [27,34–36]. It also occurs an increase in the catecholamine that binds to adrenergic β3 receptors presents in the adipocytes membranes, triggering a cascade reaction to the degradation of TG into FFA and glycerol ensuring the supply of lipids as an energy source during physical exercise [37].

In this context, other researchers examined benefits of LLLT associated with physical resistance exercise in lean humans. The authors demonstrating that phototherapy reduces lactate levels in the circulation due to increased local microcirculation and consequently increased in oxygen supply. As a consequence, there is an improvement in muscle fatigue, faster recovery of muscle damage and improved performance, both in humans and animals [34–36,38]. In this context, our research group demonstrated in exogenous obese rats that the association of low-level laser therapy (LLLT) plus moderate swimming training promoted decrease in adipocyte area and increase in the energetic demand and in the mitochondrial oxidative capacity besides greater workload (data not published).

Thus, we can suggest that aerobic plus resistance training associated with LLLT had synergistic effects for degradation on TG in adipocytes, what may explain the great decrease in percentage of fat, mainly in the visceral fat in our study. These results show us an important finding. The LLLT associated with aerobic plus resistance training promotes biomodulation even in the deep fat, in this case represents for visceral fat, which can diminish the risk to development of cardiovascular disease in obese women.

In fact, the visceral fat predisposes to atherosclerosis development since it is a prevalent source of inflammatory cytokine secretion and a possible reservoir for pro-inflammatory molecules [5]. In these sense, leptin (an adipose tissue-derived hormone) levels rise with obesity and correlate strongly with percent body fat. Central obesity (mainly

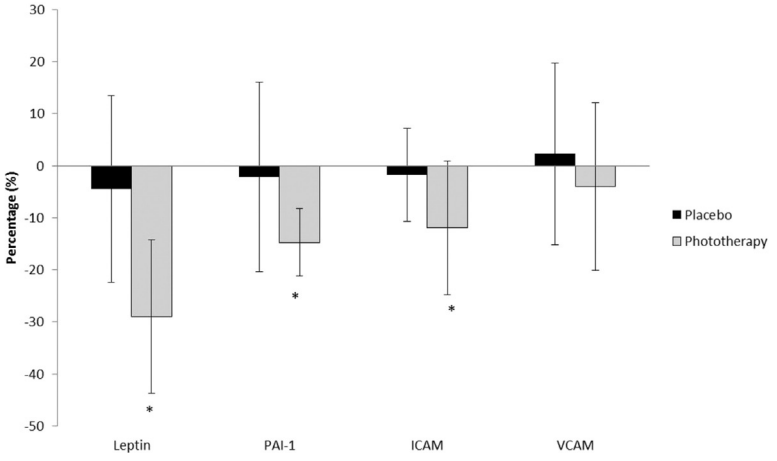

Values expressed by mean ± SD
* Statistical difference between delta values
PAI-1: plasminogen activator inhibitor, ICAM-1: intracellular adhesion molecule 1, VCAM-1: vascular cell adhesion molecule 1

Fig. 3. Effects of LLLT on inflammatory marks. Differences between delta.

the visceral fat), as well as waist and more recently neck circumferences, all of them are associated to high risk of insulin resistance and metabolic complications [42–46].

Besides that, both hyperleptinemia and insulin resistance are considered risk factors for cardiometabolic disease. Due to the leptin role in regulating blood pressure and activating the sympathetic nervous system, insulin resistance, platelet aggregation, arterial thrombosis, angiogenesis, and inflammatory vascular responses, the leptin has a close relationship with the development of coronary heart disease, when in hyperleptinemia state, as our volunteers at the beginning of treatment [39,47]. Thereby, in this current study, the LLLT associated with aerobic plus resistance training can auxiliary decrease the cardiometabolic risk observed in obesity, since this treatment reduce hyperleptinemia state and insulin resistance measured by HOMA-IR, beyond greater decrease in waist and neck circumferences compared to a placebo group.

In a recent study, the authors observed that LLLT can modulate the balance between pro and anti-inflammatory cytokines, both systemically and peripherally in lean rats [40]. Other study shows that laser irradiation with wavelength of 808 nm, similar with our study, in coronary artery, results in increase of anti-inflammatory and decrease in the pro-inflammatory interleukins levels [41]. In fact, we observed in the current study evidence that LLLT in wavelength of 808 nm promoted, beyond the effect on the reduction of adipose tissue, a systemic effect in the modulation of inflammatory process. The LLLT associated with aerobic plus resistance training decreased PAI-1, ICAM-1, VCAM-1 besides reducing circulating concentrations of leptin and insulin as discussed above.

These findings are important since in most cases of obesity, individuals have vascular endothelial cell damage that in turn expresses cell adhesion molecules 1 (CAMs), including ICAM-1 and VCAM-1. Circulating leukocytes are selective attracting and monocytes chemotactic protein 1 (MCP-1) are released by endothelial cells that stimulate to recruit mononuclear cell circulating differentiated into macrophages in the vessel wall. This development in the local inflammatory responses stimulates other cell types to produce pro-inflammatory cytokines, resulting in an inflammatory response that magnified beyond the original local area of endothelial dysfunction [32].

Furthermore, the main inhibitor of fibrinolysis, the PAI-1 (plasminogen inhibitor of fibrinolysis) increase in plasma of the obese individuals leads to a hyperthrombotic state by hypofibrinolysis, hypercoagulability and platelets activation that leads to development of atherosclerotic plaques formation, the main predictor for myocardial infarction [8,9]. Besides that, oxidative stress transforms an anti-atherosclerotic NO-producing enzyme into pro-atherosclerotic superoxide producing one, in addition to stimulates the inducible nitric oxide synthase raising the oxidative stress. Therefore, oxidative stress has been linked to increased platelet activation, characteristics in many obese individuals [32]. In a recent review, the authors showed some studies, with rats and humans, about the effect of the exercise aerobic and/or resistance training on inflammation in adipose tissue and endothelial cells, decreasing pro-inflammatory cytokine expression and increasing anti-inflammatory protein expression in this tissue [5]. These authors also show that chronic exercise as well reduce the number of pro-inflammatory monocytes and increase circulating numbers of regulatory T cells, which release anti-inflammatory cytokines and reduce chronic inflammation.

In this manner, the biophotomodulation generated by LLLT can affect the application area, as well as the surrounding regions affect metabolic changes, generating systemic effects [48]. In accordance with Novoselova and colleagues [49], the tissue irradiated with low-power laser produces signaling factors that will circulate into the lymphatic system and blood vessels. This way, associated the exercise effects with the local and systemic effects promoted by LLLT on the inflammation decreases dramatically the cardiometabolic risk in obese individuals. Finally, despite this as being a new study that uses new technologies (laser) aiming to control cardiometabolic disease in obese women, we were able to show that associated effects of exercise with LLLT, include the local and systemic improvements, is corroborating with an improvement in inflammatory state and a substantially decrease in the cardiometabolic risk factors in these individuals.

In conclusion, the results observed in the present investigation suggest that LLLT associated with aerobic plus resistance training may be a new therapeutic tool in targeting to optimize the control of cardiometabolic risk factors in obese people.

Conflict of Interest

None disclosed.

Financial Support

We thank the financial support for all research agencies like: CNPq (150177/2014-3); CNPq 300654/2013-8; FAPESP (2013/19046-0); FAPESP (2013/04136-4).

Acknowledgments

We thank Ms Jorge Camargo Oishi for the assistance with statistical analyses, Ms Cynthia Aparecida Castro and Ms Karina Ana da Silva for technical support during the training protocol and data collection and Paulo Henrique Colturato Reame for opening his gym (Oxy) for development to the project.

References

[1] F.O. Duarte, M. Sene-Fiorese, N.C. Cheik, A.S. Maria, A.E. de Aquino Jr., J.C. Oishi, E.A. Rossi, A.C. Garcia de Oliveira Duarte, A.R. Dâmaso, Food restriction and refeeding induces changes in lipid pathways and fat deposition in the adipose and hepatic tissues in rats with diet-induced obesity, Exp. Physiol. 97 (7) (Jul 2012) 882–894, http://dx.doi.org/10.1113/expphysiol.2011.064121.

[2] F.C. Corgosinho, C. Ackel-D'Elia, S. Tufik, A.R. Dâmaso, A. de Piano, L. Sanches Pde, R.M. Campos, P.L. Silva, J. Carnier, L. Tock, M.L. Andersen, G.A. Moreira, M. Pradella-Hallinan, L.M. Oyama, M.T. de Mello, Beneficial effects of a multifaceted 1-year lifestyle intervention on metabolic abnormalities in obese adolescents with and without sleep-disordered breathing, Metab. Syndr. Relat. Disord. 13 (3) (Apr 2015) 110–118, http://dx.doi.org/10.1089/met.2014.0110.

[3] N. Alexopoulos, D. Katritsis, P. Raggi, Visceral adipose tissue as a source of inflammation and promoter of atherosclerosis, Atherosclerosis 233 (1) (Mar 2014) 104–112, http://dx.doi.org/10.1016/j.atherosclerosis.2013.12.023.

[4] L. Jamar, P. Pisani, L.M. Oyama, C. Belote, D.C.L. Masquio, V.A. Furuya, J.P. Carvalho-Ferreira, S.G. Andrade-Silva, A.R. Dâmaso, D.A. Caranti, Is the neck circumference an emergent predictor for inflammatory status in obese adults? Int. J. Clin. Pract. 67 (3) (Mar 2013) 217–224, http://dx.doi.org/10.1111/ijcp.12041.

[5] T. You, N.C. Arsenis, B.L. Disanzo, M.J. Lamonte, Effects of exercise training on chronic inflammation in obesity: current evidence and potential mechanisms, Sports Med. 43 (4) (Apr 2013) 243–256, http://dx.doi.org/10.1007/s40279-013-0023-3.

[6] Jing-ya Zhou, Hui Ge, Ming-fan Zhu, Li-jun Wang, Li Chen, Yao-zong Tan, Yu-ming Chen, Hui-lian Zhu, Neck circumference as an independent predictive contributor to cardio-metabolic syndrome, Cardiovasc. Diabetol. 16 (May 2013) 12–76, http://dx.doi.org/10.1186/1475-2840-12-76.

[7] R.B. Harris, Leptin: much more than a satiety signal, Annu. Rev. Nutr. 20 (2000 July) 45–75, http://dx.doi.org/10.1146/annurev.nutr.20.1.45.

[8] V.Z. Rocha, E.J. Folco, Inflammatory concepts of obesity, Int. J. Inflamm. 2011 (May 2011) 1–14, http://dx.doi.org/10.4061/2011/529061.

[9] J. Chudek, A. Wiecek, Adipose tissue, inflammation and endothelial dysfunction, Pharmacol. Rep. 58 (Suppl.) (2006) 81–810.

[10] A.R. Dâmaso, A. de Piano, R.M. Campos, F.C. Corgosinho, W. Siegfried, D.A. Caranti, D.C. Masquio, J. Carnier, P. Sanches de L, P. Leão da Silva, C.M. Nascimento, L.M. Oyama, A.D. Dantas, M.T. de Mello, S. Tufik, L. Tock, Multidisciplinary approach to the treatment of obese adolescents: effects on cardiovascular risk factors, inflammatory profile, and neuroendocrine regulation of energy balance, Int. J. Endocrinol. 2013 (2013) 541032, http://dx.doi.org/10.1155/2013/541032.

[11] A.R. Dâmaso, R.M. Campos, D.A. Caranti, A. de Piano, M. Fisberg, D. Foschini, P.D. Sanches, L. Tock, H.M. Lederman, S. Tufik, M.T. de Mello, Aerobic plus resistance training was more effective in improving the visceral adiposity, metabolic profile and inflammatory markers than aerobic training in obese adolescents, J. Sports Sci. 32 (15) (2014) 1435–1445, http://dx.doi.org/10.1080/02640414.2014.900692.

[12] R.F. Jackson, F.A. Stern, R. Neira, C.L. Ortiz-Neira, J. Maloney, Application of low-level laser therapy for noninvasive body contouring, Lasers Surg. Med. 44 (3) (2012 Mar) 211–217, http://dx.doi.org/10.1002/lsm.22007.

[13] C. Ferraresi, O.T. de Brito, Z.L. de Oliveira, R.B. de Menezes Reiff, V. Baldissera, S.E. de Andrade Perez, E. Matheucci Junior, N.A. Parizotto, Effects of low level laser therapy (808 nm) on physical strength training in humans, Lasers Med. Sci. 26 (3) (2011 May) 349–358, http://dx.doi.org/10.1007/s10103-010-0855-0.

[14] F.R. Paolillo, J.C. Milan, I.V. Aniceto, S.G. Barreto, J.R. Rebelatto, A. Borghi-Silva, N.A. Parizotto, C. Kurachi, V.S. Bagnato, Effects of infrared-LED illumination applied during high intensity treadmill training in postmenopausal women, Photomed. Laser Surg. 29 (9) (2011 Sep) 639–645, http://dx.doi.org/10.1089/pho.2010.2961.
[15] T. Fujimura, A. Mitani, M. Fukuda, M. Mogi, K. Osawa, S. Takahashi, M. Aino, Y. Iwamura, S. Miyajima, H. Yamamoto, T. Noguchi, Irradiation with a low-level diode laser induces the developmental endothelial locus-1 gene and reduces proinflammatory cytokines in epithelial cells, Lasers Med Sci. 29 (3) (May 2014) 987–994, http://dx.doi.org/10.1007/s10103-013-1439-6.
[16] F.G. Basso, T.N. Pansani, D.G. Soares, D.L. Scheffel, V.S. Bagnato, C.A. Costa, J. Hebling, Biomodulation of inflammatory cytokines related to oral mucositis by low-level laser therapy, Photochem. Photobiol. 4 (2015 Mar), http://dx.doi.org/10.1111/php.12445.
[17] A.E. Aquino Jr., M. Sene-Fiorese, F.R. Paolillo, F.O. Duarte, J.C. Oishi, A.A. Pena Jr., A.C. Duarte, M.R. Hamblin, V.S. Bagnato, N.A. Parizotto, Low-level laser therapy (LLLT) combined with swimming training improved the lipid profile in rats fed with high-fat diet, Lasers Med. Sci. 28 (5) (2013 Sep) 1271–1280, http://dx.doi.org/10.1007/s10103-012-1223-z.
[18] S.R. Preis, J.M. Massaro, U. Hoffmann, R.B. D'Agostino Sr., D. Levy, S.J. Robins, J.B. Meigs, R.S. Vasan, C.J. O'Donnell, C.S. Fox, Neck circumference as a novel measure of cardiometabolic risk: the Framingham Heart study, J. Clin. Endocrinol. Metab. 95 (8) (2010 Aug) 3701–3710, http://dx.doi.org/10.1210/jc.2009-1779.
[19] C. Nishida, G.T. Ko, S. Kumanyika, Body fat distribution and noncommunicable diseases in populations: overview of the 2008 WHO Expert Consultation on Waist Circumference and Waist–Hip Ratio, Eur. J. Clin. Nutr. 64 (1) (2010 Jan) 2–5, http://dx.doi.org/10.1038/ejcn.2009.139.
[20] B. Geloneze, E.M. Repetto, S.R. Geloneze, M.A. Tambascia, M.N. Ermetice, The threshold value for insulin resistance (HOMA-IR) in an admixture population IR in the Brazilian Metabolic Syndrome Study, Diabetes Res. Clin. Pract. 72 (2) (2006 May) 219–220.
[21] L. Dossus, S. Becker, D. Achaintre, R. Kaaks, S. Rinaldi, Validity of multiplex-based assays for cytokine measurements in serum and plasma from "non-diseased" subjects: comparison with ELISA, J. Immunol. Methods 350 (1–2) (2009 Oct 31) 125–132, http://dx.doi.org/10.1016/j.jim.2009.09.001.
[22] J.E. Donnelly, S.N. Blair, J.M. Jakicic, M.M. Manore, J.W. Rankin, B.K. Smith, American College of Sports Medicine Position Stand. Appropriate physical activity intervention strategies for weight loss and prevention of weight regain for adults, Med. Sci. Sports Exerc. 41 (2) (2009 Feb) 459–471, http://dx.doi.org/10.1249/MSS.0b013e3181949333.
[23] W.J. Kraemer, N.A. Ratamess, D.N. French, Resistance training for health and performance, Curr. Sports Med. Rep. 1 (3) (2002 Jun) 165–171.
[24] M. Sene-Fiorese, F.O. Duarte, A.E. de Aquino Junior, R.M. Campos, D.C. Masquio, L. Tock, A.C. Duarte, A.R. Dâmaso, N.A. Parizotto, V.S. Bagnato, The potential of phototherapy to reduce body fat, insulin resistance and "metabolic inflexibility" related to obesity in women undergoing weight loss treatment, Lasers Surg. Med. 47 (6) (Jul 2015), http://dx.doi.org/10.1002/lsm.22395.
[25] R.M. da Silveira Campos, A.R. Dâmaso, D.C. Masquio, A.E. Aquino Jr., M. Sene-Fiorese, F.O. Duarte, L. Tock, N.A. Parizotto, V.S. Bagnato, Low-level laser therapy (LLLT) associated with aerobic plus resistance training to improve inflammatory biomarkers in obese adults, Lasers Med. Sci. 30 (5) (2015 Jul) 1553–1563, http://dx.doi.org/10.1007/s10103-015-1759-9.
[26] K.H. Beckmann, G. Meyer-Hamme, S. Schröder, Low level laser therapy for the treatment of diabetic foot ulcers: a critical survey, Evid. Based Complement. Alternat. Med. 2014 (2014) 626127, http://dx.doi.org/10.1155/2014/626127.
[27] P. Avci, T.T. Nyame, G.K. Gupta, M. Sadasivam, M.R. Hamblin, Low-level laser therapy for fat layer reduction: a comprehensive review, Lasers Surg. Med. 45 (6) (2013 Aug) 349–357, http://dx.doi.org/10.1002/lsm.22153.
[28] F.R. Paolillo, A. Borghi-Silva, N.A. Parizotto, C. Kurachi, V.S. Bagnato, New treatment of cellulite with infrared-LED illumination applied during high-intensity treadmill training, J. Cosmet. Laser Ther. 13 (4) (2011 Aug) 166–171, http://dx.doi.org/10.3109/14764172.2011.594065.
[29] L. Badimon, R. Hernández Vera, G. Vilahur, Atherothrombotic risk in obesity, Hamostaseologie 33 (4) (2013) 259–268, http://dx.doi.org/10.5482/HAMO-13-07-0034.
[30] B. Gustafson, A. Hammarstedt, C.X. Andersson, U. Smith, Inflamed adipose tissue: a culprit underlying the metabolic syndrome and atherosclerosis, Arterioscler. Thromb. Vasc. Biol. 27 (11) (2007 Nov) 2276–2283, http://dx.doi.org/10.1161/ATVBAHA.107.147835.
[31] S. De Ferranti, D. Mozaffarian, The perfect storm: obesity, adipocyte dysfunction, and metabolic consequences, Clin. Chem. 54 (6) (2008 Jun) 945–955, http://dx.doi.org/10.1373/clinchem.2007.100156.
[32] K. Osawa, T. Miyoshi, Y. Koyama, S. Sato, N. Akagi, Y. Morimitsu, M. Kubo, H. Sugiyama, K. Nakamura, H. Morita, S. Kanazawa, H. Ito, Differential association of visceral adipose tissue with coronary plaque characteristics in patients with and without diabetes mellitus, Cardiovasc. Diabetol. 14 (Mar 2014) 13–61, http://dx.doi.org/10.1186/1475-2840-13-61.
[33] L.M. Nguyen, A.G. Malamo, K.A. Larkin-Kaiser, P.A. Borsa, P.J. Adhihetty, Effect of near-infrared light exposure on mitochondrial signaling in C2C12 muscle cells, Mitochondrion 14 (1) (2014 Jan) 42–48, http://dx.doi.org/10.1016/j.mito.2013.11.001.
[34] C. Ferraresi, B. Kaippert, P. Avci, Y.Y. Huang, M.V. de Sousa, V.S. Bagnato, N.A. Parizotto, M.R. Hamblin, Low-level laser (light) therapy increases mitochondrial membrane potential and ATP synthesis in C2C12 myotubes with a peak response at 3–6 h, Photochem. Photobiol. 91 (2) (2015 Mar) 411–416, http://dx.doi.org/10.1111/php.12397.
[35] W.H. de Brito Vieira, R.M. Bezerra, R.A. Queiroz, N.F. Maciel, N.A. Parizotto, C. Ferraresi, Use of low-level laser therapy (808 nm) to muscle fatigue resistance: a randomized double-blind crossover trial, Photomed. Laser Surg. 32 (12) (2014 Dec) 678–685, http://dx.doi.org/10.1089/pho.2014.3812.
[36] F.R. Paolillo, R. Arena, D.B. Dutra, R. de Cassia Marqueti Durigan, H.S. de Araujo, H.C. de Souza, N.A. Parizotto, G. Cipriano Jr., G. Chiappa, A. Borghi-Silva, Low-level laser therapy associated with high intensity resistance training on cardiac autonomic control of heart rate and skeletal muscle remodeling in wistar rats, Lasers Surg. Med. 46 (10) (2014 Dec) 796–803, http://dx.doi.org/10.1002/lsm.22298.
[37] Adriano Eduardo Lima-Silva, Fernando Adami, Fábio Yuzo Nakamura, Fernando Roberto de-Oliveira, Monique da Silva Gevaerd, Fat metabolism during exercise: mechanisms of regulation, Rev. Bras.Cineantropom. Desempenho Hum. 8 (4) (2006) 106–114 (ISSN 1980-0037. Article in Portuguese).
[38] C. Ferraresi, M.V. de Sousa, Y.Y. Huang, V.S. Bagnato, N.A. Parizotto, M.R. Hamblin, Time response of increases in ATP and muscle resistance to fatigue after low-level laser (light) therapy (LLLT) in mice, Lasers Med. Sci. 30 (4) (2015 May) 1259–1267, http://dx.doi.org/10.1007/s10103-015-1723-8.
[39] S.B. Chai, F. Sun, X.L. Nie, J. Wang, Leptin and coronary heart disease: a systematic review and meta-analysis, Atherosclerosis 233 (1) (Mar 2014) 3–10, http://dx.doi.org/10.1016/j.atherosclerosis.2013.11.069.
[40] V.S. Hentschke, R.B. Jaenisch, L.A. Schmeing, P.R. Cavinato, L.L. Xavier, P. Dal Lago, Low-level laser therapy improves the inflammatory profile of rats with heart failure, Lasers Med Sci. 28 (3) (Lasers Med Sci. 2013 May) 1007–1016, http://dx.doi.org/10.1007/s10103-012-1190-4.
[41] A. Derkacz, M. Protasiewicz, R. Poręba, A. Doroszko, R. Andrzejak, Effect of the intravascular low energy laser illumination during percutaneous coronary intervention on the inflammatory process in vascular wall, Lasers Med. Sci. 28 (3) (2013 May) 763–768, http://dx.doi.org/10.1007/s10103-012-1142-z.
[42] L.L. Ben-Noun, A. Laor, Relationship between changes in neck circumference and cardiovascular risk factors, Exp. Clin. Cardiol. 11 (1) (Spring 2006) 14–20.
[43] M. Sharda, P. Jain, A. Gupta, D. Nagar, A. Soni, Correlation and comparison of various anthropometric measurements of body fat distribution and sagittal abdominal diameter as a screening tool for cardio metabolic risk factors and ischaemic heart disease in elderly population, J. Assoc. Physicians India 63 (2015) 22–26.
[44] C. Stabe, A.C. Vasques, M.M. Lima, M.A. Tambascia, J.C. Pareja, A. Yamanaka, B. Geloneze, Neck circumference as a simple tool for identifying the metabolic syndrome and insulin resistance: results from the Brazilian Metabolic Syndrome Study, Clin. Endocrinol. (Oxf) 78 (6) (Jun 2013) 874–881, http://dx.doi.org/10.1111/j.1365-2265.2012.04487.x.
[45] C.J. Hsieh, P.W. Wang, T.Y. Chen, The relationship between regional abdominal fat distribution and both insulin resistance and subclinical chronic inflammation in non-diabetic adults, Diabetol. Metab. Syndr. 6 (1) (Apr 1 2014) 49, http://dx.doi.org/10.1186/1758-5996-6-49.
[46] L.S. Rallidis, K. Baroutsi, M. Zolindaki, M. Karagianni, C. Varounis, N. Dagres, J. Lekakis, M. Anastasiou-Nana, Visceral adipose tissue is a better predictor of subclinical carotid atherosclerosis compared with waist circumference, Ultrasound Med. Biol. 40 (6) (Jun 2014) 1083–1088, http://dx.doi.org/10.1016/j.ultrasmedbio.2013.12.017.
[47] P.L. Sanches, M.T. de Mello, N. Elias, F.A. Fonseca, R.M. Campos, J. Carnier, A. de Piano, D.C. Masquio, P.L. Silva, L.M. Oyama, F.C. Corgosinho, C.M. Nascimento, L. Tock, C.A. D'Elia, S. Tufik, A.R. Dâmaso, Hyperleptinemia: implications on the inflammatory state and vascular protection in obese adolescents submitted to an interdisciplinary therapy, Inflammation 37 (1) (Feb 2014) 35–43, http://dx.doi.org/10.1007/s10753-013-9709-9.
[48] T.Y. Fukuda, M.M. Tanji, S.R. Silva, M.N. Sato, H. Plapler, Infrared low-level diode laser on inflammatory process modulation in mice: pro- and anti-inflammatory cytokines, Lasers Med. Sci. 28 (5) (Sep 2013) 1305–1313, http://dx.doi.org/10.1007/s10103-012-1231-z.
[49] E.G. Novoselova, O.V. Glushkova, D.A. Cherenkov, V.M. Chudnovsky, E.E. Fesenko, Effects of low-power laser radiation on mice immunity, Photodermatol. Photoimmunol. Photomed. 22 (1) (Feb 2006) 33–38.

Lasers Med Sci (2015) 30:815–822
DOI 10.1007/s10103-013-1444-9

ORIGINAL ARTICLE

Comparative clinical study of light analgesic effect on temporomandibular disorder (TMD) using red and infrared led therapy

Vitor Hugo Panhoca · Rosane de Fatima Zanirato Lizarelli · Silvia Cristina Nunez · Renata Campi de Andrade Pizzo · Clovis Grecco · Fernanda Rossi Paolillo · Vanderlei Salvador Bagnato

Received: 30 April 2013 / Accepted: 16 September 2013 / Published online: 3 October 2013

Abstract Low-level laser therapy (LLLT) has been widely applied in pain relief in several clinical situations, including temporomandibular disorders (TMD). However, the effects of LED therapy on TMD has not been investigated. This study aims to evaluate the effects of red and infrared LEDs on: (1) tissue temperature in ex vivo and (2) pain relief and mandibular range of motion in patients with TMD. Thirty patients between 18 and 40 years old were included and randomly assigned to three groups. The two experimental groups were: the red LED (630±10 nm) group and the infrared LED (850±10 nm) group. The irradiation parameters were 150 mW, 300 mW/cm^2, 18 J/cm^2, and 9 J/point. The positive control group received an infrared laser (780 nm) with 70 mW, 1.7 W/cm^2, 105 J/cm^2, and 4.2 J/point. LED and laser therapies were applied bilaterally to the face for 60 s/point. Five points were irradiated: three points around the temporomandibular joint (TMJ), one point for the temporalis, and one near the masseter. Eight sessions of phototherapy were performed, twice a week for 4 weeks. Pain induced by palpating the masseter muscle and mandibular range of motion (maximum oral aperture) were measured at baseline, immediately after treatment, 7 days after treatment, and 30 days after treatment. There was an increase in tissue temperature during both the red and the infrared LED irradiation in ex vivo. There was a significant reduction of pain and increase of the maximum oral aperture for all groups ($p \geq 0.05$). There was no significant difference in pain scores and maximum oral aperture between groups at baseline or any periods after treatment ($p \geq 0.05$). The current study showed that red and infrared LED therapy can be useful in improving outcomes related to pain relief and orofacial function for TMD patients. We conclude that LED devices constitute an attractive alternative for LLLT.

Keywords Laser therapy · LED therapy · TMD · Pain relief · Oral aperture

V. H. Panhoca (✉) · C. Grecco · F. R. Paolillo · V. S. Bagnato
Optics Group from Physics Institute of São Carlos (IFSC), University of São Paulo (USP), Brazil. Av. Trabalhador Sancarlense, 400-Centro, 13560-970 São Carlos, SP, Brazil
e-mail: vhpanhoca@msn.com

C. Grecco
e-mail: clovias@ursa.ifsc.usp.br

F. R. Paolillo
e-mail: fer.nanda.rp@hotmail.com

V. S. Bagnato
e-mail: vander@if.sc.usp.br

R. de Fatima Zanirato Lizarelli · R. C. d. A. Pizzo
NILO-Nucleo Integrado de Laser em Odontologia, Rua Orlandia, 1156, Jardim Paulista Ribeirão Preto, SP 14090-240, Brazil

R. de Fatima Zanirato Lizarelli
e-mail: lizarelli@hotmail.com

R. C. d. A. Pizzo
e-mail: renatacampi@gmail.com

S. C. Nunez
Department of Integrated Teaching and Research INPES/CETAO, Av. Indianápolis, 153-Moema, 04063-000 São Paulo, Brazil
e-mail: silnunez@terra.com.br

Introduction

Temporomandibular disorder (TMD) is a common clinical complaint among patients in dental practices. TMD occurs as a result of malfunction in the jaw, jaw joint, and or surrounding facial muscles, and it is characterized by pain and discomfort in facial muscles mostly, when chewing or during

jaw movement. TMDs fall into three main categories: (1) myofascial pain, is the most common form of TMD, which is characterized by discomfort or pain in the masticatory muscles and sometimes in the neck and shoulder muscles; (2) internal derangement of the joint associated with a dislocated jaw or displaced disc and an injury to the condyle; and (3) degenerative joint disease, including osteoarthritis or rheumatoid arthritis in the jaw joint [1, 2].

Managing TMD is a challenge for dental practitioners; often analgesics are prescribed to ameliorate acute pain, but the long-term treatment is difficult to project [3]. TMD also has a psychological component. Therefore, the guidelines for TMD treatment recommend noninvasive approaches to managing this condition. Low-level laser therapy (LLLT) is considered a viable noninvasive and nonpharmacological alternative.

LLLT has been reported as an analgesia for several different painful conditions, such as cervical dentin hypersensitivity, trigeminal neuralgia, headaches, and especially TMD. Previous studies have shown the beneficial effects of red [4–6] and infrared [7–11] lasers in TMD management. Therapeutic "optical window" corresponds to red and near-infrared wavelengths, where the effective tissue penetration of light is maximal [12]. For this reason, red and infrared wavelengths are used to relieve both acute and chronic pain and inflammation [13, 14].

The analgesic mechanisms of light is not clearly understood although several have been proposed, including the gate control theory, modulation of endogenous opioids production, anti-inflammatory effects, direct inhibition of neural activity and slowed conduction velocity in peripheral nerves [15]. However, several factors may influence an analgesic response: patient diagnoses, symptoms, pain duration, laser irradiation location, distance from laser probe to skin, laser type, wavelength, laser mode (continuous or pulsed), average power, power density, energy, fluence, number of sessions, laser irradiation point size, and co-interventions (e.g., exercises, dry needling, and drugs) [14].

Regarding output power, clinical studies use red laser with an average power of 15 [5] or 30 mW [6] as well as infrared laser with an average power of 17 [16], 40 [9], 50 [10, 17], 70 [18], or 100 mW [13] for reduced pain and increased orofacial function for TMD management. Moreover, infrared laser with higher power, for example, 400 mW [11, 19, 20] has also been used to relieve pain and improve mobility of the joint for TMD treatment. However, it is a well-known fact that increasing laser power and exposure time may lead to higher local temperature and risk of tissue damage [21, 22].

In contemporary research, the use of LEDs for therapeutic treatment is growing. Studies have shown that lasers and LEDs operating at similar parameters produce equivalent effects [23–26]. A review of the literature shows the effectiveness of LEDs in dentistry [26], dermatology and aesthetic medicine [24, 27–29], sport medicine [30, 31], and especially for pain relief [32].

However, to our knowledge, no previous studies have assessed the effects of LED therapy on TMD management. Therefore, this study aims to evaluate the effects of red and infrared LEDs on: (1) tissue temperature in ex vivo human hemi-head and (2) pain relief and mandibular range of motion in patients with TMD. Our hypothesis was that the use of LEDs may present a new approach for therapeutic treatment of TMD, when compared with LLLT.

Materials and methods

This study is part of a larger project that aims to develop clinical protocols LED systems for therapy. All procedures were approved by the Ethics Committee of the Federal University of São Carlos, São Carlos, Brazil (approval no. 23112.004838/2010-28). All subjects provided written informed consent and agreed to participate in the study. The study was registered with NIH ClinicalTrials (NCT01873937).

Devices used in this study

To perform LED irradiation, a prototype device (Fisioled, MM Optics Ltda, São Carlos, São Paulo, Brazil) was developed specifically for this project. The device includes two handpieces with polished acrylic tips. Each handpiece includes one red (630±10 nm) or one infrared (850±10 nm) LED with a fixed output power of 150 mW and illumination area of 0.5 cm^2.

For this clinical trial, the positive control group was treated, as suggested by the ethical committee. A 780-nm laser (Twin Laser, MM Optics Ltda, São Carlos, São Paulo, Brazil) was used, because infrared lasers are a well-accepted and efficient therapy for pain relief [33]. This wavelength is commonly used for TMD treatment [7–11]. This device has adjustable output power ranging from 5 to 70 mW and a spot area of 0.04 cm^2.

A FieldMaster TO-II optical power meter (Coherent Inc., Santa Clara, CA, USA) linked to a photodetector was used to calibrate these systems.

Thermal mapping

Thermal mapping during LED irradiation was performed on an ex vivo human hemi-head (Fig. 1a) provided by the laboratory of anatomy at the University of São Paulo's (Ribeirão Preto, SP, Brazil campus) dental school.

Subcutaneous temperature measurements were performed in the anatomical specimen. A high-precision digital thermometer (MT 600, Minipa, São Paulo, Brazil) coupled with a computer program that captured the electrical signals, was

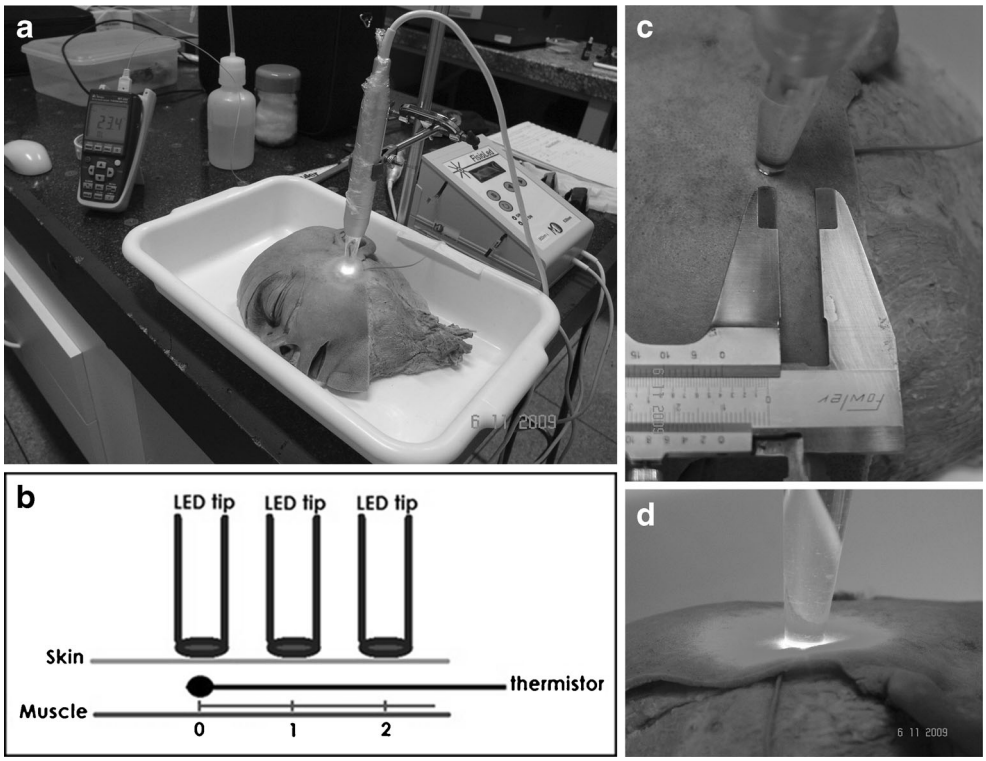

Fig. 1 The schematic representation of the experimental setup used for the measurements. Thermal map setup in the anatomical specimen (**a**); scheme showing the three positions (0, 1, and 2) of the LED considering thermistor location (**b**); pachymeter was used to determine position of the LED (**c**) and; close view of the LED tip (**d**)

positioned between the subcutaneous and muscle tissues (Fig. 1b). Three fixed distances were chosen to evaluate the thermal effect: (*d*0), 1 (*d*1), or 2 cm (d2) from the irradiation tip to subcutaneous tissue (Fig. 1c).

The irradiation was performed with red LED or infrared LED (prototype device) for 3 min. The measurements were performed three times and the mean temperature was recorded. As the same anatomical piece (Fig. 1d) was used each measurement was followed by a 5-min interval to allow the tissue to cool completely (thermal relaxation).

It is well-known that LEDs operating at higher output powers, around or above 100 mW, can generate heat [31]. Therefore, we investigated the effect of the LEDs on tissue temperature prior to the start of the clinical trial.

Clinical study

A randomized, single-blind, cross-sectional, and longitudinal clinical trial was conducted. A computer program was used for the randomization. Patients who received care at a private dental office in Ribeirão Preto, São Paulo, Brazil (NILO-Integrated Center for Laser Dentistry) were invited to participate in the study. The inclusion criteria were patients aged between 18 and 50 years with signs and symptoms of TMD. The diagnosis was made through a standard and comprehensive clinical examination based upon the research diagnostic criteria for temporomandiublar disorders [9, 10, 34]. This protocol was translated into Portuguese [35, 36] and was performed to obtain information about myofascial pain and arthralgia. The signs and symptoms were evaluated by a trained professional using the following procedures: pain during palpation of the temporomandibular joint (TMJ) area, pain on associated muscles (masseter and temporal), and limited or painful jaw movement with impaired oral aperture. The exclusion criteria were current or recent orthodontic and/or orthopedic treatment, degenerative joint disease, or patients treated with systemic medication (e.g., sedatives, muscle relaxants, analgesics, corticosteroids, or nonsteroidal anti-inflammatory agents).

Thirty patients between 18 and 40 years old (8 males and 22 females) were included and randomly assigned to three groups with ten patients in each group. The two experimental groups were: the red LED (630±10 nm) group and the infrared LED (850±10 nm) group. The patients in both groups were exposed to the LED prototype devices, with an average optical power of 150 mW, irradiance of 300 mW/cm^2, 9 J per point and fluence of 18 J/cm^2. The third group, the positive control, received the infrared laser (780 nm), with an average optical power of 70 mW, irradiance of 1.7 W/cm^2, energy of 4.2 J per point and fluence of 105 J/cm2. The LED and laser therapies were applied bilaterally to the face for 60 s/point. Five points were irradiated: three points around the TMJ, one point on the temporalis and one on the masseter (Fig. 2). Eight sessions of the phototherapy were performed, twice a week for 4 weeks.

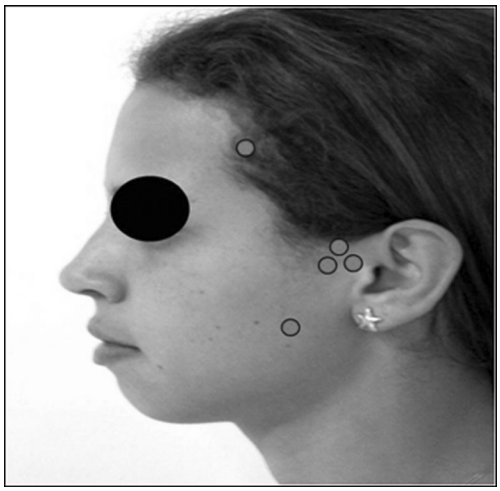

Fig. 2 Irradiation points: three points around the TMJ and one point for the temporalis and the masseter, respectively

Clinical measurements

Two parameters were used to evaluate the efficiency of the proposed treatments: range of motion (total aperture) and pain in the masseter muscle [9, 10, 35, 36]. To measure the jaw movement, a rule developed by a researcher from the Department of Oral Physiology, Institute of Head-UNIFESP (Escola Paulista de Medicina, São Paulo, adapted from the school of Gothenburg, Sweden) was used. To evaluate pain, the researcher palpited the masseter with a finger. Pain was evaluated using a numerical scale that ranged from 0 to 3: 0 (no pain), 1 (mild pain), 2 (moderate pain), and 3 (strong pain). The pain scores [35, 36] are shown in Table 1. The patients were evaluated at baseline (B), immediately after treatment, 7 days 7AT, and 30 days after treatment (30AT). During this time frame, we evaluated the progression of the treatment and classified it as an improvement, worsening or maintenance of both orofacial pain and function.

Statistical analysis

The data were expressed as mean and standard deviations. The Shapiro–Wilk test was used to analyze data normality and the homogeneity of variances using Levene's test. Two-way ANOVA with repeated measures was used to compare changes in pain score and orofacial aperture, before and after the treatment. The independent factors were group (with three levels: red LED, infrared LED, and infrared laser groups) and time (with four levels: baseline, immediately after treatment, 7 days after treatment, and 30 days after treatment), which was also considered a repeated measurement (intragroup differences). The change between baseline and all periods after treatment (delta=after treatment minus baseline) was used to compare groups using a one-way ANOVA (intergroup differences). When significant differences were found, Tukey's post-hoc test was applied. Statistica for Windows 7 (Statsoft Inc., Tulsa, Ok) was used for the statistical analysis. The significance level was set at 5 % ($p<0.05$).

Table 1 Pain scores

Degrees	Sensitivity
0	Without significant discomfort
1	Discomfort with mild pain
2	Sharp pain solely during the application of stimulus
3	Sharp pain during the application of stimulus and continuous after its removal

Results

The measurements of the subcutaneous temperatures for red and infrared LEDs are shown in Fig. 3a, b, respectively. The curves represent the heating and thermal relaxation during and immediately after LED irradiation. There was an increase in temperature during irradiation (3 min), represented by an exponential curve. The irradiation is followed by an exponential decay (cooling), which occurs for 3 to 4 min, until the initial temperature is reached (for both red and infrared wavelengths).

At position $d0$, the red LED reached a maximal temperature of 5.7 °C. There was no thermal change at positions $d1$ and $d2$. After 3 min under the infrared LED at position $d0$, subcutaneous temperatures reached 2 °C, where the largest energy deposition occurred. The maximal temperature of 0.5 °C occurred at position $d1$ (1.0 cm away) and, there was no thermal change at position $d2$.

The pain score can be seen in Fig. 4 compared with baseline, the results for all groups showed a significant reduction of pain on the right and left side of the face ($p<0.05$) at the period immediately after treatment, as well as 7 and 30 days after treatment. No significant difference was found for the pain score of each measurement compared with the prior period, except for the left side of patients in the red LED group at the period between immediately after treatment and 7 days after treatment ($p=0.04$).

There was a significant increase of the maximum oral aperture for all groups (Fig. 5). The patients that received LED therapy showed significant improvement of aperture ($p<0.05$) at the period immediately after treatment, as well as 7 and 30 days after treatment, compared with baseline. The infrared laser group only showed significant improvement 30 days after treatment ($p=0.01$). No significant difference was found for maximum orofacial aperture of each measurement compared with the prior period, except for the period between immediately after treatment and 7 days after treatment in the infrared LED ($p=0.04$) and infrared laser groups ($p=0.02$).

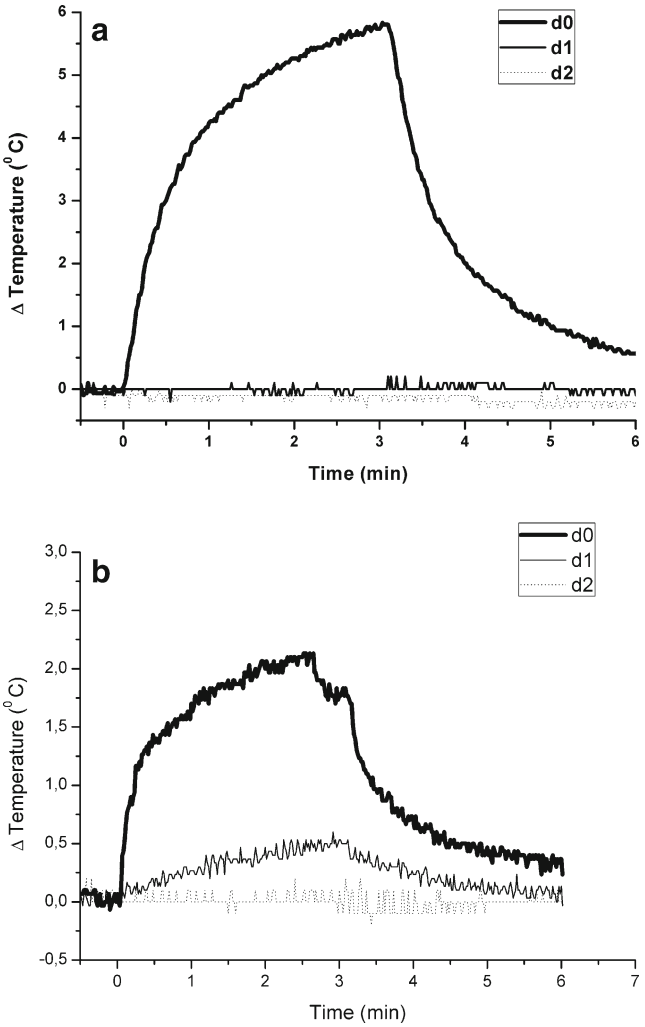

Fig. 3 Thermal map with application of the red LED (**a**) and infrared LED (**b**). The legends *d0*, *d1*, and *d2* represent the distances from the LED tip to the tissue in a vertical direction with a 90° angle. They represent the distance between the tip and the thermistor at zero, 1 cm, and 2 cm, respectively

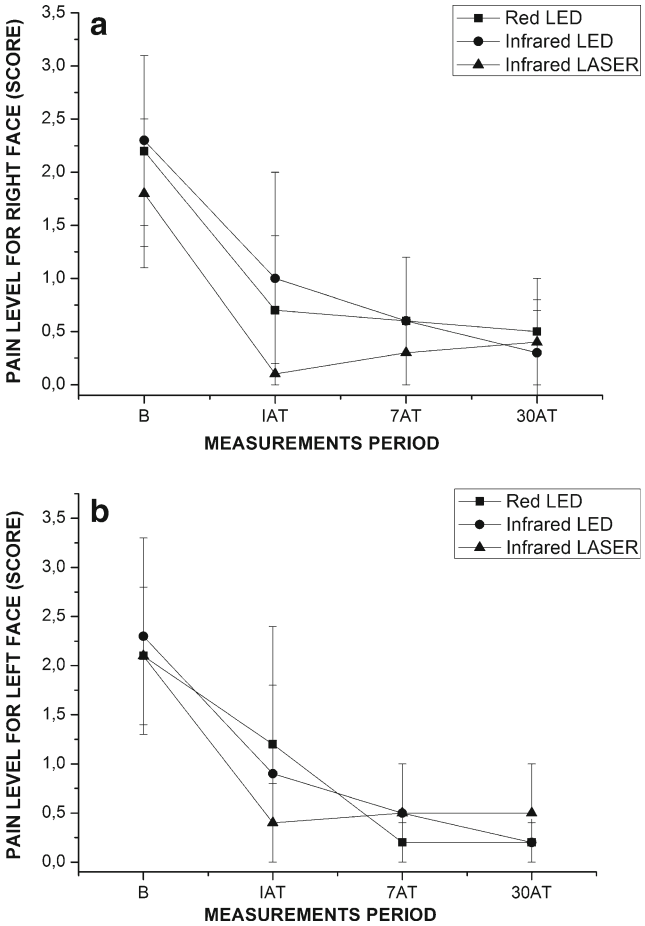

Fig. 4 Pain score for the right (**a**) and left (**b**) face. Significant intragroup differences compared with instance baseline ($p < 0.05$, two-way ANOVA with Tukey's post-hoc). No significant intergroup differences ($p \geq 0.05$, one-way ANOVA). *B* baseline, *IAT* immediately after treatment, *7AT* 7 days after treatment, *30AT* 30 days after treatment

There was no significant difference in pain scores and maximum oral aperture between groups at baseline or any periods after treatment (delta value; $p \geq 0.05$).

Discussion

This is the first study evaluating the effects of LED therapy on TMD management. The main findings of this study were: (1) that the red and infrared LED irradiation showed an increased subcutaneous temperature in the anatomical specimen, a higher temperature for the red wavelength; (2) the red and infrared LED therapy resulted in reduced pain and improved orofacial function similar to the LLLT. These data are relevant because they realize the potential development of new clinical protocols with LEDs for pain relief and improved orofacial function.

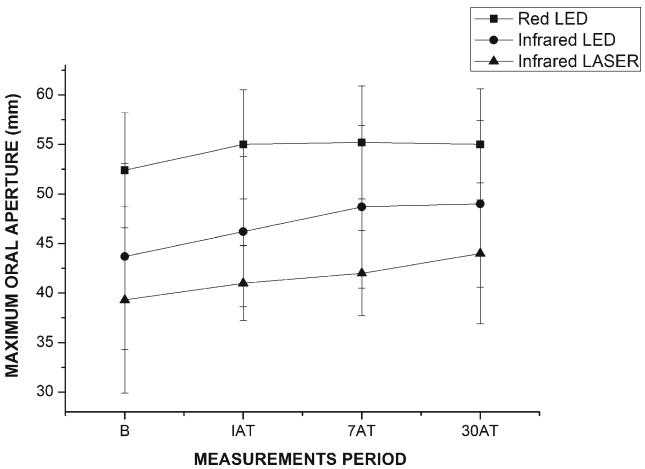

Fig. 5 Maximun oral aperture. Significant intragroup differences compared with instance baseline ($p < 0.05$, two-way ANOVA with Tukey's post-hoc). No significant intergroup differences ($p \geq 0.05$, one-way ANOVA). *B* baseline, *IAT* immediately after treatment, *7AT* 7 days after treatment, *30AT* 30 days after treatment

Although the current study applied LED therapy for TMD treatment, LEDs with higher output power reaching 3 W have been used for other purposes in dental patients without side effects, such as photo activation of dental bleaching gel [37] and curing of composite resins [38].

According to thermal map, LEDs with higher power increased tissue temperature; however, the red radiation produced higher temperatures compared with infrared radiation. In this context, red wavelengths are more absorbed by tissue surface components than infrared wavelengths. The absorbed energy can be dissipated in the form of heat around the skin surface. Conversely, the infrared wavelengths can penetrate deeply into the body tissues which has lower scattering and absorption properties [39]. Remarkably, the heat remains localized. This finding is very interesting and presents an appealing clinical approach application geometry. Considering the clinical effectiveness, it would suggest performing punctual irradiation on the target area, especially when dealing with a large area (larger than the beam diameter); the points must be equidistant for red LED, at a maximum of 1.0 cm, to ensure the uniform irradiation of the entire region. It is important to emphasize that we analyzed ex vivo specimen prior to clinical trials and living tissues is highly complex and has optical properties defined by varying rates of absorption, scattering, transmission, and reflection. Moreover, patients have the ability to thermoregulate and, therefore, the parameters of LED therapy used in the current study were safe during TMD treatment.

Clinical trials have been performed to investigate the TMJ area temperature when applying a CO_2 laser (1.0 W) positioned 10 cm above the skin [40, 41]. This laser caused a significant increase in facial temperature because it improved the microcirculation via the vasodilator reflex [40]. Moreover, after the TMJ area was exposed to phototherapy, there was a significant increase in the diameter and blood flow volume of superficial temporal artery, compared with the baseline [41].

Thermal effects can explain the reduced pain and the increased functionality, because phototherapy can lead to lymphatic drainage, improve oxygen supply and transport, and utilization of metabolic substrates [31].

Several studies [42–44] have shown that temperature changes induced by phototherapy can be associated with alteration in nerve conduction velocities which result in analgesic effects [15]. Regarding nerve conduction, in a study of Vinck et al. [32], infrared LED therapy, with an average power of 160 mW, was performed on healthy subjects and showed an immediate and localized effect on the conduction characteristics of nerves, with a reduced number of impulses per unit of time for pain relief [32]. In the current study, we used similar average power as Vinck et al. [32] (150×160 mW), but the device's geometry (probe area of 0.5×18 cm^2) is different and, consequently, the fluences are different as well. For the same reason, the LEDs and laser parameters used in our study are different.

Concerning fluence parameters, we chose the applied dose based on typical doses used in regular practice (around 100 J/cm^2 seemed reasonable). Pöntinen [45] showed that a fluence of 4 J/cm^2 at skin level will maintain an irradiance at depths in the range of 0.5–2.5 cm. When irradiating joints or muscles, a fluence of 100–300 J/cm^2 was attenuated to 2 J/cm^2 and irradiance can be maintained at certain depths [31, 45].

One of the limitations of the current study is the difference between laser and LED parameters. LED and laser prototype devices with the same geometry and parameters should be developed for future studies. However, our study showed similar effects for LED and laser therapies on TMD management.

LEDs are not monochromatic, nor coherent, and cover a much broader range of wavelengths. Whereas lasers are monochromatic, coherent, and preserve collimation during propagation. Additionally, coherence is not lost in lasers upon entering tissue, but the length of coherence is reduced and split up into small speckles throughout the irradiated volume [46]. However, our study showed that the coherence property of light was not exclusively responsible for cellular response and the outcomes of phototherapy. Therefore, LED devices constitute an attractive alternative for phototherapy. In this context, LEDs have a comparably low operational cost, allow irradiation of larger areas, and can be configured to produce multiple wavelengths with an absorption of photons by several chromophores [29, 30].

Concerning different wavelengths, red and infrared radiation can act on different sites of the tissue. For example, red light acts on mitochondria, whereas infrared acts on both mitochondria and cellular membrane [47]. The combined effects of both wavelengths can be advantageous for tissue biostimulation or biomodulation. Future studies should be performed combining red and infrared radiation for TMD treatment.

Only one clinical trial [48] has investigated the immediate effects of red LED therapy (640±10 nm) on masseter muscles of subjects with healthy TMJ. However, long-term effects were not investigated and subjects with TMD were excluded from the study. In this study, compared with the results in a placebo group, the subjects who received LED therapy showed increased muscle activity and fatigue resistance.

Future studies investigating the effects of different parameters of irradiation on pain relief and improvement of orofacial function should be performed.

Conclusions

The current study showed that red and infrared LED therapy can be useful in improving outcomes related to pain relief and mandibular range of motion for TMD patients. In addition, LED and laser therapy showed similar results. In this context,

LEDs can be considered as an attractive alternative to the use of LLLT.

Acknowledgments We would like to thank the National Council for Scientific and Technological Development (CNPq)—grant no. 552720/2009-7 and the São Paulo Research Foundation (FAPESP)—grant no. 2013/07276-1 for financial support.

References

1. Fricton JR (2004) Temporomandibular muscle and joint disorders. Pain 109:530
2. Núñez SC, Garcez AS, Suzuki SS, Ribeiro MS (2006) Management of mouth opening in patients with temporomandibular disorders through low-level laser therapy and transcutaneous electrical neural stimulation. Photomed Laser Surg 24:45–49
3. Weinberg LA (1980) The etiology, diagnosis, and treatment of TMJ dysfunction-pain syndrome. Part II: differential diagnosis. J Prosthet Dent 43:58–70
4. Ibuldu E, Cakmak A, Disci R, Aydin R (2004) Comparison of laser, dry needling and placebo laser treatments in myofascial syndrome. Photomed Laser Surg 22:306–311
5. De Medeiros JS, Vieira GF, Nishimura PY (2005) Laser application effects on the bite strength of the masseter muscle, as an orofacial pain treatment. Photomed Laser Surg 23:373–376
6. Emshoff R, Bösch R, Pümpel E, Schöning H, Strobl H (2008) Low-level laser therapy for treatment of temporomandibular joint pain: a double-blind and placebo-controlled trial. Oral Surg Oral Med Oral Pathol Oral Radiol Endod 105:452–456
7. Conti PCR (1997) Low level laser therapy in the treatment of temporomandibular disorders (TMD): a double blind pilot study. J Craniomandib Pract 15:144–149
8. Gur A, Sarac AJ, Cevik R, Altindag O, Sarac S (2004) Efficacy of 904 nm gallium arsenide low level laser therapy in the management of chronic myofascial pain in the neck: a double-blind and randomized trial. Lasers Surg Med 35:229–235
9. Salmos-Brito JA, de Menezes RF, Teixeira CE, Gonzaga RK, Rodrigues BH, Braz R, Bessa-Nogueira RV, Gerbi ME (2013) Evaluation of low-level laser therapy in patients with acute and chronic temporomandibular disorders. Lasers Med Sci 28:57–64
10. Ahrari F, Madani AS, Ghafouri ZS, Tunér J (2013) The efficacy of low-level laser therapy for the treatment of myogenous temporomandibular joint disorder. Lasers Med Sci (in press)
11. Gökçen-Röhlig B, Kipirdi S, Baca E, Keskin H, Sato S (2012) Evaluation of orofacial function in temporomandibular disorder patients after low-level laser therapy. Acta Odontol Scand 4:1–6
12. Huang YY, Chen ACH, Carroll JD, Hamblin MR (2009) Biphasic dose response in low level light therapy. Dose Response 7:358–383
13. de Moraes Maia ML, Ribeiro MA, Maia LG, Stuginski-Barbosa J, Costa YM, Porporatti AL, Conti PC, Bonjardim LR (2013). Evaluation of low-level laser therapy effectiveness on the pain and masticatory performance of patients with myofascial pain. Lasers Med Sci (in press)
14. Jang H, Lee H (2012) Meta-analysis of pain relief effects by laser irradiation on joint areas. Photomed Laser Surg 30(8):405–417
15. Chow R et al (2011) Inhibitory effects of laser irradiation on peripheral mammalian nerves and relevance to analgesic effects: a systematic review. Photomed Laser Surg 29:365–381
16. Kulekcioglu S, Sivrioglu K, Ozcan O, Parlak M (2003) Effectiveness of low–level laser therapy in temporomandibular disorder. Scand J Rheumatol 32:114–118.
17. Ferreira L A, de Oliveira R G, Guimarães J P, Carvalho A C P, De Paula, M V Q (2013). Laser acupuncture in patients with temporomandibular dysfunction: a randomized controlled trial. Lasers Med Sci (in press)
18. Hotta PT, Hotta TH, Bataglion C, Bataglion SA, de Souza Coronatto EA, Siéssere S, Regalo SCH (2010) Emg analysis after laser acupuncture in patients with temporomandibular dysfunction (TMD). Implications for practice. Complement Ther Clin Pract 16(3):158–160
19. Fikackova H, Dostalova T, Navratil L, Klaschka J (2007) Effectiveness of low-level laser therapy in temporomandbular joint disorders: a placebo-controlled study. Photomed Laser Surg 25:297–303
20. Oz S, Gokçen-Rohlig B, Saruhanoglu A, Tuncer EB (2010) Management of myofacial pain: low-level laser therapy versus occlusal splints. J Craniofac Surg 21:1722–1728
21. Walsh LJ (1997) The current status of low level laser therapy in dentistry, part 1, soft tissue applications. Aust Dent J 42(4):247–254
22. Stadler I, Lanzafame RJ, Oskoui P, Zhang RY, Coleman J, Whittaker M (2004) Alteration of skin temperature during low-level laser irradiation at 830 nm in a mouse model. Photomed Laser Sur 22(3):227–231
23. Sopena EP, Serra MC, Sopena M, Lopez-Silva SM (1996) Cuban experience for therapy in dentistry with light-emitting diodes. Proc SPIE 2630:147–154
24. Corazza AV, Jorge J, Kurachi C, Bagnato VS (2007) Photobiomodulation on the angiogenesis of skin wounds in rats using different light sources. Photomed Laser Surg 25:102–106
25. Bastos JLN, Lizarelli RFZ, Parizotto NA (2009) Comparative study of laser and LED systems of low intensity applied to tendon healing. Laser Physics 19(9):1925–1931
26. Lizarelli RFZ, Miguel FAC, Freitas–Pontes KM, Villa GEP, Nunez SC, Bagnato VS (2010) Dentin hypersensitivity clinical study comparing LILT and LEDT keeping the same irradiation parameters. Laser Physics Letters 7(11):805–811
27. Barolet D (2008) Light-emitting diodes (LEDs) in dermatology. Semin Cutan Med Surg 27(4):227–238
28. Paolillo FR, Borghi-Silva A, Parizotto NA, Kurachi C, Bagnato VS (2011) New treatment of cellulite with infrared-LED illumination applied during high-intensity treadmill training. J Cosmet Laser Ther 13(4):166–171
29. Paolillo FR, Milan JC, Aniceto IV, Barreto SG, Rebelatto JR, Borghi-Silva A, Bagnato VS (2011) Effects of infrared-LED illumination applied during high-intensity treadmill training in postmenopausal women. Photomed Laser Surg 29(9):639–645
30. Paolillo FR, Corazza AV, Borghi-Silva A, Parizotto NA, Kurachi C, Bagnato VS (2013) Infrared LED irradiation applied during high-intensity treadmill training improves maximal exercise tolerance in postmenopausal women: a 6-month longitudinal study. Lasers Med Sci 28:415–422
31. Paolillo FR, Lins EC, Corazza AV, Kurachi C, Bagnato VS (2013) Thermography applied during exercises with or without infrared light-emitting diode irradiation: individual and comparative analysis. Photomed Laser Surg 31(7):349–355
32. Vinck E, Coorevits P, Cagnie B, De Muynck M, Vanderstraeten G, Cambier D (2005) Evidence of changes in sural nerve conduction mediated by light emitting diode irradiation. Lasers Med Sci 20:35–40
33. Petrucci A, Sgolastra F, Gatto R, Mattei A, Monaco A (2011) Effectiveness of low-level laser therapy in temporomandibular disorders: a systematic review and meta-analysis. J Orofac Pain 25(4):298
34. Dworkin SF, LeResche L (1992) Research diagnostic criteria for temporomandibular disorders: review, criteria, examinations and specifications, critique. J Craniomandib Disord 6(4):301–355
35. Pereira FJ Jr, Huggins KH, Dworkin SF et al (2004) Critérios de diagnóstico para pesquisa das desordens temporomandibulares RDC/

TMD. Tradução oficial para a língua portuguesa. J Bras Clin Odontol Int 8:384–395
36. Komisnky M, Lucena LBS, Siqueira JTT et al (2004) Adaptação cultural do questionário "Research diagnostic criteria for temporomandibular disorders" axis II para o português. Jl Bras Clin Odontol Int 4(1):51–61
37. Florez FLE, Andrade MF, Campos EA, Oliveira Júnior OB, Bagnato VS, Panhoca VH (2011) In-office dental bleaching efficacy assessment in function of the light exposure regime by digital colorimetric reflectance spectroscopy. J Dent Oral Hyg 3(8):99–105
38. Leonard DL, Charlton DG, Roberts HW, Cohen ME (2002) Polymerization efficiency of LED curing lights. J Esthet Restor Dent 14(5):286–295
39. Svanberg S (2002) Tissue diagnostics using lasers. In: Waynant RW (ed) Lasers in medicine. CRC Press, Boca Raton, FL, pp 135–169
40. Makihara E, Makihara M, Masumi SI, Sakamoto E (2005) Evaluation of facial thermographic changes before and after low-level laser irradiation. Photomed Laser Ther 23(2):191–195
41. Makihara E, Masumi SI (2008) Blood flow changes of a superficial temporal artery before and after low-level laser irradiation applied to the temporomandibular joint area. J Jpn Prosthodont Soc 52(2):167–170
42. Lowe AS, Baxter GD, Walsh DM, Allen JM (1994) Effect of low intensity laser (830 nm) irradiation on skin temperature and antidromic conduction latencies in the human median nerve: relevance of radiant exposure. Lasers Surg Med 14(1):40–46
43. Lowe AS, Baxter GD, Walsh DM, Allen JM (1995) The relevance of pulse repetition rate and radiant exposure to the neurophysiological effects of low-intensity laser (820 nm/pulsed wave) irradiation upon skin temperature and antidromic conduction latencies in the human median nerve. Laser Med Sci 10(4):253–259
44. Noble JG, Lowe AS, Baxter GD (2001) Monochromatic infrared irradiation (890 nm): effect of a multisource array upon conduction in the human median nerve. J Clin Laser Med Surg 19(6):291–295
45. Pöntinen PJ (2000) Laseracupuncture. In: Simunovic Z (ed) Lasers in medicine and dentistry: basic and up-to-date clinical application of low-energy-level laser therapy (LLLT). Vitgraf, Rijeka, Croatia, pp 55–475
46. Hode T, Jenkins P, Jordison S, Hode L. (2011). To what extent is coherence lost in tissue? SPIE BiOS-International Society for Optics and Photonics, Bellingham, WA, pp. 788703–788703
47. Eells JT, Wong-Riley MT, VerHoeve J, Henry M, Buchman EV, Kane MP, Gould LJ, Das R, Jett M, Hodgson BD, Margolis D, Whelan HT (2004) Mitochondrial signal transduction in accelerated wound and retinal healing by near-infrared light therapy. Mitochondrion 4(5):559–567
48. Kelencz CA, Muñoz IS, Amorim CF, Nicolau RA (2010) Effect of low-power gallium-aluminum-arsenium noncoherent light (640 nm) on muscle activity: a clinical study. Photomed Laser Surg 28(5):647–652

cepof.ifsc.usp.br

Grupo de Óptica / CePOF, Instituto de Física de São Carlos, Universidade de São Paulo
Av. Trabalhador Sancarlense, 400, Centro, CP 369, 13560-970, São Carlos - SP
Telefones: (16) 3373-9810; 3373-9823 - Fax: 3373-9811